TOWARDS REDOX CONTROL OF ORGANOMETALLIC CATALYSTS BEARING FERROCENE-BASED LIGANDS

BY

SHUOREN DU
杜硕人

OCTOBER 2013

Department of Chemistry
Imperial College London

A thesis submitted in partial fulfillment of the requirements for the award of Doctor of Philosophy of Imperial College London

TABLE OF CONTENTS

DECLARATION/PUBLICATION 6

ABSTRACT 7

ACKNOWLEDGEMENTS 8

ABBREVIATIONS 10

CHAPTER 1: *Introduction* 13

1.1. Overview of Redox-Active Ligands 15

1.2. Categorization of Redox-Active Ligands Designed for Transition Metals 17

1.2.1. Categorization from Mirkin and Allgeier 17

1.2.2. Categorization from Lyaskovskyy and de Bruin 21

1.3. Ferrocene and Cobaltocene Incorporated Redox-Active Ligands 25

1.3.1. Cobaltocene/cobaltocenium-based redox-active ligands 25

1.3.2. Ferrocene-derived redox-active ligands 27

1.4. Electrochemistry and Chemical Redox Agents 32

1.4.1. Cyclic voltammetry 32

1.4.2. Ferrocenium hexafluorophosphate as oxidant 36

1.5. Palladium-catalyzed Carbonylation of Aryl Halides 38

1.5.1. Mechanisms 39

1.5.2. Conclusion 46

1.6. Summary 46

1.7. References 47

CHAPTER 2: *Redox Control in Palladium-Catalyzed Intra- and Inter-molecular Alkoxy/aminocarbonylation Reactions supported by 1,1'-bis(Diaryl/alkylphosphino)ferrocenes* 55

2.1. Introduction 57

2.2. Chemical oxidation of dichloropalladium 1,1'-bis(diphosphino)ferrocenes 58

2.3. Intramolecular alkoxycarbonylation reactions of 2-halobenzylalcohols 61

2.3.1. Realization of redox control and the mechanism of the processes 61

2.3.2. The optimized conditions for the alkoxycarbonylation of 2-bromobenzylalcohol catalyzed by $[Pd(dppf\text{-}Fe^{III})Cl_2][PF_6]$ 69

2.3.3. Efficiency of the redox control on the $Pd(dppf)Cl_2$ catalyzed alkoxycarbonylation reaction of 2-bromobenzylalcohol 74

2.4. The intermolecular aminocarbonylation reactions of halobenzene and benzylamine 77

2.5. The intramolecular aminocarbonylation reaction of 2-bromobenzylamine, and the intermolecular alkoxycarbonylation reaction of bromobenzene and benzylalcohol 82

2.6. Conclusion 84

2.7. References 84

CHAPTER 3: *Novel Ferrocenyl N-P Ligands for Palladium-Catalyzed Carbonylation Reactions* 88

3.1. Introduction 90

3.2. Synthesis of Novel New Ferrocenyl N-P Ligands 91

3.2.1. Synthesis of the aminoferrocene precursor 91

3.2.2. Synthesis of ligands 92

3.3. Synthesis of Palladium Complexes 103

3.4. Electrochemical Studies and Chemical Oxidation of Complexes 107

3.5. Catalytic Investigations 110
3.6. Conclusions 113
3.7. References 114

CHAPTER 4: *Synthesis of Ferrocene-based Dimines and Oxidative Purification of Halogenated Ferrocenes* 116

4.1. Introduction 118
4.2. Oxidative Purification of Halogenated Ferrocenes 120
4.2.1. Purification of 1,1'-dibromoferrocene 120
4.2.2. Oxidative purification of monohaloferrocenes and 1,1'-dihaloferrocenes 125
4.3. Synthesis of Ferrocenyl-incorporated Diimines 132
4.4. Synthesis of Ferrocen-1,1'-diyl-containing Diimines 141
4.4.1. Synthesis of 1,1'-bis(amino)ferrocene 141
4.4.2. Synthesis of bis-bidentate diimine ligands 142
4.5. Conclusion 147
4.6 References 147

CHAPTER 5: *Investigations of Palladium-Catalyzed Suzuki-Miyaura Cross-coupling and Rhodium-catalyzed Hydrogenation Reactions* 150

5.1. Introduction 152
5.2. Synthesis of 1,1'-bis(Methylthio)ferrocene-containing Complexes 154
5.2.1. Synthesis of methylchloropalladium complexes 154
5.2.2. Synthesis of rhodium complexes bearing fc[P, P] and fc[S, S] ligand 156
5.3. Studies on the Redox Properties of Complexes 158
5.4. Catalytic investigations 164

5.4.1. Suzuki-Miyaura cross-coupling reactions 164
5.4.2. Rhodium-catalyzed hydrogenation of styrene 174
5.5. Conclusion 175
5.6. References 176

CHAPTER 6: *Conclusion and Future work* 178

CHAPTER 7: *Experimental* 182
7.1. General 184
7.2. Compounds synthesized in chapter 2 186
7.3. Compounds synthesized in chapter 3 191
7.4. Compounds synthesized in chapter 4 195
7.5. Compounds synthesized in chapter 5 198
7.6. References 201

APPENDICES 202

DECLARATION

The work described in this thesis was carried out in the Department of Chemistry, Imperial College London, between October 2009 and September 2013. The entire body of work is my own unless otherwise stated to the contrary and has not been previously submitted for a degree at this or any other university.

PUBLICATION

‘‘Oxidative purification of halogenated ferrocenes’’, Inkpen, M.; Du, S.; Driver, M.; Albrecht, T.; Long, N. J. *Dalton Trans* **2013**, *42*, 2813.

ABSTRACT

This thesis is mainly concerned with the synthesis and characterization of redox -active substituted ferrocene ligands, their complexation with palladium, the redox properties of the complexes and their applications as carbonylation catalysts with a view to controlling the catalytic behaviour *via* a change in the oxidation state of the ferrocene unit. Chapter 1 presents the concept of redox-active ligands and redox control in transition metal-catalyzed processes, with the emphasis on the utilization of ferrocene/cobaltocene as a 'redox centre'. Cyclic voltammetry, by which the redox properties of the compounds synthesized in this work were electrochemically characterized, and the choice of the appropriate chemical oxidizing agent are also introduced. Finally, the palladium-catalyzed alkoxy-/aminocarbonylation processes of aryl halides are briefly reviewed. Chapter 2 is concerned with the chemical oxidation of some previously synthesized ferrocene-incorporated palladium diphosphines, and the observation and discussion of the different catalytic performance of the oxidized and non-oxidized catalysts in the alkoxy-/aminocarbonylation reactions of aryl halides. Chapter 3 involves the synthesis of ferrocenyl N-P ligands and their coordination to palladium, as well as studies on the redox behaviour of the palladium complexes and their applications as catalysts to realize redox control on the alkoxycarbonylation of 2-halobenzylalcohol. Chapter 4 describes the synthesis of ferrocenyl or ferrocen-1, 1'-diyl diimine ligands, and the unexpected oxidation of the ferrocene redox units upon the complexation of these ligands to various transition metals including nickel, iron, cobalt and palladium. Chapter 5 details explorations into the redox control of Suzuki-Miyaura cross-coupling and hydrogenation reactions through the use of some ferrocene-based palladium and rhodium complexes. Chapter 6 presents the conclusions of the thesis and suggestions for future work. Experimental details for chapters 2 - 5 are given in chapter 7.

ACKNOWLEDGEMENT 致谢

First of all I would like to express gratitude to my fantastic supervisor, Professor Nick Long, for the opportunity to study and research at Imperial College London, one of the top universities in the world; for all his guidance, support, encouragement, advice and patience throughout the past four years spent as his PhD student; for he is always reliable in replying to emails; for his excellent supervising skills so I can be at all time motivated but never too stressed; for everything I have learnt during these project; and of course for all the treasured practical opportunities he has introduced to me: conferences, supervising MRes project and the collaborative project with Dr. Chris Blackman in UCL. I absolutely enjoy doing my PhD in your group!

My special thanks must go to Dr. Mike Inkpen, who is so talented in chemistry, for all his invaluable support during those times when I was so defeated by ferrocenes. Without both his technical assistance, crazy but interesting thoughts on my progress as this project developed and expert proof reading skill, this thesis would not have been realized. Also, buddy, working with you on the paper we have published and the one in progress is definitely an amazing experience from which I have learnt a lot. Oh, I almost forgot the Ferrocene conference in Hannover Germany, we made the perfect Imperial team!

Many other people have given me advice and inspiration on chemistry, thanks in particular to Dr. Phil Miller for training me working with CO and H_2 gas cylinders, and for his great help in our discussions on catalysis. Of course, my huge thanks to Dr. Tim Albrecht for giving me access to his electrochemistry lab and delicate apparatus, as doing cyclic voltammetry experiments is also an important part of this project. It is definitely a rewarding practice by doing different things in Nick's synthesis lab and in Tim's physical chemistry lab.

Acquisition of data would not have been possible without the help of Mr. Peter Haycock and Mr. Dick Sheppard for NMR analysis; Mr. John Barton and Ms. Lisa Haigh for mass spectrometry; Mr. Stephen Boyer for elemental analysis; Dr. Andrew

White for X-ray crystallography; Dr. Emanule Instuli for his training sessions on electrochemical measurements; Dr. George Britovsek and Dr. Atanas Tomov for their kind offer to use the GC in their lab when the GC on the 6th floor was down; and Dr. Jay Hall for teaching me how to do GC analysis, and buying my first pint of Guiness!

To all the members of the Long group, past and present, thank you for being so friendly and helpful at all time. Sheena, it has been a great time to fight with you as in our final year, and thank you for all the encouragements. Anna, you made a perfect neighbour in the office. Andy, you are talented in chemistry definitely, and thanks for all your help in the lab. Juan, thank you for your understanding when I had to 'invade' into your fumehood, you are such a nice man and I wish you all the best. Graeme, I may not have obtained the 1,1'-bis(azido/amino)ferrocene in time if it was not with your help… It's an enjoyable experience to be with you, Long group lovelies, every one of you contributes to my PhD!

I also have to say thank you to my friends here in Imperial for all their support, especially my girlfriend Wendy for taking great care of me everyday and helped me calm down whenever I got too emotional.

感谢中国留学基金委 CHINA SCHOLARSHIP COUNCIL 提供给我国家公派留学的机会和慷慨资助，使得我可以在伦敦这样一个消费水平极高的国际化大都市潜心科研学术，不为经济问题困扰。感谢中国驻英国大使馆教育处的工作人员这些年来给予的关怀与帮助，让我身在帝都的每一分钟都感到组织就在身边，从而心中底气足。田公参夫妇和蔼的笑容和温暖的鼓励，还有他们准备的温馨年夜饭；力老师一如既往的对我生活上的关照，对我在帝国理工中国学生学者联谊会工作中的绝对支持，以及对我在帝国理工公派留学生联络工作中的信任；大使馆逢年过节的招待会中家乡的美味以及刘晓明大使对留学生表达的祖国对我们的期望，等等。这些都是我留英学习期间难忘的回忆。

最终特别感谢我亲爱的爸妈，先是遗传给我在语言上的天赋和敏锐的思辨能力，再是后天在为人、学习、音乐等等各方面的培养，以及二十几年来不懈的谆谆教诲和对我的人生观、世界观、价值观的正确影响，使我终于可以争取到在伦敦帝国理工这样一所世界一流学府学习的机会。这一天，你们盼得比我久。

ABBREVIATIONS

^{o}C	degrees Celsius
δ	chemical shift (ppm)
μ	micro-
aq.	aqueous
Ar	aryl
br	broad signal
Bz	benzyl
$CDCl_3$	deuterated chloroform
CD_2Cl_2	deuterated methylene chloride
CO	carbon monoxide
COD	1,5-cyclooctadiene
Cp	cyclopentadienyl
Cp*	1,2,3,4,5-pentamethylcyclopentadienyl
d	doublet
dd	doublet of doublets
DCM	dichloromethane
DMSO	dimethylsulfoxide
dippf	1,1'-bis(di-*iso*-propylphosphino)ferrocene
dippf-Fe^{III}	1,1'-bis(di-*iso*-propylphosphino)ferrocenium
dppc	1,1'-bis(diphenylphosphino)cobaltocene
dppf	1,1'-bis(diphenylphosphino)ferrocene
dppf-Fe^{III}	1,1'-bis(diphenylphosphino)ferrocenium
dtbpf	1,1'-bis(di-*tert*-butylphosphino)ferrocene
dtbpf-Fe^{III}	1,1'-bis(di-*tert*-butylphosphino)ferrocenium
$E_p^{1/2}$	half wave potential
EI	electron impact ionization
E_p^{a}	anodic peak potential

E_p^c	cathodic peak potential
Et_2O	diethyl ether
Et_3N	triethylamine
EtOH	ethanol
$FeCp_2$	ferrocene
FeCpCp*	1,2,3,4,5-pentamethylferrocene
$FeCp^*_2$	decamethylferrocene
Fc	ferrocenyl
fc	ferrocen-1,1'-diyl
g	gram(s)
hr(s)	hour(s)
I	current
i_p^a	anodic peak current
i_p^c	cathodic peak current
^{i}Pr	*iso*-propyl
J	coupling constant (Hz)
L	litre(s) / ligand (if stated)
L-L	bidentate ligand
M	mole per litre
m/z	mass/charge ratio
MeCN	acetonitrile
MHz	megahertz
min(s)	minute(s)
mL	millilitre(s)
mmol(s)	millimole(s)
MeOH	methanol
MS	mass spectrometry
N_3^-	azide
NEt_3	triethylamine

OTf	trifate
PF_6^-	hexafluorophosphate
Ph	phenyl
P-P	bidentate diphosphines
PPh_3	triphenylphosphine
ppm	parts per million
pt	pseudo-triplet
s	singlet
t	tripet
TBAP	tetrabutylammonium hexafluorophosphate
^{t}Bu	*tert*-butyl
THF	tetrahydrofuran
TMEDA	N,N,N',N'-tetramethylenediamine
V	voltage
v_s	scan rate

Chapter 1

Introduction

昨夜西风凋碧树，独上西楼，望尽天涯路。

—— 晏殊《蝶恋花》

Redox-active compounds are of great significance for their applications in catalysis,[1-11] as well as their potential to be 'intelligent' materials,[12, 13] and sensors for ions[14-16] and small molecules.[17, 18] With ideal chemical redox agents or applied potentials, a redox-active compound can be interconverted between its two (or more) oxidation states. Therefore these compounds are often referred to as 'redox switches' (or 'redox partners'). Redox-active transition metal complexes, as one of the most important types of redox-active compound, have therefore drawn considerable attention because of their role as highly efficient and selective catalysts.[2-11] In redox processes of these coordination compounds, while the behaviour of some involve only the oxidation or reduction of the metal,[3, 10] ligands of some other metal complexes participate in the redox processes as a much more prominent role in a catalytic cycle than the metals.[19] In the latter cases, the ligand is referred to as a 'redox-active ligand' or 'redox non-innocent ligand',[20, 21] which can be switched between two or more oxidation states through a series of approaches. The aim of this introduction is to (i) provide a general insight into the redox-active complexes that are based on a redox-active ligand and their applications in homogeneous catalysis, (ii) to give a brief introduction into electrochemistry and chemical redox agents, and (iii) to briefly review the palladium-catalyzed carbonylation of aryl halides as a catalytic process where redox-active ligands can potentially be used to control the reactivities of the palladium catalysts.

1.1. Overview of Redox-active Ligands

It is of great interest to incorporate redox-active groups into various metal-binding ligands. Cryptand and crown sequestering agents with ferrocenyl,[22-25] cobaltocenyl[16, 26] and other redox-active groups[27, 28] have been synthesized. These ligands offer electrochemical control over the thermodynamic binding affinities of transition metals, and have been used in various metal systems.[27, 29] The compounds featuring redox-active ligands have been applied in the electrochemical recognition of alkali and alkaline earth metal cations,[14, 16, 22-24, 28, 30, 31] and designed for electrochemical detection of numerous anionic guest species.[14,16, 32]

Several redox-active ligands that alter the reactivity of their bound metals as a function of ligand oxidation state have been designed and successfully synthesized. Redox-active ligands of this type are used to provide electrochemical control over stoichiometric and

catalytic reactions of transition metals, and therefore yield compounds with electrochemically switchable states of reactivity and selectivity.[33] Catalysts derived from these ligands may be active in one particular oxidation state, but become rather inactive after reduction or oxidation.[6, 9, 11] Moreover, they may exhibit selectivities for specific transformations, which are dependent upon the oxidation state of the complex.[5] With a redox-active group, no further conventional synthetic steps are needed to control the electron richness of the ligand, as well as the central metal.

In addition to the ligand-based approaches for controlling the reactivities of metal centres as mentioned above, there are metal-based approaches that are also effective. By changing the d-electron count of a certain transition metal, both the steric and electronic environment of the metal's coordination sphere can be drastically altered.[34] In this case, it is difficult to determine the effect of the electrochemical control on a transition metal as the steric properties of the metal or even the modes of ligand binding are also changed.

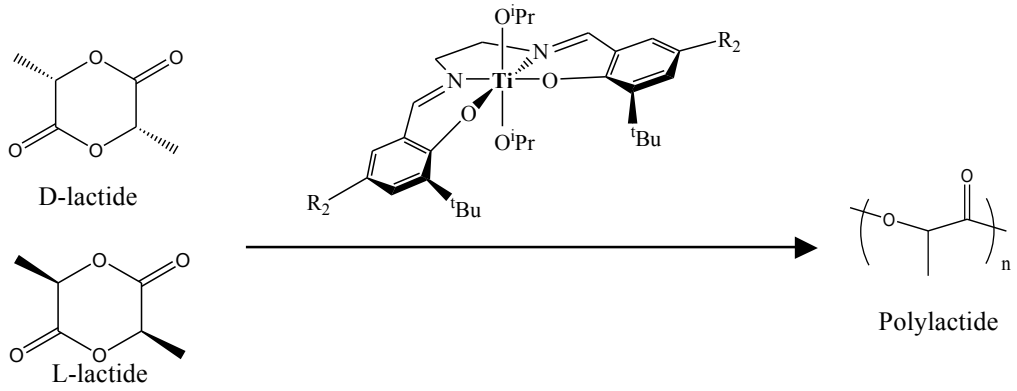

Figure 1.1. Scheme of a titanium-catalyzed ring-opening polymerization (ROP) reaction of *rac*-lactide[i]

However, a ligand-based approach allows for more subtle changes in the electronic properties of the centre metal. There are numerous examples indicating that subtle changes in the electron-donating properties of the ligand can lead to remarkable effects in the reactivity of transition metals. For example, in the catalytic reaction of the ring-opening polymerization

[i] Figure 1.1 adapted from reference 35.

of *rac*-lactide, titanium-salen initiators bearing electron-donating substituents incorporated into the aryl groups (R group in figure 1.1) offer higher reactivity than the corresponding catalysts with electron-withdrawing groups.[35]

Based on these facts, in this project, it was decided to focus on the use redox-active complexes where the redox processes are centred on the ligand but not the metal centre.

1.2. Categorization of Redox-active Ligands designed for Transition Metals

Redox-active ligands, which are specially designed for controlling the reactivity and selectivity of transition metals, were first categorized by Mirkin and Allgeier[33] based on the method that a redox-active ligand takes to alter the stoichiometric activity and the coordinating properties of its bound metals. Recently, the categories of redox-active ligands have been specified again by Lyaskovskyy and de Bruin according to the role these ligands play in catalytic processes.[19] Both categorizations will be illustrated.

1.2.1. Categorization from Mirkin and Allgeier

A. Substitutionally-inert redox-active ligands

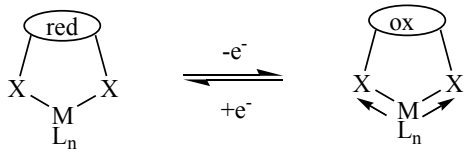

electron-rich electron-poor

Figure 1.2. Concept of substitutionally-inert redox-active ligands[ii]

(X= strongly binding ligand)

For ligands that fall into this class, the redox-active group is incorporated into a ligand which forms a strong, substitutionally inert interaction with a particular transition metal (Figure 1.2). Changes in the oxidation state of the ligand affect the reactivity of the metal by

[ii] Figure 1.2 adapted from reference 33.

altering its electronic nature without changing its formal oxidation state, usually by way of through-bond electron donation or withdrawal as well as through-space dipole interactions.[5, 36-40]

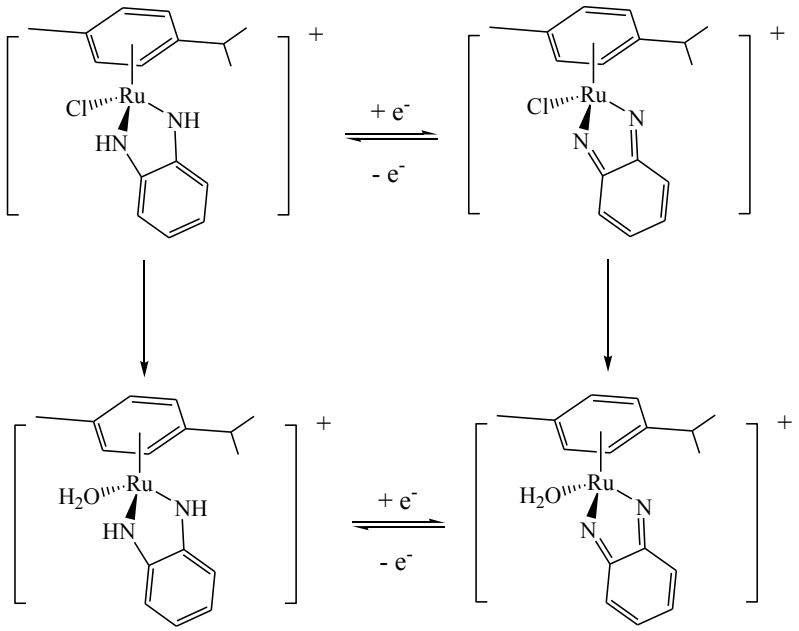

Figure 1.3. Redox and hydrolysis process of a ruthenium aryl complex[iii]

For example, in a research study on the ruthenium halide complexes that have potential as anticancer agents,[40] ligand-based oxidation was observed during the hydrolysis of the ruthenium complex shown at the top left in figure 1.3. It is discovered that the hydrolysis of this diamino complex also leads to the formation of both chlorinated and hydrolyzed diimino products. The formation of the π-acceptor chelating ligand is described to decrease the rate of hydrolysis as it attracts electrons on the ruthenium centre and thus reduces the lability of the chloride.

In general, the substitutionally-inert redox-active ligands offer effective electrochemical control over the electronic properties of their bound transition metal, without significant concomitant changes in the steric properties of the complex.

[iii] Figure 1.3 adapted from reference 40.

B. Redox switchable hemilabile ligands (RHLs)

Similarly to the substitutionally-inert redox-active ligands, the RHLs do not bring changes in the formal oxidation state of the metal centre during a redox process. However, the RHLs have the advantage of offering electrochemical control on both the steric and the electronic environment of the coordination site or a set of coordination sites at a transition metal.[8, 41-44]

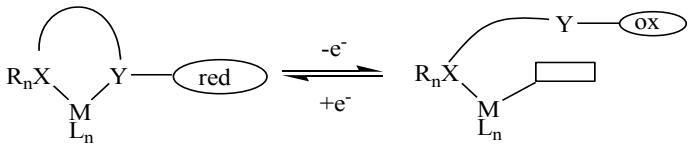

Figure 1.4. Concept of the RHLs (X = strongly binding ligand; Y = weakly binding ligand; R = substituent of tunable electronic nature; ▭ = ligand or solvent molecule)[iv]

Pioneered and extensively studied by Mirkin's group, the RHLs are defined as multidentate ligands that possess at least one substitutionally inert centre and one substitutionally labile centre (figure 1.4). A redox-active group is covalently attached to the substitutionally labile portion of the ligand, whose binding affinity with the central metal is controlled by adjusting the state of charge of the redox-active moiety. In some cases, dissociation of the labile portion of the ligand[45] in favour of a stronger binding ligand or solvent molecule occurs when attempting to modulate the strength of the metal-ligand bond. The electronic nature of the central metal in a RHL-based complex can therefore be tailored through both choosing different R groups and changing the oxidation state of the ligand.

Although the RHLs are still in their early stage of development, a RHL system that avoids proton-coupled electrochemistry has been established by Mirkin and his co-workers to provide a foundation for the synthesis and application of complexes with the RHLs.[41] As demonstrated in figure 1.5, the rhodium complex **1.1** exhibits ligand dissociation upon oxidation of the ferrocenyl groups. The weak Rh-O bond, which is a result of the p-π conjugation effect between the oxygen atom and the ferrocenyl moiety, is further weakened by the oxidation of the ferrocenyl moieties to the extent of dissociation to form the

[iv] Figure 1.4 adapted from reference 43.

aryl-bridged dimer **1.2**, with the geometry of the complex converting from square-planar to piano-stool.

1.1

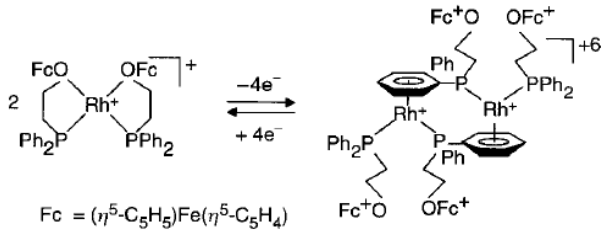

1.2

Figure 1.5. The redox-controlled behaviour of rhodium complex **1.1** with RHLs[v]

This oxidation state-dependent behaviour of complex **1.1** is significant proof for the RHL concept. It shows how RHLs provide tuneability with regard to both the electronic and steric properties of the transition metal to which they are bound, and how useful they are in designing systems with electrochemically switchable selectivities for desired transformations.

Complexes supported by RHLs undergo both electronic and steric transformations during redox processes, making it complicated to study the nature of the changes on their catalytic activities during redox processes.

C. Redox-active ligands as reactive (leaving) fragments

Whilst the aforementioned redox-active ligand may alter the coordination chemistry of the metal in a reversible fashion, other redox-active ligand-based transition metal complexes also exist to demonstrate electrochemically induced irreversible changes in their reactivities. Such redox-active ligands may be completely expelled as leaving fragments from the coordination sphere of the central metals, or change their binding mode upon oxidation or reduction (Figure 1.6).[46, 47]

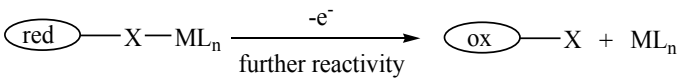

Figure 1.6. Concept of the redox-active ligands as reactive fragments[vi]

[v] Figure 1.5 taken from reference 41.

[vi] Figure 1.6 adapted from reference 33.

This project consequently focuses on the electronic effects that substitutionally inert redox-active ligands exert on the coordination chemistry of the transition metal where the catalytic process is taking place, especially when these ligands are oxidized or reduced.

1.2.2. Categorization from Lyaskovskyy and de Bruin

According to Lyaskovskyy and de Bruin, two main types of redox-active ligands (also named as redox non-innocent ligands) are defined by their role in the catalytic cycle.[19] Redox -active ligands of the first type participate in the catalytic cycle only by accepting/donating electrons, while those of the second type actively participate in the formation/breaking of substrate covalent bonds. In the latter case, the active sites for the catalytic transformation from the substrate to the product are actually ligand-radicals or substrate-centred radical species generated upon the oxidation of either the chelating ligands[48-52] or the substrate after oxidative addition to the metal centre of the catalyst.[53-55] Therefore, redox non-innocent ligands of the second type will not be further discussed as the intrinsic catalytic reactivities of their complexes are not metal-based.

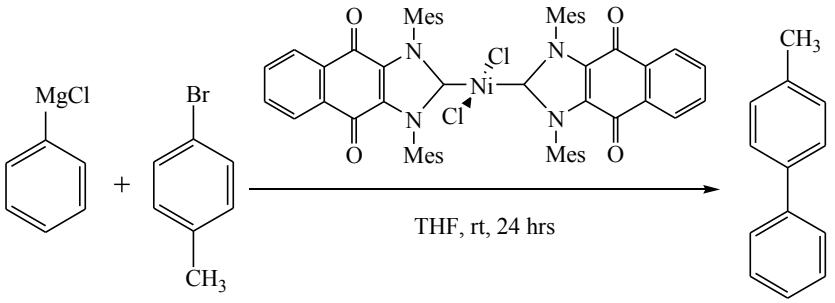

Figure 1.7. Scheme of the Kumada cross-coupling reaction of 4-bromotoluene and PhMgCl catalyzed by redox-active nickel complex (5 mol% catalyst loading)[vii]

Redox-active ligands of the first type can also be classified into two main groups according to the strategies adapted by the ligand in catalysis. The first strategy involves the oxidation or reduction of the ligand as a tool for tuning the electronic properties, such as the Lewis acidity of the metal.[2,4-6, 9, 11, 56] A very good example has been illustrated by Bielawski's research group in their studies on controlling the activity of Kumada cross-coupling reactions

[vii] Figure 1.7 and 1.9 adapted from reference 6, figure 1.8 taken from reference 6.

by applying a nickel catalyst supported by a redox-active N-heterocyclic carbene ligand, 1,3-dimesitylnaphthoquinimidazolium (figure 1.7).[6]

Since 1972, Kumada *et al.* have reported the reactions of organomagnesium reagents and alkenyl or aryl halides that are catalyzed by Ni(II) complexes, which are often referred to as Kumada cross-coupling reactions.[57-60] In this work by Bielawski and his co-workers, the reaction of PhMgCl and 4-bromotoluene (MePhBr) catalyzed by Ni(II) was successfully switched by chemically oxidizing/reducing the ligand, which alters the electron density on the nickel without changing its formal oxidation state.

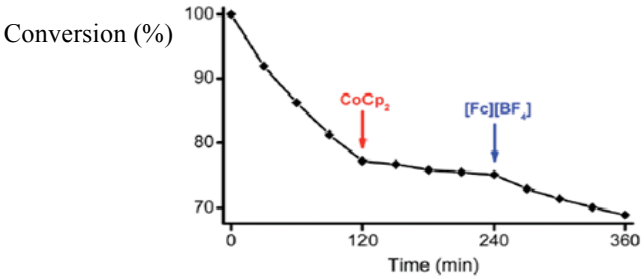

Figure 1.8. Catalytic conversion of the reaction of 4-bromotoluene and PhMgCl during the *in situ* oxidation and reduction of Ni(II) catalyst (Y axis represents the percentage conversion of 4-bromotoluene monitored by GC over 30 min intervals)

As demonstrated in figure 1.8, the neutral Ni(II) complex is clearly more catalytically active than its anionic counterpart. In the first 2 hours before the reducing agent was added, the reaction was found to proceed with a first-order rate constant (k_{obs}) of 4.7×10^{-5} s^{-1}, and a conversion of 23% had occurred within this reaction time. At this point, $CoCp_2$ (2 equivalents relative to Ni to oxidize both of the ligands on the nickel) was added, and a decrease in the catalytic activity by an order of magnitude ($k_{obs} = 2.7\times10^{-6}$ s^{-1}) was observed. After a further 2 h, the re-formation of the oxidized ligand caused by the introduction of $[Fc][BF_4]$ (also 2 equivalents relative to Ni) afforded nearly a 5-fold restoration of catalytic activity ($k_{obs} = 1.2\times10^{-5}$ s^{-1}).[6]

This difference in the catalytic activities between the neutral and anionic nickel complex was elucidated by the authors *via* the mechanism and the intermediates involved in a typical Kumada cross-coupling cycle. As shown in figure 1.9, before the catalytic process

begins, the Ni(II) complex is first reduced by 2 equivalents of PhMgCl to generate the catalytically active Ni(0) species, which then undergoes oxidative addition with MePhBr. Transmetalation then followes to produce nickel diaryl species, and subsequent reductive elimination releases the cross-coupled product with the regeneration of Ni(0) species. It is reasoned that (i) the reduction of Ni(II) to Ni(0) species could be easier with a less electron-rich system for both the generation of catalytically active Ni(0) species and the reductive elimination step, and (ii) that the transmetalation with PhMgCl favours a more positive metal centre as this step involves the bond formation between the nickel and a negatively charged carbon atom. Consequently, the higher catalytic reactivity of the oxidized nickel complex than its non-oxidized version was expected as the metal centre in the neutral complex is less electron-deficient .[6]

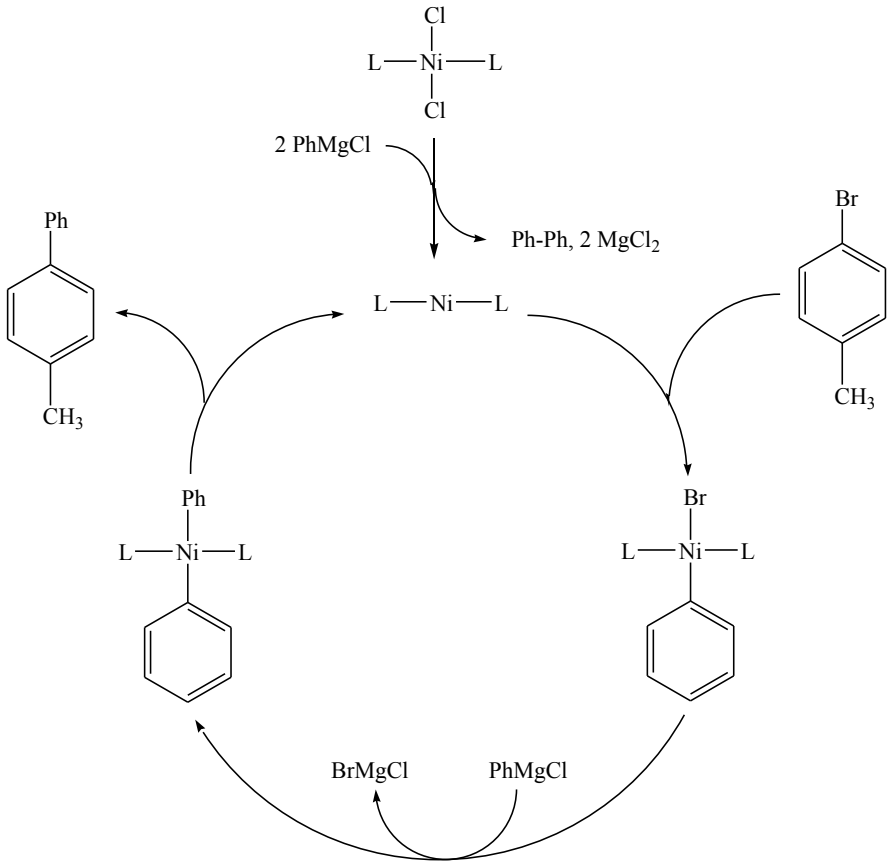

Figure 1.9. Catalytic cycle of the Kumada cross-coupling reaction of MePhBr and PhMgCl (L = ligand)

Redox-active ligands, such as 1,3-dimesitylnaphthoquinimidazolium that can control the catalytic activity of the central metal by tuning its Lewis acidity with no changes in its structure or the formal oxidation state, are the main interest of this project. This type of control on a catalytic process by using the redox properties of the catalyst is named 'redox control'.

The second strategy adopted by the redox-active ligands of the first type in the catalytic cycle can be described as 'electron reservoir' according to Lyaskovskyy and de Bruin.[19] Without changing the d-electron configuration of the metal, some redox-active ligands allow the metal to store electrons on the ligand when excessive electron density is generated on the metal, and release the electrons to the metal when a certain amount of electrons on the metal centre is required.[61, 62]

Quantities of important transformations in the metal-based catalytic processes are based on the electronic transfer between the metal and the substrate, such as the most common oxidative addition step and reductive elimination step. These transformations are usually easy for noble metals like palladium, platinum and rhodium, but difficult for cheap metals like iron and cobalt. However, the 'electron reservoir' strategy of some redox-active ligands to a very large extent promotes the electronic communication in the catalytic cycles between the metal and the substrate *via* ligand-based electron-donation or acceptations where both single unpaired electrons and electron-pairs can be involved, and therefore solves the difficulties in catalytic transformations for first-row transition metals[63-70] or late transition metals.[71-74]

Nonetheless, this strategy is only adopted by redox-active ligands when uncommon oxidation states of the metal need to be avoided in the catalytic processes or a certain electron density on the metal is required for transformations which are otherwise unrealizable. In other words, the redox processes on the ligand take place *via* particular steps in the catalytic cycles, but not as a tool to control catalytic processes when the ligands are supposed to be oxidized or reduced before the catalytic cycle, thus causing a series of changes in the reactivities of the metal towards transformations at various steps. Therefore, the 'electron reservoir' properties of redox-active ligands will not be further discussed.

1.3. Ferrocene and Cobaltocene Incorporated Redox-Active Ligands

In coordination chemistry, the ferrocenyl and cobaltocenyl moieties have played significant roles as backbones or substituents in ancillary ligands due to the specific and unique geometries and redox properties that ferrocene and cobaltocene possess.[25, 75-79] The reversible one-electron redox behaviour, as well as the structural durability, of ferrocene or cobaltocene derivatives make themselves ideal electroactive ligands to perturb *via* redox approaches, the electronic properties and stoichiometric reactivities of the transition metal complexes[80-85] containing ferrocenyl or cobaltocenyl moieties. Therefore, cobaltocene- and ferrocene-based ligands offer great potential within homogeneous transition metal catalysis, for inducing higher or lower electrophilicity (the latter for ferrocenium/cobaltocenium version of the ligands) and consequently an enhancement or a decrease in the reactivity of a catalytically active metal centre.

1.3.1. Cobaltocene/cobaltocenium-based redox-active ligands

Within all the cobaltocenyl chelating ligands, 1,1'-bis(diphenylphosphino)cobaltocene (dppc) is of the greatest significance in terms of the applications of its redox properties. One example has been illustrated by Lorkovic *et al*., where it can be used as an electrochemically tuneable ligand to alter the coordination chemistry of the metal centre.

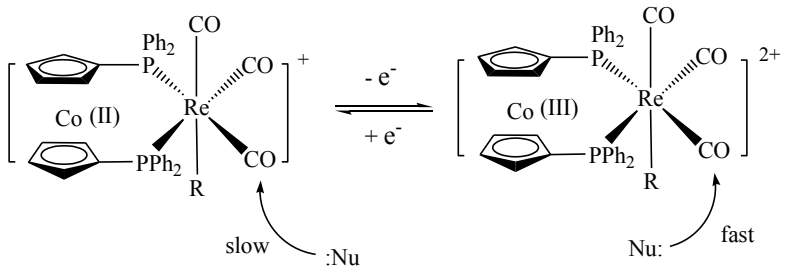

Figure 1.10. Redox couple of dppc-containing rhenium carbonyl complexes [viii]

(Complex **1.3** when R = MeCN; Complex **1.4** when R = CO)

As shown in figure 1.10, rhenium carbonyl complexes containing dppc/dppc-Co^{III} ligands were prepared and characterized in both oxidation states. N-oxides (Me_3NO and

[viii] Figure 1.10 adapted from reference 36.

Me_2PhNO) and azide (N_3^-) performed as molecular and anionic nucleophiles, reacting selectively and irreversibly with metal bound carbonyls. The differences in the reactivities of the rhenium carbonyl moieties between the oxidized and reduced forms of either complex are of orders of magnitude. In MeCN at 25 °C, the one electron oxidation of the dppc ligand results in a 200 fold increase in the rate of reaction of complex **1.3** and Me_3NO/Me_2PhNO, and a 5400 times faster reaction of complex **1.4** and N_3^-. These results clearly show that the binding strength between the rhenium and carbonyl carbon decreases as a result of ligand oxidation.[36]

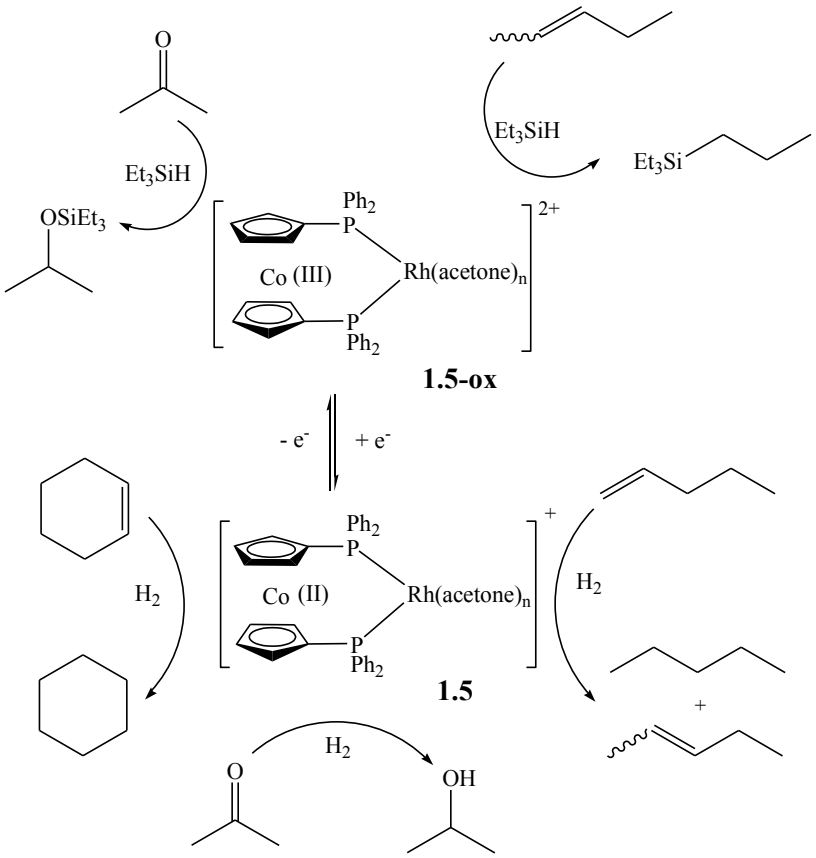

Figure 1.11. The catalytic behaviour of complex **1.5** in each state of charge[ix]

Another classic example of the applications of the dppc ligand in its electrochemical control of the reactivities of homogeneous transition metal catalyst has also been elucidated by Lorkovic *et al*. In this research study on the rhodium(I)-catalyzed isomerization and

[ix] Figure 1.11 adapted from reference 5.

reduction of ketones and alkenes, a dppc-containing rhodium complex **1.5** was found to be catalytically active towards different processes of transformation when the cobalt is in its different oxidation states. This catalytic selectivity induced by the redox nature of dppc is demonstrated in figure 1.11. While **1.5-ox** turned out to be the more efficient and durable hydrosilylation catalyst, **1.5** is more reactive towards hydrogenation processes.[5] The latter fact is attributed to the more basic phosphines employed by dppc-Co^{II} than dppc-Co^{III}, which lead to a more electron-rich rhodium centre that is favoured by the oxidative addition of hydrogen.[86-89] Although the trend correlating the catalytic reactivities for hydrosilylation of olefins or ketones with the basicity of the transition metal has not been found in the literature, this work undoubtedly indicates different consequences from switching the state of charge of the rhodium centre for hydrogenation or hydrosilylation. Most importantly, after numerous studies on how reactivity and selectivity of homogeneous transition metal catalysts can be affected by ligand "donicity",[90-94] for the first time the effect of changes in the ligand charge state on catalytic reactivity was described.

1.3.2. Ferrocene-derived redox-active ligands

The recognition of the 'sandwich' structure of ferrocene is one of the milestones in the field of organometallic chemistry.[95] The reversible one-electron redox behaviour and high stability of ferrocene, as well as the well-established methods for the modification of the cyclopentadienyl group of ferrocene towards more complex structures results in ferrocene still being of great interest.[25, 44, 75, 76, 96] The incorporation of ferrocene as a redox-active moiety of the ligand is indeed the focus of this project and the research group, where a large range of ligands formed *via* substitution of ferrocene by various donor hetero atoms has been synthesized.[97-101]

One of the most significant results in our group on the applications of the redox properties of ferrocene has been the successful synthesis of the titanium redox-active complex shown in figure 1.12, and the investigations of its reversible catalytic activities towards the ring-opening polymerization (ROP) of *rac*-lactide. The switch between the two different oxidation states of complex **1.6** was realized by chemical redox agents, silver triflate (AgOTf) in CH_2Cl_2 as the oxidant and decamethylferrocene ($FeCp^*_2$) as the reductant.[9]

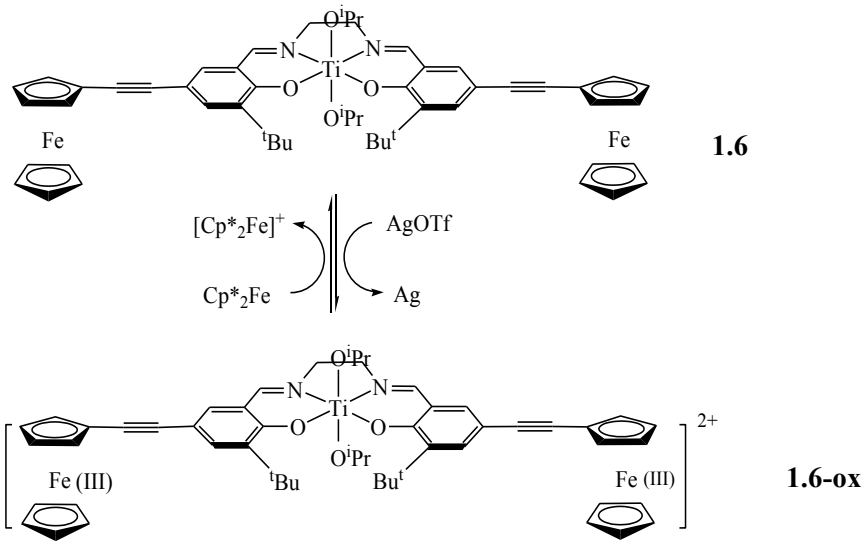

Figure 1.12. Scheme of the redox switches of complex **1.6/1.6-ox**[x]

Analysis of the conversion data (figure 1.13a) indicates that the non-oxidized ligand supports an approximately 30 times more rapid polymerization, suggesting that the titanium centre bearing a more electron-withdrawing ligand framework offers a slower rate of the ROP of *rac*-lactide. The redox behaviour of the ligand is clearly shown to relay an electronic effect to the titanium centre.

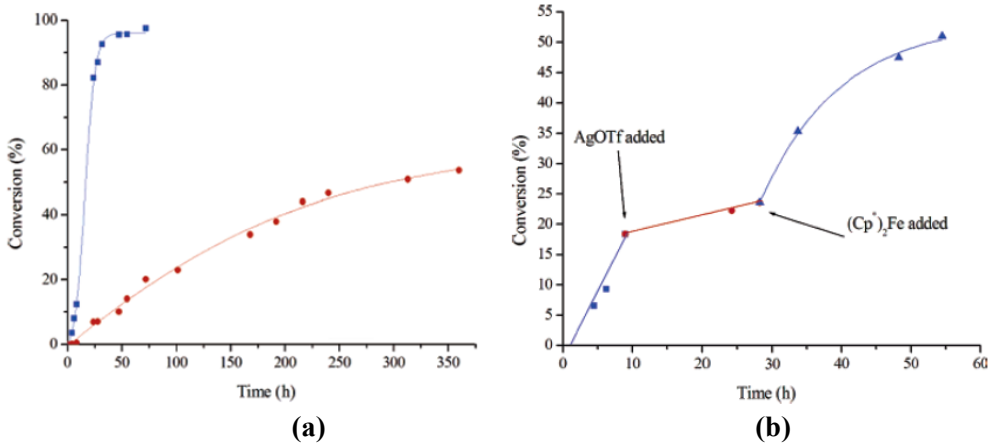

Figure 1.13. (a) Plots of the consumption of *rac*-lactide versus time for complex **1.6** in both states of charge[xi] (b) A plot of conversion versus time for the polymerization of *rac*-lactide during *in situ* oxidation and reduction of complex **1.6** (toluene, 70 °C, 1 mol % catalyst load)

[x] Figure 1.12 is adapted from reference 9.

[xi] Figure 1.13 is taken from reference 9.

In order to demonstrate a genuine switching effect, the reversible nature of the redox activity of complex **1.6** in this catalytic polymerization has also been investigated. As plotted in figure 1.13b, a 18% conversion of the reaction was afforded by **1.6** after 8 hours. At this point, AgOTf was added to oxidize the ferrocenyl substituents on the ligand backbone to their ferrocenium counterparts, and a marked decrease in the conversion of monomer was observed. After a further 20 hours, Cp^*_2Fe was added for the re-formation of the neutral ligand, which was accompanied by a corresponding increase in the catalytic activity of the complex.

As neither AgOTf nor $FeCp^*_2$ afforded any polymerization activity under comparable conditions, this return in catalytic activity to approximately the same magnitude as that observed prior to oxidation confirmed the redox shuttle between **1.6** and **1.6-ox**. All these results suggest that remote redox-active ligand substituents may be exploited to control the activity of the metal centre, again giving evidence that redox couples can be used to oscillate a catalyst between sites of differing activities. This work is recognized as a significant advance as for the first time the application of redox switchable catalysts in single-site polymerization catalyst technology was demonstrated.

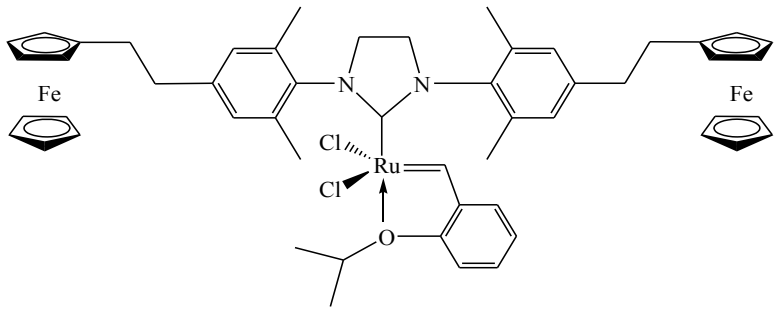

Figure 1.14. Structure of the diferrocenyl-tagged Grubbs-Hoveyda type catalyst[xii]

In efforts to develop further chemistry in this area, compounds capable of reversible processes have also been studied in other research institutes. For instance, the ruthenium complex shown in figure 1.14 was reported by Süβner and Plenio to be an olefin -metathesis homogeneous catalyst of the Grubbs-Hoveyda type bearing a diferrocenyl redox-active ligand. The solubility of the complex can be tuned by switching between Fe^{II}/Fe^{III} of the ferrocenyl moieties, which is consequently referred to as the solubility-determining redox-active tag.[4]

[xii] Figure 1.14 adapted from reference 4.

The data in figure 1.15 describe the catalytic reactivity of the ruthenium complex in the ring-closing metathesis (RCM) reaction of N-tosyldiallylamide. The neutral complex catalyzed the reaction to completion in toluene by itself, while the oxidized complex lost its catalytic activity towards the reaction as it precipitated out of solution. The oxidized catalyst can be readily separated from the reaction mixture or the crude product, recycled by filtration and reactivated with full restoration of catalytic activity by chemical reduction.

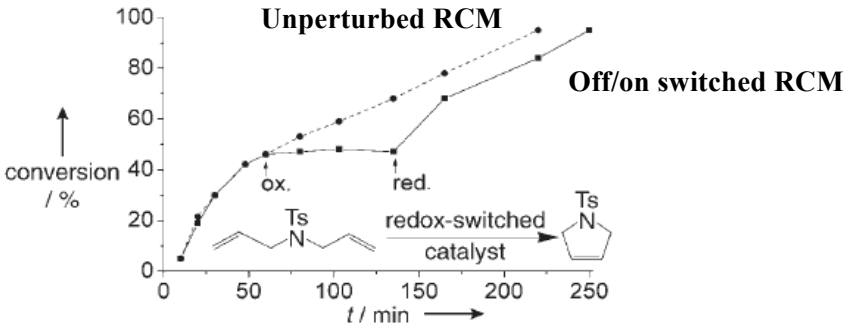

Figure 1.15. Switching of the ruthenium-catalyzed RCM reaction of N-tosyldiallylamide in toluene (Ts = *p*-toluenesulfonyl)[xiii]

Again, switching of the catalytic activities of the transition metal complex was realized *via* ligand-based redox processes. However, in this case the electronic effect on ruthenium caused by oxidation was unclear, as the loss of activity of the oxidized catalyst was due to it becoming insoluble in the homogeneous catalytic system. It would be more interesting to see the control of a redox-active ligand on the electronic properties of the metal centre.

More recently, in 2011, successful redox control of ROP of *L*-lactide and trimethylene carbonate was realized by the use of ferrocene-derived late transition metal complexes. Figure 1.16 shows the yttrium (**1.7**) and indium (**1.8**) complexes bearing the same ligand 1,1'-di(2-*tert*-butyl-6-diphenylphosphiniminophenoxy)ferrocene), which can alter the electronic environments of the central metals by undergoing Fe^{II}/Fe^{III} redox processes. The yttrium redox partners **1.7/1.7-ox** were found to be capable of controlling the ROP of *L*-lactide, and **1.8/1.8-ox** were observed to possess different catalytic activities towards the ROP of trimethylene carbonate.[11]

[xiii] Figure 1.15 taken from reference 4.

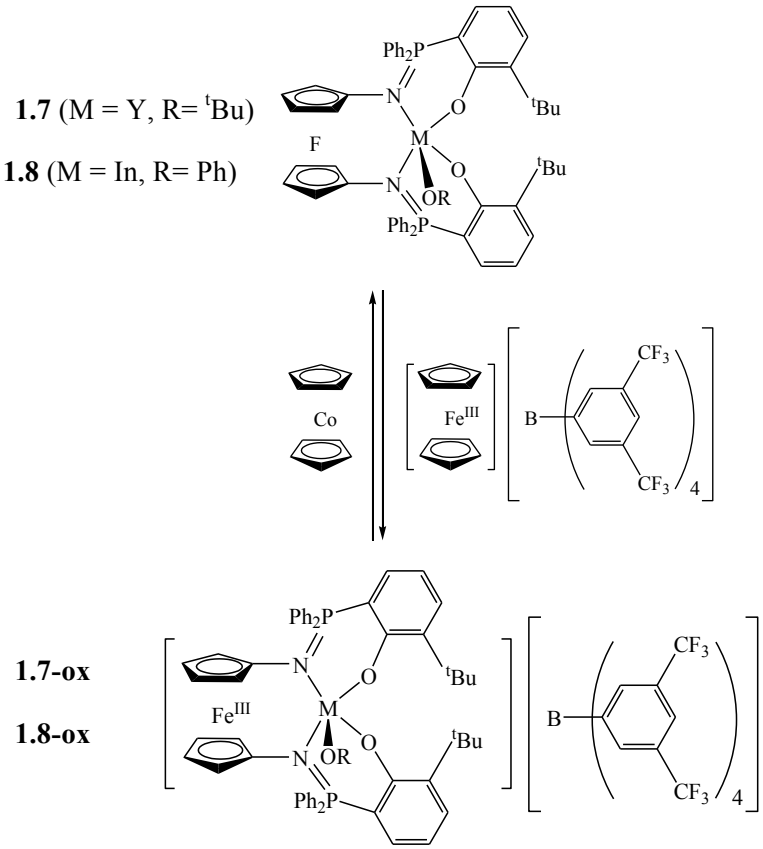

Figure 1.16. Scheme describing the redox behaviour of **1.7** and **1.8**[xiv]

The ROP of *L*-lactide catalyzed by the yttrium redox switches was first described. While a high conversion of 74% was given by **1.7** in 3 hours at room temperature, no conversion was observed in the presence of **1.7-ox**. Polymerization with the catalyst switched *in situ* between its oxidized and reduced states was also performed under the same conditions (figure 1.17). After 1 hour, the polymerization with **1.7** reached 24% conversion, but then halted upon the oxidation of the catalyst. Once the reductant was added to the reaction mixture, the polymerization resumed with the same rate as that before the switch was performed. The same redox switch cycles were then repeated for three consecutive times, and only minimal change in the rate of the reaction was observed. The lack of activity of **1.7-ox** was then investigated by carrying out a stoichiometric reaction of **1.7-ox** and *L*-lactide, and the formation of a new species which is unreactive toward further polymerization was found to be the explanation.

[xiv] Figure 1.16 adapted from reference 11.

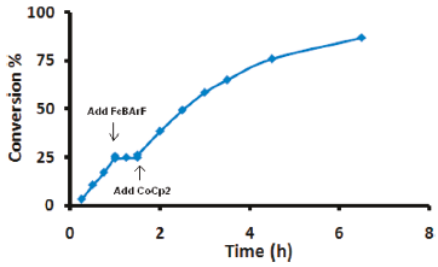

Figure 1.17. Plot of conversion versus time for the ROP of *L*-lactide with **1.7** oxidized and reduced *in situ* (rt, THF, 1 mol% catalyst load)[xv].

This fact that the oxidation of the redox-active ligand decreases the rate of the ROP of *L*-lactide is consistent with the observation by Gregson and coworkers in their work on the ROP of *rac*-lactide.[9] However, a reverse effect was developed by using the redox switches of **1.8/1.8-ox** to catalyze the ROP of trimethylene carbonate, which was carried out in benzene-d_6 at room temperature with 1 mol% catalyst load. After 1 day, while the reaction catalyzed by **1.8-ox** reached 49% conversion, **1.8** afforded only 2% conversion. These results suggest that a decrease in the electronic density at the indium centre through the oxidation of the chelating ligand increased the rate of ROP of trimethylene carbonate. Therefore, the metal dependency on the redox control on polymerization by the redox-functionalized ligand was discovered.

1.4. Electrochemistry and Chemical Redox Agents

1.4.1. Cyclic voltammetry

Before initiating the investigations on what the effects of redox behaviour of a redox -active compound would have on its catalytic activities, it is necessary to choose an appropriate chemical redox agent by first ascertaining the oxidative potential of the compound. The electrochemical characterizations of redox-active compounds are usually carried out using cyclic voltammetry. The cyclic voltammograms (CV) are produced by first dissolving a small amount of the test compounds in a suitable solvent with a suitable

[xv] Figure 1.17 taken from reference 11.

electrolyte. The dilute solutions are then placed in an electrochemical cell equipped with a working electrode, a counter/auxiliary electrode and a reference electrode.[102] For the electrochemical experiments of the ferrocene-based ligands and complexes prepared in this project, tetrabutylammonium hexafluorophosphate (TBAP) was used for the electrolyte, a platinum disk (Φ = 25 μm) was chosen for the working electrolyte, a silver wire (Φ = 1 mm) for the reference electrode, and a platinum coil (Φ = 1 mm) for the counter electrode.

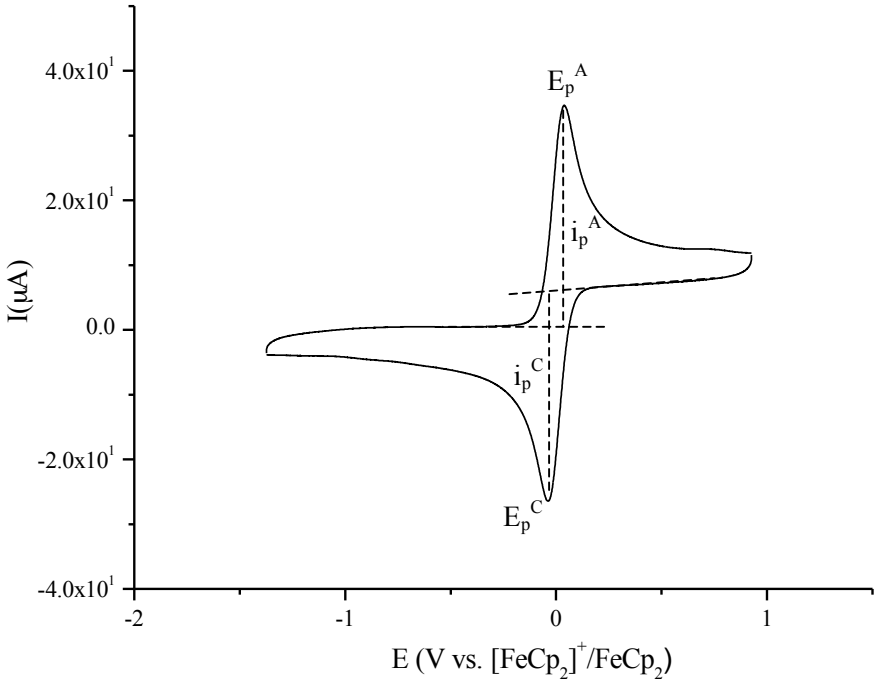

Figure 1.18. Cyclic voltammogram of ferrocene

(10 mM in MeCN with 0.1 M TBAP, rt, scan rate: 50 mV/s)

Ferrocene derivatives are ideal for electrochemical study as ferrocene has a reversible one electron Fe^{II}-Fe^{III} redox process between ferrocene and ferrocenium. The redox properties of the ferrocenyl compounds can be affected by changes in the electron density on the iron centre caused by inducing different substituents on the cyclopentadienyl rings, giving an impact on the observed redox potential. Figure 1.18 shows the cyclic voltammogram of ferrocene produced by a 0.1 M solution of ferrocene in acetonitrile.

E_p^A is the anodic potential, where the oxidation occurs and the oxidation current reaches

its peak value (i_p^A). E_p^C is, on the opposite, namely the cathodic potential at which the reduction occurs and the reduction current reaches its peak value (i_p^C). ΔE_p is a measure of reversibility ($\Delta E_p = E_p^A - E_p^C$), and $E_p^{1/2}$ is the half wave redox potential ($E_p^{1/2} = 1/2\Delta E_p + E_p^C = E_p^A - 1/2\Delta E_p$). The redox potential and the reversibility of the redox process(es) of a certain compound can be extracted from these important parameters, giving a measure of how readily the compound oxidizes.[102]

The reversibility of a redox process is also affected by the relative rates of electron transfer to and from the redox species at the electrode vs. the diffusion of the compound from and to the electrode in that particular solution. An electrochemically reversible process is realized when the rate of electron transfer is much faster than the diffusion process. In a cyclic voltammogram, this reversibility manifests itself in several ways including the ratio of peak currents resulting from oxidation and reduction (i_p^A / i_p^C), the distance in potential between the redox peaks (ΔE_p), and the changes on the values of peak position (E_p^A, E_p^C) and peak current (i_p^A, i_p^C) caused by using different scan rates.

For a completely reversible one electron redox process at room temperature, ΔE_p is approximately 59 mV, and the peak potentials are independent of sweep rate. The maximum reduction current and oxidation current are equal to each other ($i_p^A / i_p^C = 1$), and these peak currents are both proportional to the square root of the scan rate ($i_p \propto v_s^{1/2}$). It is worth mentioned here that regardless of the reversibility of a particular process, the peak currents depend on the voltage sweep rate.

However, in reality a theoretically reversible system is hard to achieve as the electron transfer is not ideally efficient. Usually a larger separation between the redox peaks (a greater ΔE_p value) can be observed when increasing the sweep rate, because there is less responding time for the system towards the changes in the potential. Also, a system that is reversible at low scan rates may even become irreversible under fast sweep if the electrode kinetics are too slow for the concentrations to adjust to equilibrium values.

The term ‘quasi-reversible’ is used for a system lying between the limiting cases of ‘reversible’ and ‘irreversible’, where the surface concentrations of the oxidized and reduced species on the electrodes of interest depend on both the electron transfer rates and the rate of mass transport.[102] Thus, in a quasi-reversible system, the reversibility is dependent on the

sweep rate: ΔE_p is greater than 59 mV and this separation of the peaks varies with different scan rates; a similar but not same size of the peak for reduction relative to the peak for oxidation can be observed, and the peak current also varies with $v_s^{1/2}$, but is not proportional to it.

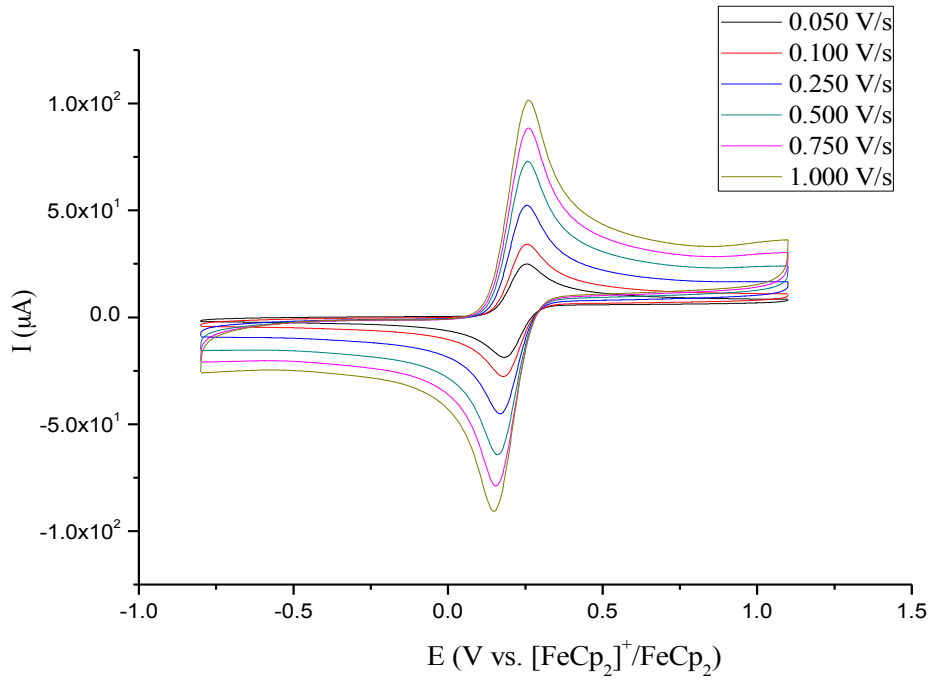

Figure 1.19. Cyclic voltammogram of ferrocene at different scan rates

(0.1 M in MeCN, potential window: -0.8 V ~ 1.1 V)

An example of the 'quasi-reversible' system of ferrocene in acetonitrile is shown in figure 1.19. The voltage between the platinum disk and the counter electrode was set between -0.800 V and 1.100 V, and the scan rate between 0.050 V/s and 0.100 V/s. The resulting current was measured three times at each scan rate, and the current cycles for the last sweeps for each scan rate were then selected as the plots in the cyclic voltammogram. All the useful data is listed in the table in figure 1.20. ΔE_p is larger than 59 mV, increasing in its value with the increase of the sweep rate. $E_{1/2}$ varies slightly at different scan rates, and the peak current values at each particular sweep rate are almost equal ($i_p^A / i_p^C \approx 1$). The linear relationship of the peak currents (i_p^A and i_p^C) to the square root of the sweep rate after linear correction is also shown in figure 1.20.

v_s (V/s)	E_p^A (V)	E_p^C (V)	ΔE_p (V)	$E_{1/2}$ (V)	i_p^A (10^{-5} A)	i_p^C (-10^{-5} A)	i_p^A / i_p^C
0.050	0.257	0.179	0.078	0.218	2.413	2.418	0.998
0.100	0.257	0.178	0.079	0.218	3.357	3.357	1.000
0.250	0.256	0.171	0.085	0.214	5.170	5.158	1.002
0.50	0.257	0.162	0.095	0.210	7.191	7.126	1.009
0.750	0.259	0.153	0.106	0.206	8.655	8.636	1.002
1.000	0.261	0.150	0.111	0.206	9.857	9.819	1.004

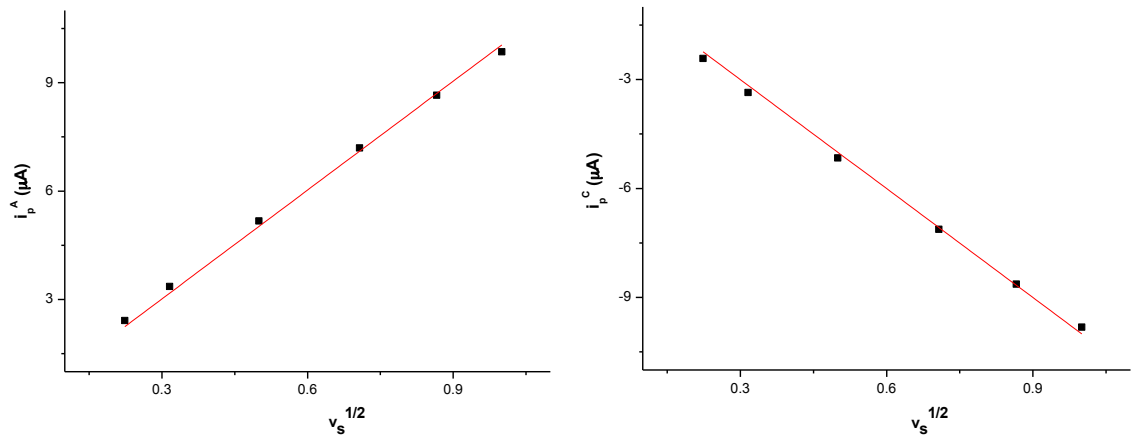

Figure 1.20. Table of the electrochemical data acquired and linear relationship of i_p to $v_s^{1/2}$ after linear correction

1.4.2. Ferrocenium hexafluorophosphate as oxidant

All the redox processes in this thesis were realized *via* chemical reactions of the compounds to be oxidized/reduced and suitable redox reagents. Despite the disadvantages of chemical redox agents compared to electrochemical approaches, such as uncertainty on the purity and stability of the reagents and the formation of byproducts as the result of chemical reactions,[103] this method avoids the use of large amounts of electrolyte(s), which could bring more difficult purification problems. Besides, rapid large-scale preparations would be more easily done by simply mixing the substrate and the redox agent in solution than working with complicated electrochemical devices.

Therefore, finding the appropriate chemical reagents is crucial to obtain the desired redox couples. As this work is largely related to ferrocene, ferrocene or other metallocene based redox agents were first taken into consideration.

The ferrocenium ion is a mild one-electron oxidant which engages usually in an outer -sphere electron-transfer reaction.[104-107] It is readily available as salts of a variety of counter anions including the most commonly used $[BF_4]^-$ and $[PF_6]^-$, and these air-stable salts can be made quite easily from cheap precursors.[108, 109] The byproduct generated from the oxidation by ferrocenium salts is simply ferrocene, which is fairly inert and can be easily removed by washing the product with a non-polar solvent such as n-hexane.

However, complete removal of excess ferrocenium salts from an oxidized ionic product is rather difficult. Ferrocenium ion was electrochemically detected by Connelly and Geiger in a product whose purity has been confirmed by elemental analysis.[103] This problem is often solved by using the stoichiometric amount or even less than one equivalent of the oxidant,[110] but the separation of the substrate and product is then required. The oxidized compounds in this project are transition metal complexes, which decompose during column chromatography, thus a difference in the solubility between the redox switches is desired so that the product can be purified *via* washing or recrystallization. This change in the solubility after oxidation depends on both the solvent and the counter anion. As the metal complexes cannot dissolve in non- or low polar solvents, ferrocenium salts with a suitable anion must be found to further decrease the solubility of a certain complex after oxidizing it.

$[FeCp_2][PF_6]$ was selected to be the ideal oxidant because of its availability and solubility. $[FeCp_2][PF_6]$ and $[FeCp_2][BF_4]$ are the only two ferrocenium salts that are commercially available. $[FeCp_2][PF_6]$ is cheaper, soluble in chlorinated solvents like CH_2Cl_2 and $CHCl_3$, but poorly soluble in other organic solvents, while $[FeCp_2][BF_4]$ is soluble in most of the common polar solvents including THF, MeOH, and MeCN. As $[FeCp_2][PF_6]$ has manifested itself in numerous different cases to be an excellent oxidant for transition metal complexes,[111-113] the anion of $[PF_6]^-$ was then thought to be a better counter anion for ferrocenium ion since it decreases the solubility of ferrocene after oxidation to ferrocenium much more than $[BF_4]^-$ does.

In principle, the reversibility of the $[FeCp_2]^+/[FeCp_2]$ redox couple suggests that the

ferrocenium ion can be used to oxidize only substrates with oxidation potentials higher than that of ferrocene. Although the oxidation potential of the ferrocenium ion can be improved by ring substitution with electron-withdrawing groups,[114, 115] the stability of these modified ferrocenes, which are prepared *via* ring-substitution of ferrocene followed by oxidation, is not as ideal as the ferrocenium salt.[116] The preparation of substituted ferrocenyl oxidant, however, can be avoided when the oxidation process of the substrate is irreversible.[117, 118] When the product distribution is not governed by the Nernst equation, the driving force of the chemical reaction can lead to the oxidation of substrates with higher oxidation potential than the ferrocenium ion.[103]

1.5. Palladium-catalyzed Carbonylation of Aryl Halides

In order to study the redox control of metal complexes bearing redox-active ligands in catalysis, suitable catalytic processes has to be found. Classic catalytic reactions are preferred as their mechanisms have been well-studied, and thus make it easier to explain the 'redox switching' that can possibly be realized. Among the well-established transition metal catalyzed processes, the rhodium-catalyzed hydrogenation[6] and the nickel-catalyzed cross -coupling reactions[5] have been previously introduced as the catalytic applications of redox -active ligands. Nonetheless, the classic palladium-catalyzed processes, among which the 2010 Nobel Prize in Chemistry was awarded for palladium-catalyzed cross-coupling, present ideal candidates for redox-controlled catalysis. Since the palladium-catalyzed carbonylation reactions of aryl halides is also one of the research topics in our laboratory, the synthesis of redox-active palladium catalysts and their applications in carbonylation processes were taken as a significant part of this project.

Carbonylation reactions have found significance in synthetic organic chemistry,[121] and are increasingly favoured in pharmaceutical chemistry for the atom-efficient introduction of carbonyl centres.[122] The palladium-catalyzed carbonylation of aryl halides was first established by Richard Heck in the 1970s. In his reports, Heck described these reactions as the formation of acylpalladium intermediates, which are then attacked by a nucleophile to eventually form the products (figure 1.21).[123-125]

Base is generally required in these reactions to reduce the Pd(II) catalyst precursors to Pd(0) active species that actually initiates the reaction, to deprotonate alcohols or amines or by other chemical processes to generate nucleophiles (Nu:), and to react with acid (HX) generated in the reaction.[126] Products of these reactions, which depend on the types of the nucleophiles, can be carboxylic acids (hydroxycarbonylation reaction), carboxylate esters (alkoxycarbonylation), amides (aminocarbonylation), aldehydes (reductive carbonylation), and ketones (carbonylative cross-coupling).[127] This review will focus on alkoxycarbonylation and aminocarbonylation reactions catalyzed by palladium complexes.

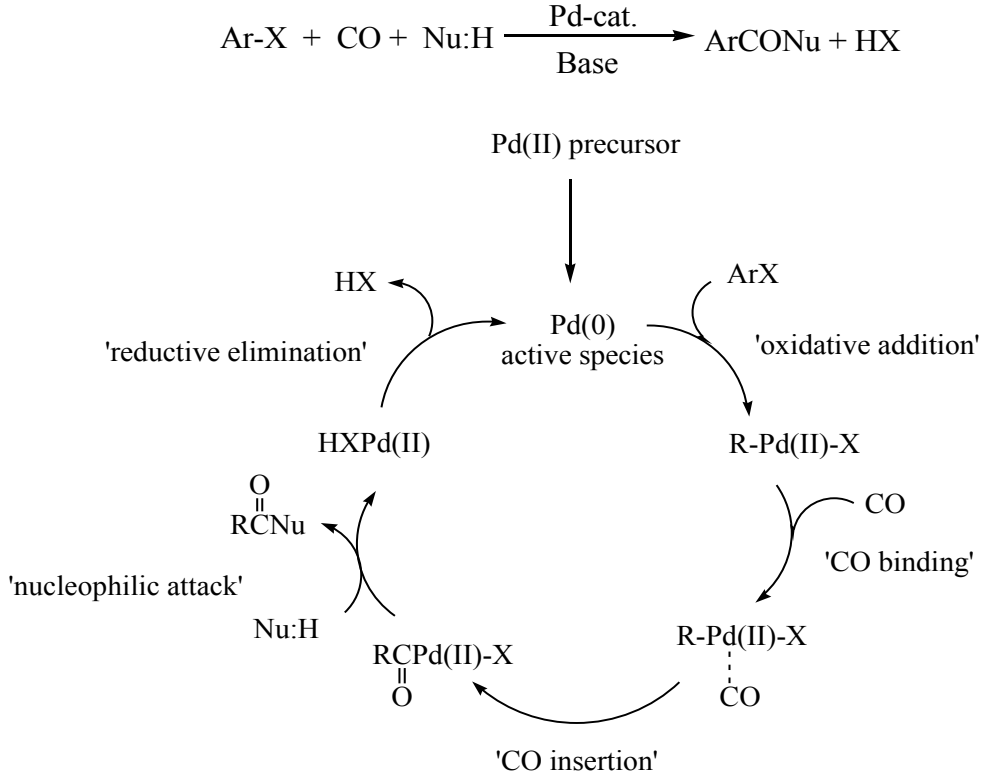

Figure 1.21. General reaction scheme and catalytic cycle for palladium-catalyzed carbonylation of aryl halides[xvi]

1.5.1. Mechanisms

Quantities of mechanistic studies have been carried out on carbonylation reactions and yet some uncertainties and disagreements still remain regarding the 'rate-determining step', as

[xvi] Figure 1.21 and 1.23 adapted from reference 5.

well as the later steps of the mechanism. This is inevitable due to the complicated nature of the carbonylation reaction, which includes the following aspects: (a) the electronic and steric effects of the ligands of the catalyst precursor; (b) the concentration and type of the base, which affects the concentration of the nucleophilic anion and influences the reductive elimination of HX from Pd; (c) the choice of halide, the electronic and steric properties of the substrate; (d) the solvent effect on the stabilization of transition states and charged intermediates; and (e) the actual pressure of carbon monoxide (CO) and the presence of other potential ligands.[128] Therefore, it is usually not reasonable to extend the conclusions of the research study on one particular carbonylation reactions to others. In some cases, conflicting conclusions may be drawn from studies involving different substrates or catalysts.[129, 130]

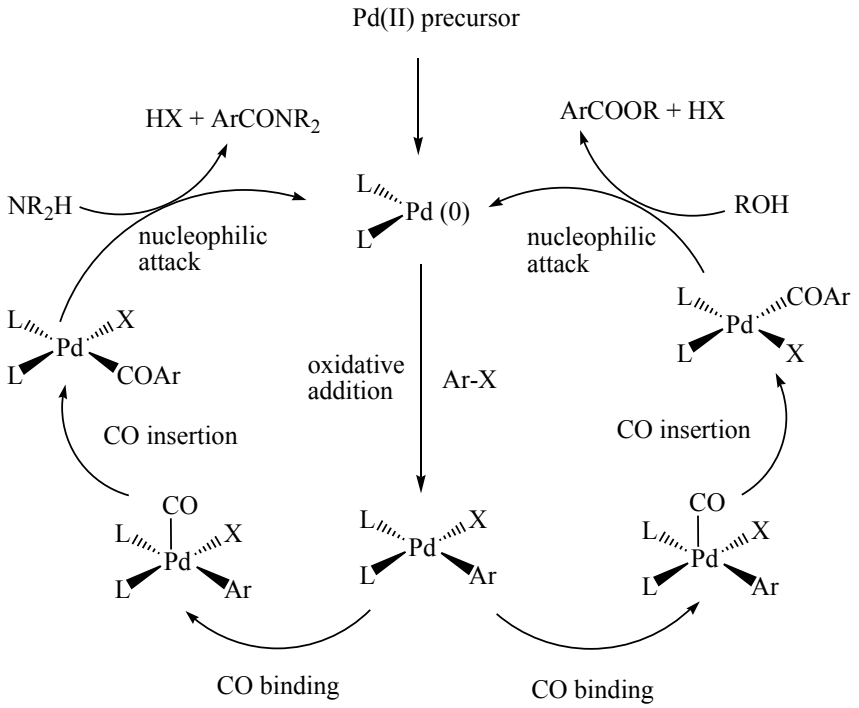

Figure 1.22. Simplified mechanisms for alkoxycarbonylation and aminocarbonylation[xvii]

Mechanisms for palladium-catalyzed alkoxycarbonylation and aminocarbonylation of aryl halides are shown in Figure 1.22, demonstrating the main steps in a catalytic cycle: (I) formation of catalytically active Pd(0) species; (II) oxidative addition of aryl halide to the palladium centre; (III) the binding of CO with palladium intermediate; (IV) carbonyl insertion;

[xvii] Figure 1.22 and 1.24 adapted from reference 122.

(V) nucleophilic attack on the palladium centre and formation of the product, which is followed by the return of the Pd(0) initiator. An alternative for steps III and IV is nucleophilic attack on the CO coordinated with palladium to form a carbamate or carboxylate ligand, followed by reductive elimination for product release.[126] Each of these steps will be further discussed in detail.

(I) Catalyst Formation

Palladium catalysts for carbonylation reactions can be either obtained from pre-formed complexes, or prepared *in situ* using simple commercially available palladium sources and the desired ligands. Many of the palladium compounds suitable for carbonylation are Pd(II) catalyst precursors, which have to be reduced to catalytically active Pd(0) species to initiate the reaction. This step is often influenced by the base and the presence of excess ligand.

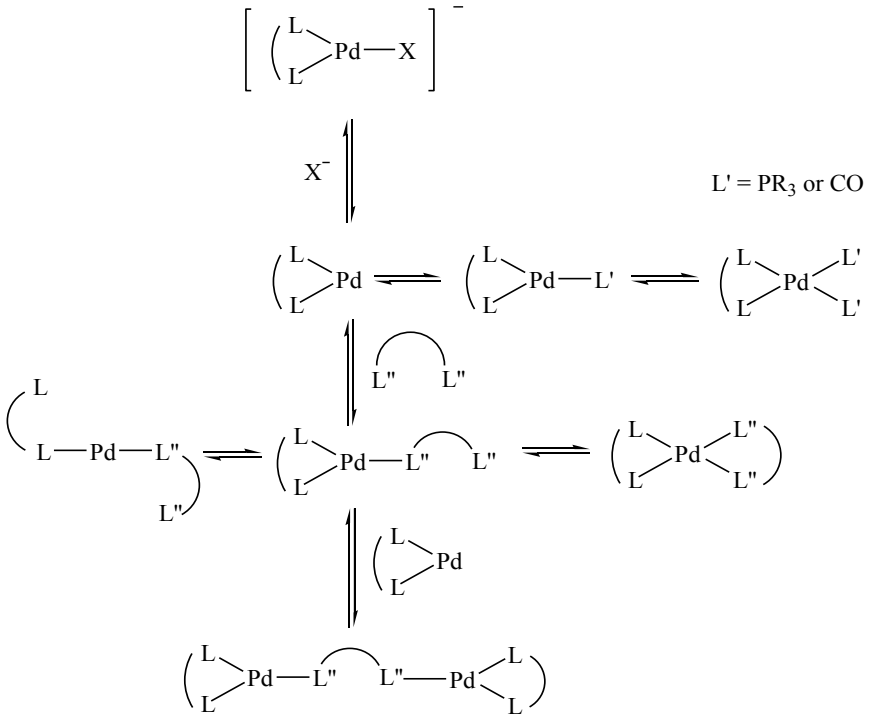

Figure 1.23. Precatalytic equilibria for PdL_2 systems[xviii]

The reactive 14-electron Pd(0) species will be in equilibrium with carbonyl Pd(II) species and anionic species in the reaction system.[131] The carbonyl group reduces the electron

[xviii] Figure 1.23 adapted from reference 121.

density of the metal centre by back-bonding of d-electrons of palladium. Therefore, these carbonyl species are generally not active for oxidative addition.[132] For bidentate diphosphine ligands, the equilibria become more complicated with the involvements of anion, CO and phosphines (figure 1.23). The amount of palladium available to the catalytic cycle can be significantly diminished by these equilibria, for instance, under high pressures of CO. Additional ligands affect these equilibria with electronic and steric factors, thus influencing the catalytic activity of the palladium. Osborn observed that a noticeably narrow range for phosphine cone angle of 160-180° was necessary for good catalytic conversions.[133]

Therefore, increase of the CO pressure can result in shifts of the equilibria of the Pd(0) species towards additional CO coordination to palladium, and thus deactivates the palladium species towards further interactions.

(II) Oxidative Addition

The oxidative addition of aryl halides to Pd(0) species is believed to be the very first step of the catalytic cycle for most palladium-catalyzed synthetic organic reactions.[134] As this transformation is also vital in other coupling chemistry, the oxidative addition step has been thoroughly investigated in both theoretical and experimental studies.[135]

Increase in electron density on the palladium centre reduces the activation energy for the formation of the Pd(II) organometallic intermediate.[136-138] As a consequence, while the aryl-substituted phosphines can be used as suitable ligands for the carbonylation of aryl iodides and bromides, alkyl-substituted phosphines, as stronger electron-donating ligands, are required to promote the oxidative addition of aryl chlorides. Oxidative addition was reported by Milstein to be the rate limiting step for the carbonylation of aryl chlorides,[139, 140] but this conclusion was then defeated by Osborn.[133]

In studies of palladium-catalyzed coupling mechanisms it has been shown that bulky electron-rich alkyl phosphines significantly accelerates oxidative addition,[141] which is another factor behind the limiting cone angle values observed by Osborn. It has also been shown that when oxidative addition occurs readily and is not the rate-limiting step, then carbonylation reactions favour catalysts with less electron density on palladium.[142]

(III) CO Binding

The introduction of CO into the coordination sphere of palladium takes place right after the formation of aryl-halo palladium species. This step has proved to be highly sensitive to steric factors of the substrate, as it is a rapid reaction for simple phenyl-halo palladium complexes, but can be rate limiting when the coordination of CO to palladium is hindered by steric factors.[122]

A good example of sterically hindered CO binding is shown in figure 1.24, which illustrates the difficulties in the attempts to carbonylate 2-bromo-m-xylene. In this sterically constrained environment, the aryl group lies in the vertical plane orientating the two methyl groups into positions close to the axial binding sites of palladium, which is the access for the coordination of CO. In this case, both of the coordinating sites for CO are restricted, and CO binding is thereby strongly inhibited. Consequently, after oxidative addition of 2-bromo-*m*-xylene to palladium, reductive elimination becomes the dominating activity, and thus leads to the formation of *m*-xylene as the major product.[122]

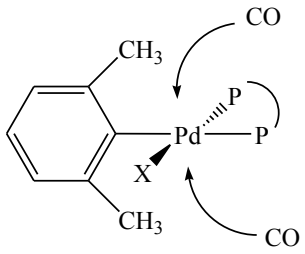

Figure 1.24. Steric influence on the binding of CO with palladium[122]

(IV) Carbonyl Insertion / Nucleophilic attack at CO

According to the initial work on carbonylation by Heck, the next step in the cycle is the combination of *cis*-related carbonyl and aryl groups, leading to the formation of palladium acyl species. The low reactivity of $[PdCl(COMe)(PPh_3)_2]$ with iodobenzene[143] was taken by Hidai as strong evidence for the carbonyl insertion route.[144] Other evidence for the rapid carbonyl insertion step at room temperature was also obtained by Milstein[139, 140] and Chatt.[145] As demonstrated by Moser[146] for $[PdBr(COPh)(PPh_3)_2]$ and Milstein[147] using ^{13}CO and $[PdCl(COCH_2Ph)(PMe_3)_2]$, the formation of the acylpalladium intermediate is irreversible in most cases. However, Osborn[133] reported a reversible carbonyl insertion in the study of

[PdCl(COPh)(PCy_3)$_2$], which again emphasizes the significant influence of the electronic and steric properties of the phosphine ligand on the reactivity of the palladium intermediate in the carbonylation process.

The possibilities of direct formation of the acyl palladium species from the five-coordinate trigonal intermediate [PdAr(X)(CO)(PR_3)$_2$] and indirect formation from the square-planar four-coordinate species [PdAr(X)(CO)(PR_3)] generated *via* the dissociation of one phosphine ligand, which is inhibited by the presence of excess phosphines, have both been considered by Heck.[142] As the carbonyl insertion step requires *cis* location of the carbonyl and aryl groups, the two structures that are most likely to be adopted by the five-coordinated palladium intermediate formed *via* CO binding, as well as the equilibrium between the five- and four-coordinate intermediates, are shown in figure 1.25. For bidentate ligands, the stability of the chelating ring strongly affects this equilibrium, which explains the trend of reactivities of the diphosphines (C_3 >> C_4 > C_2) observed by Milstein.[139, 140]

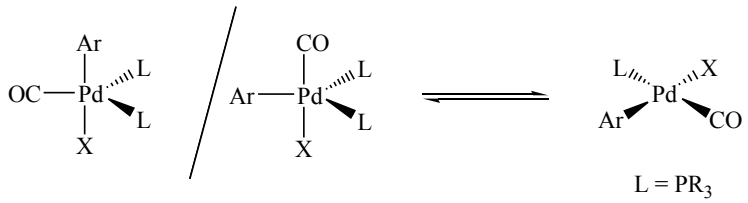

Figure 1.25. Scheme of the equilibria of the trigonal intermediates for carbonyl insertion step and their ligand dissociation product[xix]

The rate of the carbonyl insertion step can be altered by the strength of the Pd-carbonyl and Pd-aryl bonds. As the back-bonding of d-electrons from palladium to its ligands is involved in both of these bonds, this back-donation is much more pronounced for the Pd-carbonyl bonds. Increased electron density on palladium caused by the introduction of alkyl-substituted diphosphines results in a stronger back-bonding effect, and therefore slower carbonyl insertion. Therefore, for reactions where the oxidative addition is not the rate determining step, aryl-substituted diphosphines often give faster reactions than their corresponding alkyl analogues.[142]

[xix] Figure 1.25 adapted from reference 142.

In the meantime, steps after oxidative addition could proceed *via* an alternative route. Proposed by Yamamoto, in some cases the carbonyl ligand is attacked by the nucleophile, generating a carbamate or carboxylate ligand, and the product is then formed from reductive elimination of the aryl group and carbamate or carboxyl ligand.[148, 149] Investigations of this reductive elimination indicate that this step occurs after initial dissociation of one neutral ligand, leading to a trigonal transition state.[150]

(V) Nucleophilic Attack

Carbonylation product generation from the reaction of the acyl palladium intermediate and the nucleophile then occurs either by direct nucleophilic attack at the acyl carbon or by initial bonding of the nucleophile to the palladium centre. The former route was suggested by Heck in his initial work and is believed to be dominant for most alkoxy-/aminocarbonylation reacions.[123-135] Nonetheless, the kinetic study by Yamamoto on $[PdI(Ph)(PPh_3)_2]$ supports the latter mechanism.[151] Yamamoto suggested that there may be significant differences in the catalytic cycles between aryl iodide and bromide substrates, and between amino- and alkoxy-products.[152] He proposed that the aminocarbonylation products are formed *via* the carbamoyl intermediate $[PdAr(CONR_2)L_2]$ rather than $[PdX(COAr)L_2]$ suggested by Heck; and for the products of alkoxycarbonylation formed *via* the common iodide intermediate $[PdI(COAr)L_2]$, it is the binding of the alkoxide group to palladium that precedes the reductive elimination rather than nucleophilic attack on the acyl ligand.

As described above, there are many features and pathways involved in the mechanism of palladium-catalyzed carbonylation of aryl halides, and the amount of the catalytically active species is affected by various equilibria involving coordination of excess ligands or carbonyls. All of these factors make it extremely difficult to predict the optimized reaction conditions for any combination of substrate and nucleophile. While some aspects are clear, such as the need for stronger electron donating alkyl-phosphine ligands for the oxidative addition of aryl chlorides and relatively weaker electron donating arylphosphine ligands for the carbonyl insertion of most aryl bromides and iodides, many other factors such as steric effects of the ligands and substrates can have a major influence on these carbonylation reactions.

1.5.2. Conclusion

Palladium-catalyzed carbonylation reactions of aryl halides offer an attractive tool for atom-efficient synthesis. The electronic and steric properties of the ligand used in the palladium-catalyzed carbonylation reactions have been noticed to have an influence on the rate of each step in the catalytic cycle, and thus result in the different catalytic behaviour of the palladium centre. As studies on the use of redox-active ligands to control the reactivity of carbonylation reactions have not been carried out, it would be interesting to see if there is a difference in the catalytic activities of the palladium centre when the ligand is in its different oxidation states.

1.6. Summary and Aims of the Thesis

Redox-active ligands provide a novel tool for controlling the activity and selectivity of transition metal complexes, and thus show great promise in the redox control of transition metal catalysis. Of all the types of redox-active ligands and all their roles in catalytic processes, substitutionally inert redox-active ligands that do not directly interact with the substrate but tune the catalytic reactivities by altering the electronic properties of the central metal *via* ligand based redox processes are of the greatest interest in this project. The chemistry of ferrocene and its application as a redox unit in the redox-active ligand backbone has been well established; similarly the chemistry involved in palladium catalyzed carbonylation of aryl halides has also been well documented.

This project combines these areas through the design and synthesis of ferrocene-based redox-active ligands, the complexation of these ligands mainly to palladium but also other transition metals such as rhodium, electrochemical characterization and chemical oxidation of the complexes. In additional, there are the applications of the non-oxidized and oxidized complexes as catalysts for the alkoxy-/aminocarbonylation of aryl halides and other catalytic processes including rhodium-catalyzed hydrogenation of styrene and Suzuki-Miyaura cross-coupling of aryl bromide.

Hence, chapter 2 describes (i) the successful chemical oxidation of three previously synthesized palladium complexes bearing ferrocene-based diphosphines, whose ligand-based

one-electron reversible redox behaviour has been characterized electrochemically, using ferrocenium hexafluorophosphate as the efficient oxidative agent, and (ii) the investigations on the redox control realized by the three redox switches in alkoxy-/aminocarbonylation reactions of aryl halides (X= Br, I). The synthesis and characterization of a series of new ferrocenyl N-P ligands and their palladium complexes is reported in chapter 3, where the chemical oxidation of the complexes, as well as the comparison of the catalytic activities of these oxidized and non-oxidized complexes towards the alkoxycarbonylation reactions of 2-halobenzylalcohol (X = Br, I) are also addressed. Chapter 4 discusses the synthesis of ferrocene-based diimine ligands which are designed for redox-active palladium catalysts, and their unusual complexation reactions. Also in chapter 4, another important part of this project involves the synthesis of the whole series of mono-/1,1'-dihaloferrocenes (X = F, Cl, Br, I) and the purification of these compounds using an advanced separation method based on the different oxidation potentials of the compounds in a certain mixture. Chapter 5 is concerned with the studies towards the redox control of the palladium-catalyzed Suzuki-Miyaura cross-coupling reaction of phenylboronic acid and 4-bromotoluene, and the rhodium-catalyzed hydrogenation reaction of styrene, supported by the ferrocene unit within the ligands used.

1.7. References

1. Fujiwara, M.; Terashima, S.; Endo, Y.; Shiokawa, K.; Ohue, H. *Chem. Commun.* **2006**, 4635.
2. Ringenberg, M. R.; Kokatam, S. L.; Heiden, Z. M.; Rauchfuss, T. B. *J. Am. Chem. Soc.* **2008**, *130*, 788
3. Magenau, A. J. D.; Strandwitz, N. C.; Gennaro, A.; Matyjaszewski, K. *Science*, **2011**, *332*, 81.
4. Süβner, M.; Plenio, H. *Angew. Chem., Int. Ed.* **2005**, *44*, 6885.
5. Lorkovic, I. M.; Duff, R. R., Jr.; Wrighton, M. S. *J. Am. Chem. Soc.* **1995**, *117*, 3617.
6. Tennyson, A. G.; Lynch, V. M.; Bielawski, C. W. *J. Am. Chem. Soc.* **2010**, *132,* 9420.
7. Liu, G.; He, H.; Wang, J. *Adv. Synth. Catal.* **2009**, *351*, 1610.

8. Slone, C.; Mirkin, C. A.; Yap, G. P. A.; Guzei, I. A.; Rheingold, A. L. *J. Am Chem. Soc.* **1997**, *119*, 10743.
9. Gregson, C. K. A.; Gibson, V. C.; Long, N. J.; Marshall, E. L., Oxford, P. J., White, A. J. P. *J. Am. Chem. Soc.* **2006**, *128*, 7410.
10. Broderick, E. M.; Guo, N.; Wu, T; Vogel, C. S.; Xu, C.; Sutter, J.; Miller, J. T.; Meyer, K.; Cantat, T.; Diaconescu, P. L. *Chem. Commun.* **2011**, *47*, 9897.
11. Broderick, E. M.; Guo, N.; Vogel, C. S.; Xu, C.; Sutter, J.; Miller, J. T.; Meyer, K.; Mehrkhodavandi, P.; Diaconescu, P. L. *J. Am. Chem. Soc.* **2011**, *133*, 9278.
12. Yasuda, T.; Tanabe, K.; Tsuji, T.; Coti, K. K.; Aprahamian, I.; Stoddart, J. F.; Kato, T. *Chem. Commun.* **2010**, *46*, 1224.
13. Kamada, J.; Koynov, K.; Corten, C.; Juhari, A.; Yoon, J. A.; Urban, M. W.; Balazs, A. C.; Matyjaszewski, K. *Macromolecules* **2010**, *43*, 4133
14. Beer, P. D.; Blackburn, C.; McAleer, J. F.; Sikanyika, H.; *Inorg. Chem.* **1990**, *29,* 378.
15. Beer, P. D.; Drew, M. G. B.; Hazlewood, C.; Hesek, D.; Hodacova, J.; Stokes, S. E. *J. Am. Chem. Soc., Chem. Commun.* **1993**, 229.
16. Beer, P. D.; Keefe, A. D.; Sikanyika, H.; Blackburn, C.; McAleer, J. F. *J. Chem. Soc.*, *Dalton Trans.* **1990**, 3289.
17. Mirkin, C. A.; Wrighton, M. S. *J. Am. Chem. Soc*. **1990**, *112*, 8596.
18. Edelman, P. G.; Wang, J. *Biosensors and Chemical Sensors: Optimizing Performance Through Polymeric Materials*; American Chemical Society: Washington DC, 1992.
19. Lyaskovskyy, V.; de Bruin, Bas *ACS Catal.* **2012**, *2*, 270.
20. Kaim, W.; Schwederski, B. *Coord. Chem. Rev.* **2010**, *254*, 1580.
21. Kaim, W. *Coord. Chem. Rev.* **1987**, *76*, 187.
22. Plenio, H.; Diodone, R. *J. Organomel. Chem.* **1995**, *492*, 73.
23. Medina, J. C.; Goodnow, T. T.; Rojas, M. T.; Atwood, J. L.; Lynn, B. C.; Kaifer, A. E.; Gokel, G. W. *J. Am. Chem. Soc*. **1992**, *114*, 10583.
24. Hall, C. D.; Chu, S. Y. F. *J. Organomet. Chem*. **1995**, *498*, 221.
25. Togni, A.; Hayashi, T. *Ferrocenes: Homogeneous Catalysis*, *Organic Synthesis, Material Science*; VCH: New York, 1995.
26. Plenio, H.; Burth, D. *Organometallics* **1996**, *15*, 1151

27. Echegoyan, L. E.; Yoo, H. K.; Gatto, V. J.; Gokel, G. W.; Echegoyan, L. *J. Am. Chem. Soc.* **1989**, *111*, 2440;
28. Echegoyan, L.; Gokel, G. W.; Echegoyen, L. E.; Chen, Z. H.; Yoo, H. *J. Inclusion Phenom. Mol. Recognit. Chem.* **1989**, *7*, 257.
29. Saji, T. *Chem. Lett*. **1986**, 275.
30. Chen, Z.; Gokel, G. W.; Echegoyen, L. *J. Org. Chem*. **1991**, *56*, 3369.
31. Saji, T.; Kinoshita, I. *J. Chem. Soc. Chem*. *Commun*. **1986**, 716.
32. Delavaux-Nicot, B.; Guari, Y.; Douziech, B.; Mathieu, R. *J. Chem. Soc. Chem. Commun.* **1995**, 585.
33. Allgeier, A. M., Mirkin, C.A. *Angew. Chem. Int. Ed.* **1998**, *37*, 894.
34. Kuchynka, D. J.; Kochi, J. K. *Inorg. Chem*. **1988**, *27*, 2574.
35. Gregson, C. K. A.; Blackmore, I. J.; Gibson, V. C.; Long, N. J.; Marshall, E. L. *Dalton Trans.* **2006**, 3134.
36. Lorkovic, I. M.; Wrighton, M. S.; Davis, W. M. *J. Am. Chem. Soc.* **1994**, *116*, 6220.
37. Yeung, L. K.; Kim, J. E.; Chung, Y. K.; Rieger, P. H.; Sweigart, D. A. *Organometallics* **1996**, *15*, 3891.
38. Degrand, C.; Besançon, J.; Radecki-Sudre, A. *J. Electroanal. Chem*. **1984**, *160*, 199.
39. Degrand, C.; Radecki-Sudre, A. *J. Organomet. Chem.* **1984**, *268*, 63.
40. Bugarcic, T.; Habtemariam, A.; Deeth, R. J.; Fabbiani, F. P. A.; Sadler, P. J. *Inorg. Chem.* **2009**, *48*, 9444.
41. Singewald, E. T.; Mirkin, C. A.; Stern, C. L. *Angew. Chem. Int. Ed. Engl*. **1995**, *34*, 1624.
42. Sassano, C. A., Mirkin, C. A. *J. Am. Chem. Soc*. **1995**, *117*, 11379.
43. Allgeier, A. M.; Slone, C. S.; Mirkin, C. A.; Liable-Sands, L. M.; Yap, G. P. A.; Rheingold, A. L. *J. Am. Chem. Soc.* **1997**, *119*, 550.
44. Allgeier, A. M.; Singewald, E. T.; Mirkin, C. A.; Stern, C. L. *Organometallics* **1994**, *13*, 2928.
45. Sembring, S. B.; Colbran, S. B.; Craig, D. C. *Inorg. Chem*. **1995**, *34*, 761.
46. Hayashi, Y.; Osawa, M.; Kobayashi, K.; Wakatsuki, Y. *Chem. Commun*. **1996**, 1617.
47. Sato, M.; Mogi, E.; Kumakura, S. *Organometallics*, **1995**, *14*, 3157.
48. Que, Li.;Tolman, W. B. *Nature* **2008**, *455*, 333.

49. Whittaker, J. W. *Chem. Rev.* **2003**, *103*, 2347.
50. Chaudhuri, P.; Hess, M.; Flörke, U.; Wieghardt, K. *Angew. Chem., Int. Ed.* **1998**, *37*, 2217.
51. Königsmann, M.; Donati, N.; Stein, D.; Schönberg, H.; Harmer, J.; Sreekanth, A.; Grützmacher, H. *Angew. Chem., Int. Ed.* **2007**, *46*, 3567.
52. Wang, K; Stiefel, E. I. *Science* **2001**, *291*, 106.
53. Schauer, P. A.; Low, P. J. *Euro. J. Inorg. Chem.* **2012**, *3*, 390.
54. Dzik, W. L.; de Bruin, B. *Specialist Periodical Report in Organometallic chemistry*; Fairlamb, I. Lymann, J., Eds.; RSC Publishing: Cambridge, 2011.
55. King, E. R.; Hennessy, E. T.; Betley, T. A. *J. Am. Chem. Soc.* **2011**, *133*, 4917.
56. Ringenberg, M. R.; Rauchfuss, T. B. *Eur. J. Inorg. Chem.* **2012**, *3*, 490.
57. Tamao, K.; Sumitani, K.; Kumada, M. *J. Am. Chem. Soc*. **1972**, *94*, 4374.
58. Tamao, K.; Kiso, Y.; Sumitani, K.; Kumada, M. *J. Am. Chem. Soc*. **1972**, *94*, 9268.
59. Hayashi, T.; Konishi, M.; Fukushima, M.; Mise, T.; Kagotani, M.; Tajika, M.; Kumada, M. *J . Am. Chem. Soc.* **1982**,*104*,180.
60. Hayashi, T.; Konishi, M.; Kobori, Y.; Kumada, M.; Higuchi, T.; Hirotsu, K. *J. Am. Chem. Soc*. **1984**, *106*, 158.
61. Muckerman, J. T.; Polyansky, D. E.; Wada, T.; Tanaka, K.; Fujita, E. *Inorg. Chem.* **2008**, *47*, 1787.
62. Boyer, J. L.; Rochford, J.; Tsai, M.-K; Muckerman, J. T.; Fujita, E. *Coord. Chem. Rev.* **2010**, *254*, 309
63. Forum Issure on Redox Non-Innocent Ligands: *Inorg. Chem.,* **2011**, *50,* 9737.
64. van der Vlugt, J. I. *Eur. J. Inorg. Chem.* **2012**, *3*, 363.
65. Dzik, W. I.; van der Vlugt, J. I.; Reek, J. N. H.; de Bruin, B. *Angew. Chem., Int. Ed.* **2011**, *50*, 3356.
66. Dzik, W. I.; Zhang, P. X.; de Bruin, B. *Inorg. Chem.* **2011**, *50*, 9896.
67. Chirik, P. J; Wieghardt, K. *Science* **2010**, *327*, 794.
68. Bouwkamp, M. W.; Bowman, A. C. Lobkovsky, E.; Chirik, P. J. *J. Am. Chem. Soc.* **2006,** *128,* 13340.
69. Smith, A. L.; Hardcastle, K. I.; Soper, J. D. *J. Am. Chem. Soc.* **2010**, *132*, 14358.

70. Smith, A. L.; Clapp, L. A.; Hardcastle, K. I.; Soper, J. D. *Polyhedron* **2010**, *29*, 164.
71. Lippert, C. A.; Riener, K.; Soper, J. D. *Euro. J. Inorg. Chem.* **2012**, *3*, 554.
72. Lippert, C. A.; Arnstein, S. A.; Sherrill, C. D.; Soper, J. D. *J. Am. Chem. Soc.* **2010**, *132*, 3879.
73. Heyduk, A. F.; Zarkesh, R. A.; Nguyen, A. I. *Inorg. Chem.* **2011**, *50*, 9849.
74. Nguyen, A. I.; Zarkesh, R. A.; Lacy, D. C.; Thorson, M. K.; Heyduk, A. F. *Chem. Sci.* **2011**, *2*, 166.
75. Long, N. J. *Metallocenes: An Introduction to Sandwich Complexes*; Blackwell Science: Oxford, 1998.
76. Stepnicka, P. *Ferrocenes: Ligands, Materials and Biomolecules*; John Wiley & Sons Ltd: West Sussex, 2008.
77. Beer, P. D.; Nation, J. E.; Harman, M. E.; *J. Organome. Chem*. **1992**, *441,* 465.
78. Rudie, A. W.; Lichtenberg, D. W.; Katcher, M. L.; Davison, A. *Inorg. Chem.* **1978**, *17*, 2859.
79. Moriuchi, T.; Ikeda, I.; Hirao, T. *Organometallics* **1995**, *14*, 3578.
80. Wolf, M. O.; Wrighton, M. S. *Chem. Mater.* **1994**, *6*, 1526.
81. Mao, F.; Tyler, D. R.; Keszler, D. *J. Am. Chem. Soc.* **1989**, *111*, 130.
82. Mao, F.; Tyler, D. R.; Bruce, M. R. M.; Bruce, A.; Rieger, A. L.; Rieger, P. L. *J. Am. Chem. Soc.* **1992**, *114*, 6418.
83. Carriedo, G. A.; Connelly, N. G.; Perez-Carreno, E.; Orpen, A.G.; Rieger, A. L.; Rieger, P. H.; Riera, V.; Rosair, G. M. *J. Chem. Soc., Dalton Trans.* **1993**, 3103.
84. Bardaji, M.; Brown, N. C.; Connelly, N. G.; Davies, R.; Opern, A. G.; Rosair, G. M.; Seear, N. R. *J. Organomet. Chem.* **1994**, *474*, C21.
85. Atkinson, F. L.; Christofides, A.; Connelly, N. G.; Lawson, H. J.; Lowyns, A. C.; Orpen, A. G.; Rosair, G. M., Worth, G. H. *J. Chem. Soc., Dalton Trans.* **1993**, 1441.
86. Schrock, R. R.; Osborn, J. A. *J. Chem. Soc., Chem. Commun.* **1970**, 567.
87. Schrock, R. R.; Osborn, J. A. *J. Am. Chem. Soc.* **1976**, *98*, 2134.
88. Cullen, W. R.; Kim, T.-J.; Einstein, F. W. B.; Jones, T. *Organometallics.* **1983**, *2*, 714.
89. Cullen, W. R.; Kim, T.-J.; Einstein, F. W. B.; Jones, T. *Organometallics.* **1985**, *4*, 346.
90. Tolman, C. A. *Chem. Rev.* **1977**, *77,* 313.

91. Jacobsen, E. N.; Zhang, W.; Güler, M. L. *J. Am. Chem. Soc*. **1991**, *113*, 6703.

92. Nishiyama, H.; Yanaguchi, S.; Kondo, M.; Itoh, K. *J. Org. Chem.* **1992**, *57*, 4306.

93. Rajanbabu, T. V.; Casalnuovo, A. L. *J. Am. Chem. Soc.* **1992**,*114*, 6265.

94. Rajanbabu, T. V.; Ayers, T. A.; Casalnuovo, A. L. *J. Am. Chem. Soc.* **1994**, *116,* 4101.

95. Wilkinson, G.; Rosenblum, M.; Whiting, M. C.; Woodward, R. B.; *J. Am. Chem. Soc.* **1952**, *74*, 2125.

96. Butler, I. R.,; Cullen, W. R.; Kim, T. -J.; Jones, T.; Einstein, F. W. B. *J. Chem. Soc., Chem. Commun.* **1984**, 719.

97. Gibson, V. C.; Long, N. J.; Marshall, E. L.; Oxford, P. J.; White, A. J. P.; Williams, J. *J. Chem. Soc., Dalton Trans.* **2001**, 1162.

98. Gibson, V. C.; Haliwell, C. M.; White, A. J. P.; Long, N. J.; Oxford, P. J.; Smith, A. M.; Williams, D. J. *J. Chem. Soc., Dalton Trans.,* **2003**, 918.

99. Gibson, V. C.; Gregson, C. K. A.; Haliwell, C. M.; White, A. J. P.; Long, N. J.; Oxford, P. J.; Williams, D. J. *J. Organomet. Chem.,* **2005**, *690*, 6271.

100. Oxford, P. J. PhD Thesis, Imperial College London, 2003.

101. Gregson, C. K. A. PhD Thesis, Imperial College London, 2006.

102. Fisher, A.C. *Electrode Dynamics;* Oxford University Press, 2003.

103. Connelly, N. G.; Geiger, W. E. *Chem. Rev.* **1996**, *96*, 877.

104. Carney, M. J.; Lesniak, J. S.; Likar, M. D.; Pladziewicz, J. R. *J. Am. Chem. Soc.* **1984**, *277*, 113.

105. Connelly, N. G.; Forrow, N. J.; Gracey, B. P.; Knox, S. A. R.; Orpen, A. G. *J. Chem. Soc., Chem. Commun.* **1994**, 2109.

106. Connelly, N. G.; Forrow, N. J.; Gracey, B. P.; Knox, S. A. R.; Orpen, A. G. *J. Chem. Soc., Chem. Commun.* **1985**, 14.

107. Connelly, N. G.; Metz, B.; Orpen, A. G. *J. Chem. Soc., Chem. Commun.* **1985**, 16.

108. Smart, J. C.; Pinsky, B. L. *J. Am. Chem. Soc.* **1980**, *102*, 1009.

109. Hendrickson, D. N.; Sohn, Y. S.; Gray, H. B. *Inorg. Chem.* **1971**, *10*, 1559.

110. Ge, Y. W.; Ye, Y.; Sharp, P. R. *J. Am. Chem. Soc.* **1994**, *116*, 8384.

111. Broadley, K.; Connelly, N. G.; Geiger, W. E. *J. Chem. Soc., Dalton Trans*. **1983**, 121.

112. Ryan, O. B.; Tilset, M. *J. Am. Chem. Soc.***1991**, *113*, 9554.

113. Bianchini, C.; Meli, A.; Peruzzini, M.; Vacca, A.; Laschi, F.; Zanello, P.; Ottaviani, F. M. *Organometallics* **1994**, *13*, 4176.

114. Geiger, W. E. *In Organometallic Radical Processes,* Trogler, W. C., Ed. Elsevier: New York, 1990.

115. Schumann, H.; Lentz, A.; Weimann, R.; Pickardt, J. *Angew. Chem., Int. Ed. Engl.* **1994**, *33*, 1731.

116. Atwood, C. A. PhD dissertation, University of Vermont, 1994.

117. Fonseca, F. M.; Geiger, W. E.; Bitterwolf, T. E.; Rheingold, A. L. *Organometallics* **1988**, *7,* 567.

118. Brammer, L.; Connelly, N. G.; Edwin, J.; Geiger, W. E.; Orpen, A. G.; Sheridan, J. B. *Organometallics* **1988**, *7*, 1259.

119. Luca, O. R.; Crabree, R. H. *Chem. Soc. Rev.* **2013**, *42*, 1440.

120. Praneeth, V. K. K.; Ringenberg, M. R.; Ward, T. R. *Angew. Chem. Int. Ed.* **2012**, *51*, 10228.

121. Skoda-Földes, R.; Kollar, L. *Curr. Org. Chem.* **2002**, *6*, 1097.

122. Barnard, C. F. J. *Org. Process Res. Dev.* **2008**,*12*, 566.

123. Schoenberg, A.; Bartoletti, I.; Heck, R. F. *J. Org. Chem.* **1974**, *39*, 3318.

124. Schoenberg, A.; Heck, R. F.; *J. Org. Chem.* **1974**, *39*, 3327.

125. Schoenberg, A.; Heck, R. F. *J. Am. Chem. Soc.* **1974**, *96*, 7761.

126. Hidai, M.; Hikita, T.; Wada, Y.; Fujikura, Y.; Uchida, Y. *Bull. Chem. Soc. Jpn.* **1975**, *48*, 2075.

127. Brennführer, A.; Neumann, H.; Beller, M. *Angew. Chem.*, *Int. Ed.* **2009**, *48*, 4114.

128. Barnard, C. F. J., *Organometallics* **2008**, *27*, 5402.

129. Beller, M.; Cornils, B.; Frohning, C.D.; Kohlpainter, C. W. *J. Mol. Catal.* **1995**, *104*, 17.

130. Kollar, L. Eds. *Modern Carbonylation Methods*; Wiley: Weinheim, 2008.

131. Amatore, C.; Jutand, A. *Acc. Chem. Res.* **2000**, *33*, 314.

132. Portnoy, M.; Milstein, D. *Organometallics* **1993**, *12*, 1655.

133. Huser, M.; Youinou, M.-T.; Osborn, J. A. *Angew. Chem., Int. Ed. Engl.* **1989**, *28*, 1386.

134. Tsuji, J., *Palladium Reagents and Catalysis: New Perspectives for the 21st Century*; Wiley: Chichester , 2004.

135. Zinovyeva, V. A.; Luo, C.; Fournier, S.; Devillers, C. H.; Cattey, H.; Doucet, H.; Hierso, J.-C.; Lucas, D. *Chem. Eur. J.* **2011**, *17*, 9901.

136. Parshall, G. W. *J. Am. Chem. Soc.* **1974**, *96*, 2360.

137. Amatore, C.; Pfluger, F.; *Organometallics* **1990**, *9*, 2276.

138. Qadir, M.; Mochel, T.; Hii, K. K. *Tetrahedron* **2000**, *56*, 7975.

139. Ben-David, Y.; Portnoy, M.; Milstein, D. *J. Am. Chem. Soc.* **1989**, *111*, 8742.

140. Ben-David, Y., Portnoy, M., Milstein, D., *J. Chem. Soc., Chem. Commun.* **1989**, 1816.

141. Hamann, B. C.; Hartwig, J. F. *J. Am. Chem. Soc.* **1998**, *120*, 7369.

142. Garrou, P. E.; Heck, R. F. *J. Am. Chem. Soc.* **1976**, *98*, 4115.

143. Stille, J. K.; Wong, P. K. *J. Org. Chem.* **1975**, *40,* 532.

144. Hidai, M.; Kolura, M.; Uchida, Y. *J. Org. Chem.* **1973**, *52*, 431.

145. Booth, G., Chatt, J., *J. Chem. Soc. A*. **1966**, 634.

146. Moser, W. R.; Wang, A. W.; Kildahl, N. K.; *J. Am. Chem. Soc.* **1988**, *110*, 2816.

147. Milstein, D. *J. Chem. Soc., Chem. Commun.* **1986**, 817.

148. Ozawa, F.; Sugimoto, T.; Yuasa, Y.; Santra, M.; Yamamoto, T.; Yamamoto, A.; *Organometallics* **1984**, *3*, 683.

149. Ozawa, F.; Sugimoto, T.; Yamamoto, T.; Yamamoto, A. *Organometallics*, **1984**, *3*, 692.

150. Ozawa, F.; Ito, T.; Nakamura, Y.; Yamamoto, A. *Bull. Chem. Soc. Jpn.* **1981**, *54*, 1868.

151. Ozawa, F.; Soyama, H.; Yanagihara, H.; Aoyama, I.; Takino, H.; Izawa, K.; Yamamoto, T.; Yamanoto, A. *J. Am. Chem. Soc.* **1985**, *107*, 3235.

152. Ozawa, F.; Kawasaki, N.; Okamoto, H.; Yamamoto, T.; Yamamoto, A. *Organometallics* **1987**, *6*, 1640.

Chapter 2

Redox Control in Palladium-catalyzed Intra- and Inter-molecular Alkoxy/aminocarbonylation Reactions Supported by 1,1'-bis(Diaryl/alkylphosphino)ferrocenes

众里寻她千百度，蓦然回首，那人却在，灯火阑珊处。

—— 辛弃疾《青玉案》

2.1. Introduction

The modification of ferrocene by phosphine groups has led to a large family of chelating ligands that have found widespread application in homogeneous catalysis.[1-4] Symmetrical ferrocen-1,1'-diyl rigid chelating ligands, especially when the substituents are phosphines, have been of great interest in homogeneous catalysis as they offer a large ligand bite angle and consequently high catalytic activities for their binding metals in certain cases.[5]

In particular, palladium complexes of ligand 1,1'-bis(diphenylphosphino)ferrocene (dppf) exhibit excellent catalytic reactivity for selective cross-coupling reactions.[6,7] After the first report of this novel ligand in 1965, the development of dppf in transition metal-catalyzed organic transformations including Kumada-Hayashi, Suzuki, Heck and Hartwig-Buchwald coupling reactions continued to flourish all the way to the 21st century.[8] The derivatives of dppf can be obtained by changing the substituents on the phosphorus centre, which alters both the electronic and steric properties of the ligand. 1,1'-Bis(di-*iso*-propylphosphino)ferrocene (dippf) and 1,1'-bis(di-*tert*-butylphosphino)ferrocene (dtbpf), among compounds of the type $fc(PR_2)_2$, have also found application in highly efficient palladium-catalyzed cross-coupling reactions due to the large bite angle and bulky electron rich phosphine possessed by these ligands.[9, 10]

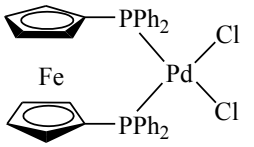

[*Pd(dppf)Cl*$_2$] **(2.1)**

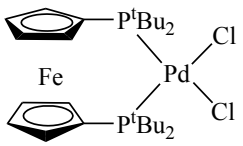

[*Pd(dtbpf)Cl*$_2$] **(2.2)**

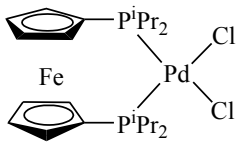

[*Pd(dippf)Cl*$_2$] **(2.3)**

Figure 2.1. Redox-active palladium complexes of the type $Pd(fc(PR_2)_2)Cl_2$

Furthermore, the dichloropalladium complex bearing dppf/dippf/dtbpf (figure 2.1) has been electrochemically shown to undergo ligand-based one-electron reversible redox process without a change in the oxidation state of the palladium centre (figure 2.2).[11-14] This ligand -based oxidation causes little change in the steric properties of a complex of the type $[Pd(fc(PR_2)_2)Cl_2]$ (**2.1** R = Ph; **2.2** R = ^{t}Bu; **2.3** when R = ^{i}Pr) compared with using different R groups, and it is considered the best approach to induce a genuine electronic effect on the

palladium centre. Therefore, it is of great interest to investigate how the catalytic activity of **2.1**/**2.2**/**2.3** can be affected by the ligand state of charge. Nonetheless, chemical oxidations of these palladium complexes bearing substitutionally-inert ferrocene-based redox active ligands that lead to analytically pure products has not previously been reported.

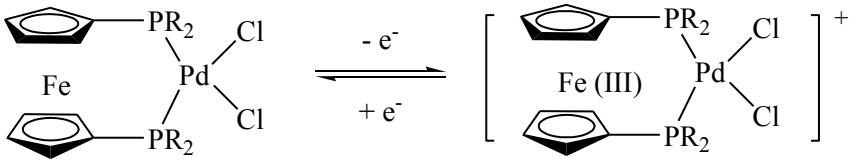

Figure 2.2. Scheme of the redox behaviour of $[Pd(fc(PR_2)_2)Cl_2]$ (R = Ph, ^{t}Bu, ^{i}Pr)

In this chapter, the chemical oxidation of complexes **2.1**, **2.2** and **2.3**, as well as the redox control on the catalytic reactivities of these complexes towards the intramolecular alkoxycarbonylation reactions of 2-halobenzylalcohol (X = Br, I), is reported. The different catalytic behaviour of these oxidized/non-oxidized complexes is explained via the catalytic cycle of the palladium-catalyzed carbonylative cross-coupling reactions, and similar redox control realized on other types of carbonylation processes is also discussed.

2.2. Chemical oxidation of dichloropalladium 1,1'-bis(diphosphino)ferrocenes

2.1, **2.2** and **2.3** were prepared adopting referenced procedures.[15-18] Since it is crucial to obtain the oxidized version of these complexes in order to investigate the effects of the catalytic properties of the palladium centre caused by ligand-based oxidation, a suitable chemical redox agent has to be found.

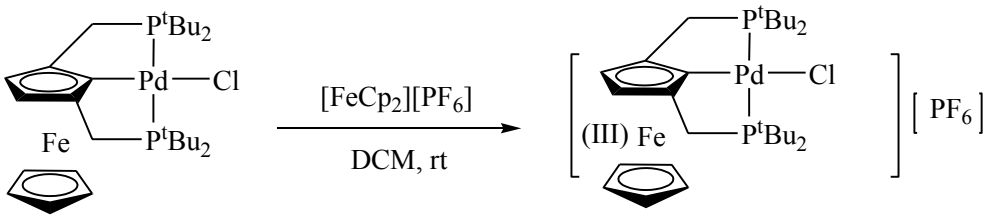

Figure 2.3. Scheme of ligand-based chemical oxidation of a ferrocene complex[19]

The first reported example of ferrocene-based phosphine chelate oxidation centred on the iron atom[19] was the oxidation reaction of the chloropalladium ferrocene-based pincer complex (figure 2.3) and ferrocenium hexafluorophosphate ($[FeCp_2][PF_6]$). Therefore, the oxidations of **2.1**, **2.2** and **2.3** were carried out using the same oxidant under similar conditions (figure 2.4). In order to avoid difficulties in the separation of the oxidized complexes from the ferrocenium salt as mentioned in chapter 1, less than one equivalent of the oxidant was used in each of the reactions.[20, 21]

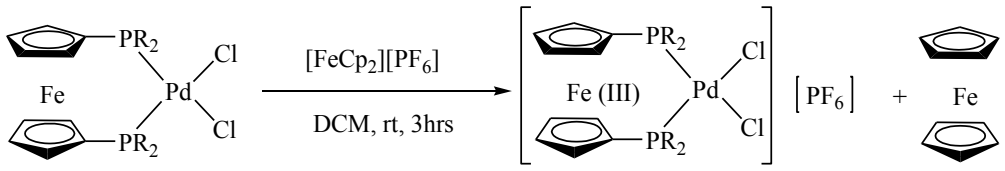

Figure 2.4. Scheme of the synthesis of **2.1-ox** ($[Pd(dppf\text{-}Fe^{III})Cl_2][PF_6]$, R = Ph), **2.2-ox** ($[Pd(dtbpf\text{-}Fe^{III})Cl_2][PF_6]$, R = ^{t}Bu) and **2.3-ox** ($[Pd(dippf\text{-}Fe^{III})Cl_2][PF_6]$, R = ^{i}Pr)

The formation of **2.1-ox**/**2.2-ox**/**2.3-ox** was confirmed by (i) their paramagnetic ^1H NMR spectra, (ii) $^{31}P\{^1H\}$ NMR spectra, where two singlets assigned to the non-oxidized and oxidized complexes were found at different chemical shifts, and (iii) colour change from the non-oxidized complexes. A drop in the solubility of **2.1**/**2.2**/**2.3** after oxidation was discovered, (the above observations are summarized in table 2.1) and this is utilized for the purification of the oxidation products: the separation of **2.1-ox**/**2.2-ox**/**2.3-ox** from the remaining non- oxidized complex and $FeCp_2$ generated from the oxidation reaction was achieved by washing the crude product with toluene (to dissolve and remove **2.1**)/Et_2O (**2.2**)/DCM (**2.3**).

The purity of the isolated products was confirmed by elemental analyses. Although the mass spectrometry of the three oxidized complexes gave no evidence for the molecular ion of **2.1-ox**/**2.2-ox**/**2.3-ox**, peaks for the fragments of $[Pd(dppf\text{-}Fe^{III})Cl_2]^+$, $[Pd(dtbpf\text{-}Fe^{III})]^{2+}$, and $(Pd[dippf\text{-}Fe^{III}])^{2+}$ were found in their electrospray mass spectra, respectively.

The lower stability of **2.1-ox**/**2.2-ox**/**2.3-ox** than its non-oxidized counterpart was observed. While all the non-oxidized complexes are air and moisture stable both in the solid

state and in solution, **2.1-ox** and **2.2-ox** was found to be air and moisture stable only in the solid state. The THF solution of **2.1-ox** were left open to air, and the colour change of the dark green solution to dark brown was observed within 15 mins. Mass analyses of the resulting solution indicated the formation of phosphine oxide, as a result of the further oxidation of **2.1-ox** by oxygen. Similar oxidation of the toluene solution of **2.2-ox** was also observed, whilst **2.3-ox** was found to be of poor solubility.

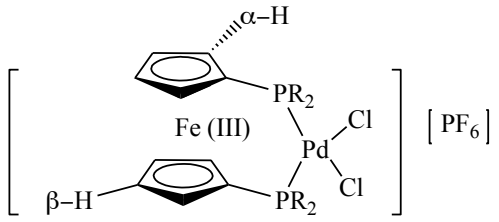

Complex	α-H (ppm)	β-H (ppm)	PR_2 (s) (ppm)	Colour (as solid)	Solubility[a]
2.1	4.40 (pt)	4.20 (pt)	34.0	orange	MeOH
2.1-ox	4.33 (br)	3.92 (br)	33.7	dark green	THF
2.2	4.67 (pt)	4.50 (pt)	66.6	dark purple	Et_2O
2.2-ox	4.21 (br)	4.21 (br)[b]	11.0[c]	brown	toluene
2.3	4.59 (pt)	4.50 (pt)	63.0	orange	DCM
2.3-ox	4.52 (br)	4.47 (br)	65.3	dark green	-

Table 2.1. ^{1}H NMR ($CDCl_3$, 298 K, 400 Hz) and $^{31}P\{^{1}H\}$ NMR ($CDCl_3$, 298 K, 162 Hz) spectral data and physical properties of the redox switches obtained[i]

As the redox switches of **2.1/2.1-ox**, **2.2/2.2-ox** and **2.3/2.3-ox** were successfully synthesized and purified, investigations on their catalytic activities towards carbonylation processes were subsequently carried out.

[i] (a) The solvent required for complete dissolution of the complex (0.01 mol in 5mL). Chlorinated solvents were found to offer better dissolution for these palladium complexes; For **2.2-ox**, (b) the signal for the all the protons on the ferrocene-1,1'-diyl group is one broad peak; (c) the signals for $[PF_6]^-$ was also found in its $^{31}P\{^{1}H\}$ NMR spectrum as multiplets at -145.8 ppm ($^{1}J_{F,P}$ = 683.65 Hz). Further details of the spectral data are found in Chapter 7 Experimental.

2.3. Intramolecular alkoxycarbonylation reactions of 2-halobenzylalcohols

2.3.1. Realization of redox control and the mechanism of the processes

The alkoxycarbonylation reactions of the bifunctional substrates of 2-halobenzylalcohol (X = Br, I) towards phthalide catalyzed by the palladium redox switches synthesized were first studied. Under an atmospheric pressure of CO and in the presence of NEt_3, the reactions of 2-bromobenzylalcohol (Br-substrate, figure 2.5) in toluene were carried out at 120 ºC for 18 hours, and the reactions of 2-iodobenzylalcohol (I-substrate) at 100 ºC for 3 hours. This is because the I-substrate is more active towards the oxidative addition to palladium, which is in many palladium-catalyzed processes the rate-limiting step,[22-24] as the bond strength of C-Br is larger than that of C-Br. Each reaction was repeated at least 3 times to give an appreciation of reproducibility ($n \geq 3$), and the products obtained were analyzed by gas chromatography.[ii]

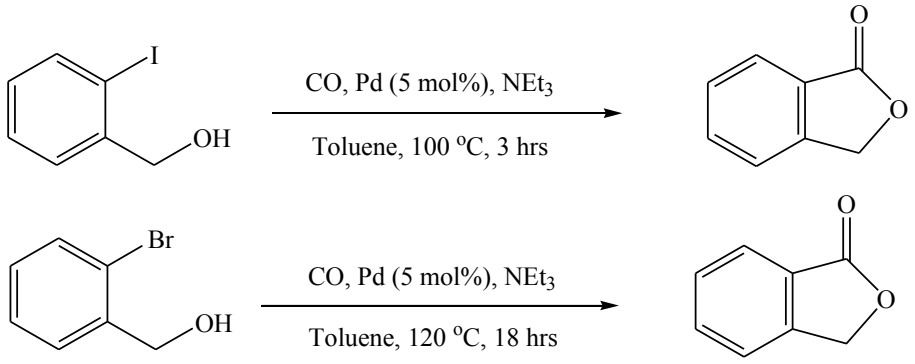

Figure 2.5. Scheme of palladium-catalyzed alkoxycarbonylation of 2-halobenzylalcohols

The carbonylation reaction of the I-substrate catalyzed by **2.1**/**2.1-ox** was first carried out. While an 87 ± 1% yield was afforded by **2.1**, **2.1-ox** offered a slightly higher yield of 95 ± 3 %. For the reactions of the less activated Br-substrate, a yield of 54 ± 3 % was given by **2.1**, suggesting a more difficult oxidative addition step than that for the I-substrate. Nonetheless, high reactivity was exhibited by **2.1-ox** which afforded a 91 ± 2 % yield, showing a noticeable change in the catalytic behaviour of **2.1** caused by ligand-based oxidation. As an initial redox control has been observed, the carbonylation reactions of

[ii] The catalytic activities of the palladium complexes in each carbonylation reaction were measured via the isolated yields of phthalide. Reaction rate was not measured.

2-halobenzylalcohols catalyzed by the redox switches of **2.2/2.2-ox** and **2.3/2.3-ox** were also carried out for further investigations.

Phosphine ligands modified by *tert*-butyl groups have received great attention for being reported to offer great efficiencies towards various challenging palladium-catalyzed processes since these sterically bulky and strongly electron-donating alkylphosphines to a large extent promote the oxidative addition step in some cases.[25-30] Therefore, **2.2** is expected to exhibit high reactivities towards the carbonylation reactions of 2-halobenzylalcohols because its *tert*-butyl featured bidentate ligand dtbpf is electron-rich and has a large bite angle, both of which impart activities to this palladium catalyst.[31-34] Indeed, complete conversions from both substrates to phthalide were afforded by both **2.2** and **2.2-ox**, where the electron density on the phosphine is reduced by the ferrocen-1,1'-diylium group.

The poorest catalytic results were given by the redox partners of **2.3/2.3-ox**. Although the *iso*-propylphosphine incorporated ferrocene ligands have been reported to be effective tools for enhancing the activities of palladium catalysts especially towards Suzuki cross-coupling reactions,[34-36] no product was obtained from the reaction of the Br/I- substrate catalyzed by **2.3**. Furthermore, while a moderated yield of 50 $\pm$ 3 % was afforded by **2.3-ox** for the reactions of the Br-substrate, a lower yield of 21 $\pm$ 2 % was obtained from the **2.3-ox** catalyzed reaction of the I-substrate. It was still quite interesting to discover that **2.3-ox** exhibited higher activities than its non-oxidized version.

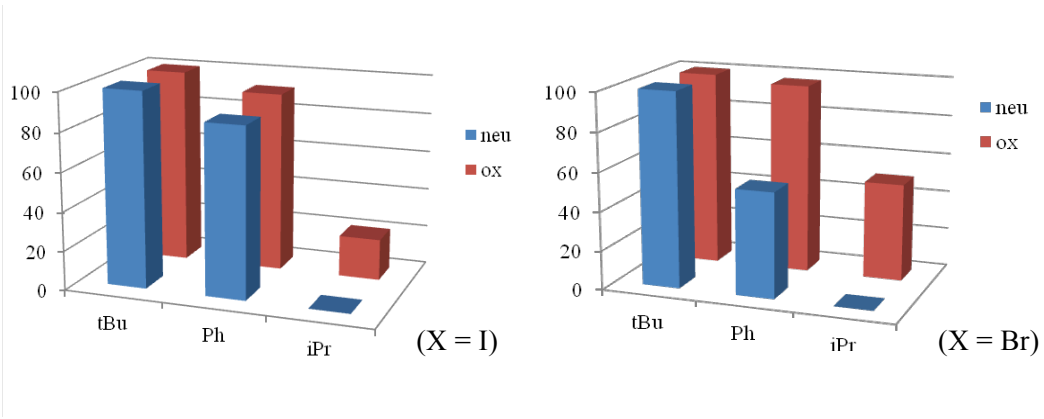

Figure 2.6. Bar charts of the yields (%) of the alkoxycarbonylation of 2-halobenzylalcohols (X = Br or I) catalyzed by the redox switches of the type $PdCl_2(fc(PR_2)_2)$, R = Ph, ^{t}Bu, ^{i}Pr (neu = non-oxidized complexes; ox = oxidized complexes)

The catalytic data was summarized and compared (figure 2.6), and the catalytic cycle of palladium-catalyzed alkoxycarbonylation reactions (figure 2.7) considered in order to find plausible explanations for these results.

Firstly, the palladium redox switches synthesized are Pd(II) catalyst precursors which have to be reduced to Pd(0) species before initiating the catalytic cycle of palladium-catalyzed carbonylation reactions.[37] However, the formation of the catalytically active Pd(0) species is considered to be a rapid process when compared with its following oxidative addition step, where electron-rich palladium centres are favoured as the increase in the electron density on the palladium centre reduces the activation energy for this transformation (figure 2.7).[38-40]

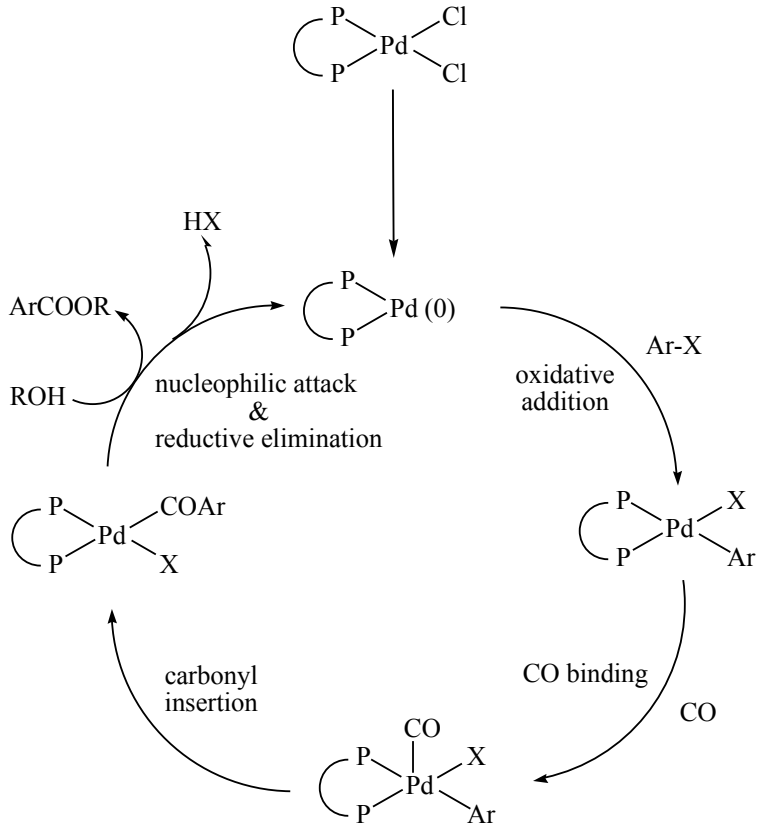

Figure 2.7. Catalytic cycle of the alkoxycarbonylation reactions catalyzed by dichloro -palladium complexes with bidentate phosphine ligands (P-P)[iii]

The excellent yields given by **2.2** can therefore be attributed to it bearing the most basic palladium centre among all the catalysts used, which greatly promote the oxidative addition

[iii] Figure 2.7 adapted from reference 42.

step in the reactions of 2-bromo/iodobenzylalcohol even when the ferrocen-1,1'-diyl group is oxidized to its ferrocen-1,1'-dilyium version.[41] Nonetheless, neither the higher catalytic reactivities of **2.1** compared with those of **2.3**, nor the higher activities of **2.1-ox/2/3-ox** than their non-oxidized versions can be explained by the relative ease of the oxidative addition step. In these cases, better yields were given by the relatively electron-deficient palladium centres, which make it necessary to look into other steps of the catalytic cycle.

The CO binding step occurs following oxidative addition. The introduction of CO into the coordination sphere of palladium is reported to be a rapid reaction for simple phenyl-halo Pd(II) organometallic intermediates, but can be rate-determining for sterically constrained aryl-halo Pd(II) intermediates.[42]

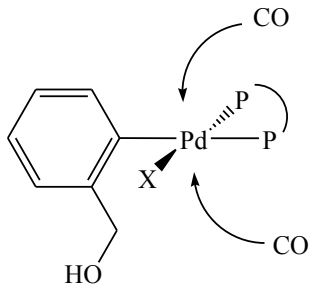

Figure 2.8. CO binding step for palladium-catalyzed carbonylation reactions of 2-halobenzylalcohols supported by bidentate diphosphines (X = Br or I)

For the carbonylation reactions of 2-halobenzylalcohols, the palladium intermediate [ArXPd(P-P)] generated after oxidative addition is described in figure 2.8. The alcohol branch on the aryl group can be orientated away from the vertical plane by distortion of the square-planar palladium species into a square-pyramidal geometry, leaving the axial binding sites of palladium, which are the access points for the coordination of CO, unblocked.[43] In terms of the sizes of different bidentate phosphines chelating to palladium, the dippf ligand is least likely to restrict the coordination sites for CO binding compared with dtbpf and dppf, as the *iso*-propyl group is a smaller substituent compared to the *tert*-butyl group or the phenyl group. However, the redox partners of **2.3/2.3-ox** are the least catalytically reactive among the three redox switches synthesized. Besides, oxidation on the ferrocen-1,1'-diyl moieties on these redox active palladium complexes is unlikely to cause any remarkable change in their

steric properties. Consequently, steps that depend more on electronic factors, other than CO binding, have to be considered for the unexplained catalytic results.

According to the catalytic cycle in figure 2.7, the combination of *cis*-related carbonyl and aryl groups that leads to the formation of an acylpalladium intermediate is the next step. The rate of carbonyl insertion is pronouncedly affected by the back-bonding of d-electrons from palladium to the carbonyl group. Increased electronic density on palladium results in stronger back-donation and consequently stabilization of the Pd-CO bond, leading to slower carbonyl insertion.[44] For this reason, it has been reported that for the carbonylation reactions where the oxidative addition is of similar difficulties, aryl-substituted phosphines often give faster reactions than their corresponding alkyl analogues.[42]

The lower catalytic activity of **2.3** than **2.1**/**2.2** can then be explained: (i) The dippf ligand is not able to promote the oxidative addition of the substrates to palladium so efficiently as dtbpf, leaving this step still as rate-determining; (ii) For the same reaction catalyzed by **2.1**/**2.3**, the carbonyl insertion of the intermediate of [ArXPd(dippf)CO] is slower than [ArXPd(dppf)CO] as the alkylphosphine ligand of dippf is more electron-rich than the arylphosphine dppf. Moreover, the better catalytic performance of **2.1-ox**/**2.3-ox** than their non-oxidized counterparts can also be explained via the carbonyl insertion step, as the ligand-based oxidation of **2.1**/**2.3** reduces the electron density on the palladium centre.

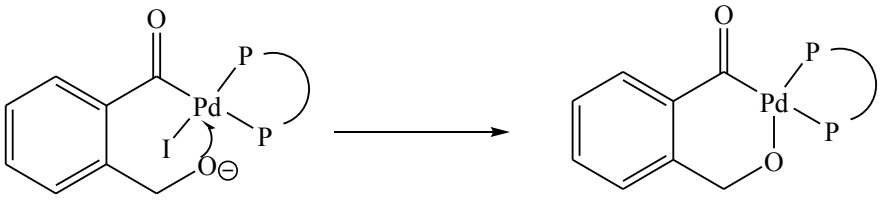

Figure 2.9. The nucleophilic attack step for carbonylation of 2-iodobenzylalcohol[iv]

The subsequent nucleophilic attack and reductive elimination step, which is also known as the product formation step, varies with substrates featuring different halide groups. For the palladium-catalyzed alkoxycarbonylation reaction of 2-iodobenzylalcohol, the formation of phthalide has been described by Morin-Phelippeau *et al*.[45] as the substitution of iodide by alkoxide, which leads to the formation of the stable 6-membered palladacycle shown in figure

[iv] Figure 39 adapted from reference 45.

2.9, preceding the reductive elimination of this resulting Pd(II) intermediate. Based on this mechanism, a more electron-deficient palladium is more active towards the intramolecular nucleophilic attack by an adjacent alkoxide group. This is consistent with the facts that for the reactions of 2-iodobenzylalcohol, **2.1/2.3** is less catalytically reactive than **2.1-ox/2.3-ox**, and that dppf is a better supporting ligand than dippf.

On the other hand, for the alkoxycarbonylation reaction of aryl bromide, the classic catalytic cycle proposed by Heck[46-48] has not been challenged. According to his initial studies, the nucleophilic attack occurs at the acyl carbon of $[Ar(CO)PdL_2]$ (L = ligand), rather than the palladium centre, giving the carbonylation product. In the case of 2-bromobenzylalcohol, the nucleophilic attack step is demonstrated in figure 2.10. Decrease of the electron density at the palladium centre causes the shift of electrons from the acyl carbon to palladium, and thus makes the acyl carbon more attractive to nucleophiles. Consequently, the higher catalytic yields of the reaction of 2-bromobenzylalcohol afforded by **2.1-ox**/**2.3-ox** than **2.1/2.3** can also be attributed to the more rapid nucleophilic attack on the more electron-deficient [ArBrPd(P-P)] intermediates derived from the oxidized complexes.

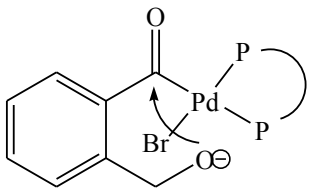

Figure 2.10. The proposed product formation step of the alkoxycarbonylation reaction of 2-bromobenzylalcohol catalyzed by palladium diphosphines

In summary, the data obtained from the alkoxycarbonylation reactions of 2-halobenzyl -alcohols catalyzed by the palladium redox switches synthesized, including the redox control observed in these reactions, can be illustrated via the following hypothesis: (i) oxidative addition is the rate-determining step for these reactions. Complete conversion from the starting material to the product can be realized if the oxidative addition step is greatly promoted; (ii) when the oxidative addition step is still rate-limiting, the catalysts with relatively less electron density on palladium afford more rapid carbonyl insertion and product formation steps.

Evidence is then required to support the hypothesis, which could potentially explain the remaining question: for the reactions catalyzed by **2.3-ox**, why were lower yields obtained from the reactions of the I-substrate than those from the less active Br-substrate? As it is well known that the reactivities of the palladium-catalyzed coupling processes depend not only on the catalyst used, but also on the reaction conditions[49] such as temperature and the solvent, the differences in the reaction conditions for the I- and Br-substrates were considered. While the same solvent and CO pressure were used for both substrates, the reactions of the Br-substrate were carried out at a higher temperature of 120 ºC, with a longer time of 18 hours. These conditions were applied to the **2.3/2.3-ox** catalyzed carbonylation reactions of the I-substrate (3 hours at 100 ºC), and surprisingly 100% yields were afforded by both catalysts (figure 2.11). The same results were also given by these reactions completed within 3 hours, which indicate the important role of temperature. According to the hypothesis proposed for this type of reaction, it is concluded that (i) for the alkoxycarbonylation of 2-iodobenzylalcohol catalyzed by **2.3/2.3-ox**, 120 ºC is the crucial temperature to fully overcome the difficulties in the oxidative addition step; (ii) at the lower temperature of 100 ºC, **2.3** could neither completely activate the I-substrate towards oxidative addition, nor be favoured by the carbonyl insertion or the product formation steps due to the relative electron-rich palladium centre of the Pd(II) derived from **2c**, and consequently afforded no carbonylation product; (iii) at 100 ºC a 21$\pm$ 2 % yield of the reaction of the I-substrate was given by **2.3-ox** as a result of the less reactive oxidative addition but more accelerated carbonyl insertion and product-formation steps when compared with the case of **2.3**.

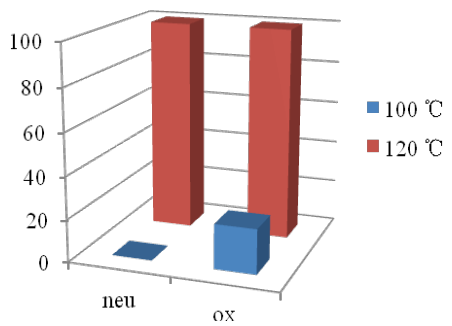

Figure 2.11. Bar chart of the yields (%) of the alkoxycarbonylation reaction of 2-iodobenzylalcohol catalyzed by **2.3/2.3-ox** at different temperature

Since an interesting temperature effect had been observed for the palladium-catalyzed alkoxycarbonylation reactions of 2-iodobenzylalcohol, further experiments were carried out to investigate this temperature impact on the reactions of the Br-substrate.

The alkoxycarbonylation reactions of 2-bromobenzylalcohol catalyzed by each catalyst (**2.1, 2.1-ox, 2.2, 2.2-ox, 2.3, 2.3-ox**) were repeated at 100 ºC, and the results were compared with those obtained from the original reactions at 120 ºC (figure 2.12). As expected for a less activated catalytic process, at 100 ºC **2.3** still exhibited no reactivity; **2.1**, **2.1-ox** and **2.3-ox** were all less active at 100 ºC than at 120 ºC. Nevertheless, it was also observed that at 100 ºC, no product was afforded by **2.1-ox,** which gave an excellent yield of 91 $\pm$ 2 % for the reaction at 120 ºC. Furthermore, for the reactions catalyzed by the redox switches of both **2.1/2.1-ox** and **2.2/2.2-ox** at 100 ºC, an inverse redox control was observed: the non-oxidized catalysts were found more active than their oxidized versions in these cases.

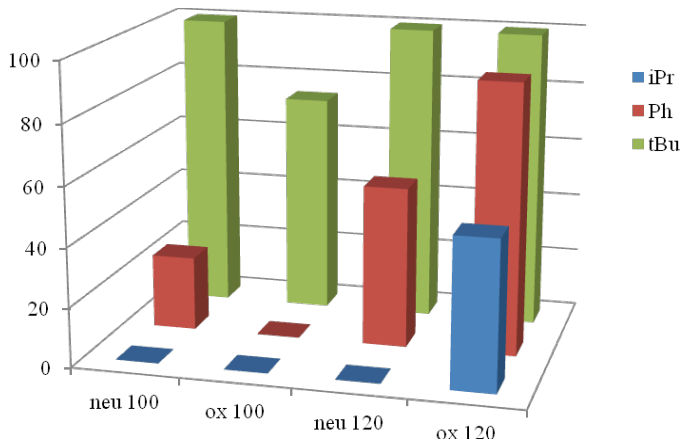

Figure 2.12. Bar chart of the yields (%) of the alkoxycarbonylation reaction of 2-bromobenzylalcohol at different temperatures catalyzed by the redox switches of the type $[PdCl_2(fc(PR_2)_2)]$, R = Ph, ^{t}Bu, ^{i}Pr

Again, analyses via the mechanism of these catalytic reactions, utilizing the proposed hypothesis, was undertaken to explain these results. The lower catalytic yields offered by **2.1-ox/2.2-ox** than their non-oxidized counterparts could be attributed to the less activated oxidative addition step at 100 ºC than that at 120 ºC. As this step favours electron-rich

palladium systems,[38-40] temperature becomes crucial for the activity of the oxidative addition of the substrate to an electron-deficient palladium species. Therefore, while the bulky and electron-rich dtbpf ligand can still support a 100 % conversion from the reactant to the product at 100 ºC, this cannot be repeated when the ligand is oxidized. A 74 $\pm$ 1 % yield was afforded by **2.2-ox** as a result of an incompletely activated oxidative addition step.

The 0 % yield of the reactions catalyzed by **2.1-ox/2.3-ox** at 100 ºC is considered as a result of the completely inactivated oxidative addition step. Although the oxidative addition of the Br-substrate to the electron-deficient palladium centre in [Pd(dippf-Fe^{III})]/[Pd(dppf-Fe^{III})] was successful at 120 ºC, such transformation may not be achieved at a lower temperature of 100 ºC.

Consequently, the catalytic activities of the oxidized palladium complexes depend more on the temperature than their non-oxidized counterparts due to the difficulties in the oxidative addition step for electron-deficient palladium systems; and the two inverse redox control processes observed at 100 ºC and 120 ºC can be explained as an overall effect of the more difficult oxidative addition step and the more rapid carbonyl insertion and product formation steps caused by the ligand-based oxidation of **2.1**/**2.2**/**2.3**.

As the various influences of temperature on the alkoxycarbonylation reactions of 2-halo -benzylalcohols have been observed and elucidated, studies on the effects of conditions other than temperature on the reactivities of these catalytic reactions were carried out in order to fully understand the redox control observed.

2.3.2. The optimized conditions for the alkoxycarbonylation of 2-bromobenzylalcohol catalyzed by [Pd(dppf-Fe^{III})Cl_2][PF_6]

Apart from achieving redox control in certain catalytic processes, it is also the aim of this work to achieve high yields of challenging catalytic reactions using accessible catalysts under mild conditions. It has been reported that the efficiency of the palladium-catalyzed coupling reactions depend on numerous factors including the temperature, the substrate, the type and amount of the palladium source, the solvents and the base.[49] Therefore the CO pressure is desired to remain atmospheric. As to the palladium sources, the redox switches of **2.1/ 2.1-ox**, **2.2/2.2-ox** and **2.3/2.3-ox** were compared via various aspects.

Firstly, the preparations of the palladium complexes of **2.2** and **2.3** required the synthesis of air-sensitive ligands (dtbpf and dippf), while dppf is air-stable at room temperature and thus was more easily obtained. Furthermore, among the aryl-/alkylphosphines of the type of $ClPR_2$ (R = Ph, ^tBu and ^iPr), which are the starting materials for the ligands dppf, dippf and dtbpf, respectively, $ClPPh_2$ is the cheapest. Besides, although improvements on the catalytic performance of both **2a** and **2c** caused by ligand-based oxidation in the alkoxycarbonylation reactions of 2-bromobenzylalcohol were noticed, an excellent yield of 91 $\pm$ 2 % was obtained from the reactions catalyzed by **2.1-ox,** while only a 50 $\pm$ 3 % yield was given by **2.3-ox**. Therefore, the redox switches of **2.1/2.1-ox** were selected to study the effect of reaction conditions on the catalytic behaviour.

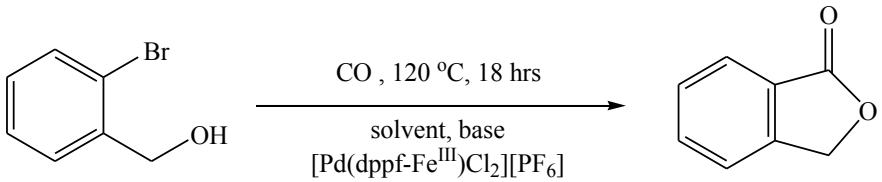

Figure 2.13. Scheme of the alkoxycarbonylation reaction of 2-bromobenzyalcohol catalyzed by **2.1-ox** with variable conditions

Since excellent yields were obtained from the reactions of 2-iodobenzylalcohol catalyzed by each palladium catalyst (figure 2.6 and 2.11), the alkoxycarbonylation reaction of 2-bromobenzylalcohol was chosen to investigate on which factors the high reactivity of **2.1-ox** relies. According to the temperature effect on the catalytic behaviour of **2.1-ox** towards the reactions of the Br-substrate observed (figure 2.12), 120 ºC was used for a successful oxidative addition step, and the effects of the solvent, the base and the amount of **2.1-ox** were studied (figure 2.13).

The impact of the percentage of **2.1-ox** in the reaction mixture on the catalytic yield was first studied. While other conditions were maintained, reactions with different amounts of catalyst (1 mol%, 2 mol% and 3 mol%), were carried out. It was discovered that the original 5 mol% catalyst loading is the minimum to ensure a good yield of this reaction. The quantity of the phthalide obtained distinctly decreases as less catalyst was used, until no product could be afforded when the catalyst loading drops to 1 mol% (figure 2.14).

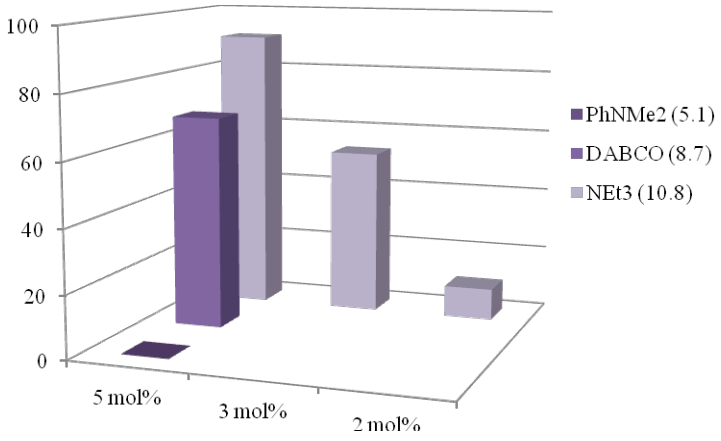

Figure 2.14. Bar chart of the yields (%) of the alkoxycarbonylation reactions of 2-bromobenzylalcohol using different amounts of [Pd(dppf-Fe^{III})Cl_2][PF_6] and different bases (pK_a values are given in the brackets)[v]

After the determination of the minimum catalyst loading, experiments into how the catalytic reactivity of **2.1-ox** is affected by the basicity of the homogeneous reaction mixture for the carbonylation of 2-bromobenzylalcohol were carried out. In the presence of different tertiary amines and 5 mol% of the catalyst, the reactions demonstrated a strong dependence on the base used. As shown in figure 2.14, base with a higher pK_a value[50] obviously supports a better yield for the reaction.

In the catalytic cycle of the alkoxycarbonylation reaction of the Br-substrate catalyzed by **2.1**, the base is involved in two steps. The first is the formation of the catalytically active Pd(0) species.[37] In the case of **2.1-ox**, the base assists the detachment of the two chlorides. The other is the product formation step, where the base assists the nucleophilic attack and the regeneration of the Pd(0) species.[42, 46-48] For these reactions, the product is formed upon the completion of the nucleophilic attack of the alkoxide formed via the removal of the proton on the alkoxy group at the acyl carbon (figure 2.15). The following reductive elimination step involves the dissociation of the bromo- ligand on the palladium, giving a bromide anion, and the regeneration of the Pd(0) species. The anion, together with the tertiary amine and the removed proton, form an ammonium bromide salt that precipitates from the solution of the reaction mixture.

[v] The data in all the bar charts in this chapter is summarized in Chapter 7 Experimental.

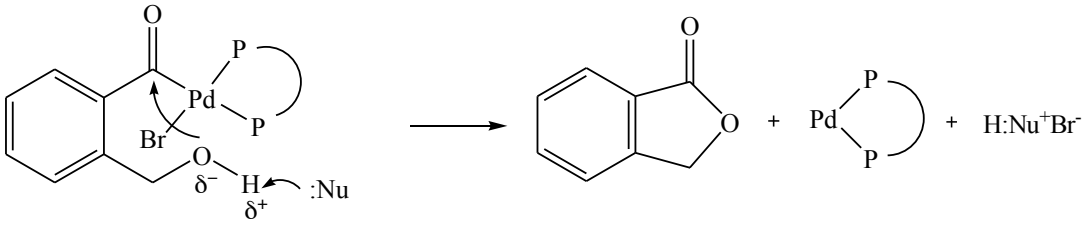

Figure 2.15. Product formation step of the palladium-catalyzed alkoxycarbonylation reaction of 2-bromobenzylalcohol in the presence of Lewis base.

In another part of this project, it has been discovered that the Suzuki cross-coupling reaction of 4-bromotoluene and phenylboronic acid at 80 ºC catalyzed by 2 mol% of **2.1-ox** in the presence of K_3PO_4 could give an 84 $\pm$ 3 % yield of 4-phenyltoluene (this will be further discussed in chapter 5). Knowing that K_3PO_4 (pK_a = 1.6) [51] is a weaker base than any of the tertiary amines in figure 2.14, and that the generation of the catalytically active Pd(0) species is also the first step in the catalytic cycle for the palladium-catalyzed Suzuki-Miyaura cross-coupling reactions, it can be concluded that this step is not likely to be rate-limiting for the carbonylation reaction catalyzed by the same catalyst at a higher temperature of 120 ºC with a stronger base.

Thereby, the cause of the base dependency of the **2.1-ox** catalyzed alkoxycarbonylation reactions of the Br-substrate must be related to the product formation. It has been reported by Hartwig[52, 53] and others[26, 54, 55] that the reductive elimination step is usually more rapid for electron-deficient Pd(II) complexes as they are easier to be reduced. Thus it is concluded that the reductive elimination step for the reactions catalyzed by **2.1-ox** is relatively rapid as the electrons on the palladium centre shift to the ferrocen-1,1'-diylium moiety. This again confirms that the catalyst formation step at the beginning of the catalytic cycle is not rate-limiting for **2.1-ox** or the other oxidized catalysts.

Consequently, the product formation step, where the base assists the deprotonation of the hydroxyl group on the Pd(II) intermediate ($[ArCOBrPd(dppf\text{-}Fe^{III})]^+$) formed after the carbonyl insertion step and the regeneration of Pd(0) species ($[Pd(dppf\text{-}Fe^{III})]^+$), could be responsible for the base effect observed.

It has been illustrated that electron-deficient palladium species afforded more rapid nucleophilic attack. In this case, the extent of the acceleration on this step caused by the electron-withdrawing bidentate ligand depends on the rate of the formation of the nucleophile. From this point of view, it is quite straightforward to explain the different catalytic yields offered by different bases as a stronger base affords more rapid deprotonation and therefore produces the alkoxide nucleophile more quickly.

Since the importance of a strong base for the optimized yield of the carbonylation of 2-bromobenzylalcohol catalyzed by **2.1-ox** has been discussed, the solvent effect was then studied. Based on the high temperature and the homogeneous nature of the carbonylation reaction, solvents of high polarities and high boiling points are preferred. Among solvents of this type, EtOH and MeCN can also be potential nucleophiles that can cause competitive reactions. Therefore, the same reactions in the presence of NEt_3 at 120 ºC, along with control experiments using **2.1** as the catalyst, were carried out in THF.

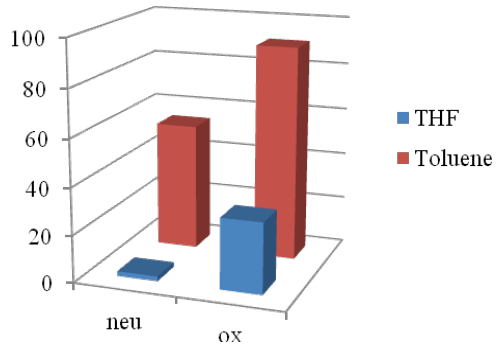

Figure 2.16. Bar chart for the solvent effect on the carbonylation reaction of 2-bromobenzyalcohol catalyzed by **2.1/2.1-ox**

As clearly shown in figure 2.16, toluene proved to be a more suitable solvent than THF for this reaction since higher yields were given by toluene with catalysts in both oxidation states, and this is attributed to the lower boiling point of THF (66 ºC) than toluene (110 ºC). It was also observed that even in THF, **2.1-ox** still offered better catalytic yields than **2.1** at 120 ºC, which again indicates the electronic nature of this redox control.

To summarize, the excellent catalytic reactivity of **2.1-ox** towards the carbonylation reaction of 2-bromobenzylalcohol relies on various factors such as the base, the solvent, the temperature and the catalyst loading. The optimized reaction conditions have been found to be at 120 ºC in the presence of NEt_3, toluene and 5 mol% of the catalyst. The mechanism behind the optimized catalytic yield was also studied, and the two reductive elimination processes in the catalytic cycle for this reaction is another reason for the good activity of this oxidized catalyst.

2.3.3. Efficiency of the redox control on the [Pd(dppf)Cl_2] catalyzed alkoxycarbonylation reaction of 2-bromobenzylalcohol

The extent that the ligand-based oxidation of **2.1** increases the catalytic activity towards the alkoxycarbonylation of 2-bromobenzylalcohol has also been studied. Under the optimized conditions for [Pd(dppf-Fe^{III})Cl_2][PF_6], reactions catalyzed by various palladium phosphines were carried out (figure 2.17) to compare their catalytic activities.

[Pd(dppf)CH_3Cl] was used to catalyze the reaction in order to study the influence of the non-chelating substituent on palladium, as the same bidentate phosphine ligand is contained in both this compound and **2.1**. Moreover, **2.1-ox** was compared with [Pd(PPh_3)$_4$], where excess phosphine ligand is a feature, in terms of their catalytic capabilities. Another commonly used catalyst, [Pd(PPh_3)$_2Cl_2$], was also used to gain a full understanding of this particular reaction.

According to the data in figure 2.17, under the same conditions, [Pd(dppf)CH_3Cl] is slightly more catalytically reactive than **2.1.** Two possible explanations for this difference between the catalytic behaviour of the two complexes of similar formation are discussed. On the one hand, if both catalyst precursors followed the same catalytic cycle for the reaction, then based on the fact that these two catalysts possess the same bidentate ligand and that the dissociation of the non-chelating ligands and the activation of the substrate takes place during the oxidative addition step (figure 2.7), the catalyst formation step for [Pd(dppf)CH_3Cl] must be a quicker process than that for **2.1**. This hypothesis is supported by some research studies, which claimed that palladium methyl complexes readily undergo reductive elimination, and that reductive elimination occurs faster in palladium complexes bearing electron-donating

reacting ligands than those with weakly electron-donating substituents.[55-58]

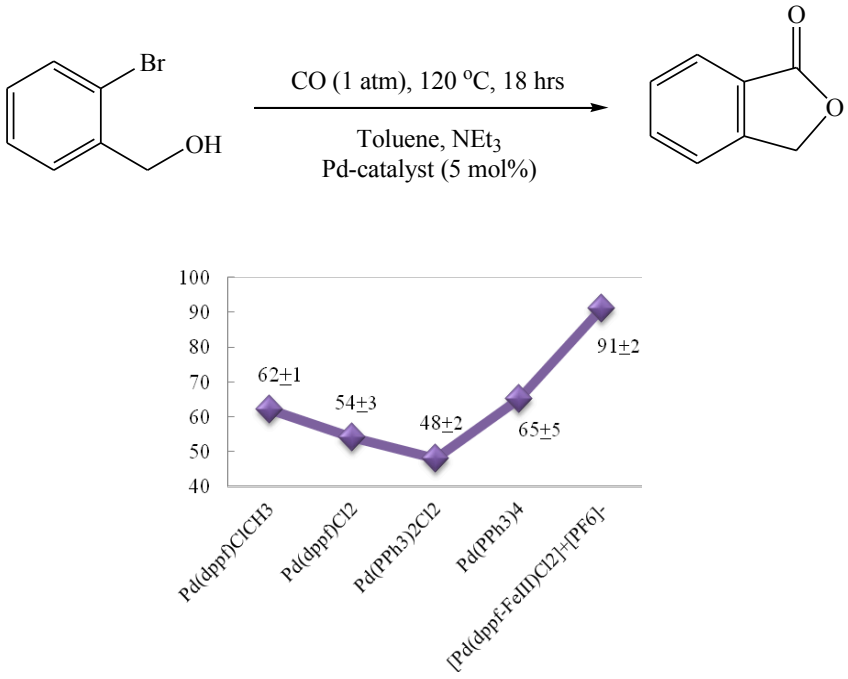

Figure 2.17. Alkoxycarbonylation reactions of 2-bromobenzylalcohol catalyzed by different palladium complexes

On the other hand, as it has been reported that [Pd(dppf)CH_3Cl] can be treated as an oxidative adduct in the studies on the influence of ligands on the rate of CO insertion into palladium-methyl bond,[59] it is possible that in this carbonylation reaction [Pd(dppf)CH_3Cl] binds with CO in the beginning of the catalytic process, followed by reductive elimination leading to the formation of the intermediate [(CO)Pd(P-P)], which undergoes oxidative addition with the substrate (figure 2.18). Since the [Pd(CO)L_2] catalytically active species has also been proposed by Heck in his initial studies on the alkoxycarbonylation of aryl halides, the catalytic cycle described in figure 2.18, which is proposed based on the work of Dekker *et al*. and Heck *et al*.[46-48, 59] is more likely to be the case for the alkoxycarbonylation reaction of 2-bromobenzylalcohol catalyzed by [Pd(dppf)CH_3Cl]. In this case, the oxidative addition of the substrate to the [Pd(CO)(P-P)] intermediate is supposed to be more rapid than the corresponding [Pd(P-P)] species as the carbonyl group is a б-donor that increases the electron density on the palladium centre. This explains higher catalytic reactivity of [Pd(dppf)CH_3Cl] than that of **2.1**.

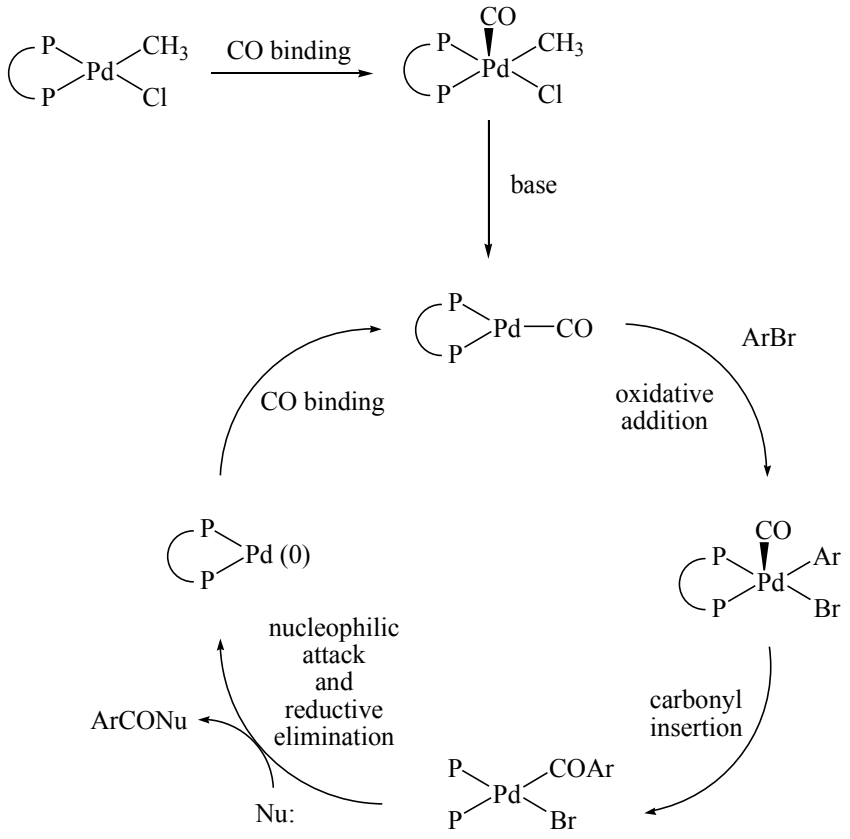

Figure 2.18. Possible catalytic cycle proposed for the alkoxycarbonylation reaction of 2-bromobenzylalcohol catalyzed by [Pd(dppf)CH_3Cl] [vi]

In terms of the catalytic behaviour of **2.1** and [Pd(PPh_3)$_2Cl_2$], the advantages of bidentate chelating phosphines with a large bite angle[60-65] (**2.1** in this case) was revealed. Moreover, although [Pd(PPh_3)$_4$] contains more phosphine ligands than the other catalysts and thus afforded higher catalytic yield than other non-oxidized catalysts, **2.1-ox** remained the most efficient catalyst. Consequently it is discovered that the ligand-based oxidation on **2.1** has a greater enhancement on its catalytic reactivity than the changes on the ligands.

The excellent catalytic performance of **2.1-ox** in the alkoxycarbonylation reaction of 2-bromobenzylalcohol under optimized conditions (91 $\pm$ 2 %) was also compared with some published work on this particular reaction. It was noticed that this yield afforded by **2.1-ox** is highest among the literature value, where the reactions are reported to be catalyzed by other metals,[66] under larger pressure of CO ,[66-67] or carried out in advanced micro-reactors.[68]

[vi] Mechanism proposed in the figure is derived from reference 46-48 and 59.

2.4. The intermolecular aminocarbonylation reactions of halobenzene and benzylamine

Since a noticeable redox control has been realized on the alkoxycarbonylation reactions of 2-halobenzylalcohols catalyzed by **2.1/2.1-ox**, the same redox partners were again used to catalyze the intermolecular aminocarbonylation reactions of halobenzene (PhX, X = Br, I) and benzylamine ($BzNH_2$) in order to further study the redox control on the catalytic behaviour of **2.1** and to evaluate the proposed hypothesis for this redox control.

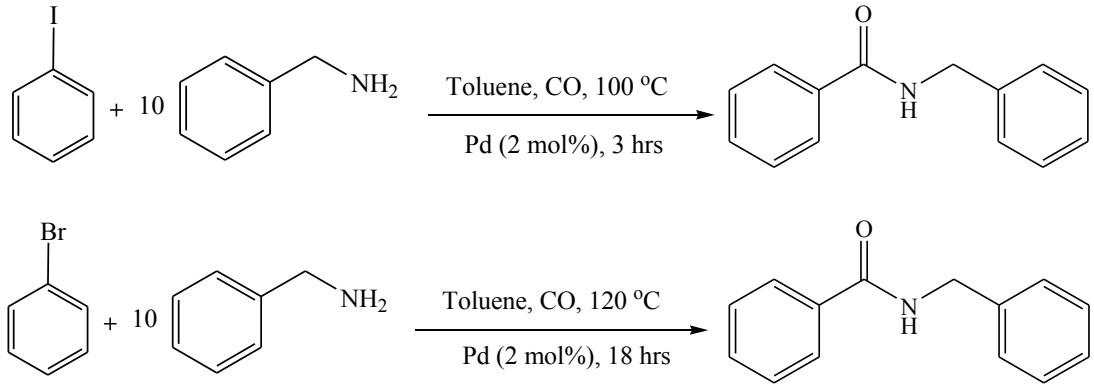

Figure 2.19. Schemes of the aminocarbonylation reactions of halobenzene and benzylamine

As shown in figure 2.19, the reactions of PhX (X = Br, I) and $BzNH_2$ catalyzed by 2 mol% of **2.1/2.1-ox** under an atmospheric pressure of CO in toluene towards the formation of N-benzylbenzamide were investigated. 10 equivalents of benzylamine were used as both the substrate and the base, and the reactions of PhI and PhBr were carried out at 100 ºC and 120 ºC, respectively.

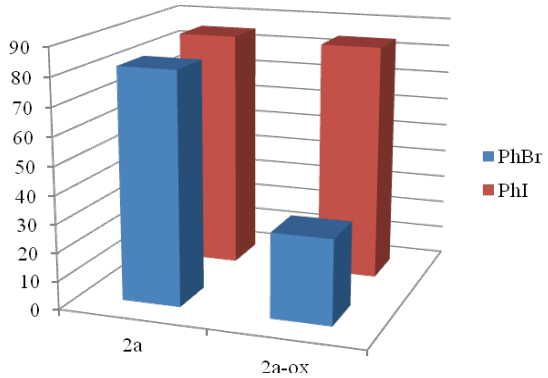

Figure 2.20. Bar chart of the yield (%) of the aminocarbonylation of PhX (X = Br, I) and $BzNH_2$ catalyzed by **2.1/2.1-ox**

It was found that while both **2.1** and **2.1-ox** afforded high yields for the reactions of PhI, little difference between the catalytic activities of the redox partners was observed (figure 2.20). The good catalytic reactivity of **2.1** is consistent with previous work in our laboratory, which investigated the influence of bite angle and flexibility of the bidentate diphosphine ligands on the catalytic property of the palladium centre, on the same reaction.[69] The similar catalytic yields afforded by **2.1/2.1-ox** suggests that under the given conditions, the activity of the reaction might have been driven to its maximum.

However, in the case of the aminocarbonylation of PhBr, redox control was observed as the oxidized catalyst offered a lower yield of 30 $\pm$ 5 % than its non-oxidized counterpart, which gave an 82 $\pm$ 2 % yield. As this redox control was different from that observed for the alkoxycarbonylation reactions of 2-bromobenzylalcohol under optimized conditions, where better yields were afforded by **2.1-ox**, the different conditions used for the two different types of reactions were compared.

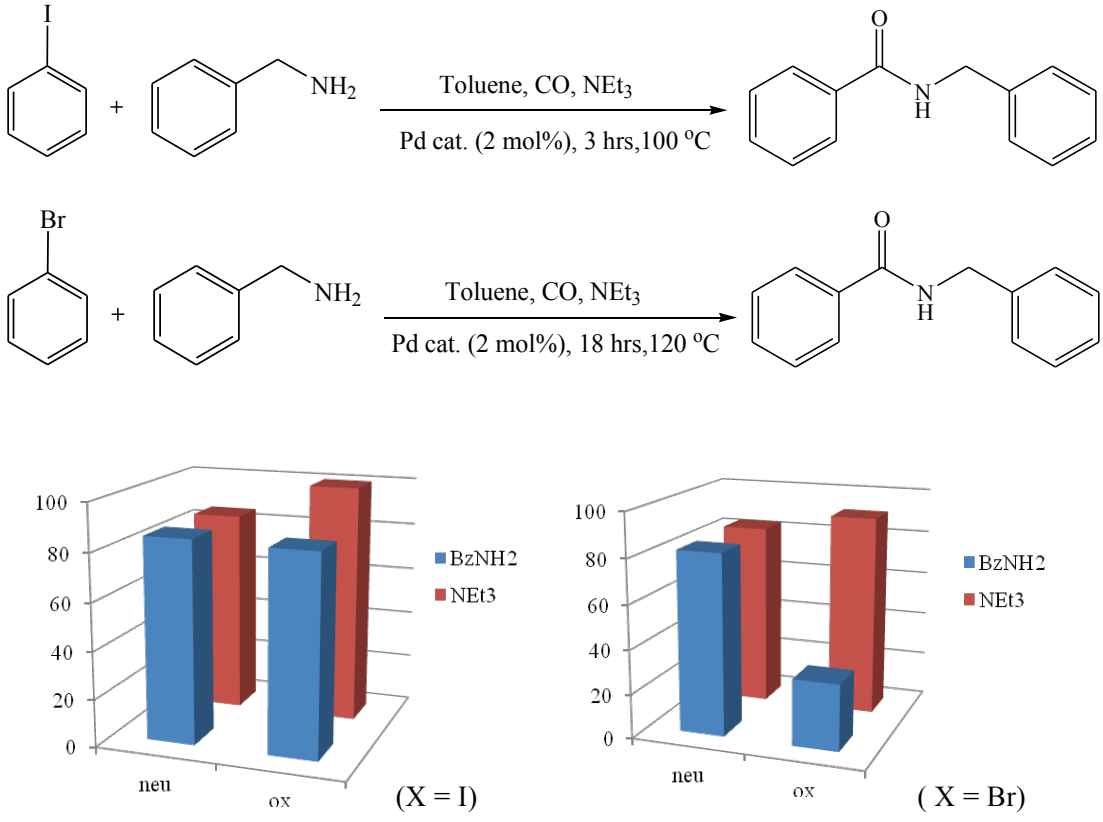

Figure 2.21. Schemes of the aminocarbonylation reaction of PhX (X = Br, I) and $BzNH_2$ catalyzed by **2.1/2.1-ox** using NEt_3 as the base, and the bar charts of the yields (%)

It was noticed that a stronger base, i.e. NEt_3[50] and a higher catalyst loading of 5 mol% were used to optimize the catalytic yield of the reaction of 2-bromobenzylalcohol. As it has been explained in the previous section that the catalytic behaviour of **2.1-ox** depends on both the basicity and the percentage of palladium in the reaction system, the reaction of PhX (X = Br, I) and $BzNH_2$ using NEt_3 as the base instead of excess $BzNH_2$ (figure 2.21) was first carried out in order to study the base effect in these reactions.

Indeed a base dependency of the catalytic reactivity of **2.1-ox** was observed for both halo- substrates. In the presence of NEt_3 the oxidized catalyst offered a complete conversion from iodobenzene to the product, and a high yield of 91 $\pm$ 1 % from bromobenzene. For both substrates, **2.1-ox** is more catalytically reactive than **2.1**, which undoubtedly suggests the return of the high catalytic activity of **2.1-ox** and confirms the proposed hypothesis.

This base dependency is again similarly explained via the product formation step in the catalytic cycle of the palladium-catalyzed carbonylation reactions. In these intermolecular aminocarbonylation reactions, this step also differs for PhI and PhBr (figure 2.22).[45-48] One of the protons in the primary amine group must be removed by the base, and a stronger Lewis base is preferred as it removes one of the hydrogens in the amine group more efficiently, especially in an electron-deficient palladium centre of **2.1-ox**. This indicates the reason why the reactions catalyzed by the non-oxidized catalyst were less affected by the change of the base (figure 2.21).

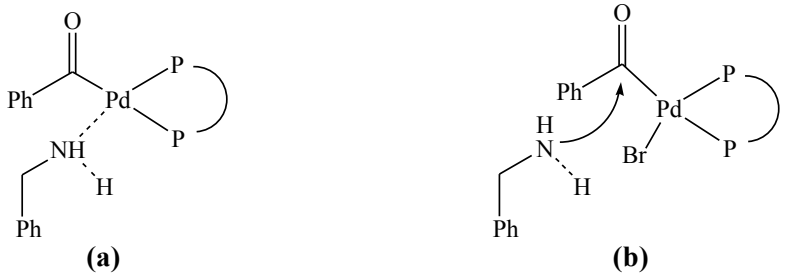

Figure 2.22. Proposed intermediates during the nucleophilic attack of the aminocarbonylation reactions of $BzNH_2$ and PhI (a)/PhBr (b)

However, the catalytic behaviour of **2.1-ox** varies significantly with the base. For the reactions of PhI, after the carbonyl insertion step, the iodo- ligand in [(PhCO)IPd(dppf-Fe^{III})] is replaced by the nucleophile,[45] which is formed from the deprotonation of $BzNH_2$ assisted

by the base (figure 2.22a). In the meantime, the resulting electron-poor Pd(II) intermediate readily proceeds reductive elimination and regenerates the catalytically active Pd(0) species,[55] and thus decreases the demand for a strong Lewis base. These, altogether, explain why NEt_3 can support the reaction of PhI and $BzNH_2$ catalyzed by **2.1-ox** towards a 100 % yield while the excess benzylamine can still support the reaction to give a good yield of 84 $\pm$ 2%.

Nonetheless, for the reactions of PhBr, the nucleophilic attack occurs at the acyl carbon (figure 2.22b),[46-48] and thus the removal of a proton from the amine group in benzylamine precedes the rapid reductive elimination step.[55-58] In this case the rate of the nucleophilic attack is affected more by the rate of the deprotonation for the formation of the nucleophile, which explains the necessity of a strong Lewis base for the maximization of the catalytic capability of **2.1-ox** in this reaction. It also explains the huge difference in the yields of the reactions catalyzed by the ferrocen-1,1'-diylium complex when using NEt_3 and $BzNH_2$ as the base, respectively.

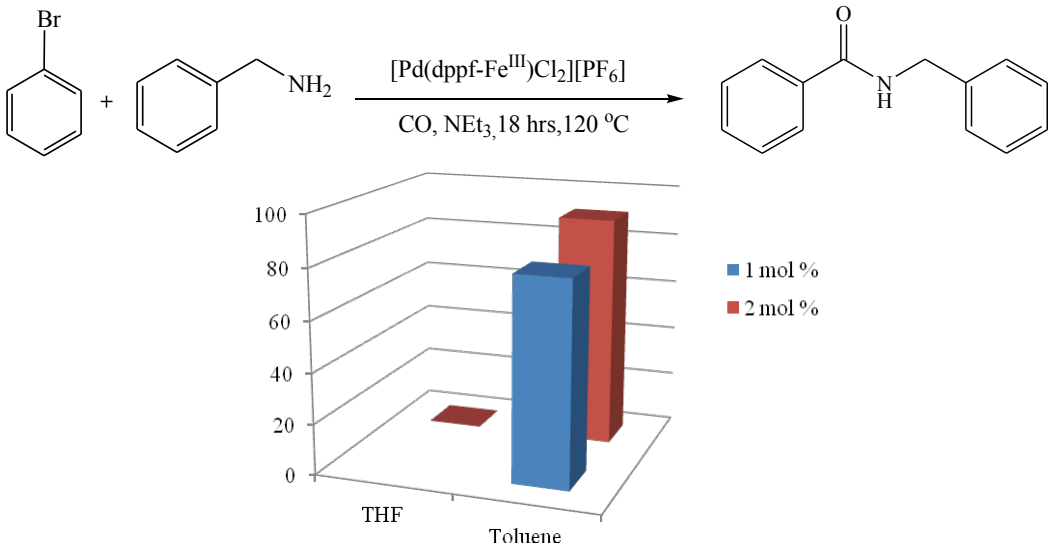

Figure 2.23. Scheme of the aminocarbonylation reactions of PhBr and $BzNH_2$ using different amounts of **2.1-ox** and different solvents, and the bar chart of the yields (%)

As the base effect in the reactions of halobenzene (X = Br, I) and benzylamine has been studied, investigations on the influence of catalyst loading and the solvent on the catalytic performance of **2.1-ox** towards the aminocarbonylation reaction of PhBr and $BzNH_2$ were then carried out (figure 2.23). Since it has been shown that 2 mol % **2.1-ox** is

enough for a good yield when a suitable base is present, the catalyst loading was thereby reduced to 1 mol %, and a decrease in the yield from 91 ± 1% to 80 ± 1% was observed. It was also found that no product was obtained from the reaction with 2 mol% **2.1-ox** carried out in THF instead of toluene. These results suggest that a considerable amount of 2 mol% catalyst loading and a solvent of high boiling point were required for the impressive performance of the oxidized catalyst, which is consistent with the findings on the dependence of the high catalytic reactivity of **2.1-ox** towards the alkoxycarbonylation of 2-bromobenzylalcohol.

In general, similar redox control was realized on the intermolecular aminocarbonylation reactions of halobenzene (X = Br, I) and benzylamine. Increase in the catalytic activity of **2.1** towards these processes was realized by its ligand-based oxidation, and the reactivity of the corresponding ferrocen-1,1'-diylium version of the catalyst was also found to rely on several factors such as the catalyst loading, the base and the solvent.

Nevertheless, the extent of the improvement of the catalyst performance of **2.1** caused by the ligand-based oxidation towards the aminocarbonylation reaction of PhBr and $BzNH_2$, and the alkoxycarbonylation reaction of 2-bromobenzylalcohol, are quite different. While the same optimized reaction conditions were applied (atmospheric pressure of CO, 120 ºC, NEt_3 and toluene), a greater enhancement was observed in the catalytic yield in the latter reaction than the former reaction (figure 2.6 and 2.21). This difference will be discussed below.

Firstly, as the oxygen atom is more electronegative than the nitrogen atom, the hydroxyl group (in 2-bromobenzylalcohol) is supposed to be less nucleophilic than the primary amine group (in $BzNH_2$). Furthermore, according to the proposed hypothesis for the redox control observed in these carbonylation processes, the more rapid nucleophilic attack is afforded by electron-deficient palladium systems. Thus it is considered that when the electron density on the intermediate of [(ArCO)BrPd(dppf)] was reduced by the ligand-based oxidation, the nucleophilic attack of weaker nucleophiles may be more accelerated than stronger nucleophiles, leading to different levels of improvement on the catalytic yields. This explains the bigger difference between the catalytic yields afforded by **2.1** and **2.1-ox** for the alkoxycarbonylation reactions of 2-bromobenzylalcohol than that for the aminocarbonylation reactions of PhBr and $BzNH_2$.

However, this hypothesis cannot yet been confirmed because, so far, the amino-/alkoxy -carbonylation processes investigated are intramolecular and intermolecular, respectively. As there are distinctive differences between these two types of reactions, it is then necessary to compare intramolecular aminocarbonylation with intramolecular alkoxycarbonylation, and intermolecular alkoxycarbonylation with intermolecular aminocarbonylation in order to fully understand the mechanism of the redox effect on these palladium-catalyzed reactions.

2.5. The intramolecular aminocarbonylation reaction of 2-bromobenzylamine, and the intermolecular alkoxycarbonylation reaction of bromobenzene and benzylalcohol

To further investigate the nature of the redox control observed, the intermolecular alkoxycarbonylation reaction of PhBr and benzylalcohol (BzOH), and the intramolecular aminocarbonylation reaction of 2-bromobenzylamine, both catalyzed by the redox partners of **2.1/2.1-ox,** were carried out under the optimized conditions for the alkoxycarbonylation reaction of 2-bromobenzylalcohol and the aminocarbonylation reaction of PhBr and $BzNH_2$. The yields obtained from the intramolecular reactions of 2-bromobenzylamine/alcohol and the intermolecular reactions of PhBr and $BzOH/BzNH_2$ were summarized in figure 2.24.

It can be seen from figure 2.24 that for both the intermolecular and intramolecular reactions catalyzed by **2.1/2.1-ox**, the differences between the activities of the non-oxidized and the oxidized catalysts are bigger in the alkoxycarbonylation processes than in the aminocarbonylation processes. These results confirm the hypothesis that the nucleophilic attack of weaker nucleophiles is more accelerated by the decrease of the electron density on the palladium centre than stronger nucleophiles in the catalytic cycle of palladium-catalyzed carbonylation reactions. This discovery again broadens the scope of the comprehension of the redox control.

The stronger nucleophilicity of the primary amine group than the hydroxyl group was also revealed in the catalytic yields of the intermolecular reactions of benzylamine/alcohol and bromobenzene. Catalyzed by either the non-oxidzed or the oxidized catalyst, the yield of the aminocarbonylation reaction is higher than that of the alkoxycarbonylation reaction. This

can be understood as a stronger nucleophile undergoes the nucleophilic attack step more quickly than a weaker nucleophile.

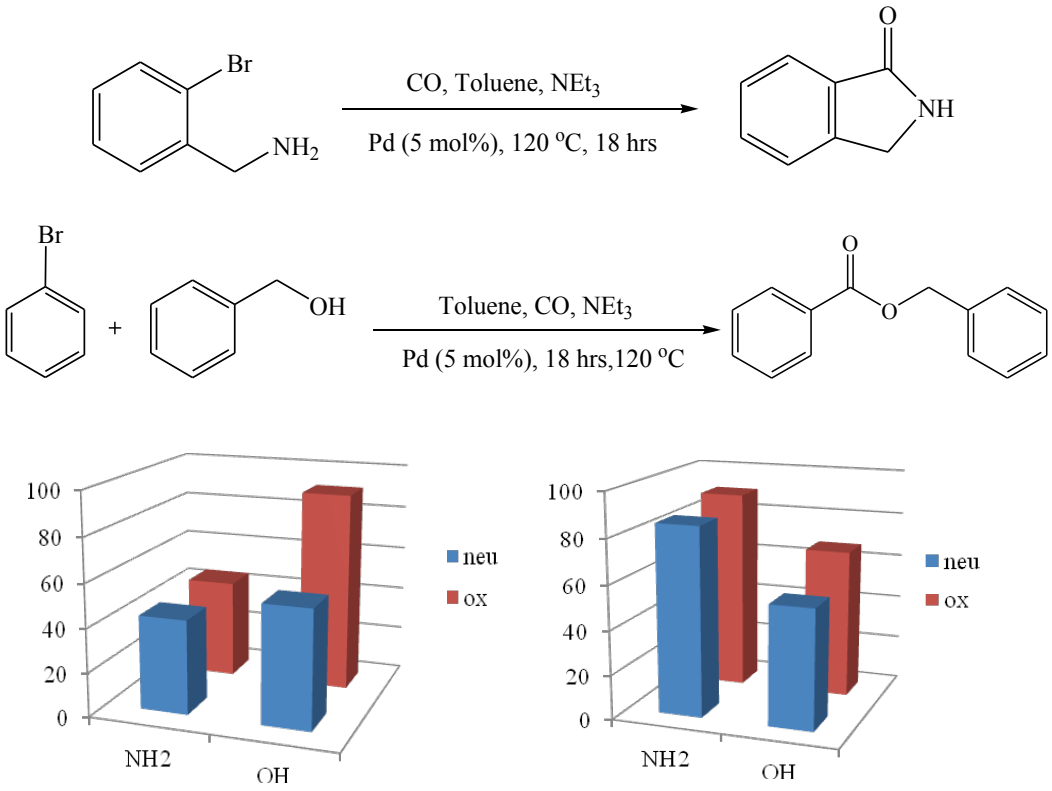

Figure 2.24. Schemes of the alkoxycarbonylation reaction of PhBr and BzOH, and the aminocarbonylation reaction of 2-bromobenzylamine; the bar charts of the yields (%) of the intramolecular reactions of 2-bromobenzylalcohol/amine (left) and intermolecular reactions of PhBr and BzOH/$BzNH_2$ (right) catalyzed by **2.1/2.1-ox**.

An inverse trend was found in the intramolecular reactions of 2-bromobenzylalcohol /amine where yields afforded by the aminocarbonylation processes were lower than those afforded by the alkoxycarbonylation processes. Although the reason is not clear, it has been discussed that this might be attributed to the boiling point of 2-bromobenzylamine (117 ºC). The solvent effect observed in the alkoxycarbonylation reaction of 2-bromobenzylalcohol and the aminocarbonylation of bromobenzene and benzylamine has revealed the importance of the boiling point of the homogeneous reaction mixture. Therefore, the lower boiling point of the 2-bromobenzylamine than the reaction temperature may cause insufficient interaction time between the catalyst and the substrate, and thus lead to the low yield of the reaction.

2.6. Conclusion

A series of palladium complexes containing ferrocene-based bidentate diphosphine ligands of similar bite angle[70-73] has been successfully synthesized and chemically oxidized. Their catalytic behaviour towards carbonylation reactions of aryl halides were compared, and it is found that in general the oxidized catalysts performed better than their non-oxidized version. A hypothesis for the explanation of the higher activities of palladium centres with oxidized ligand is proposed via the catalytic cycle of palladium-catalyzed carbonylative cross -coupling reactions. It is believed that the electron-deficient palladium centres of the oxidized catalysts decelerated the oxidative addition step, but accelerated the reductive elimination, the carbonyl insertion, and the nucleophilic attack steps. This increase in the catalytic reactivity of the palladium centre caused by ligand-based oxidation is also found to depend on reaction conditions such as the temperature, the catalyst loading, the solvent and base used for the reactions.

2.7. References

1. *Ferrocenes* eds. Togni, A.; Hayashi, T. VCH, Weinheim. 1995.
2. Togni, A. *Metallocenes* eds. Togni, A.; Halterman, R. L. Wiley-VCH, Weinheim, 1998.
3. Colacot, T. J. *Chem. Rev.* **2003**, *103*, 3149.
4. Colacot, *Platinum Met. Rev.* **2001**, *45*, 22.
5. Cullen, W. R.; Woollins, J. D. *Coord. Chem. Rev.* **1981**, *39,* 1.
6. Kumada, M. *Pure Appl. Chem.* **1980**, *52*, 669.
7. Hayashi, T.; Konishi, M.; Yokopta, K. I.; Kumada, M.; *J. Chem. Soc., Chem. Commun.* **1981**, 313.
8. Siemeling, U.; Auch, T.-C. *Chem. Soc. Rev.* **2005**, *34*, 584.
9. Hayashi, T.; Konishi, M.; Kobori, Y.; Kumada, M.; Higuchi, T.; Hirotsu, K. *J. Am. Chem. Soc.* **1984**, *106*, 158.
10. Elsagir, A. R.; Gassner, F.; Gorls H.; Dinjus, E. *J. Organomet. Chem.* **2000**, *597*, 139.
11. Ong, J. H. L.; Nataro, C.; Golen, J. A.; Rheingold, A. L. *Organometallics* **2003**, *22*, 5027.

12. Blanco, F. N.; Hagopian, L. E.; McNamara, W. R.; Golen, J. A.; Rheingold, A. L.; Nataro, C. *Organometallics* **2006**, *25*, 4292.
13. Corain, B.; Longato, B.; Favero, G.; Ajo, D.; Pilloni, G.; Russo, U.; Kreissl, F. R. *Inorganica Chimica Acta,* **1989**, *157*, 259.
14. Nataro, C.; Fosbenner, S. M. *J. Chem. Educ.* **2009**, 86, 1412.
15. Butler, I. R.; Cullen, W. R.; Ni, J.; Rettig, S. J. *Organometallics*, **1985**, *4*, 2196.
16. Rausch, M . D.; Ciappenelli, D. J. *J. Organometal. Chem.***1967**, *10*, 127.
17. de Lang, R-J.; van Soolingen, J.; Verkruijsse, H. D.; Brandsma, L. *Synthetic Commun.* **1995**, *25*, 2989.
18. Colacot, T. J.; Fair Jr., R. J.; Boyko, W. J. *Phosphorous, Sulfur and Silicon* **1999**, 144, 49.
19. Koridze, A. A.; Kuklin, S. A.; Sheloumov, A. M.; Dolgushin, F.M.; Lagunova, V. Y.; Petukhova, I. I.; Ezernitskaya, M. G.; Peregudov, A. G.; Petrovskii, P. V.; Vorontsov, E. V.; Baya, M.; Poli, R. *Organometallics*, **2004**, *23*, 4587.
20. Connelly, N. G.; Geiger,W. E. *Chem. Rev.* **1996**, *96*, 877.
21. Ge, Y. W.; Ye, Y.; Sharp, P. R. *J. Am. Chem. Soc.* **1994**, *116*, 8384.
22. Zinovyeva, V. A.; Luo, C.; Fournier, S.; Devillers, C. H.; Cattey, H.; Doucet, H.; Hierso, J.-C.; Lucas, D. *Chem. Eur. J.* **2011**, *17*, 9901.
23. Ben-David, Y.; Portnoy, M.; Milstein, D. *J. Am. Chem. Soc.* **1998**, *111*, 8742.
24. Ben-David, Y., Portnoy, M., Milstein, D., *J. Chem. Soc., Chem. Commun.* **1989**, 1816.
25. Hundertmark, T.; Littke, A. F.; Buchwald, S. L.; Fu, G. C. *Org. Lett*. **2000**, *2*, 1729.
26. Fleckenstein, C. A.; Plenio, H. *Chem. Soc. Rev.* **2010**, *39*, 694.
27. Guram, A. S.; King, A. O.; Allen, J. G.; Wang, X.; Schenkel, L. B.; Chan, J.; Bunel, E. E.; Faul, M. M.; Larsen, R. D.; Martinelli, M. J.; Reider, P. J. *Org. Lett.* **2006**, *8*, 1787.
28. Salvi, L.; Davis, N. R.; Ali, S. Z.; Buchwald, S. L. *Org. Lett.* **2012**, *14*, 170.
29. Mann, G.; Incarvito, C.; Rheingold, A. L.; Hartwig, J. F. *J. Am. Chem. Soc*. **1999**, *121*, 3224.
30. Colacot, T. J.; Pu, X.; Li, H. *J. Org. Chem.* **2013**, *78*, 568.
31. Shaughnessy, K. H.; Kim, P.; Hartwig, J. F. *J. Am. Chem. Soc*. **1991**, *121*, 2123.
32. Hamann, B. C.; Hartwig, J. F. *J. Am. Chem. Soc*. **1998**, *120*, 7369.
33. Kawatsura, M.; Hartwig, J. F. *J. Am. Chem. Soc*. **1999**, *121*, 1473.

34. Colacot, T. J., Shea, H. J. *Org. Lett.* **2004**, *6*, 3731.
35. Sheloumov, A. M.; Tundo, P.; Dolgushin, F. M.; Koridze, A. A. *Eur. J. Org. Chem.* **2008**, 572.
36. Elsagir, A. R.; Gassner. F.; Goerls, H.; Dinjus, E. *J. Organomet. Chem.* **2000**, *597*,139.
37. Barnard, C. F. J., *Organometallics* **2008**, *27*, 5402.
38. Parshall, G. W. *J. Am. Chem. Soc.* **1974**, *96*, 2360.
39. Amatore, C.; Pfluger, F.; *Organometallics* **1990**, *9*, 2276.
40. Qadir, M.; Mochel, T.; Hii, K. K. *Tetrahedron* **2000**, *56*, 7975.
41. Hamann, B. C.; Hartwig, J. F. *J. Am. Chem. Soc.* **1998**, *120*, 7369.
42. Barnard, C. F. J. *Org. Process Res. Dev.* **2008**,*12*, 566.
43. Albaneze-Walker, J.; Bazaral, C.; Leavey, T.; Dormer, P. G.; Murry, J. A. *Org. Lett.* **2004**, *6*, 2097.
44. Garrou, P. E.; Heck, R. F. *J. Am. Chem. Soc.* **1976**, *98*, 4115.
45. Morin-Phelippeau, B.; Favre-Fafet, A.; Hugues, F.; Commereuc, D.; Chauvin, Y. *J. Mol. Catal.* **1989**, *51*, 145.
46. Schoenberg, A.; Bartoletti, I.; Heck, R. F. *J. Org. Chem.* **1974**, *39*, 3318.
47. Schoenberg, A.; Heck, R. F.; *J. Org. Chem.* **1974**, *39*, 3327.
48. Schoenberg, A.; Heck, R. F. *J. Am. Chem. Soc.* **1974**, *96*, 7761.
49. Doherty, S.; Robins, E. G.; Nieuwenhuyzen, M.; Knight, J. G.; Champkin, P. A.; Clegg, W. *Organometallics* **2002**, *21*, 1383.
50. Perrin, D. D. *Dissociation Constants of Organic Bases in Aqueous Solution,* Butterworths, London, 1965; Supplement, 1972.
51. Serjeant, E. P; Dempsey, B. *Ionization Constants of Organic Acids in Aqueous Solution*, Pergamon, Oxford, 1979.
52. Hartwig, J. F. *Inorg. Chem.* **2007**, *46*, 1936.
53. Hartwig, J. F. *Acc. Chem. Res.* **1998**, *31*, 852.
54. Low, J. J.; Goddard, W. A. *J. Am. Chem. Soc.* **1986**, *108*, 6115.
55. Tatsumi, K.; Hoffman, R.; Yamamoto, A.; Stille, J. K. *Bull. Chem. Soc. Jpn.* **1981**, *54*, 1857.
56. Low, J. J.; Goddard, W. A.; *J. Am. Chem. Soc.***1984**, *106*, 6928.
57. Grushin, V. V.; Marshall, W. J. *J. Am. Chem. Soc.* **2006**, *128*, 12644.

58. Roy, A. H.; Hartwig, J. F. *J. Am. Chem. Soc.* **2001**, *123*, 1232.
59. Dekker, G. P. C.; Elsevier, C. J.; Vrieze, K. *Organometallics* **1992**, *11*, 1598.
60. Tolman, C. A.; *Chemical Review*, **1977**, *77*, 313.
61. Freixa, Z.; van Leeuwen, P. W. N. M. *Dalton Trans.* **2003**, 1890.
62. Casey, C. P.; Whiteker, G. T. *Isr. J. Chem.* **1990**, *30*, 299.
63. van Leeuwen, P. W. N. M.; Kamer, P. C. J.; Reek, J. N. H.; Dierkes, P. *Chem. Rev.* **2000**, *100*, 2741.
64. Kamer, P. C. J.; van Leeuwen, P. W. N. M.; Reek, J. N. H. *Acc. Chem. Res.* **2001**, *34*, 895.
65. Dierkes, P.; van Leeuwen, P. W. N. M.; *J. Chem. Soc. Dalton Trans.* **1998**, 27.
66. Foa, M.; Francalanci, F.; Bencini, E.; Gardano, A. *J. Organomet. Chem.* **1985**, *285*, 293.
67. Wu, X.; Mahalingam, A. K.; Wan, Y.; Alterman, M. *Tetrahedron Letters* **2004**, *45*, 4635.
68. Gong, X.; Miller, P. W.; Gee, A. D.; Long, N. J.; de Mello, A. J.; Vilar, R. *Chem. Euro. J.* **2012**, *18*, 2768.
69. Jennings, L. PhD thesis, Imperial College London, 2011.
70. Cullen, W. R.; Kim, T-J.; Einstein, F. W. B.; Jones, T. *Organometallics* **1985**, *4*, 346.
71. Bulter, I. R.; Cullen, W. R.; Kim, T-J.; Rettig, S. J.; Trotter, J. *Organometallics* **1985**, *4*, 972.
72. Westmoreland, I.; Arnold, J. *Acta Crystallogr. Sect. E.*, **2006**, 2272.
73. Shafir, A.; Arnold, J. *J. Am. Chem. Soc.* **2001**, *123*, 9212.

Chapter 3

Novel Ferrocenyl N-P Ligands for Palladium-Catalyzed Carbonylation Reactions

冗繁削尽留清瘦，画到生时是熟时。

郑板桥

3.1. Introduction

N-P ligands, as the name indicates, contain both a nitrogen atom and a phosphorus atom that can coordinate to the metal centre. The chemistry of N-P ligands is well established and great advances have been made since the 1990's.[1-3] Although the two donor atoms are in the same group of the periodic table, they have quite different properties. Phosphorus is a 'softer' donor and is generally able to bind strongly to the late transition metals, whilst the nitrogen is relatively 'hard' and coordinates weakly to the metal, readily providing a site for the binding of substrates. The result of having both a hard and a soft donor atom in a ligand is referred to as 'hemilability'.[4] The advantage of hemilabile ligands is that they are capable of stabilizing the metal centre in a variety of states of charge and geometries, with or without the presence of the substrate, due to their numerous possible modes of coordination (Figure 3.1).

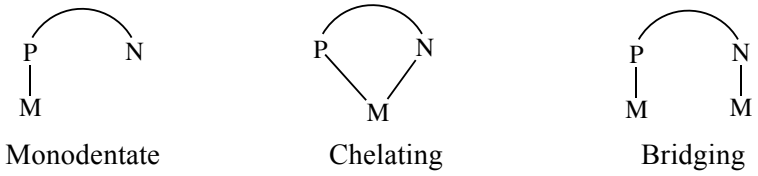

Figure 3.1. Examples of chelating modes of N-P hemilabile ligands to metal centres[i]

The most widely used of these ligands are pyridylphosphines, whose chemistry has been studied and reviewed due to the versatile nature of this type of ligand, which can dramatically influence complex behaviour.[3,5-8] Ferrocene-based N-P ligands have also attracted attention as a result of the large bite angle that these bidentate ligands can provide. Interesting work in this area includes the synthesis of (i) a pair of chiral ferrocenylphosphine-amidine ligands (figure 3.2A), which offer efficient palladium-catalyzed asymmetric allylic alkylation,[9] (ii) two planar chiral 1,2-P,N-ferrocenes (figure 3.2B) whose palladium complexes are very catalytically reactive towards Suzuki-Miyaura and Buchwald-Hartwig coupling of aryl chlorides,[10] and (iii) 1-diphenylphosphino-1'-aminoferrocene (figure 3.2C) where each of the heteroatoms are directly attached to a cyclopentadienyl (Cp) ring.[11]

Nonetheless, in these studies, the redox properties of the complexes bearing these ferrocene-based N-P ligands were not reported, either because some of the complexes were generated *in situ* during catalytic processes, or since it might not have been the main interest of these investigations. In this chapter the synthesis and redox behaviour of palladium complexes based on a series of new ferrocenyl N-P ligands, as well as their catalytic applications, are reported.

[i] Figure 3.1 adapted from reference 2.

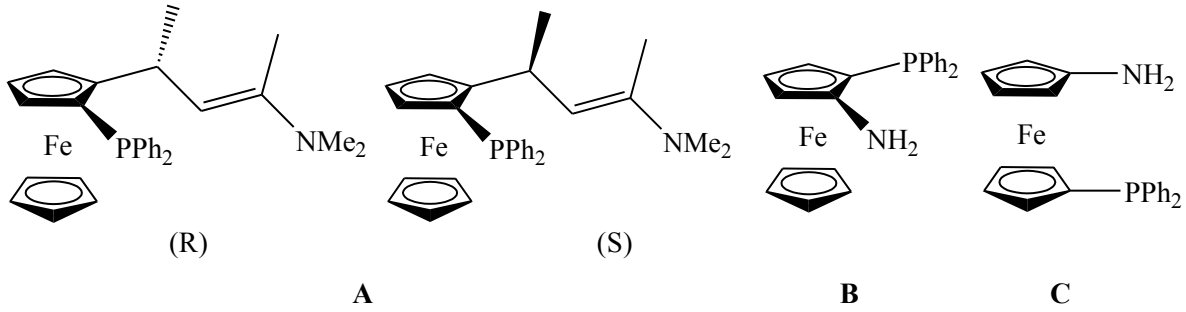

Figure 3.2. Some novel ferrocene-based N-P ligands

3.2. Synthesis of Novel New Ferrocenyl N-P Ligands

3.2.1. Synthesis of the aminoferrocene precursor

The preparation of aminoferrocene ($FcNH_2$), which is the starting material for the new ligands to be synthesized, was carried out. Since the first synthesis of $FcNH_2$ in 1955,[12] numerous improvements of the synthetic method to gain a better yield of this compound have been made.[13-20] Most recently in 2013, an environmentally benign procedure towards $FcNH_2$ was reported. In this study an optimized pathway was proposed with the sequence FcH-FcI-$FcNH_2$, using ammonia as the nitrogen source.[20] However, due to the difficulties in the purification of FcI and $FcNH_2$ via column chromatography, as well as the safety risk in handling with ammonia, this approach was not adopted here.

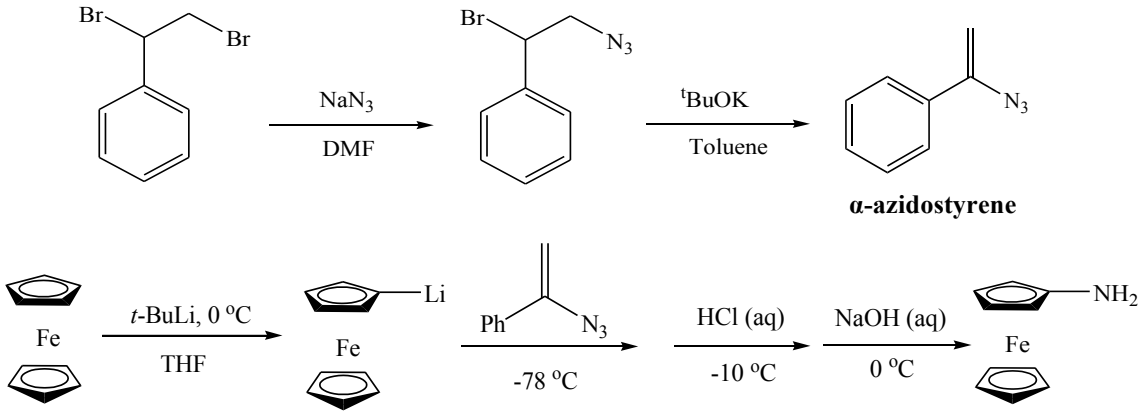

Figure 3.3. Scheme of the synthesis of aminoferrocene[ii]

In this work, the method for the preparation of $FcNH_2$ proposed by van Leusen et al. was followed (figure 3.3). This two-step strategy involves first the deprotonation of ferrocene and

[ii] Figure 3.3 adapted from reference 17 and 21.

then the use of α-azidostyrene, which requires an additional three-step synthetic route.[17, 21] The crude product can be sublimed at 120 °C under high vacuum to give pure $FcNH_2$ as an orange crystalline solid in 55 % yield (calculated from ferrocene).

3.2.2. Synthesis of ligands

The preparation of the novel ligand **3.1**, which had been initiated by a previous member of our group,[22] was first repeated via condensation reaction as shown in figure 3.4. A mixture of aminoferrocene and 2-diphenylphosphinobenzaldehyde in a 1:1 ratio in THF was heated to reflux for 5 hours, during which time the orange solution darkened to deep red. The solvent was then removed to leave an air-stable red solid crude product, which can be recrystallized from hot MeCN to obtain a dark red solid in a 90 % yield upon cooling at 0 °C overnight.

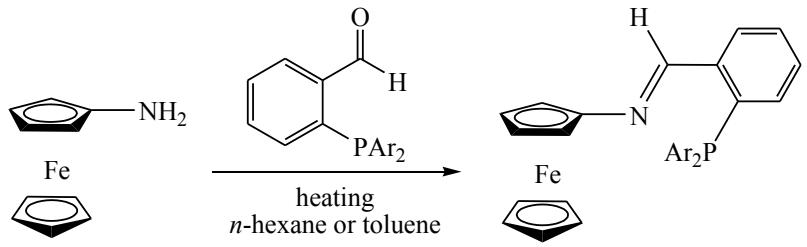

Ar =

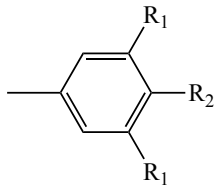

Ligand	3.1	3.2	3.3	3.4
$\mathbf{R_1}$	H	H	Me	^{t}Bu
$\mathbf{R_2}$	H	Me	H	OMe

Figure 3.4. Scheme of the synthesis of the ligand series **3.1** – **3.4**[iii]

As the synthetic method was quite straightforward and promising, ligands **3.2**, **3.3** and **3.4**, as the derivatives of **3.1**, were synthesized via similar reactions of aminoferrocene and the corresponding 2-diarylphosphinobenzaldehyde under the same conditions. Pure products of these derivatives were collected after purification via silica column chromatography and subsequent recrystallization in Et_2O. These new ligands can also be obtained in good yields (74, 78, 70% for **3.2**, **3.3**, **3.4**, respectively).

It was later found out that the preparation of **3.4** can be carried out in n-hexane at 70 °C without the formation of any by-product, and the pure product can be obtained in quantitative yield. Similar improvements of the synthetic method for ligands **3.1, 3.2** and **3.3** have also been made by changing the solvent to n-hexane (for **3.2** and **3.3**) or toluene (for **3.1**), and by

[iii] Figure adapted from reference 22.

pre-heating the mixture of the reactants to 50 °C before adding solvent. Therefore in these cases, it was realized that THF afforded more side reactions towards byproducts.

Nonetheless, it was observed that during the synthesis of **3.2** and **3.3**, a longer reaction time was required for completion of these reactions under improved conditions. This decrease in reaction rate when switching the solvent from THF, a polar solvent, to a non-polar solvent of n-hexane can be understood as solvents of higher polarity can better stabilize the dipolar intermediates of these condensation reactions, and thereby accelerate the reactions.[23] This theory can also be used to explain the extra side reactions brought by THF, as this strong and polar solvent can stabilize a wider range of intermediates and thus bear more transformation processes.

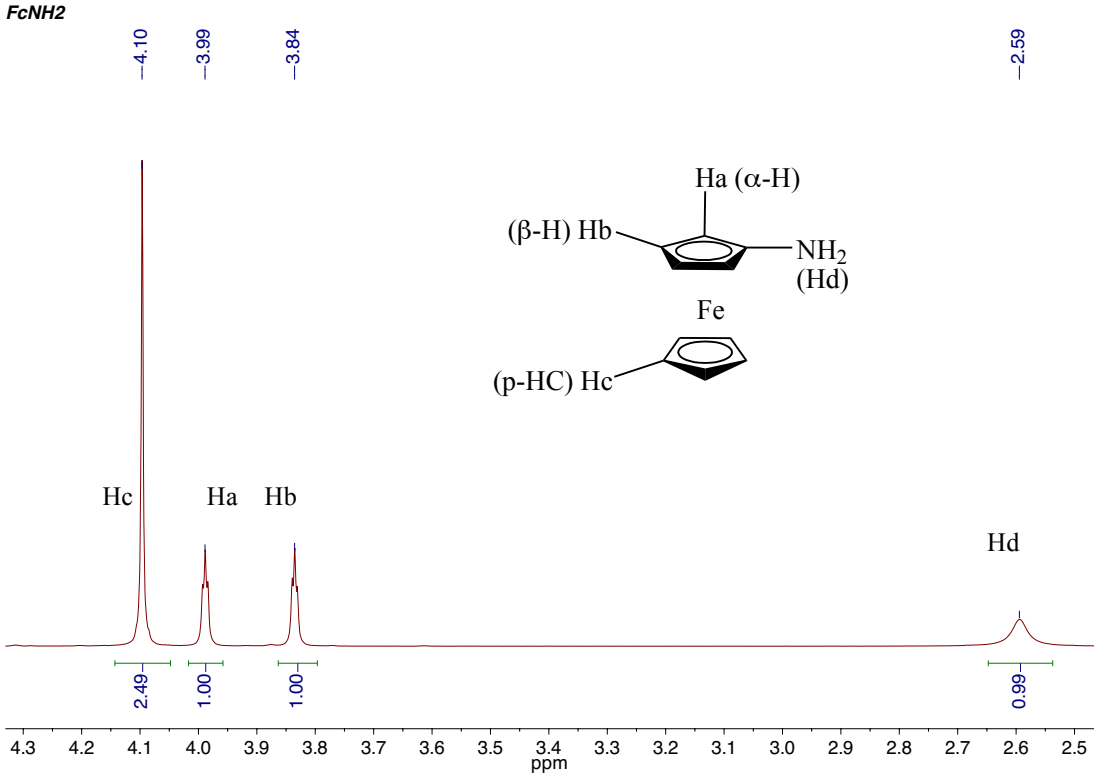

Figure 3.5. ^{1}H NMR spectrum ($CDCl_3$, 298 K, 400 MHz) of $FcNH_2$

The formation of the imine group can be confirmed by the ^{1}H NMR spectra of these ligands. In the ^{1}H NMR spectrum of aminoferrocene (figure 3.5), two pseudo-triplets exhibited by the substituted cyclopentadienyl (Cp) protons are at 3.84 ppm and 3.99 ppm, and a singlet corresponding to the unsubstituted Cp ring is at a higher chemical shift of 4.10 ppm. These suggest that the electrons on the protons on the substituted Cp are more shielded caused by the electron-donating nature of the amine substituent.

Ligand	α-H (pseudo-t)	β-H (pseudo-t)	Cp-H (s)	C=N-H (d)	$^{31}P\{^{1}H\}$ NMR (s)
3.1	4.43	4.19	3.96	9.31	-13.9
3.2	4.43	4.19	3.96	9.32	-15.8
3.3	4.46	4.18	3.94	9.36	-14.7
3.4	4.43	4.17	3.93	9.43	-14.1

Table 3.1. The chemical shifts (ppm) of protons and phosphorus atoms in ligand **3.1-3.4**[iv]

Comparing the spectra of ligands **3.1-3.4** to the spectrum of $FcNH_2$, both of the pseudo-triplets have shifted to higher frequencies than the singlet, indicating the presence of an electron-withdrawing imine substituent (Table 3.1). The hydrogen attached to the C=N carbon in each of these ligands gives a doublet, as a result of $^{4}J_{P,H}$ coupling, at a reasonably high frequency around 9.40 ppm in its ^{1}H NMR spectrum. An example of the ^{1}H NMR spectrum of ligand **3.4** is shown in figure 3.6.

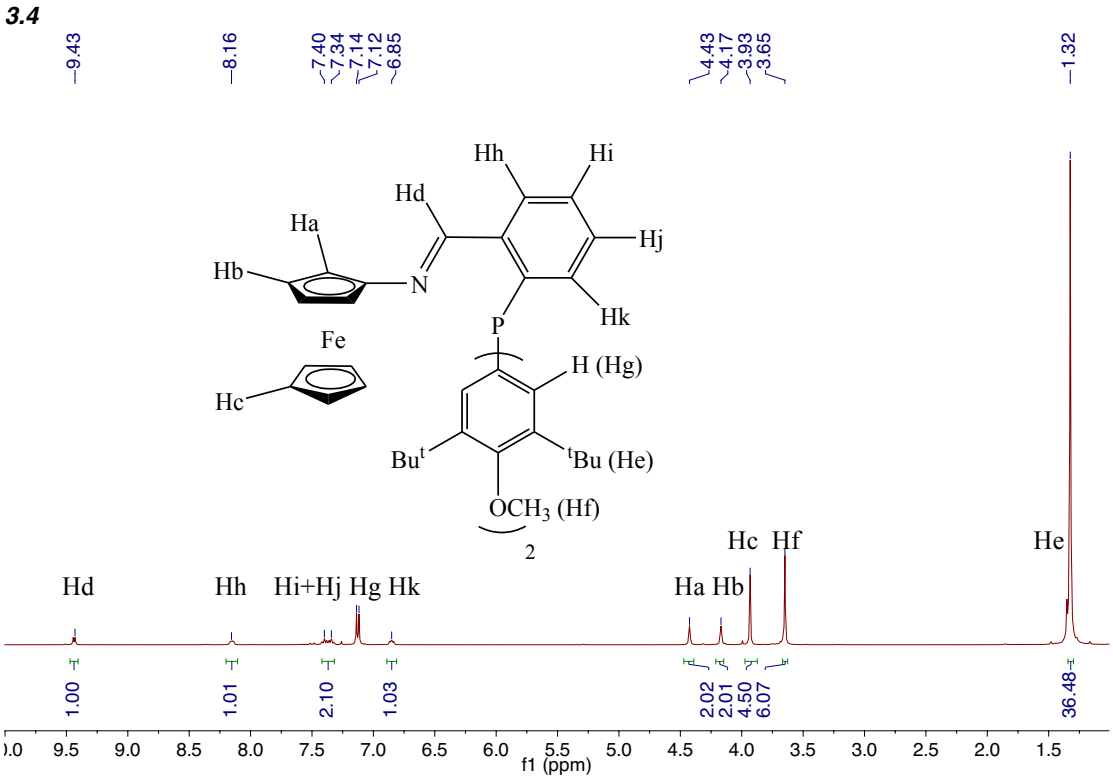

Figure 3.6. ^{1}H NMR spectrum ($CDCl_3$, 298 K, 400 MHz) of **3.4**

[iv] Conditions: ^{1}H NMR ($CDCl_3$, 298 K, 400 Hz); $^{31}P\{^{1}H\}$ NMR ($CDCl_3$, 298 K, 162 Hz)

According to figure 3.6, the signals for the hydrogen atoms on the ferrocenyl group are two pseudo-triplets at 4.43 ppm and 4.19 ppm, and a singlet at 3.93 ppm. The doublet at 9.43 ppm correspond to the C=N-H, the large peak at 1.32 ppm is the signal for the protons on the *tert*-butyl groups, and the singlet at 3.65 ppm is assigned to the methoxy group. The signals for the protons on the *ortho* position of the two aryl substituents on the phosphine group are found as a two singlets at 7.10 ppm and 7.12 ppm. This is also considered as a result of the different distances from these hydrogen atoms to the iron atom. The protons on the di-substituted aryl ring give signals as a doublet of doublet of doublets at 8.16 ppm, and three doublets of pseudo-triplets at 7.40 ppm, 7.34 ppm and 6.85 ppm, respectively.

The $^{31}P\{^{1}H\}$ NMR spectra of these ligands indicate the single environment of their phosphine groups by giving a singlet. The chemical shifts of these signals (table 3.1) are in good correlation with the literature ^{31}P value of -12.90 ppm found for an analogous compound, 2-(diphenylphosphino)benzylideneaminopiperidine (figure 3.7).[24]

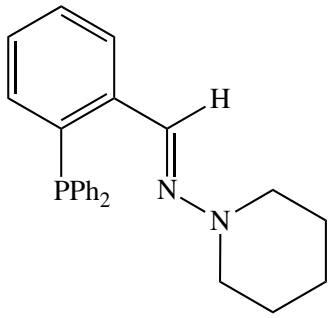

Figure 3.7. Structure of 2-(diphenylphosphino)benzylideneaminopiperidine

For complete characterization these novel N-P ligands were also analyzed by ^{13}C NMR spectroscopy. Total assignment of the spectra proved to be quite difficult due to the number of different environments of the carbons in the compound. Therefore ^{13}C-DEPT and HMQC experiments, whose results were compared with the ^{13}C-NMR spectra for complete assignment, were also carried out to gain a full understanding of these ligands. An example of the assigned carbon environments of ligand **3.4** have been summarized in Table 3.2, and the spectrum is shown in figure 3.8.

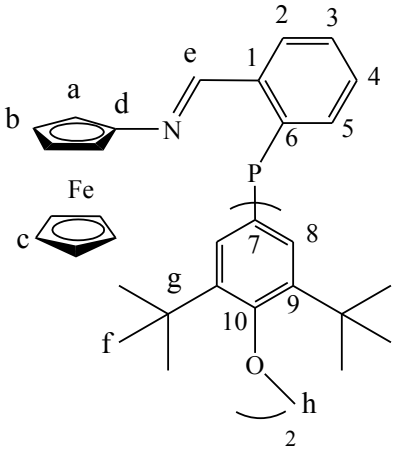

Carbon environment	Chemical shift (ppm)
Ferrocenyl a/b/c/d	63.7 / 67.2 / 69.7 / 105.1
Imine e	157.4
***tert*-butyl f/g**	32.1 / 36.0
Methoxy h	64.4
Aromatic 1~6	139.6 /126.6 / 130.1 / 128.8 / 133.0 / 139.3
Aromatic 7~10	129.9 / 132.6 & 132.8 / 143.9 / 160.5

Table 3.2. The ^{13}C NMR ($CDCl_3$, 298 K, 100 Hz) spectral data for ligand **3.4**

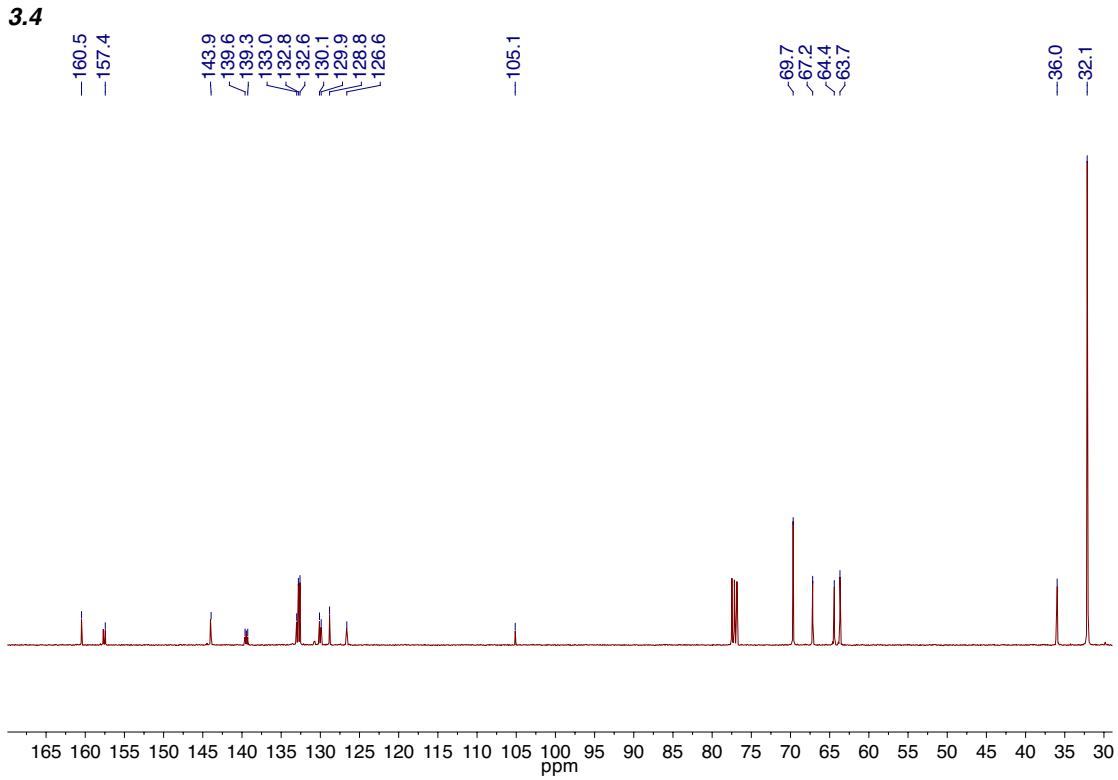

Figure 3.8. ^{13}C NMR ($CDCl_3$, 298 K, 100 MHz) spectrum of **3.4**

Elemental analyses of **3.1** and **3.4** show good agreement of the calculated values and experimental values, while **3.2** and **3.3** were found to be hydroscopic in the solid state and thus cause a decrease in the percentage of carbon and nitrogen. Peaks for the water adduct of **3.2** and **3.3** were found in their mass spectra. Apart from these characterizations, electrochemical experiments were also carried out to investigate the redox properties of the ligands.

Initial studies were carried out to examine the cyclic voltammetry of **3.1** in DCM at different scan rates with tetrabutylammonium hexafluorophosphate (TBAP) as the electrolyte. This compound was observed to undergo three oxidation processes followed by two reduction processes as shown in figure 3.9. The three oxidation peaks are assigned to the loss of one electron on the iron centre, whose electronic effect was shared by the π-conjugated systems in the molecule of **3.1** (π1, π2 and π3 in figure 3.9). It can be seen that there is no reduction process corresponding to the first oxidation peak (ox 1), and the last reduction peak (red 2) is broader than any of the oxidation peaks. Thus, the last oxidation (ox 3) and the first reduction (red 1) peaks are recognized as the characteristic redox behaviour of the ferrocenyl moiety (π1), and the second reduction peak (red 2) is understood to correspond to the electronic changes on the C=N double bond (π2) and the di-substituted aryl group (π3).

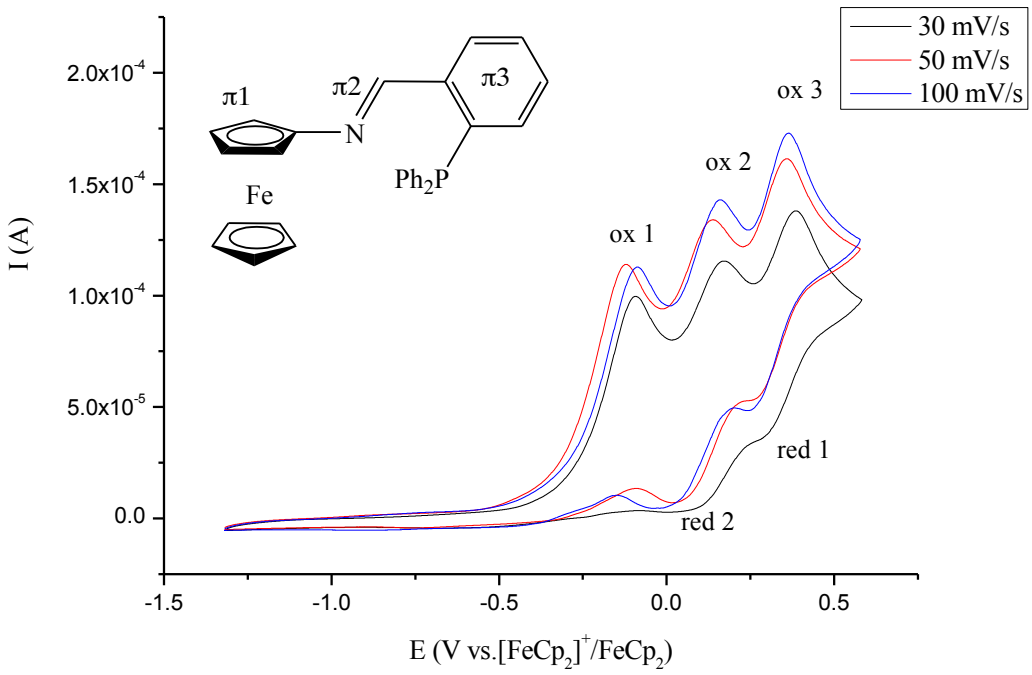

Figure 3.9. Cyclic voltammograms of **3.1** at different scan rates (50 mM in DCM with 0.1M TBAP, rt)

Although the first and second oxidation peaks have not been assigned, respectively, it was thought that this can be achieved after obtaining the cyclic voltammograms of **3.2**, **3.3** and **3.4** (figure 3.10), since the intensity of the signals for π3 relative to π2 is expected to enlarge with the increase of the number of electron-donating substituents on the phenyl groups as a result of a larger electron density. Therefore, the cyclic voltammetry of the complete ligand series was carried out and the result obtained was summarized in figure 3.10 and table 3.3. In figure 3.10 that for ligand **3.4**, the intensity of the second oxidation peak is noticeably lower than the first or the third oxidation peaks; thus the second signal is consequently assigned to the C=N double bond, and the first to the aryl group conjugated with C=N.

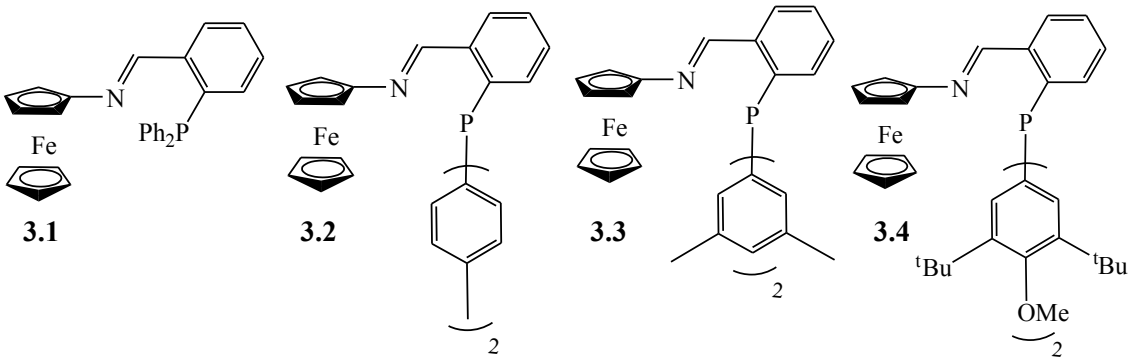

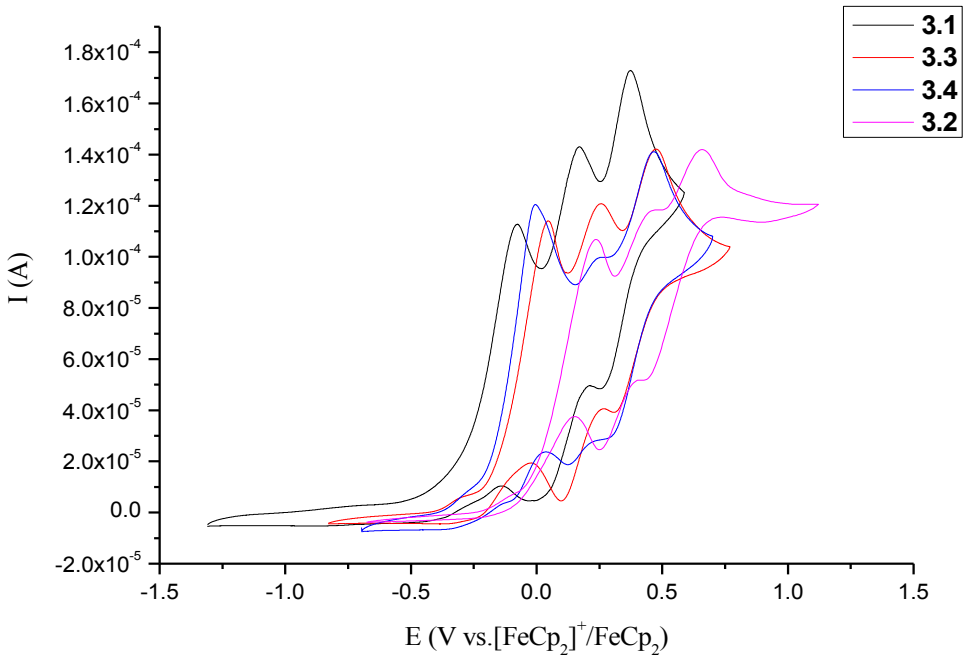

Figure 3.10. Cyclic voltammograms of **3.1**, **3.2**, **3.3** and **3.4**
(50 mM in DCM with 0.1M TBAP, rt, scan rate 100 mV/s

It can also be seen from the data in table 3.3 and figure 3.10 that for **3.2**, **3.3** and **3.4**, ligands with more electron-donating groups on the aryl groups attached to the phosphorus atom undergo oxidation more readily, which is consistent with the fact that electron-rich systems are more easily oxidized.[25, 26] However, the relatively electron-deficient ligand **3.1** is found to be the easiest to oxidize. As it has been reported that the oxidation potential(s) of certain compounds in a particular solvent depend not only on the electronic nature of the compound, but also on its geometric properties and the interactions between the molecules,[25-27] the lowest oxidation potentials of **3.1** among those of **3.2**, **3.3** and **3.4** is considered to be caused by steric factors. The substitution of the phenyl groups of **3.1** may lead to weaker interactions between the same molecules, and thus higher oxidation potentials.

Ligand	ox 1	ox 2	ox 3	red 1	red 2
3.1	-0.0674	0.179	0.383	0.259	-0.0174
3.2	0.242	0.481	0.661	0.427	0.257
3.3	0.0433	0.253	0.473	0.305	0.0944
3.4	-0.00412	0.206	0.466	0.349	0.125

Table 3.3. Oxidation and reduction potentials (vs. $[FeCp_2]^+/FeCp_2$)[v] of ligands **3.1 ~ 3.4** (50 mM in DCM with 0.1 M TBAP, rt, 100 mV/s)

Moreover, it was discovered that ligands **3.1 ~ 3.4** exhibited different redox behaviour in THF. As demonstrated in figure 3.11a, in THF **3.1** undergoes one oxidation followed by a one reduction process, the oxidation/reduction potentials of the ligand vary significantly when the sweep rate changes, and large ΔE_p values (> 400 mV), which are found to enlarge with the increase of the scan rate, are given. Similar cyclic voltammograms are offered by the other three ligands, and it was observed that broader redox peaks (figure 3.11) and a larger ΔE_p value were afforded by the ligand with more substituents (table 3.4). These results can again be explained via the delocalization of electrons on the moieties conjugated with the ferrocenyl group. As the potential on the electrode increases, the substituents can donate electrons to the π-conjugated systems and balance the loss of electron on the iron centre, and consequently extend the oxidation process.

[v] Standard $E_p^{1/2}$ of ferrocene in DCM taken from reference 28.

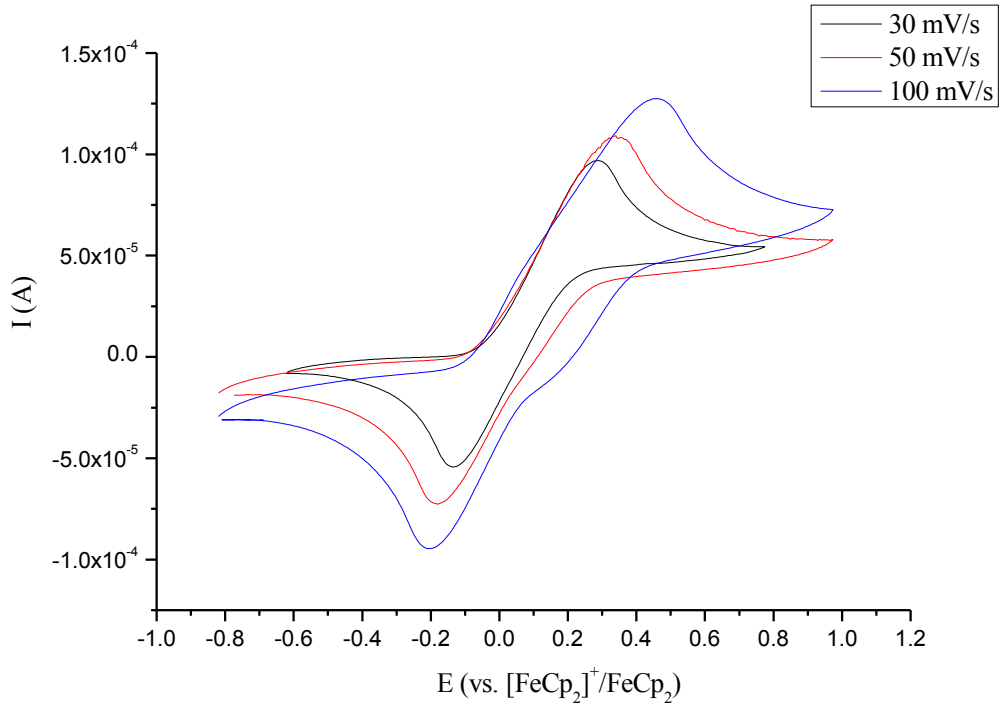

(a)

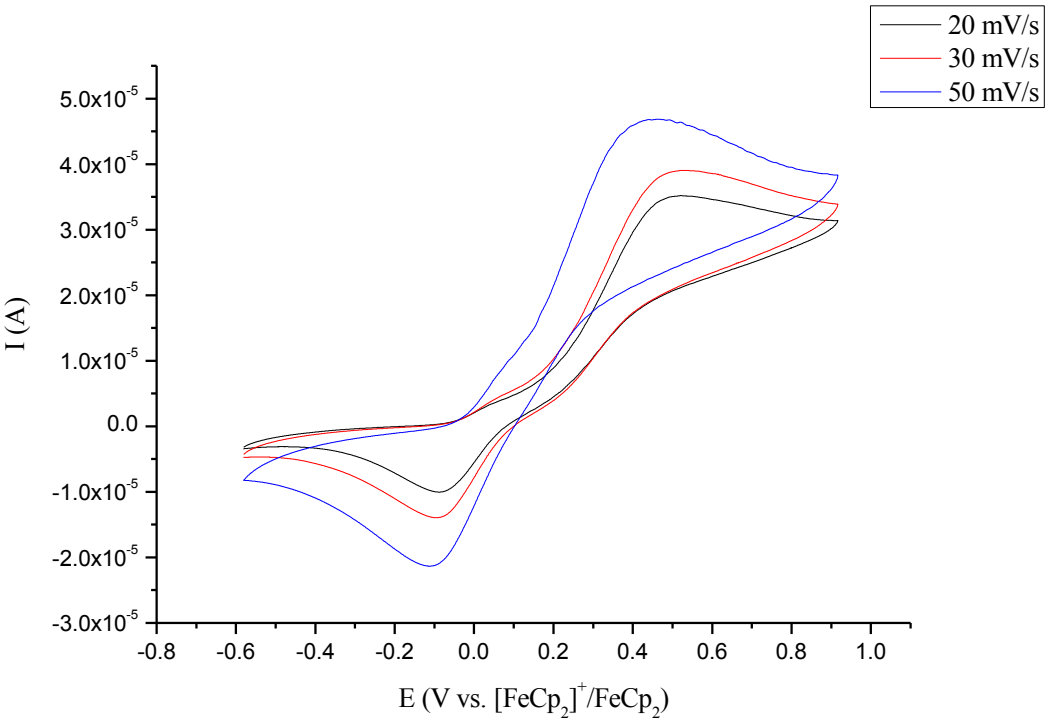

(b)

Figure 3.11. Cyclic voltammograms of **3.1** (a) and **3.2** (b) at different scan rates (50 mM in THF with 0.1 M TBAP, rt)

Further experiments confirmed that this solvent effect is caused by the coordinating nature of THF, as these ligands display the same electrochemical behaviour as in THF when only one equivalent of THF is added to the DCM solutions of the ligands. The interactions between the ligand and the THF molecule have not been understood due to difficulties in obtaining the crystal of these ligands out of their THF solution.

Ligand	ox	red	ΔE_p
3.1	0.289	-0.135	0.426
3.2	0.530	-0.0953	0.625
3.3	0.449	-0.205	0.654
3.4	0.611	-0.233	0.844

Table 3.4. Oxidation and reduction potentials (vs. $[FeCp_2]^+/FeCp_2$)[vi] of **3.1** ~ **3.4** (50 mM in THF with 0.1 M TBAP, rt, 30mV/s)

As it had been noticed that the condensation reactions of aminoferrocene and 2-diarylphosphinobenzaldehyde offered a useful tool for the synthesis of ferrocenyl-containing N-P ligands, a similar condensation reaction of $FcNH_2$ and ketone towards the formation of ligand **3.5** was also carried out (figure 3.12).

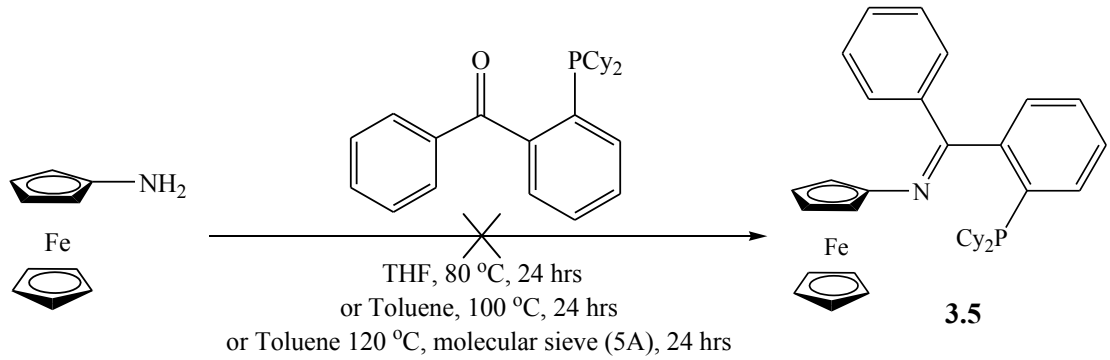

Figure 3.12. Scheme of the reaction of $FcNH_2$ and 2-(dicyclohexylphosphino)benzophenone

The reaction was first carried out in THF and heated to reflux at 80 °C, however only the starting materials were obtained after 24 hours. It was considered that this might be a result of the low reactivity of 2-(dicyclohexylphosphino)benzophenone, where electrons on the acyl group are, to a large extent, delocalized by the two adjacent phenyl groups. Consequently the

[vi] Standard Standard $E_p^{1/2}$ of ferrocene in THF taken from reference 29.

reaction mixture was then heated to 100 °C in toluene with a drop of hydrochloric acid as the catalyst. Furthermore, as the condensation reaction of amine and ketone produces water, a Dean-Stark apparatus was also used to drive the reaction towards the formation of the desired product. Nonetheless after 24 hours it was again realized that no reaction has taken place.

It has been reported that the difficult reactions of aniline and benzophenone can be overcome by the presence of molecular sieves, which can serve as a dehydrating agent as well as catalyst.[30, 31] Therefore, the reaction shown in figure 3.12 was again repeated adopting literature procedures, by heating the mixture of the reactants in toluene and molecular sieves to reflux.[32, 33] When the crude products of this reaction were examined via mass spectrometry, ^{1}H NMR and ^{31}P{H} NMR, it was observed that 2-(dicyclohexylphosphino)benzophenone and ferrocene, along with other unidentified compound(s) were obtained. There was no evidence for aminoferrocene, indicating the decomposition of this compound to ferrocene in such reaction conditions. Consequently, milder reaction conditions were tried such as using a lower temperature of 60 °C and less vigorous stirring, however there was still no evidence for the generation of **3.5** as the decomposition of $FcNH_2$ continued to take place under such reaction conditions.

As the synthesis towards **3.5** was not successful, due to both the low reactivity of the benzophenone and the low stability of aminoferrocene, efforts were not continued, and the complexation reactions of ligands **3.1** ~ **3.4**, which had been synthesized and purified successfully, to palladium was then carried out.

3.3. Synthesis of Palladium Complexes

Investigations into the coordination chemistry of the new N-P ligands synthesized with palladium were undertaken. Complexes **3.6**,[22] **3.7** and **3.8** bearing ligands **3.1**, **3.2** and **3.3**, respectively, were synthesized by stirring a solution of $Pd(CH_3CN)_2Cl_2$ and the corresponding ligand in stoichiometric amount, in DCM at ambient temperature for 5 hours (figure 3.13). After removal of the solvent and washing the crude-products with toluene, complex **3.6** was obtained as a dark green fine solid and complexes **3.7** and **3.8** were collected as dark purple solids. All the complexes are of low solubility, and incomplete dissolution of these complexes in DCM at room temperature was observed.

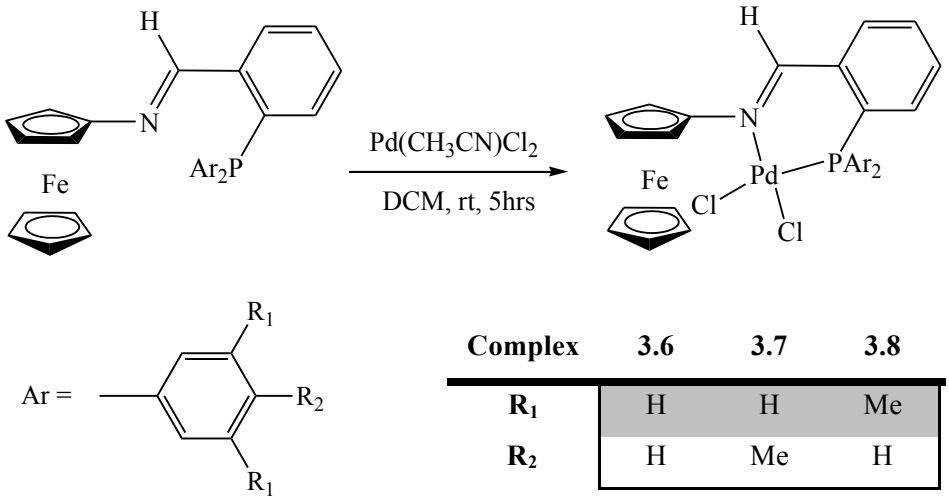

Complex	3.6	3.7	3.8
R_1	H	H	Me
R_2	H	Me	H

Figure 3.13. Scheme of the complexation reactions of ligands **3.1-3.3** to palladium

The ^1H NMR and $^{31}P\{^1H\}$ NMR spectra of each complex were compared with those of the corresponding free ligand, and changes in environments of the protons and phosphine groups were observed. Compared with the ^1H NMR spectra of the ligands, the two pseudo-triplets in the ferrocenyl region have both been shifted downfield as a result of the change in the electron environment upon complexation with the metal centre. The two singlets for the imine proton become one singlet, and this signal shifts to a lower frequency in the case of complex **3.6** but to a higher frequency in the case of **3.7** and **3.8**, indicating a closer distance from the hydrogen atom attached to the C=N carbon to the electron-rich iron atom in complex **3.6** (table 3.1 and 3.5). This is further confirmed by the crystal structure of complex **3.6** (figure 3.14). The hydrogen attached to C(7) is on the same side of the plane of the substituted Cp ring. It is also interesting to observe that the chemical shifts of (i) the proton attached to the carbon on the *6* position of the benzylidene aryl ring (C(5) for **3.6** in figure 3.14), and (ii) the protons on the unsubstituted Cp-ring vary significantly from **3.6** to **3.7** and

3.8 (table 3.5). The comparison between the ^{1}H NMR spectra of complex **3.6** and **3.7** is summarized in figure 3.15.

Complex	α-H	β-H	Cp-H	C=N-H	Aryl-H[6]	$^{31}P\{^{1}H\}$ NMR
3.6	4.85	4.29	3.72	8.90	7.79	31.7
3.7	4.55	4.18	4.14	9.98	10.01	34.3
3.8	4.58	4.28	4.20	9.89	10.71	32.5

Table 3.5. Chemical shifts (ppm) of hydrogen and phosphorus atoms in complexes **3.6-3.8**[vii]

The $^{31}P\{^{1}H\}$ NMR spectra of the complexes show a single resonance above 30 ppm, in contrast to the free ligand singlet at the region around -14 ppm (table 3.1 and 3.5). This suggests that the lone pair of electrons on the phosphorus atom are more deshielded, which is consistent with the σ-donation from the phosphine to the positively charged palladium. Elemental analyses are also consistent with the formation of these complexes.

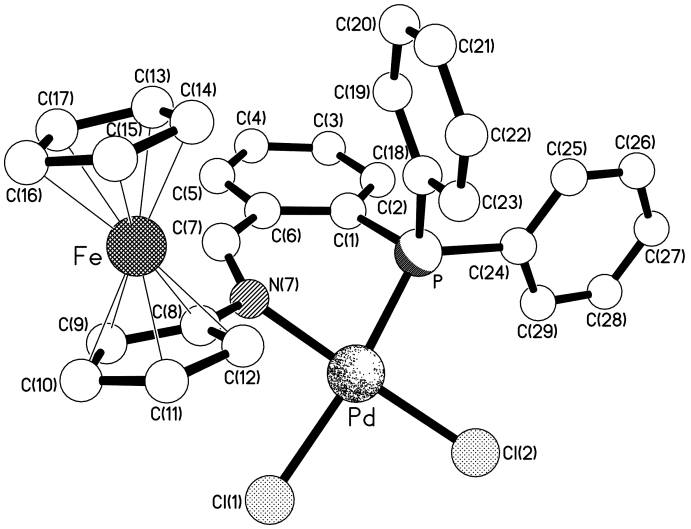

Figure 3.14. Molecule structure of **3.6**[viii]

[vii] Conditions: ^{1}H NMR ($CDCl_3$, 298 K, 400 Hz); $^{31}P\{^{1}H\}$ NMR ($CDCl_3$, 298 K, 162 Hz)

[viii] The X-ray diffraction analyses were carried out by Dr. Andrew White, Imperial College London, figure taken from reference 22.

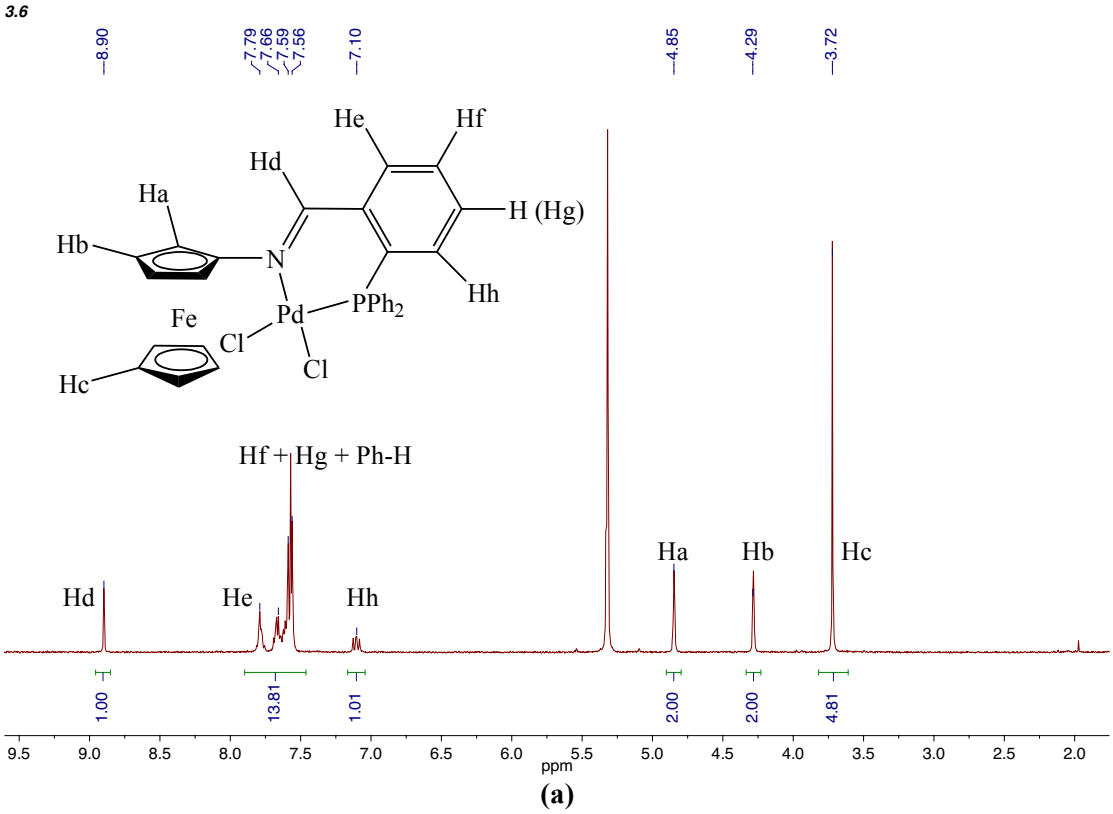

(a)

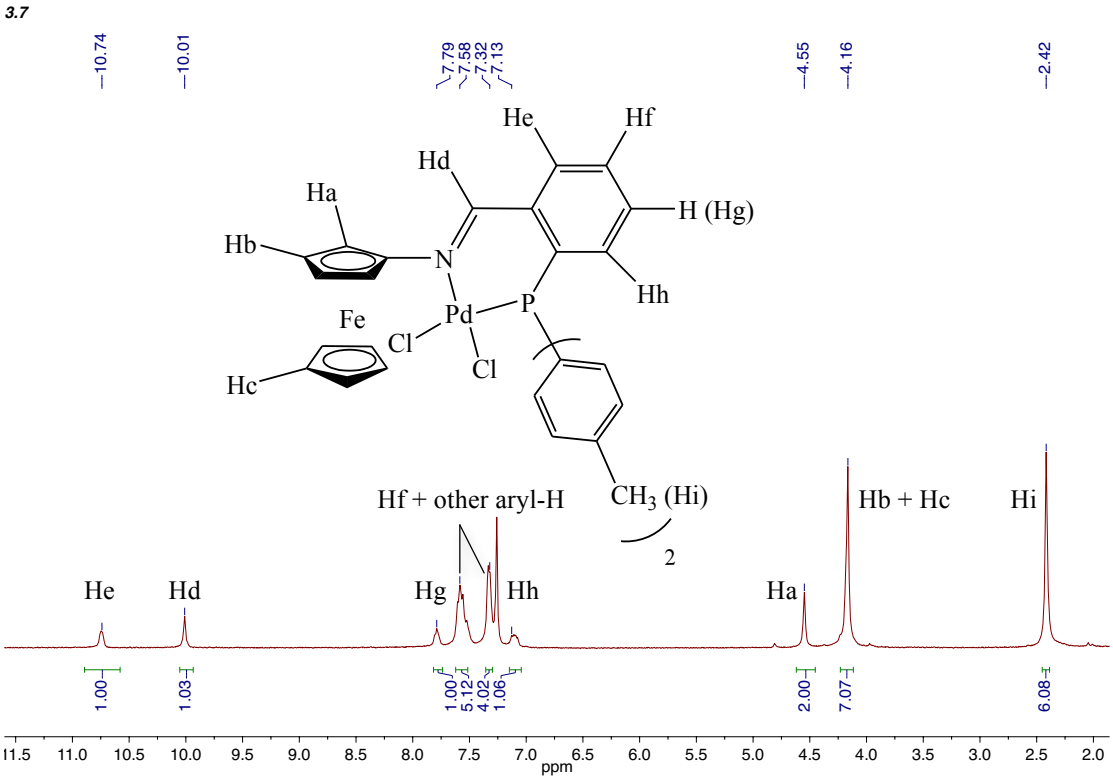

(b)

Figure 3.15. ^{1}H NMR (298 K, 400 MHz) spectra of (a) **3.6** (CD_2Cl_2) and (b) **3.7** ($CDCl_3$)

Attempts to use **3.4** to form complex **3.9** were unsuccessful. As shown in figure 3.16, different palladium sources were used for the reaction at room temperature. However, the ^{1}H NMR and $^{31}P\{^{1}H\}$ NMR spectra, as well as mass spectrum (EI) of the crude product, offer only signals for the ligand. After these crude products were washed with n-hexane, where the ligand can dissolve, the remaining solids give no resonance in their $^{31}P\{^{1}H\}$ NMR spectra, indicating that the complexation was unsuccessful.

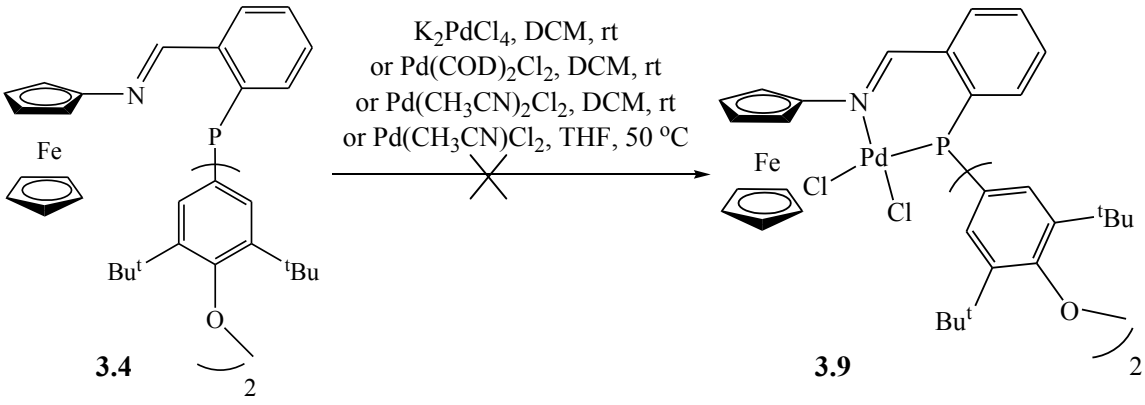

Figure 3.16. Scheme of the unsuccessful complexation reaction of **3.4**

Therefore the solvent was switched to THF, and this solution of the mixture of the ligand and the palladium precursor was heated to 50 °C. Nonetheless, instead of the desired product, a paramagnetic compound(s) was obtained according to the ^{1}H NMR spectrum of the crude product where four broad singlets were given at 1.37 ppm, 2.02 ppm, 2.39 ppm and 3.76 ppm. This is consistent with the observation that the colour of the reaction mixture changed from dark red, which is the colour of the ligand, to dark blue, which is usually the colour of ferrocenium salts, and eventually to black. In order to rule out the possibility that the formation of the ferrocenium species was caused by the involvement of oxygen during the reaction, this reaction was thereby repeated under N_2 atmosphere to prevent the oxidation of the ferrocenyl group. However, the same colour change of the reaction was noticed and the same paramagnetic product(s) was obtained.

While the peaks at 1.37 ppm and 3.76 ppm in the ^{1}H NMR spectrum may correspond to the protons on the *tert*-butyl group and ferrocenylium moiety, the other two signals cannot be assigned. Furthermore, no aryl resonance from 6 ppm to 8 ppm was observed, which indicates that the oxidation of the ferrocenyl group during the reaction might lead to decomposition of the complexation product. Nevertheless, this possibility can be ruled out as the $^{31}P\{^{1}H\}$ NMR spectrum of the crude product shows noisy signals around 38.0 ppm, which is consistent with the upfield shift of the signals for the phosphorus in **3.1** ~ **3.3** upon complexation from around -14 ppm to around 32 ppm (table 3.1 and 3.5). Therefore, the paramagnetic product could be a

palladium complex bearing the ligand **3.4**, and the higher chemical shift of 38.0 ppm of the signals in the $^{31}P\{^{1}H\}$ NMR spectrum a result of the oxidation of the ferrocenyl group. The results from mass spectrometry and elemental analysis of this crude product(s) cannot be rationalized.

3.4. Electrochemical Studies and Chemical Oxidation of Complexes

As the redox properties of the ligands **3.1** ~ **3.4** vary upon changes on the substituents on the aryl groups attached to the phosphine, cyclic voltammetry of **3.6** ~ **3.8** was carried out to electrochemically characterize these palladium complexes.

N-P ligands **3.1** ~ **3.4** were expected to be hemilabile redox-active ligands because the nitrogen atom is a weaker σ-donor than the phosphorus atom. Therefore, it was anticipated that transition metal complexes based on these ligands would undergo irreversible redox processes as the relatively weak binding between the N atom and the metal centre might not be stable towards oxidation, leading to decomposition of the complex. However, the cyclic voltammograms of **3.6-3.8** suggest that ligand-based reversible one-electron redox processes are exhibited by these complexes.

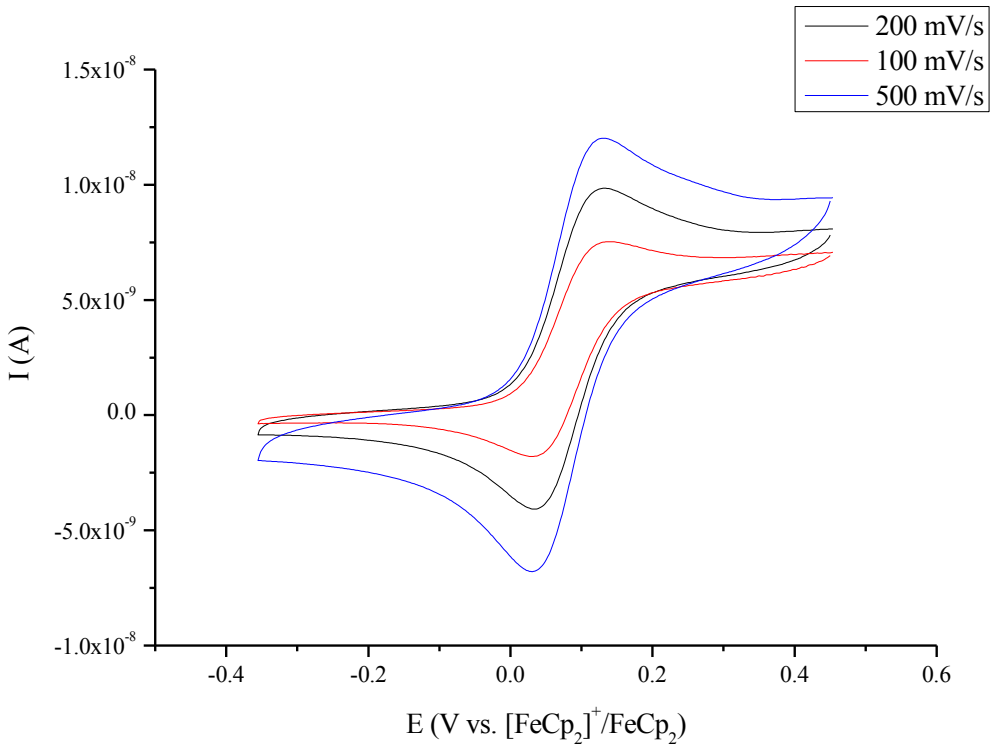

Figure 3.17. Cyclic voltammogram of complex **3.6** at different scan rate (30 mM in DCM with 0.1 M TBAP, rt)

The cyclic voltammogram of **3.6**, which indicates different redox behaviour from that of the free ligand **3.1**, is demonstrated in figure 3.17 as an example. Moreover, the values of the half-wave oxidation potentials ($E_p^{1/2}$) for these complexes are consistent with the fact that electron-rich systems are easier to be oxidized (table 3.6). This stability of these palladium complexes towards electrochemical redox processes may be explained by the stable 6-membered ring which consists of the Pd atom and the chelating P and N atoms (Pd, N, C(7), C(6), C(1), P in figure 3.14).

Complexes	E_p^a	E_p^c	ΔE_p	$E_p^{1/2}$
3.6	0.248	0.162	0.0860	0.205
3.7	0.204	0.080	0.112	0.192
3.8	0.309	0.069	0.120	0.189

Table 3.6. Selected potentials (V vs. $[FeCp_2]^+/FeCp_2$) of complexes **3.6-3.8** (30 mM in DCM with 0.1 M TBAP, rt)

Chemical oxidation of **3.6-3.8** was carried out after the electrochemical investigations on these palladium complexes. As $[FeCp_2][PF_6]$ had been proved to be an efficient redox agent as mentioned in the previous chapter, it was again used to first oxidize **3.6** (figure 3.18). After removal of the solvent, the formation of a black solid of poor solubility was obtained. The broad peaks in its ^1H NMR spectrum suggested the paramagnetic nature of the product, confirming the oxidation of the ferrocenyl group. However, no signal was observed in the $^{31}P\{^1H\}$ NMR spectra of the mixture of the product with various deuterated solvents, which included THF-d^8, acetone-d^6, DCM-d^2, DMSO-d^6 and methanol-d^4. This can either be a result of the lack of solubility of the oxidation product, or a consequence of the decomposition of complex **3.6** during the chemical redox process, where the soluble decomposition product(s) contained the oxidized ferrocenyl group but no phosphorus centres.

The oxidation of **3.6** using $[FeCp_2][BF_4]$ was also tried as the counter anion can affect the solubility. Nonetheless, although $[FeCp_2][BF_4]$ is more soluble than $[FeCp_2][PF_6]$, the product obtained did not show greater solubility. $^{31}P\{^1H\}$ NMR spectra of the samples in the same range of deuterated solvents listed above gave only noise, while ^1H NMR spectra indicated paramagnetic compounds. Moreover, the elemental analyses of the products from reactions of **3.6** and the ferrocenium salts suggested a great loss of carbon, very likely to be caused by decomposition during the oxidation reactions.

Therefore, instead of ferrocenium salts, silver salts were taken into consideration as the chemical oxidant for this type of complex. As the two chlorides in the molecule of **3.6** will be removed by the cation of Ag^{+}, leaving two empty coordination sites on the palladium centre, the compound can only be stable if the chlorides were replaced by the counter anion of the silver salt chosen. Consequently, AgOTf was used as the suitable oxidation agent, and three equivalents were added to the mixture of **3.6** in DCM to drive the reaction towards the formation of **3.6-ox** (figure 3.18). The dark orange oily solid obtained was dissolved in $CDCl_3$ to give paramagnetic ^{1}H NMR and ^{19}F NMR spectra, suggesting the successful oxidation and the coordination of triflate with palladium centre. The $^{31}P\{^{1}H\}$ NMR spectrum gave a singlet at 78.3 ppm, indicating a more deshielded electronic environment on the phosphorus atom. While no meaningful data was obtained from mass analysis of the compound, the elemental analysis supported the formation of **3.6-ox** although good consistency between the calculated and experimental values cannot be achieved due to the difficulties in drying the compound. **3.7-ox** and **3.8-ox** were prepared using the same approach.

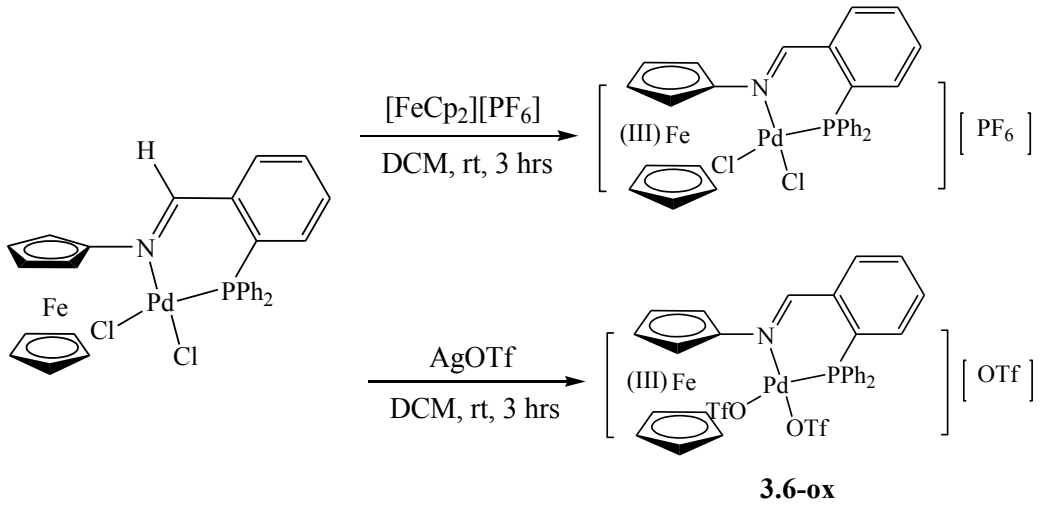

3.6-ox

Figure 3.18. Chemical oxidation of **3.6** via two different approaches

3.5. Catalytic Investigations

As both the non-oxidized and the oxidized palladium complexes containing ferrocene-based N-P ligands have been synthesized and characterized, their catalytic activities towards the alkoxycarbonylation reactions of 2-halobenyzlalcohol (X = Br or I, figure 3.19) under an atmospheric pressure of CO were investigated. Reaction conditions for the optimized yields of these reactions catalyzed by **[**$Pd(dppf\text{-}Fe^{III})Cl_2][PF_6]$ (**2.1-ox**) were used, and each of the experiments was repeated at least three times (n ≥ 3) for consistent data. The isolated yields (%) of these reactions are summarized in figure 3.20.

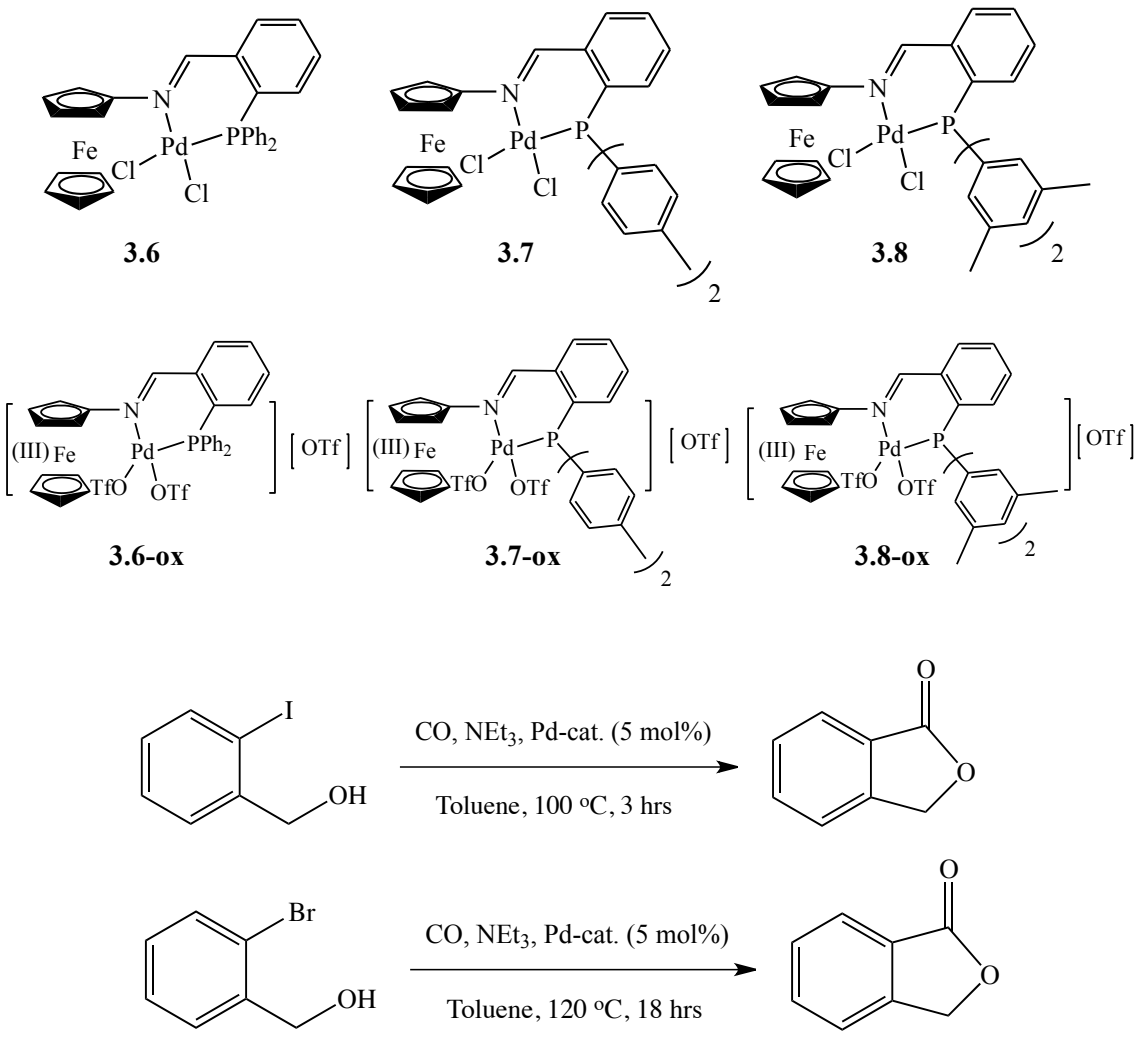

Figure 3.19. Scheme of the carbonylation reactions of 2-halobenzylalcohol (X = Br, I) catalyzed by the redox switches of **3.6/3.6-ox**, **3.7/3.7-ox** and **3.8/3.8-ox**

It can be noted from the data in figure 3.20 that (i) while these palladium complexes are generally reactive towards the alkoxycarbonylation reactions of 2-iodobenzylalcohol (I-substrate), only **3.6** exhibited weak activity for 2-bromobenzylalcohol (Br-substrate) while the

other catalysts become rather inactive; (ii) for the reactions of the Br-substrate catalyzed by the redox switches of **3.6**/**3.6-ox** and all the reactions of the I-substrate, the non-oxidized catalysts offered higher yields than their oxidized counterparts; (iii) for those non-oxidized complexes catalyzed reactions of each substrate, **3.6** afforded higher catalytic yields than **3.7** or **3.8**; and for reactions of the I-substrates catalyzed by the oxidized complexes, **3.6-ox** gave higher yields than **3.7-ox** or **3.8-ox**.

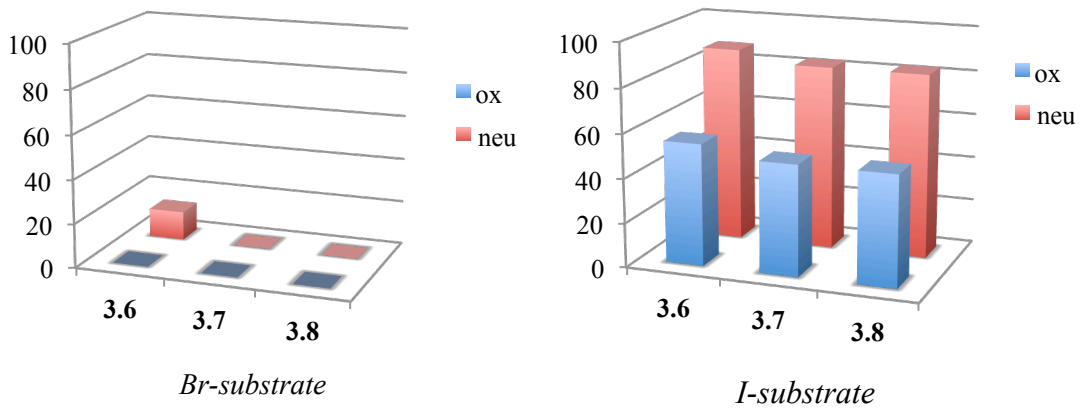

Figure 3.20. Bar charts of the catalytic yields (%) of the reactions shown in figure 3.19[ix]

The fact that these palladium complexes are reactive towards the alkoxycarbonylation of the I-substrate, but rather inactive or much less reactive towards the reactions of the Br-substrate can be understood as a result of the harder oxidative addition of the Br-substrate to palladium than the I-substrate. Based on the fact that the oxidative addition step is known to favour electron-rich palladium systems,[34-36] and that [Pd(dppf)Cl_2] (**2.1**), which bears a ferrocen -1,1'-diyl ligand offered moderate yields (54 $\pm$ 2 %) for the alkoxycarbonylation reaction of 2-bromobenzylalcohol under same conditions, dppf is compared with **3.1-3.3** (ligands of **3.6**, **3.7** and **3.8**, respectively). Firstly, each phosphine group in dppf has two phenyl units and a cyclopentadienyl (Cp) group in the ferrocen-1,1'-diyl moiety, where the iron atom is donating electrons to the Cp rings. However, the phosphine group in **3.1** bears two phenyl groups and a substituted phenyl group in conjugation with the C=N and ferrocenyl groups. As a consequence, the σ-donation to the palladium centre from the P atom in **3.6** is slightly weaker than that in **2.1**. Nonetheless, in **3.2** and **3.3** the phenyl groups are modified with electron-donating methyl groups and it is then difficult to compare the electron density on their P atoms with that in **2.1**.

[ix] Table of the data obtained given in Chapter 7. Experimental

Secondly, the other chelating atom is different in these two types of complexes. The N atom itself is a weaker σ-donor than the P atom, and as there are no electron-donating groups on the N atoms in **3.1**-**3.3**, the σ-donation from these N atoms is expected to be weaker than the P atom in dppf. This is considered the main cause for the poor performance of **3.6**-**3.8** in the alkoxycarbonylation reaction of 2-bromobenzylalcohol, as the Pd(0) species (figure 3.21) containing ligands **3.1**-**3.3** is more electron-deficient than that derived from **2.1**, and are thus, less reactive towards oxidative addition with the Br-substrate.

This weak σ-donation to palladium from the N atoms in these ferrocene-based N-P ligands also explains the lower catalytic yields of the reactions of the I-substrate afforded by the oxidized complexes than their non-oxidized versions. Based on the hypothesis proposed for the redox control in palladium-catalyzed carbonylation reactions, the effects of ligand-based oxidation are the overall results of the more difficult oxidative addition step and the easier reductive elimination, carbonyl insertion and product-formation steps. Although the oxidative addition of 2-iodobenzylalcohol to Pd(0) species derived from **3.6**-**3.8** under such conditions is not difficult as they afforded good yields for the reaction, the ligand-based oxidation of these complexes decreases the electron density on the chelating N atom and subsequently the palladium centre. This leads to a significant drop in the rate of oxidative addition, and eventually lower yields of the reaction.

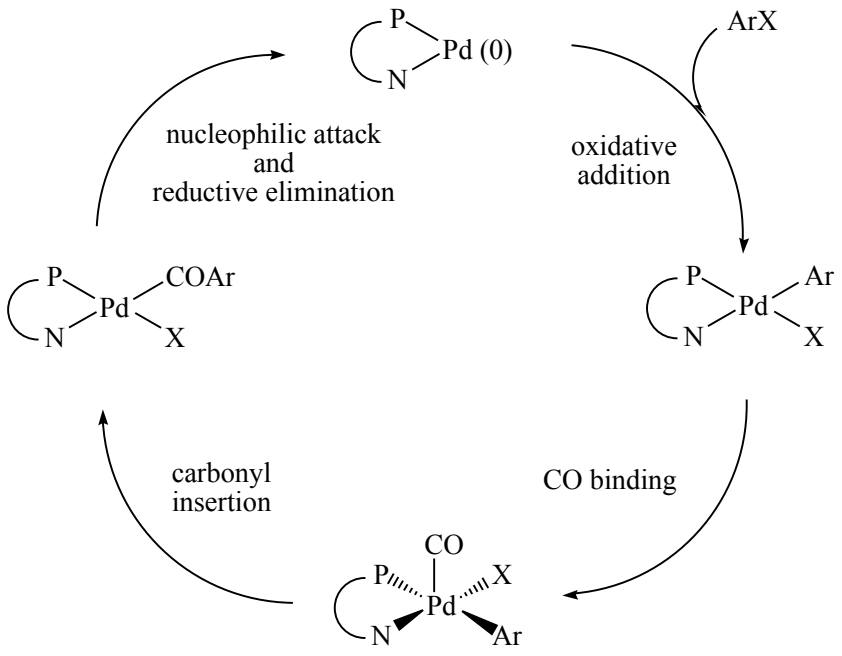

Figure 3.21. Catalytic cycle of the palladium-catalyzed alkoxycarbonylation reactions of aryl halide supported by an N-P ligand[x]

[x] Figure adapted from reference 41.

It has been mentioned in chapter 2 that the carbonyl insertion,[37] nucleophilic attack and reductive elimination[38-40] steps favour electron-deficient palladium systems. These can be used to explain the slightly higher yields afforded by **3.6** than its derivatives **3.7** or **3.8** for the reactions of the same substrate (figure 3.20). It can be seen from figure 3.19 that **3.6** possesses the most electron-deficient palladium centre compared with **3.7** and **3.8,** where the electron-donating methyl substituents in the phosphine groups lead to more electron-rich palladium systems. Therefore, while similar catalytic results were given by **3.6** ~ **3.8** for the same reaction, **3.6** could bring better yields as it offers a slightly more electron-deficient palladium centre. The higher catalytic yields of the reaction of the I-substrate afforded by **3.6-ox** than **3.7-ox** or **3.8-ox** can also be understood in the same way.

3.6. Conclusions

A series of novel ferrocenyl N-P ligands (**3.1-3.4**) and their palladium complexes (**3.6-3.8**) have been synthesized from aminoferrocene. The redox properties of both the ligands and the complexes were characterized electrochemically, and the chemical oxidations of the complexes towards the formation of ferrocenylium complexes using AgOTf as the redox agent were successfully carried out. The catalytic behaviour these palladium redox switches towards the alkoxycarbonylation reactions of 2-halobenzylalochol (X= Br, I) was investigated, and different redox control (oxidized complexes were found to afford higher catalytic yields than their non-oxidized counterparts) from that observed for the same reactions under the same conditions catalyzed by the palladium diphosphines as discussed in chapter 2 was discovered. This is considered to be a result of the different chelating atoms of the two types of complexes (N-P and P-P).

3.7. References

1. Newkome, G. R. *Chem. Rev.* **1993**, 2067.
2. Espinet, P.; Soulantica, K. *Coord. Chem. Rev.* **1999**, 499.
3. Zhang, Z. Z.; Cheng, H. *Coord. Chem. Rev.* **1996**, 1.
4. Jeffrey, J. C.; Rauchfuss, T. B. *Inorg. Chem.* **1979**, *18*, 2658.
5. Miller, P.; Long, N. J.; de Mello, A. J.; Vilar, R.; Passchier, J.; Gee, A. *Chem. Commun.*, **2006**, 546.
6. Kobayashi, J.; Mori, Y.; Okamoto, K.; Akiyama, R.; Ueno, M.; Kitamori, T.; Kobayashi, S. *Science*, **2004**, *304*, 1305.
7. Lee, C-C; Sui. G, Elizarov, A.; Shu, C. J.; Shin, Y-S; Dooley, A. N.; Huang, J.; Daridon, A.; Wyatt, P.; Stout, D.; Kolb, H. C.; Witte, O. N.; Satyamurthy, N.; Heath, J. R.; Pehlps, M. E.; Quake, S. R.; Tseng, H-R.; *Science*, **2005**, *310*, 1793.
8. Durran, S. E.; Smith, M. B.; Slawin, A. M. Z.; Steed, J. W. *J. Chem. Soc., Dalton Trans.,* **2000**, 2771.
9. Hu, X.; Chen, H.; Dai, H.; Hu, X.; Zheng, Z. *Tetrahedron*: Asymmetry **2003**, *14*, 2073.
10. Metallinos, C.; Zaifman, J.; Belle, L. V.; Dodge, L.; Pilkington, M. *Organometallics* **2009**, *28*, 4534.
11. Butler, I. R.; Quayle, S. C. *J. Organomet. Chem.* **1998**, *552*, 63.
12. Arimoto, S.; Haven, A. C., Jr. *J. Am. Chem. Soc.* **1955**, *77*, 6295.
13. Herberhold, M.; Ellinger, M.; Kremnitz, W.; *J. Organomet. Chem.* **1983**, *241*, 227.
14. Knox, G. R.; Pauson, P. L.; Willison, D.; Solcaniova, E.; Toma, S. *Organometallics* **1990**, *9*, 301.
15. Bildstein, B.; Malaun, M.; Kopacka, H.; Wurst, K.; Mitterboeck, M.; Ongania, K. –H.; Opromolla, G.; Zanello, P. *Organometallics* **1999**, *18*, 4325.
16. Shafir, A.; Power, M. P.; Whitener, G. D.; Arnold, J. *Organometallics* **2000**, *19*, 3978.
17. Van Leusen, D.; Hessen, B. *Organometallics* **2001**, *20*, 224.
18. Butler, D. C. D.; Richards, C. J. *Organometallics* **2002**, *21*, 5433.
19. Heinze, K.; Schlenker, M. *Eur. J. Inorg. Chem.* **2004**, 2974.
20. Leonidova, A.; Joshi, T.; Nipkow, D.; Frei, A.; Penner, J-E.; Konatschnig, S.; Patra, M.; Gasser, G. **2013**, *32*, 2037.
21. Smolinsky, G. *J. Org. Chem.* **1962**, *27*, 3557.
22. Guan, W. Msci. Dissertation, **2006**, Imperial College London.
23. Reichardt, C. *Solvent Effects in Organic Chemistry*, **1990** Marburg, Germany: Wiley-VCH.
24. Clarke, M. L.; Slawin, A. M. Z.; Wheatley, M. V.; Woollins, J. D. *J. Chem. Soc. Dalton Trans*. **2001**, 3421.

25. Zanello, P. *Inorganic Electrochemistry Theory, Practice and Application* RCS Publishing, 2003.
26. Zanello, P.; de Biani, F. F.; Nervi, C. *Inorganic Electrochemistry Theory, Practice and Application 2nd Edition* RCS Publishing, 2012.
27. Hirotsu, M.; Kuwamura, N.; Kinoshita, I.; Kojima, M.; Yoshikawa, Y.; Ueno, K. *Dalton Trans.* **2009**, 7678.
28. Aranzaes, J. R.; Daniel, M.-C.; Astruc, D. *Can. J. Chem.* **2006**, *84*, 288.
29. Noviandri, I.; Brown, K. N.; Fleming, D. S.; Gulyas, P. T.; Lay, P. A.; Masters, A. F.; Philips, L. *J. Phys. Chem. B* **1999**, *103*, 6713.
30. Taguchi, K.; Westheimer, F. H. *J. Org. Chem.* **1971**, *11*, 1570.
31. Ross, N. A.; MacGregor, R. R.; Bartsch, R. A. *Tetrahedron,* **2004**, *60*, 2035.
32. Stork, G.; Brizzolara, A.; Landesman, H.; Szmuszkovicz, J.; Terrell, R.; *J. Am. Chem. Soc*. **1965**, 85, 217.
33. Bonnett, R.; Emerson, T. R.; *J. Chem. Soc.* **1965**, 4518.
34. Parshall, G. W. *J. Am. Chem. Soc.* **1974**, *96*, 2360.
35. Amatore, C.; Pfluger, F.; *Organometallics* **1990**, *9*, 2276.
36. Qadir, M.; Mochel, T.; Hii, K. K. *Tetrahedron* **2000**, *56*, 7975.
37. Fleckenstein, C. A.; Plenio, H. *Chem. Soc. Rev.* **2010**, *39*, 694.
38. Hartwig, J. F. *Inorg. Chem.* **2007**, *46*, 1936.
39. Hartwig, J. F. *Acc. Chem. Res.* **1998**, *31*, 852.
40. Low, J. J.; Goddard, W. A. *J. Am. Chem. Soc.* **1986**, *108*, 6115.
41. Barnard, C. F. J., *Organometallics* **2008**, *27*, 5402.

Chapter 4

Synthesis of Ferrocene-based dimines and
Oxidative Purification of Halogenated Ferrocenes

衣带渐宽终不悔，为伊消得人憔悴。

—— 柳永

4.1. Introduction

In the previous chapters, the utilization of palladium complexes bearing ferrocene-based bidentate *N-P* and diphosphine (*P-P*) ligands has been discussed. In order to further explore the family of heteroatom-substituted ferrocenes, the design and synthesis of a series of symmetric ferrocene-based diimine (*N-N*) compounds, including bis(iminoferrocene) (figure 4.1a) and *N,N'*-substituted ferrocen-1,1'-diyl ligands (figure 4.1b), is reported in this chapter.

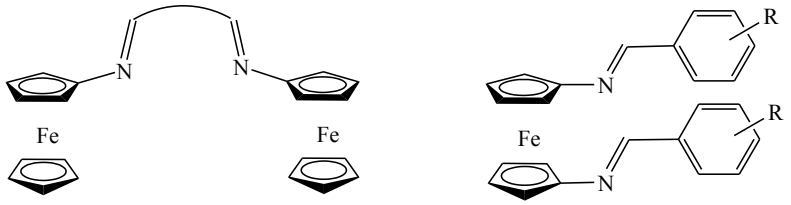

(a) (b)

Figure 4.1. Structures of the designed symmetric ferrocene-based diimine ligands

The use of diimine ligands in transition metal catalyst systems has become of great interest due to the similar properties of *N* and *P* atoms.[1-4] One of the most significant advances in transition metal-catalyzed processes supported by imine-based ligands has been α-olefin polymerization. This is catalyzed by a range of palladium and nickel complexes containing α-diimine ligands, as discovered by Brookhart *et al*.[5] Since then a new class of catalysts have been formed via variations in the substituents on the N-atoms, which impart control over the polymer molecular weight and branching. Subsequent research by Laine[6-8] and Gibson[9] have demonstrated that group 10 complexes of asymmetrical pyridyl imines (figure 4.2) were also active catalysts for ethylene polymerization.

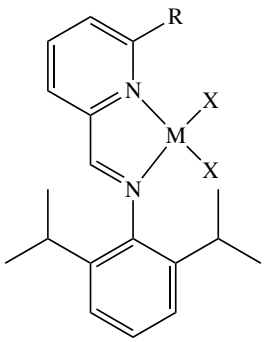

Figure 4.2. Structure of pyridyl imines developed by Gibson *et al.*
(M = Pd, Ni; R = Me, H ; X = Me, Cl, Br)[9]

Inspired by this work of Gibson and co-workers, a range of mono- and di-N-substituted ferrocene ligands, as well as their nickel and palladium complexes, have been synthesized in our laboratory (figure 4.3). Further investigations by Long *et al.* showed that the nickel dibromide complexes can be used as active dimerization pre-catalysts in the presence of MAO. [10]

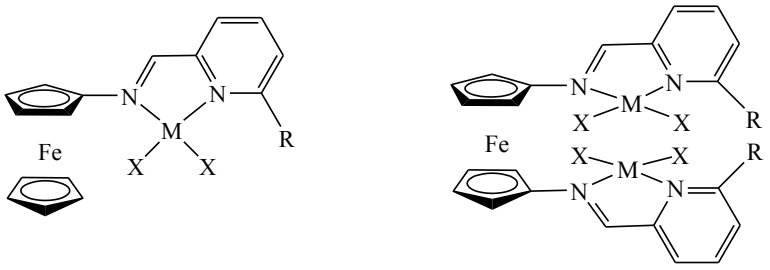

Figure 4.3. Ferrocene-derived pyridyl imine complexes synthesized in our group[10]
(M = Ni, X = Br, R = Me or H; M = Pd, X = Cl, R = H)

In 2004 Hor *et al*. reported that the dichloropalladium complex bearing the ligand N, N'-bis(benzylidene)iminoferrocene (previously synthesized by Long *et al.*)[11] exhibited high activity in the Suzuki-Miyaura cross-coupling reaction in aqueous media (figure 4.4), even after five times of recycle (94 % yield from the first use of the catalyst, and 83 % from the fifth use).[12] Therefore, it was thought to be of great interest to investigate the behaviour of ferrocene-based diimine ligands in other catalytic processes, such as palladium-catalyzed carbonylation reactions.

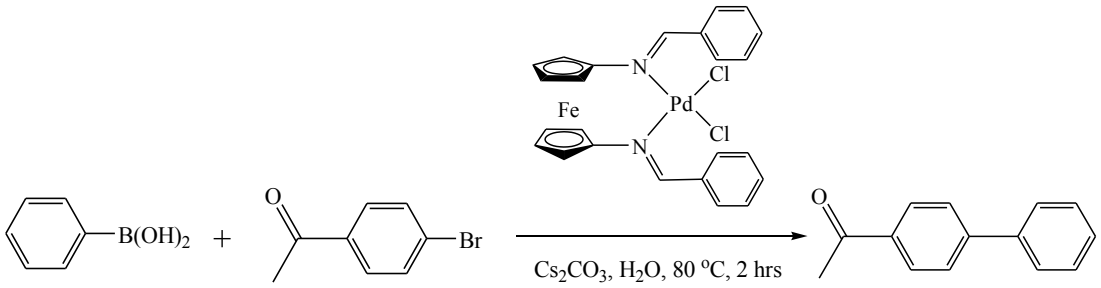

Figure 4.4. Scheme of the Suzuki-Miyaura cross-coupling reactions in aqueous media using a 1,1'-N-substituted ferrocenediyl Pd(II) complex (2 mol%) as catalyst precusor

In this chapter, the synthesis of ferrocene-imine ligands from aminoferrocene ($FcNH_2$) or 1,1'-bis(amino)ferrocene ($fc(NH_2)_2$), and their coordination chemisty is addressed. The redox behaviour of these complexes and their catalytic reactivities towards the carbonylation reaction is also discussed. In addition, a more straightforward and effective method for the

purification of 1,1'-dibromoferrocene ($fcBr_2$), which was used to prepare $fc(NH_2)_2$ (figure 4.5),[13] is demonstrated based on the difference in the oxidation potentials of $fcBr_2$ and the impurities of bromoferrocene (FcBr) and ferrocene ($FeCp_2$). This advanced separation method has been applied to purification of the whole series of monohaloferrocenes (FcX, X = F, Cl, Br, I) and 1,1'-dihaloferrocenes (fcX_2), which is also discussed in this chapter.

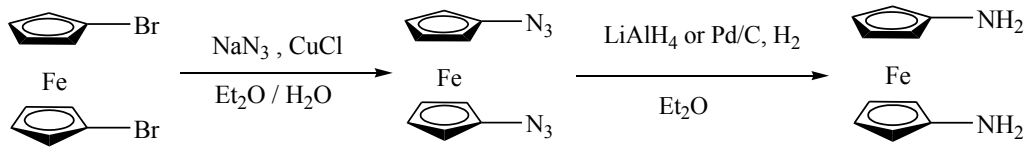

Figure 4.5. Scheme of the preparation of $fc(NH_2)_2$

4.2. Oxidative Purification of Halogenated Ferrocenes

4.2.1. Purification of 1,1'-dibromoferrocene

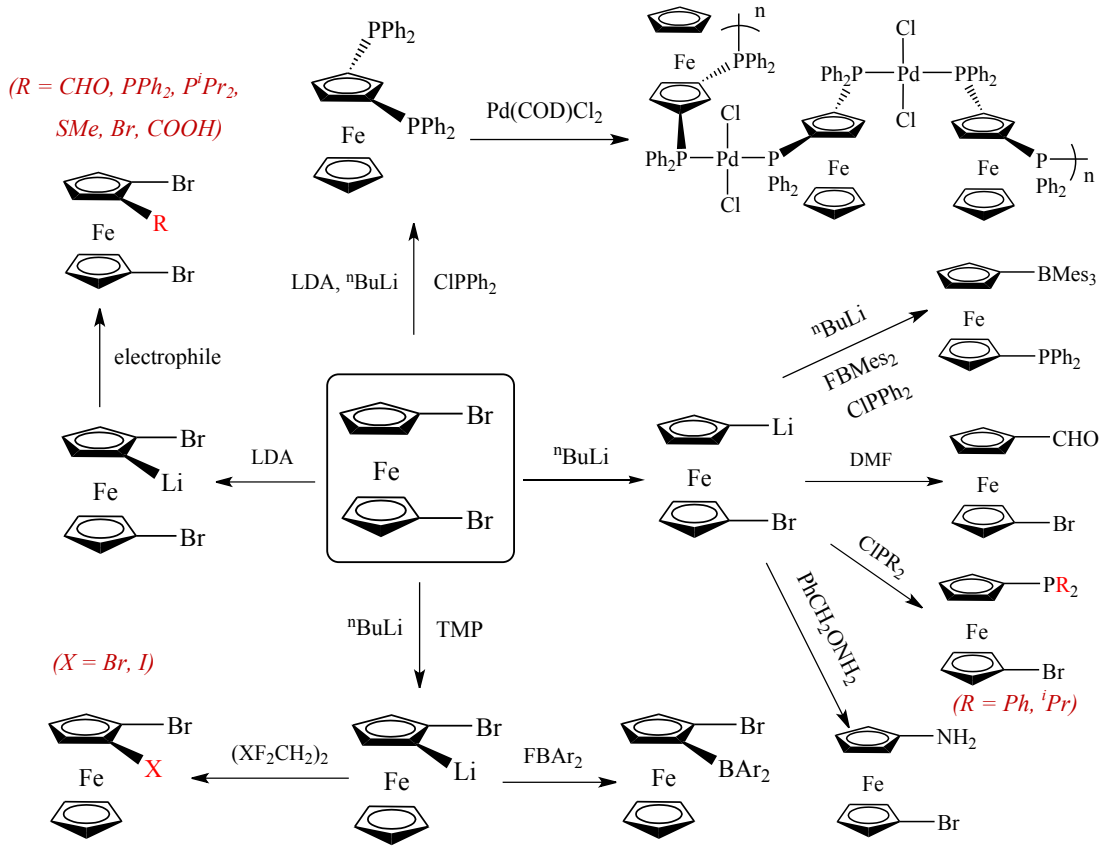

Figure 4.6. Scheme of the preparation of various materials from $fcBr_2$ (LDA = lithium diisopropylamide, TMP = trimethyl phosphate)

1,1'-Dibromoferrocene ($fcBr_2$) has found great significance in the synthesis of a large range of ferrocene-containing compounds. Via different approaches in the lithiation of $fcBr_2$, the synthetic possibilities can be extended to a variety of important reactive materials and novel compounds, including polymers (figure 4.6).[14-24]

Despite the wide application of $fcBr_2$, obtaining large quantities of this compound has not been straightforward. While synthetic routes via (bromocyclopentadienyl)thallium[25] or 1,1'-chloromercuriferrocene[26, 27] involve expensive and toxic starting materials, other routes via 1,1'-dilithioferrocene[20] and 1,1'-bis(tri-*n*-butylstannyl)ferrocene[28] lead to the formation of $fcBr_2$ in mixtures that are difficult to separate. The preparation of $fcBr_2$ in our laboratory was carried out adopting the procedure reported by Arnold *et al.*[13] It was observed that the reaction of 1,1'-dilithioferrocene-TMEDA and $(Br_2HC)_2$ in Et_2O generated a mixture of FcBr, $FeCp_2$ and $fcBr_2$. The isolation of $fcBr_2$ using conventional techniques such as sublimation,[29] column chromatography and recrystallization[13] was found to be extremely difficult. This is considered to be a result of the comparable polarities and solubilities of the three compounds in the mixture.

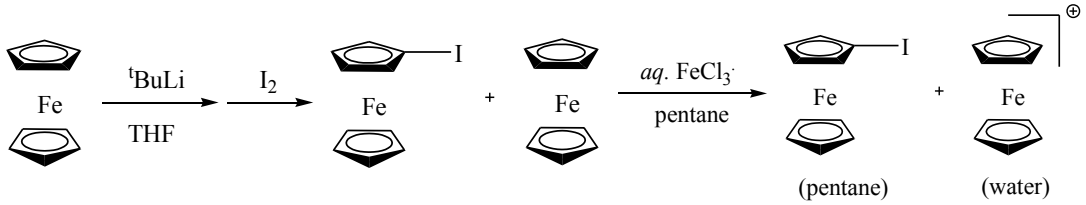

Figure 4.7. Scheme of the facile purification of FcI by Goeltz and Kubiak[30]

Similar issues with the separation of FcI from $FeCp_2$ were recently discussed in 2011 by Goeltz and Kubiak,[30] who developed an advanced purification method based on the different oxidation potentials of these two species. In their work, the large-scale reaction (14.98 g $FeCp_2$) of mono-lithiated ferrocene and elemental I_2 leads to the formation of $FeCp_2$ and FcI. As it was suggested by cyclic voltammetry of this crude product in DCM with TBAP, that the oxidation potential of FcI is 0.170 V higher than that of $FeCp_2$, they used a saturated aqueous solution of $FeCl_3$, which is a mild oxidant,[31] to repeatedly wash the solution of the mixture in pentane. Through the washings, $FeCp_2$ was converted into $[FeCp_2][Cl]$, which was readily extracted into the aqueous phase as this ionic compound was soluble in water. The aqueous layer was discarded (figure 4.7), and pure FcI was obtained without the need for difficult column chromatography or recrystallization.

In fact, the concept of separating mixtures utilizing their redox behaviour has been illustrated in 1995 by Cunningham and McMillin[32] in their work on the synthesis of FeCpCp* (pentamethylferrocene). The reaction of NaCp*, LiCp and $FeCl_2$ gave the crude products including $FeCp_2$, FeCpCp* and $FeCp^*_2$ (decamethylferrocene), whose oxidation potentials

are in descending order. Taking the mixture in Et_2O, they added excess HBF_4 to this solution, so that $FeCp^*_2$ and FeCpCp* were oxidized into [FeCpCp*][BF_4] and [$FeCp^*_2$][BF_4] as green precipitates. This solid was dissolved in EtOH and MeOH (1 : 1 volume), and treated with excess sodium ascorbate which reduced the ferrocenium species. The resulting mixture of FeCpCp* and $FeCp^*_2$ was again oxidized by HBF_4, and pure FeCpCp* was extracted from the solution (Figure 4.8).[32]

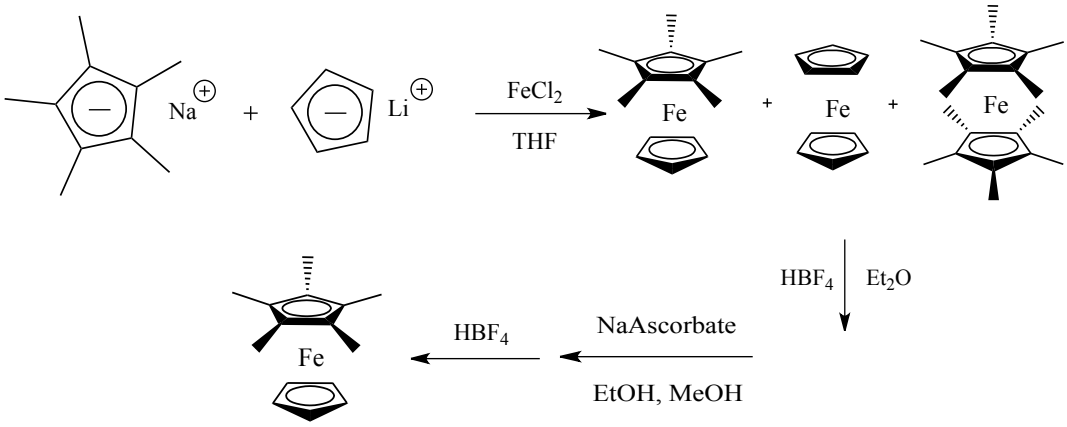

Figure 4.8. Scheme of the synthesis and isolation of FeCpCp* by Cunningham and McMillin[32]

Inspired by these findings, the oxidation potentials of $FeCp_2$, FcBr and $fcBr_2$ were determined by cyclic voltammetry, which suggested the ascending order of the $E_p^{1/2}$ of these compounds (figure 4.9).

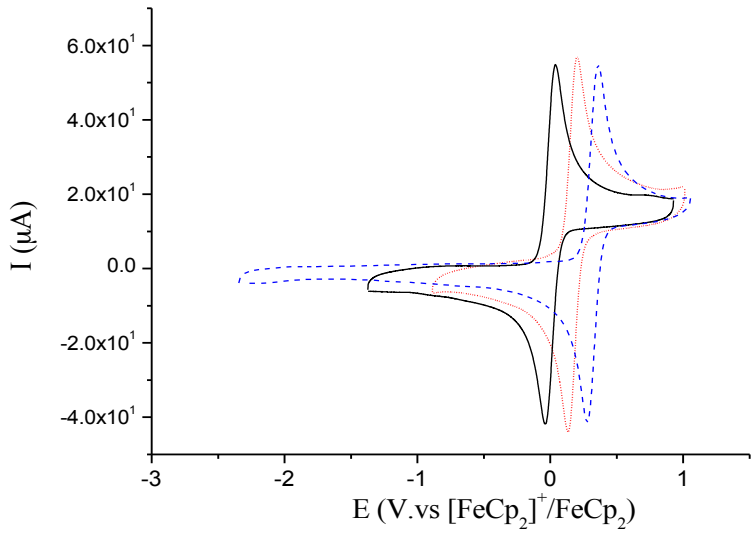

Figure 4.9. Cyclic voltammogram of $FeCp_2$/FcBr/$fcBr_2$ (10 mM in DCM with 0.1 M TBAP)

Consequently, it was expected that $fcBr_2$ could be separated from $FeCp_2$ and FcBr by oxidizing these two contaminants into their ferrocenium versions. As the purification strategy developed by Goeltz and Kubiak involves the use of a solution of an oxidant that is much cheaper and more accessible than that used by Cunningham and McMillin, $FeCl_3$ was selected as the redox agent for the isolation of $fcBr_2$.

Therefore, the mixture of $FeCp_2$, FcBr and $fcBr_2$ obtained from the initial preparation of $fcBr_2$ (molar ratio of $FeCp_2$: FcBr : $fcBr_2$ obtained from the ^{1}H NMR of this crude product was 0.02 : 1 : 2.5) was dissolved in 300 mL *n*-hexane, and this solution was treated with *aq.* $FeCl_3$ (200 mL per washing). Changes of the molar percentages of these compounds were monitored by ^{1}H NMR. It was found that selective oxidation could be achieved by simply varying the concentration of *aq.* $FeCl_3$. While only one wash with 0.2 M *aq.* $FeCl_3$ (200 mL) proved sufficient for removing $FeCp_2$ from mixtures to give a dark blue (the colour of ferrocenium salts) aqueous phase, 0.5 M (200 mL *aq.* $FeCl_3$) was found to be an inadequate concentration for the efficient elimination of FcBr as indicated in figure 4.10. However, 2.0 M *aq.* $FeCl_3$ (200 mL) to a large extent accelerated the process of isolation of $fcBr_2$. In a separate experiment, 2 washings of 200 mL saturated *aq*. $FeCl_3$ were sufficient to oxidize all contaminants from the crude product (in 300 mL *n*-hexane) of another large scale synthesis of $fcBr_2$ (started from 18.6 g / 0.1 M of ferrocene), where $FeCp_2$: FcBr : $fcBr_2$ = 0.1 : 1 : 5.5. Subsequent filtration of the organic layer through anhydrous Na_2SO_4 and a thin pad of silica followed by the removal of solvent readily gave the pure $fcBr_2$ as an orange solid in a good yield of 67% (calculated from ferrocene).

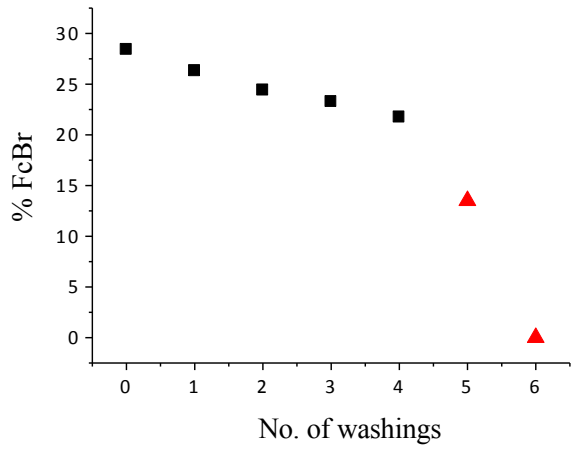

Figure 4.10. The decreasing molar percentage of FcBr in the crude product of $fcBr_2$ with 4 sequential washings of 200 mL 0.5 M (black squares) followed by 2 washings of 200 mL 2.0 M aqueous $FeCl_3$ (red triangles)[i]

[i] Percentage of mixture monitored by ^{1}H NMR ($CDCl_3$, 298 K, 400 Hz) spectroscopy.

This isolation of $fcBr_2$ in the two-phase system of water (300 mL solution of $FeCl_3$) and other organic solvents (300 mL solution of the mixture of $FeCp_2$, FcBr and $fcBr_2$), such as pentane and Et_2O has also been successfully carried out, and it was observed that after the contaminants had been removed from the organic phase, only the solution in n-hexane gave the pure $fcBr_2$ as an organic needle-like solid after the evaporation of solvent. In contrast, an orange/brown oily solid was formed when using Et_2O or pentane. Further investigations also show that the removal of solvent from the solution of pure $fcBr_2$ in toluene or dry THF also give the product as oily solid. The reason behind these facts is still unclear.

4.2.2. Oxidative purification of monohaloferrocenes and 1,1'-dihaloferrocenes

As the straightforward separation of $fcBr_2$ from FcBr and $FeCp_2$ has been developed based on the oxidation potentials of these compounds, the synthesis and purification of the whole series of monohaloferrocenes (FcX, X = I, Br, Cl, F; experimental details in figure 4.11 and table 4.1) and 1,1'-dihaloferrocenes (fcX_2, figure 4.14 and table 4.3) was carried out to extend the application of this purification method, named 'oxidative purification'.[33] These products was characterized by ^{1}H NMR, ^{13}C NMR (^{19}F NMR for FcF and fcF_2), accurate mass/elemental analyses and cyclic voltammetry (table 4.1).

The preparation of the monohaloferrocenes was first carried out, since the synthetic routes for all of these products have been reported.[30, 34-36] However, during the synthesis of FcI following the procedure by Goeltz and Kubiak[30] (scheme in figure 4.7), the formation of fcI_2 along with $FeCp_2$ and FcI was observed. As the oxidative purification only removes the contaminant that has a lower oxidation potential than the desired product, which is the main drawback of this isolation approach, the generation of fcI_2 must be avoided in the preparation of FcI. In the report by Goeltz and Kubiak, the mono-lithiation of ferrocene was realized by using 0.8 eq. of ^{t}BuLi. It was thought that a further decrease of the ratio of ^{t}BuLi/$FeCp_2$ might prevent the 1,1'-dilithiation of ferrocene,[37] which is the cause for the formation of fcI_2, so the amount of ^{t}BuLi was thereby reduced to 0.7 eq. in the reaction. Nonetheless, fcI_2 was again found in the crude product obtained, even when only 0.4 eq. of ^{t}BuLi was used in another separate experiment.

Consequently other lithiation methods had to be adopted for the synthesis of FcI. In the year of 2011, the successful mono-lithiation of ferrocene towards the formation of FcBr was reported by Sünkel and Bernhartzeder.[34] In this reference, the use of a combination of 2 eq. of ^{t}BuLi and 0.12 eq. of ^{t}BuOK at the low temperature of -78 °C was described as crucial for the exclusive mono-lithiation of ferrocene (figure 4.11). This preparation of FcBr was thus repeated at a 5 times larger scale (table 4.1, 2.0 g of $FeCp_2$ in reference) in our laboratory, and the crude product was obtained as a mixture of $FeCp_2$ and FcBr only. With the $FeCp_2$ easily

removed by washing the *n*-hexane solution (300 mL) of the mixture with 0.2 M *aq.* $FeCl_3$ (200 mL × 2), pure FcBr was collected as a brown oily solid. Therefore, this mono-lithiation method was adopted in the synthesis of FcI (figure 4.11a), and no fcI_2 was found in the crude products containing $FeCp_2$ and FcI. After the oxidative purification of this (table 4.1), pure FcI was obtained in a moderate yield of 47 % (from ferrocene), which is much higher than that reported by Goeltz and Kubiak (28 % from ferrocene).[30]

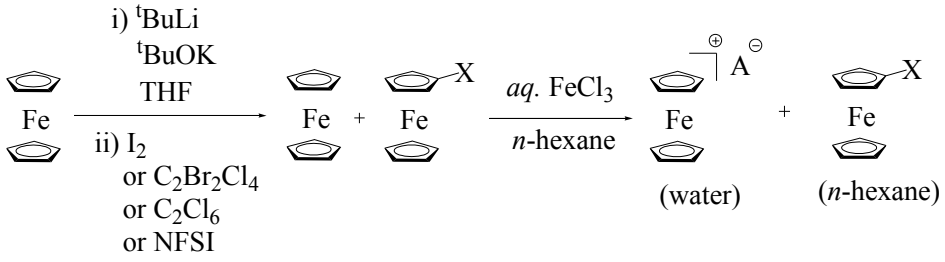

Figure 4.11. Scheme of the synthesis and purification of FcX
(X = I, Br, Cl, F; A = Cl^-, $[FeCl_4]^-$ or $[FeCl_3]^-$)

Product	Scale (g. of $FeCp_2$)	Molar ratios of FcH/FcX	$[FeCl_3]$ (M)	No. of washings	Yield (%)
FcF	1.9	1: 0.25	0.2	2	15
FcCl	4.0	1 : 17	0.2	2	64
FcBr	10.0	1 : 11	0.2	2	88
FcI	6.0	1 : 17	0.2	1	47

Table 4.1. Experimental details for the optimized oxidative purifications of FcX
(X = F, Cl, Br, I)[ii]

FcCl was then prepared following the high-yield synthetic route published by Sünkel and Bernhartzeder in the year of 2012 where the mono-lithiation of ferrocene using ^{t}BuLi and ^{t}BuOK was again mentioned. In this reference, it was reported that a mixture of $FeCp_2$, FcCl and $fcCl_2$ with the molar ratio of 5 : 94 : 1 was obtained from 1.0 g of $FeCp_2$. However, when this reaction was repeated on a larger scale (table 4.1 and figure 4.11), no formation $fcCl_2$ was observed. Although this can be understood as for the same experiments, side reactions, which lead to the generation of more by-product(s), may dominate when carried out in small-scale, it

[ii] Mixture was dissolved in 300 mL *n*-hexane and washed by 200 mL *aq.* $FeCl_3$; percentage of mixtures monitored by ^{1}H NMR ($CDCl_3$, 298 K, 400 Hz) spectroscopy; yields calculated from $FeCp_2$)

is possible that this formation of $fcCl_2$ in the reported synthesis was caused by inappropriate experimental techniques during the lithiation step. In repeated experiments towards FcBr by another member in our laboratory, it was observed that $fcBr_2$ could be obtained if ^{t}BuLi was added quickly into the suspension of $FeCp_2$ and ^{t}BuOK in THF, or the stirring of the reaction mixture was not vigorous.

In order to confirm the species in the aqueous phase after the successful oxidative purifications of FcI, FcBr, FcCl and $fcBr_2$, as well as those of fcI_2, $fcCl_2$ and FcF that can potentially be realized, the *n*-hexane solutions of pure $FeCp_2$, FcBr, FcI, FcCl were each separately washed by *aq*. $FeCl_3$ of the appropriate concentration. The resulting aqueous phases were analyzed by mass spectrometry, and peaks attributed to $[FeCp_2]^+$, $[FcBr]^+$, $[FcCl]^+$ and $[FcI]^+$ were found in the positive ion mode, whilst those assigned to $[FeCl_4]^-$ and $[FeCl_3]^-$ were observed in the negative ion mode.

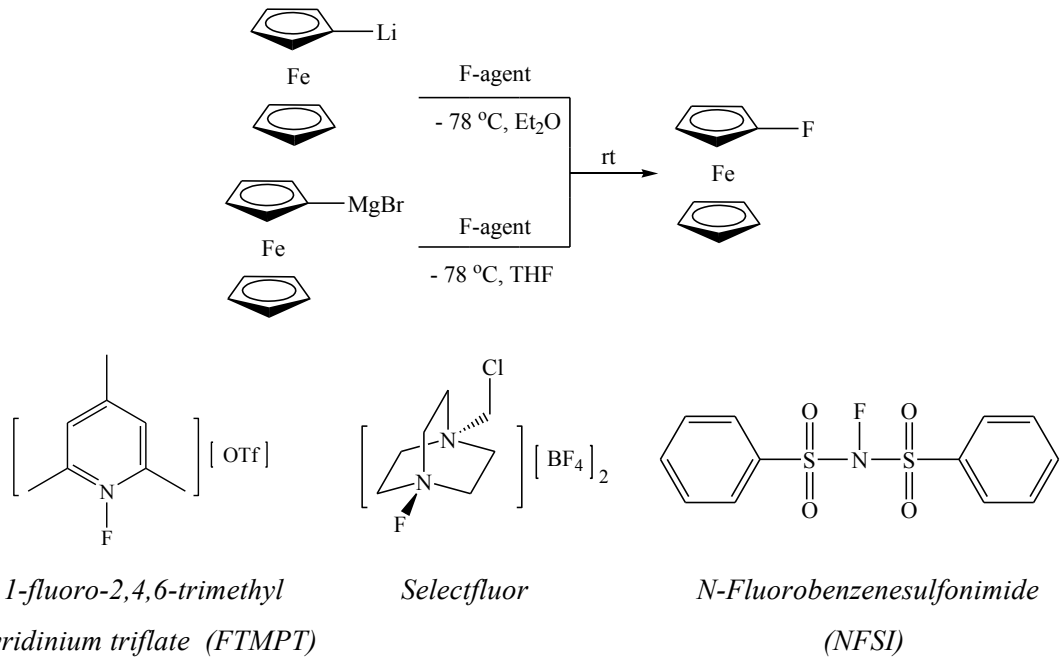

1-fluoro-2,4,6-trimethyl pyridinium triflate (FTMPT)

Selectfluor

N-Fluorobenzenesulfonimide (NFSI)

Figure 4.12. Scheme of the synthesis of FcF and the structure of the fluorinating agents used[iii]

The synthesis of FcF was not straightforward due to the difficulties in finding a successful fluorinating agent. It has been reported that FcF can be prepared via the reaction of lithioferrocene (FcLi) and perchloryl fluoride,[36] which is now not accessible due to its toxicity. Therefore, several fluorinating agents[38-40] have been tried to react with FcLi[34] or ferrocenyl Grignard reagent[41] (FcMgBr) (figure 4.12). The crude products of these reactions were

[iii] The preparation of FcLi / FcMgBr adopted from reference 34 / 38; reaction conditions adopted from reference 36, 39, 40.

quenched with H_2O, extracted with *n*-hexane, and examined by ^1H NMR spectroscopy. It was discovered that the only successful fluorination was the reaction of NFSI with FcLi (figure 4.11 and 4.12), which afforded FcF and $FeCp_2$ with the molar ratio of 4 : 1, while the other entries in table 4.2 gave only $FeCp_2$ as a result of the unsuccessful fluorine-metal exchange[42] in these reactions.

F-agent	FcM	Formation of FcF
FTMPT	FcLi	No
FTMPT	FcMgX	No
Selectfluor	FcLi	No
Selectfluor	FcMgX	No
NFSI	FcLi	15% yield from $FeCp_2$
NFSI	FcMgX	No

Table 4.2. Summary of the attempts to prepare FcF

The FcF obtained was separated from $FeCp_2$ by dissolving the mixture in 300 mL *n*-hexane and washing this solution 2 times with 0.2 M *aq*. $FeCl_3$ (200 mL, table 4.1). The organic phase was then washed with H_2O and filtered through anhydrous Na_2SO_4 and silica, and after the removal of the solvent pure FcF was obtained as a yellow solid in a yield of 15 %, which is higher than that reported in literature (10 %).[36] The ^1H NMR spectrum of FcF is shown in figure 4.13.

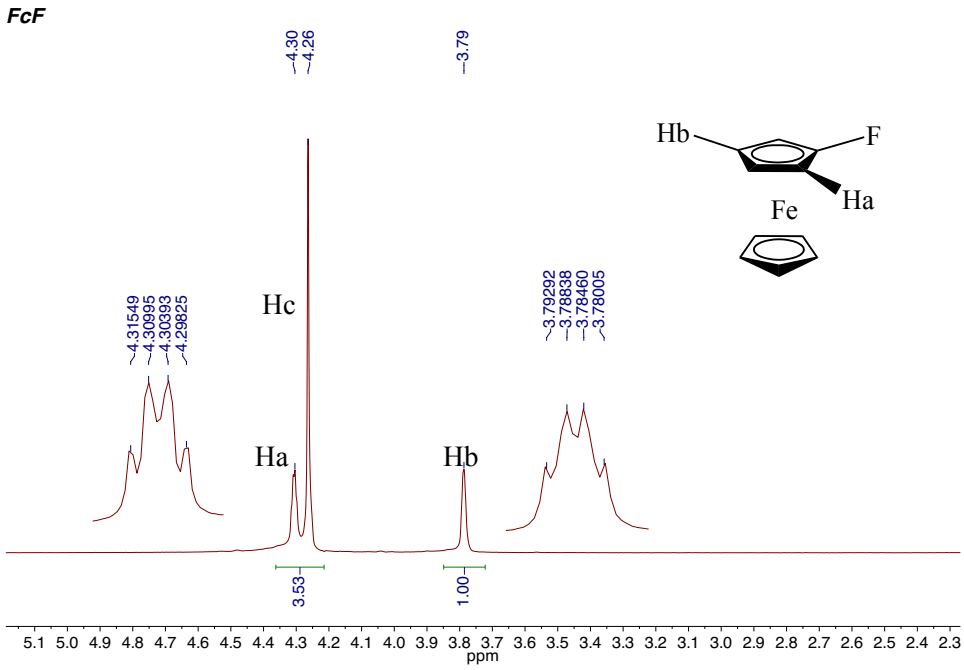

Figure 4.13. ^1H NMR ($CDCl_3$, 298 K, 400 MHz) spectrum of FcF

As the optimized oxidative purification conditions for all the monohaloferrocenes have been developed, the synthesis and isolation of 1,1'-dihaloferrocenes (experimental details shown in figure 4.14 and table 4.3) was then carried out.

The initial work of the oxidative purification of fcI_2 was carried out by another member in our laboratory.[43] In his investigations, a crude product containing $FeCp_2$, FcI and fcI_2 with the molar ratio of 0.9 : 1.5 : 1 was obtained from the reaction of 1,1'-dilithioferrocene-TMEDA (fcLi-TMEDA), which was generated from 21.14 g $FeCp_2$, and elemental I_2 in *n*-hexane. fcI_2 can be isolated by washing the *n*-hexane solution (300 mL) of the mixture 10 times with 200 mL 0.5 M *aq.* $FeCl_3$.

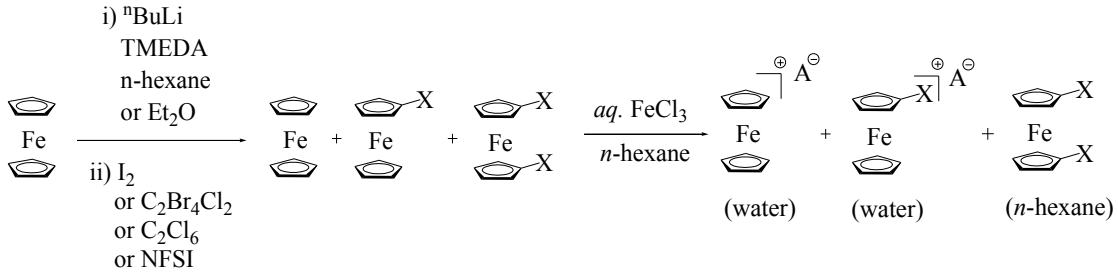

Figure 4.14. Scheme of the synthesis and purification of fcX_2
(X = I, Br, Cl, F; A = Cl^-, $[FeCl_4]^-$ or $[FeCl_3]^-$)

Product	Scale (g. of $FeCp_2$)	Molar ratios of FcH/FcX/fcX_2	[$FeCl_3$] (M)	No. of washings	Yield (%)
fcF_2	1.86	2 : 1 : 0.43	2.0	2	5
$fcCl_2$	9.30	0.1 : 1 : 43	3.0	3	75
$fcBr_2$	18.60	0.1 : 1 : 5.5	Saturated	2	67
fcI_2	21.14	0.4 : 1 : 3.8	1.5	3	19

Table 4.3. Experimental details for the optimized oxidative purifications of fcX_2
(X = F, Cl, Br, I) [iv]

This experiment was repeated at the same scale (figure 4.14), and the crude fcLi-TMEDA obtained was washed three times with *n*-hexane to remove the FcLi generated in the reaction mixture. Upon completion of this reaction, a mixture of $FeCp_2$, FcI and fcI_2 with the

[iv] Mixture dissolved in 300 mL *n*-hexane and washed by 200 mL *aq.* $FeCl_3$; percentages of mixtures monitored by ^{1}H NMR ($CDCl_3$, 298 K, 400 Hz) spectroscopy; yields calculated from $FeCp_2$)

molar ratio of 0.4 : 1 : 3.8 was obtained (table 4.3). By washing the *n*-hexane solution (300 mL) of this mixture with *aq.* $FeCl_3$ of an increased concentration of 1.5 M, $FeCp_2$ and FcI were removed after only 3 washings. In order to further simplify the purification procedure, saturated *aq*. $FeCl_3$ was also used to wash the crude product from another separate reaction towards fcI_2.

However, it was observed that saturated *aq*. $FeCl_3$ could effectively oxidize fcI_2 and cause a noticeable decrease in its yield. Compared with the purification of $fcBr_2$, where 2 washings of saturated *aq*. $FeCl_3$ is required to remove FcBr without significant loss of the desired product, it can be seen that fcI_2 is easier to chemically oxidize than $fcBr_2$. This is consistent with the fact that fcI_2 has a lower oxidation potential than $fcBr_2$ (table 4.4).

The synthesis of $fcCl_2$ via the reaction of $fcLi_2$-TMEDA and C_2Cl_6 (figure 4.14) in *n*-hexane was successful. Contaminants could be eliminated by washing the *n*-hexane solution of the crude product 3 times with 3.0 M *aq*. $FeCl_3$ (200 mL), and a good 75 % yield of $fcCl_2$ was obtained (table 4.3).

The synthesis of fcF_2 is first reported in this thesis. The reaction of $fcLi_2$-TMEDA and NFSI in Et_2O leads to the formation of $FeCp_2$, FcF and fcF_2 (figure 4.14), with $FeCp_2$ as the majority of the crude product (table 4.3). This mixture was dissolved in *n*-hexane and washed 2 times with 2.0 M *aq*. $FeCl_3$, and pure fcF_2 was collected as a yellow solid in a 5 % yield after drying the organic phase and subsequent removal of solvent. This low yield of fcF_2 is attributed to the very limited reactivity of the metal-fluorine exchange during the reaction. In attempts to improve the yield of fcF_2, the same reaction of fcLi-TMEDA and NFSI was also carried out in DME, a stronger solvent that can completely dissolve both the reactants. Nonetheless, only an increase in the rate of the reaction was observed according to the rapid colour change of the mixture. The ^{1}H NMR and ^{19}F NMR spectra of fcF_2 are shown in figure 4.15.

Since the whole series of FcX and fcX_2 have been synthesized and isolated via oxidative purification, cyclic voltammetry experiments of these compounds were carried out and their oxidation potentials were compared (table 4.4). It is quite surprising that FcF has the lowest oxidation potential among the FcX series, and that the redox potential of fcF_2 is the lowest among fcX_2, as the fluorine is the most electronegative halide group and should cause the most electron-deficient iron centre. However, this relatively low redox potential of fcF_2 was confirmed via the significant product loss observed when using a 3.0 M *aq*. $FeCl_3$ solution (200 mL) to wash the *n*-hexane solution (300 mL) of pure fcF_2. In addition, for both series of FcX and fcX_2, the brominated ferrocenes have the highest oxidation potentials, and the order of the oxidation potentials is: Br > Cl > I > F. In order to further understand the electronic effects of these halide groups on ferrocene, the ^{1}H NMR spectroscopic data of FcX and fcX_2 is summarized in table 4.4 and compared.

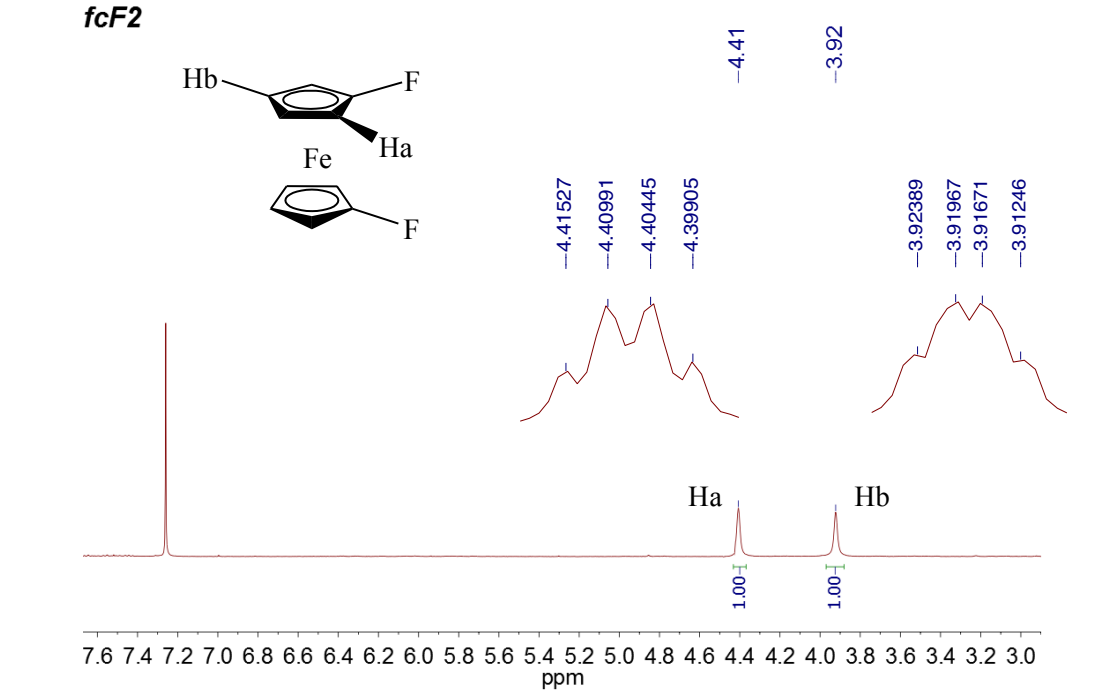

(a)

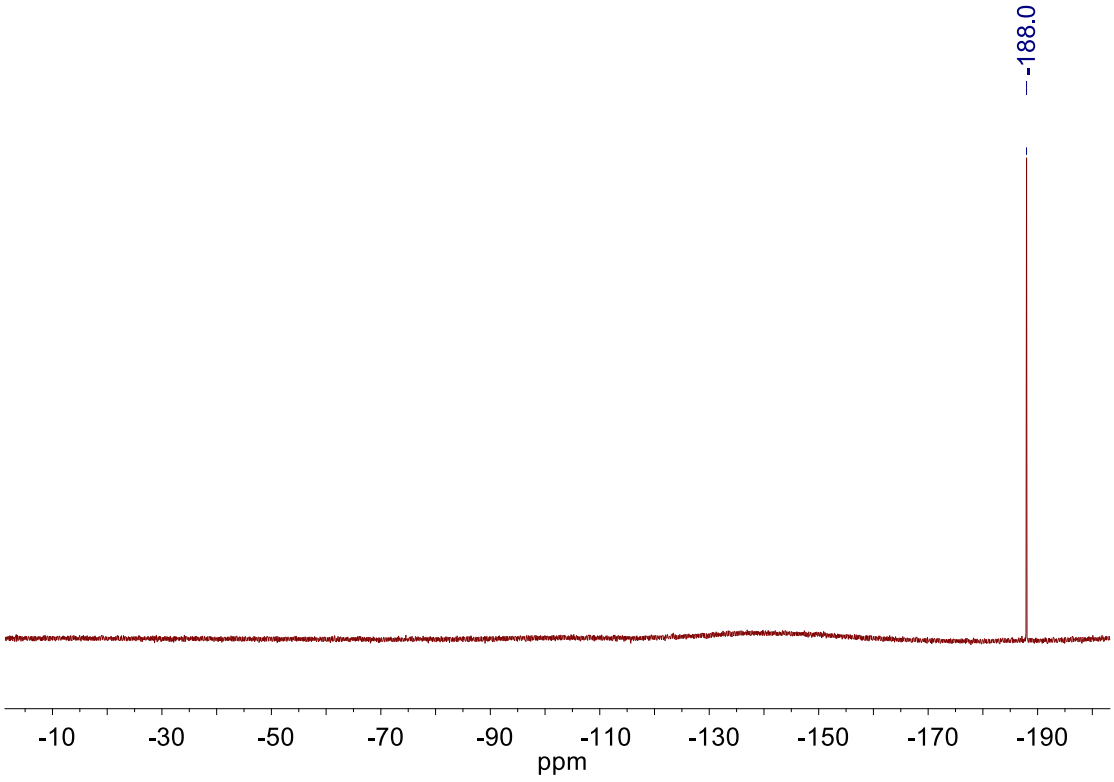

(b)

Figure 4.15. ^{1}H NMR (a) ($CDCl_3$, 298 K, 400 MHz) and ^{19}F NMR (b) ($CDCl_3$, 298 K, 377 MHz) spectra of fcF_2

It can be seen from table 4.4 that (i) signals for the protons on the unsubstituted Cp-ring of FcX, which indicates a general electronic effect of the halide substituent, shift downfield with increasing electronegativity of the halide group; (ii) signals for the protons on the substituted Cp-rings of both FcX and fcX_2 suggest overall inductive and resonance effects of the halide substituent. The chemical shift of the β-hydrogens of FcX/fcX_2, whose electronic environment is less directed by both effects, increases with decreasing electronegativity but increasing size of the halide. The chemical shift of the α-hydrogens of FcX/fcX_2, where both inductive and resonance effects are relatively strong, gives the trend: Br > I > Cl > F. (iii) It is also worth mentioning that while the signals for the protons on the substituted Cp-rings of both fluorinated ferrocenes are unresolved doublets of doublets (can also be doublets of pseudo-triplets) as a result of the strong coupling between hydrogen and fluorine (figure 4.13 and 4.15a), other halogenated ferrocenes give the characteristic pseudo-triplets (example of the ^{1}H NMR of $fcBr_2$ is shown in figure 4.16).

Compound	**$E_{1/2}$ (V vs. $[FeCp_2]^+/FeCp_2$)**	**Cp-H (s) (ppm)**	**β-H (ppm)**	**α-H (ppm)**
FcI	0.155	4.19	4.15	4.41
FcBr	0.167	4.23	4.10	4.42
FcCl	0.160	4.24	4.05	4.39
FcF	0.131	4.26	3.79 (dd)	4.30 (dd)
fcI_2	0.287	-	4.18	4.37
$fcBr_2$	0.319	-	4.17	4.43
$fcCl_2$	0.312	-	4.13	4.41
fcF_2	0.233	-	3.92 (dd)	4.40 (dd)

Table 4.4. Half-wave potentials (10 mM in MeCN with 0.1 M TBAP, rt) and ^{1}H NMR spectral data of FcX and fcX_2 (X = I, Br, Cl, F), where Cp-H is the proton attached to the unsubstituted Cp-ring[v]

Apart from these analyses, the difficulties in the storage of FcBr was also noticed. The decomposition of a fresh pure sample was observed even after overnight storage under an N_2 atmosphere in the freezer, with the container completely shielded from light. This is quite unusual, as other halogenated ferrocenes are fairly air- and moisture-stable. The reason for this phenomenon is still unclear.

[v] (a) Oxidative purification of FcBr, FcI, $fcBr_2$ and fcI_2 has been published (reference 33). (b) Experimental detals for FcCl, FcF, $fcCl_2$ and fcF_2 can be found in chapter 7 Experimental.

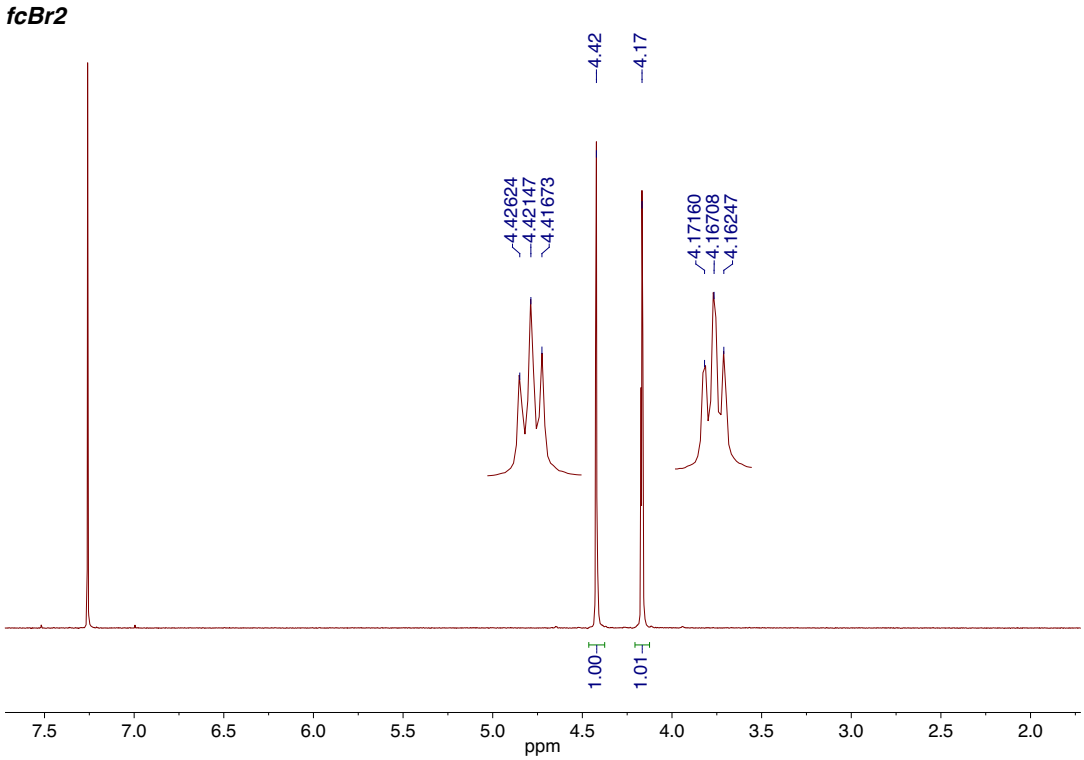

Figure 4.15. ^{1}H NMR ($CDCl_3$, 298 K, 400 MHz) spectrum of $fcBr_2$

4.3. Synthesis of Ferrocenyl-incorporated Diimines

The iron and cobalt complexes bearing the same pincer ligand shown in figure 4.17 were previously synthesized in our laboratory.[44] These complexes were found to be catalytically reactive towards ethylene polymerization, and undergo ligand-based oxidation, which leads to their ferrocenylium versions. It was considered that stronger electronic effects could be induced on the metal centre upon ligand-based oxidation if the ferrocenyl redox moieties were directly attached to the chelating N atoms.

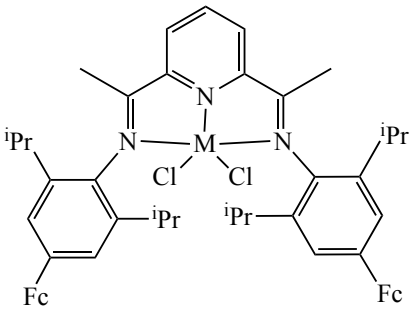

Figure 4.17. The redox-active cobalt and iron catalysts for ethylene polymerization[44]
(Fc = ferrocenyl group)

As has been mentioned in chapter 3 that the condensation reactions of $FcNH_2$ and aldehydes offer a useful tool for the syntheses of ferrocenyl-incorporated imine compounds, an analogue (**4.1**) of the pincer ligand shown in figure 4.17 was prepared via the reaction of $FcNH_2$ and 2,6-pyridinedicarbaldehyde (figure 4.18). A red/purple product was obtained in a 95 % yield. The formation of **4.1** was confirmed by the ^{1}H NMR and ^{13}C NMR (figure 4.20) spectra of the product, as well as mass spectrometric and elemental analyses.

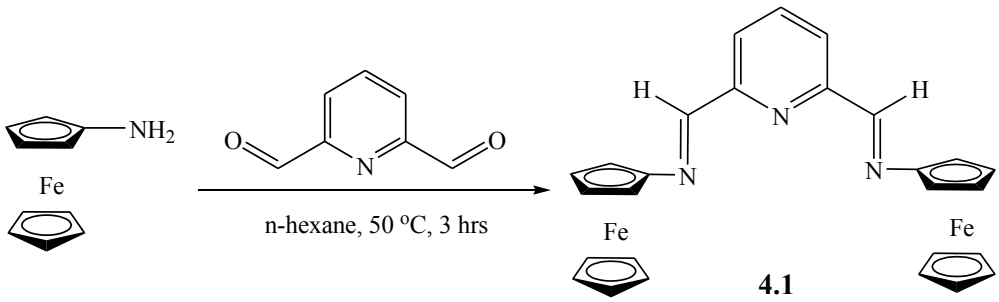

Figure 4.18. Scheme of the preparation of **4.1**

The cyclic voltammogram of **4.1** (figure 4.19) shows two consecutive reversible redox processes with their $E_p^{1/2}$ at -0.269 V and 0.173 V (vs. $[FeCp_2]^+/FeCp_2$), which are assigned to the two conjugated ferrocenyl moieties in **4.1**.

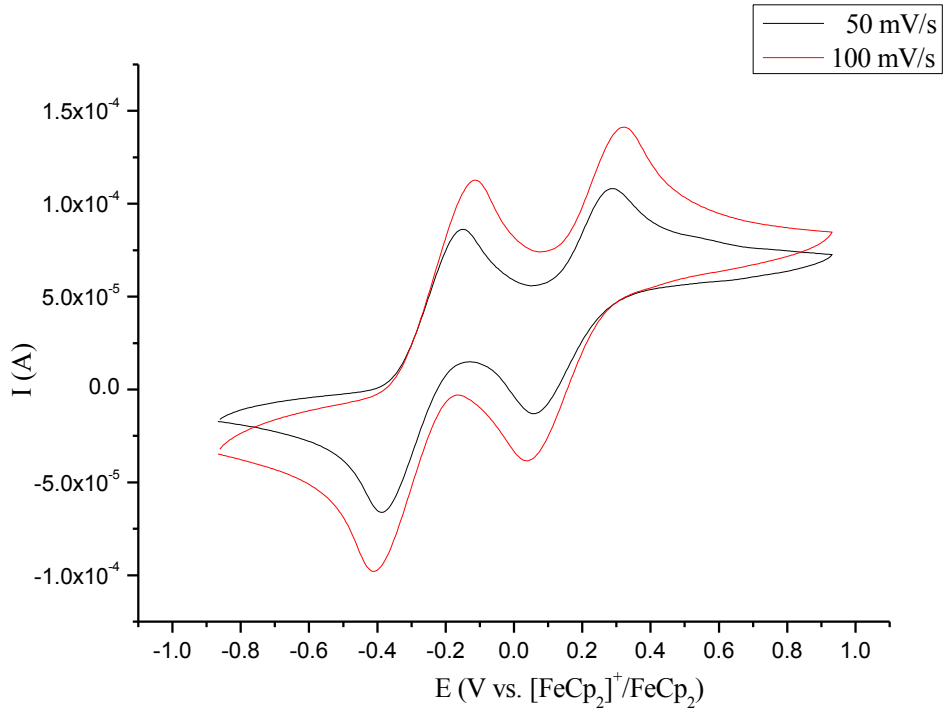

Figure 4.19. Cyclic voltammogram of **4.1** (30 mM in DCM with 0.1 M TBAP, rt) at different scan rates

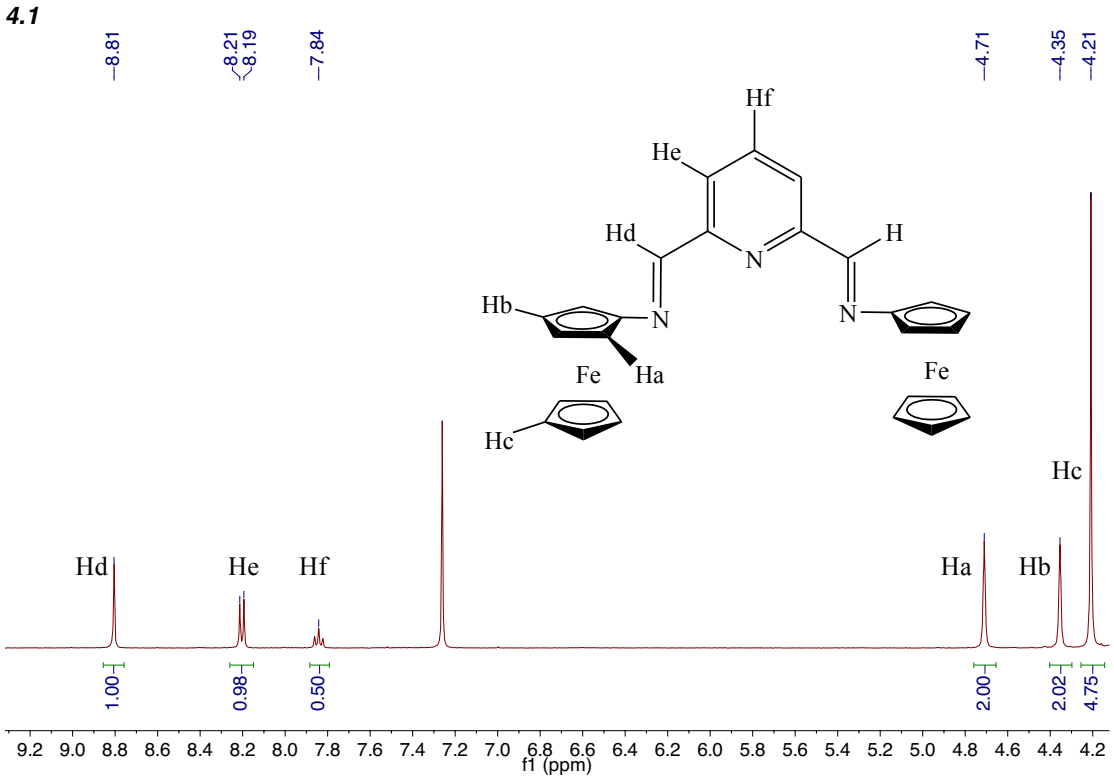

(a)

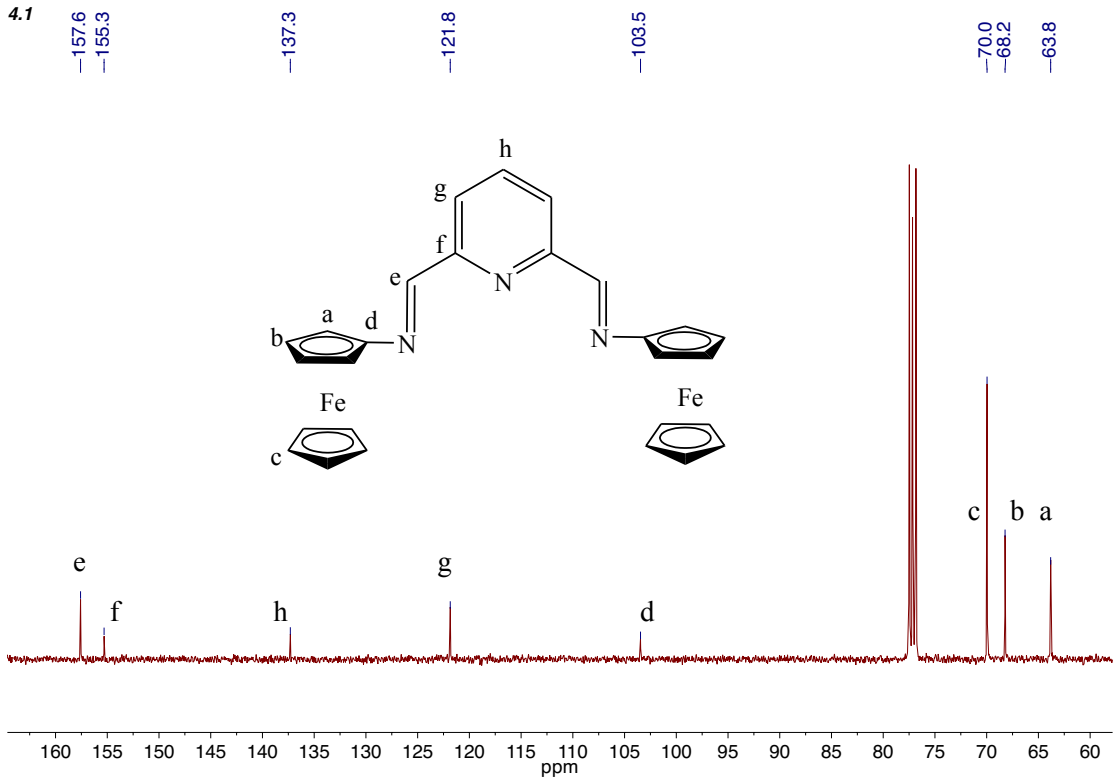

(b)

Figure 4.20. ^{1}H NMR ($CDCl_3$, 298 K, 400 MHz) and ^{13}C NMR ($CDCl_3$, 298 K, 100 MHz) spectra of **4.1**

As this new ligand has been both structurally and electrochemically characterized, the synthesis of **4.1**-containing transition metal complexes were then carried out (figure 4.21). However, the complexation of **4.1** was found to be complicated. Using the same metal sources and the same reaction conditions for the synthesis of the cobalt complex shown in figure 4.17,[44] a paramagnetic compound was obtained from the reaction of **4.1** and $CoCl_2$ according to the ^1H NMR spectrum of the crude product which gave broad signals. This is consistent with the dark blue colour of this product, which is the characteristic colour of the ferrocenium salts, suggesting the ferrocenyl moieties in **4.1** or a **4.1**-containing complex have been oxidized to their ferrocenylium versions. These observations are quite similar with the complexation of **3.4** to palladium as discussed in chapter 3.

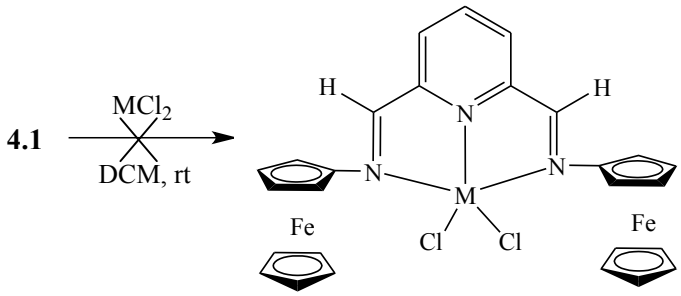

Figure 4.21. Scheme of the unsuccessful complexation of **4.1** to cobalt (M = Co) or iron (M = Fe)

The reactions of **4.1** and $FeCl_2$ also afforded similar dark blue paramagnetic products. The ^1H NMR spectra of the crude products obtained from the complexation reaction of **4.1**, as well as the results from their mass and elemental analyses cannot be rationalized. The cause of the oxidation occurred during the reaction is still unclear.

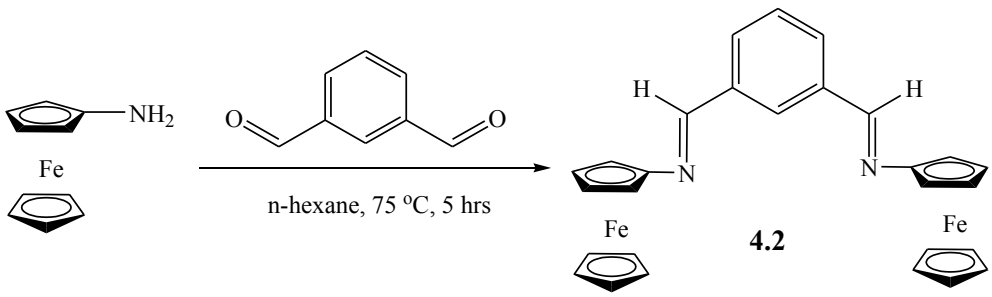

Figure 4.22. Scheme of the synthesis of **4.2**[45]

The synthesis of **4.2** as an analogue of **4.1** was carried out since **4.2** has two coordination sites and is thus a suitable ligand for a Pd(II) complex.[45] It was observed that the reaction of $FcNH_2$ and isophthalaldehyde (figure 4.22) required a higher temperature and

longer time (75 °C and 5 hours) than that for the preparation of **4.1** (55 °C and 3 hours), suggesting a higher activity of 2,6-pyridinedicarbaldehyde than isophthalaldehyde towards the reaction of $FcNH_2$.

The condensation reaction of a primary amine and an aldehyde can be described as the nucleophilic addition of the primary amine to the carbonyl group followed by the transfer of one of the protons from nitrogen to oxygen and subsequent elimination of water.[45] Therefore, for the reactions of the same primary amine, aldehydes with more electron-deficient acyl carbon atoms are preferred as they are more reactive towards nucleophilic addition. This explains the higher reactivity of 2,6-pyridinedicarbaldehyde than isophthalaldehyde, as the electron density on the acyl carbon atoms in 2,6-pyridinedicarbaldehyde are lower due to the negative inductive effect of the N atom on the pyridine ring.

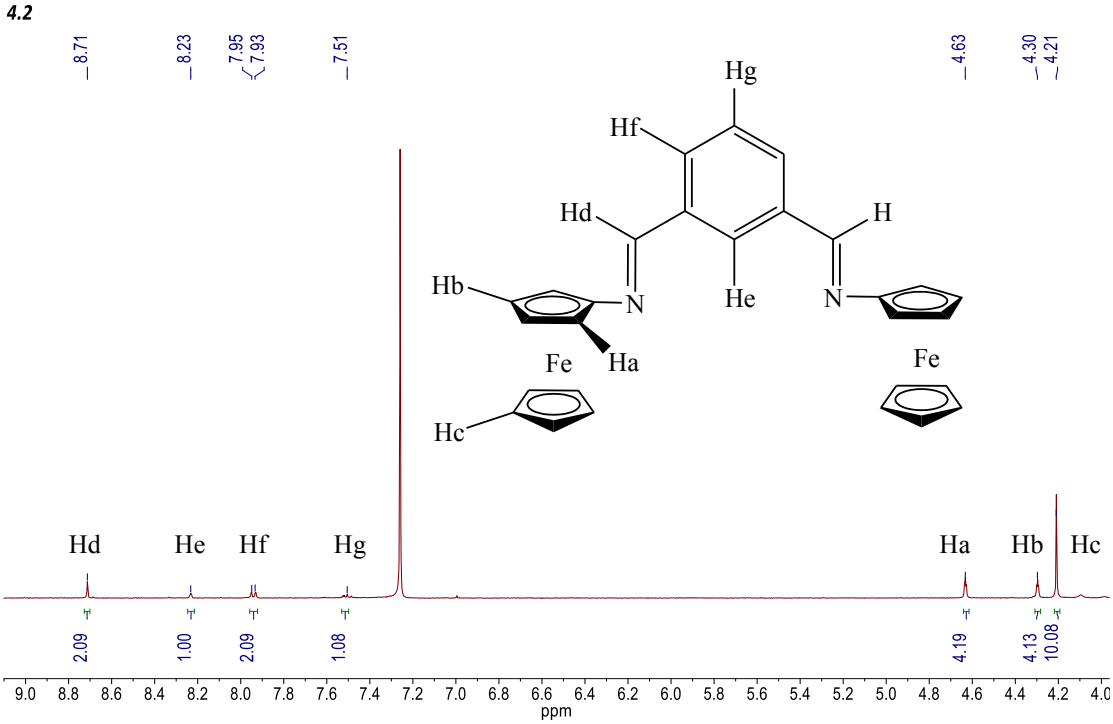

Figure 4.23. ^{1}H NMR ($CDCl_3$, 298 K, 400 MHz) spectrum of **4.2**

The formation of **4.2** was confirmed by the ^{1}H NMR (spectrum shown in figure 4.23) and ^{13}C NMR spectra, mass spectrum and elemental analysis of the red product, which was obtained in a 92 % yield. The cyclic voltammogram of this diimine ligand is given in figure 4.24, where two reversible redox processes with the $E_p^{1/2}$ of 0.093 V and 0.865 V (vs. $[FeCp_2]^+/FeCp_2$) were found, indicating quite a different redox behaviour from **4.1**.

The complexation of **4.2** to palladium was found to be complicated. While the elemental analysis of the dark purple product obtained from the reaction shown in figure 4.25 indicated the formation of **4.3**, the ^{1}H NMR spectrum of **4.3** in $CDCl_3$ suggested the decomposition of

4.3 into **4.2** and other unidentified species. In order to rule out the possibility that **4.3** is air-sensitive in solution, the NMR sample was also prepared in a N_2 atmosphere. Nonetheless, a very similar spectrum was obtained. Results from mass spectrometry also indicated the decomposition of **4.3**.

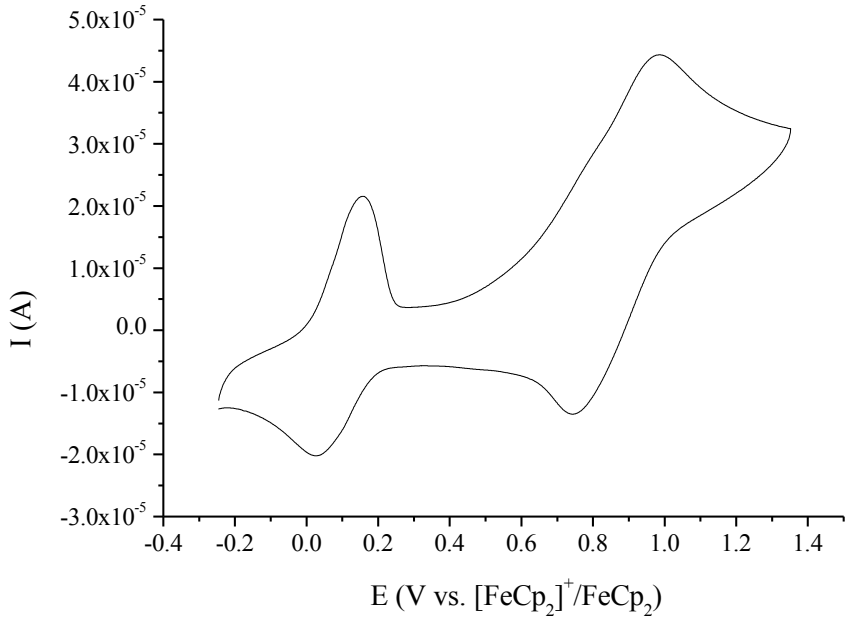

Figure. 4.24. Cyclic voltammogram of **4.2** (50 mM in DCM with 0.1 M TBAP, rt, 100 mV/s)

Therefore, it is considered that **4.3** might decompose in solution, giving **4.2** as the decomposition product. However, the cyclic voltammogram of **4.3** (50 mM in DCM with 0.1 M TBAP, rt) show no redox process, suggesting different species from **4.2** in this investigated solution. Furthermore, after removal of the solvent from the NMR sample of **4.3**, the same dark purple product was obtained. This was washed with *n*-hexane to extract **4.2**, and the solvent was removed from this colourless *n*-hexane layer before $CDCl_3$ was added. However, no product was obtained according to the ^{1}H NMR spectrum of this $CDCl_3$ layer. This indicated that no actual decomposition of **4.3** had occurred, although the ^{1}H NMR spectrum of **4.3** lead to an opposite conclusion.

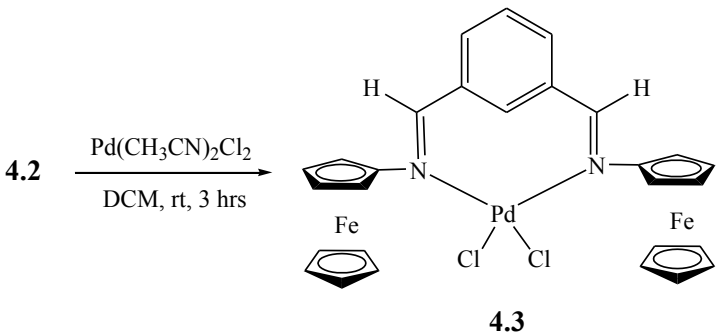

4.3

Figure 4.25. Scheme of the complexation of **4.2** to palladium

While the instability of **4.3** in solution is difficult to explain, it was considered that the atomic radius of the palladium atom might be too small for effective binding with **4.2**. Therefore, another metal of square planar molecular geometry of a larger size than palladium, platinum, was used to complex with **4.2**.

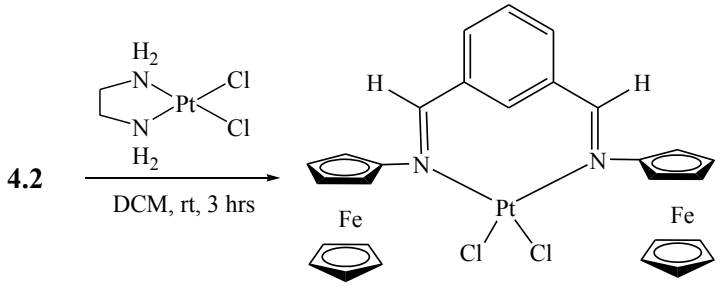

Figure 4.26. Complexation of **4.2** to platinum

A black slurry was obtained from the reaction shown in figure 4.26, which was found insoluble in common organic solvents including DMSO, THF, DCM. As a consequence, a ^{1}H NMR spectrum with noticeable signals cannot be obtained. The binding of **4.2** with platinum was not suggested by mass spectrometry as only the signal for **4.2** found in the mass spectrum of the complexation product. This crude product was then washed 3 times with THF and DCM to remove possible contaminants, and sent for elemental analysis. Anal. Calcd. for $C_{28}H_{24}Cl_2Fe_2N_2Pt$: C 43.87, H 3.16, N 3.66. Found: C 40.61, H 2.85, N 1.26. While the experimental carbon percentage is found to be more than 3 % away from the calculated values, significant decreases in the percentage of all the examined atoms were noticed when these found values were compared with those from the analysis of **4.2** (Anal. Calcd. for $C_{28}H_{24}Fe_2N_2$, C 67.22, H 4.84, N 5.60). This suggested the complexation of **4.2** to a platinum centre, although the product cannot be further purified due to its poor solubility.

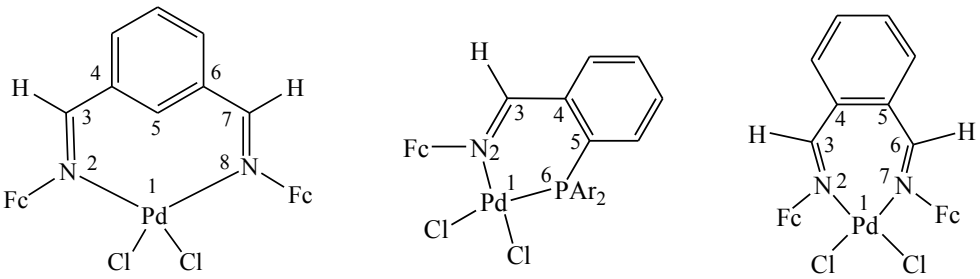

4.3 **3.6** **4.4**

Figure 4.27. Structures of complexes **4.3**, **3.6** and the proposed structure of **4.4**

As the complexation of **4.2** to platinum was also found complicated, the ligand, rather than the metal, was considered as the main cause of the instability of **4.3** in solution. As it can be seen from figure 4.25, an 8-membered ring is formed by the palladium and other atoms on the ligand backbone (figure 4.27). For the palladium complexes bearing the ferrocenyl N-P ligands reported in chapter 3, which are stable in solution, 6-membered rings are given (**3.6** is given in figure 4.27 as an example). It was thought that the 6-membered ring structure of **3.6** might be more stable than the 8-membered ring structure of **4.3**, which can explain the higher stability of **3.6** in solution. Therefore, the 7-membered ring analogue of **4.3** (**4.4** in figure 4.27) was considered as a possible stable palladium complex, and the synthesis of the ligand in **4.4** was carried out (figure 4.28).

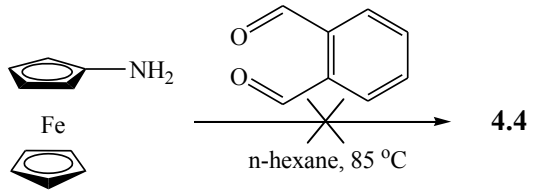

Figure 4.28. Scheme of the unsuccessful synthesis of **4.4**

It was observed that the condensation reaction of $FcNH_2$ and phthaldialdehyde required a higher temperature of 85 °C than the reaction of $FcNH_2$ and isophthalaldehyde (figure 4.22), suggesting the steric hindrance of the two *ortho*-related carbonyl groups in phthaldialdehyde (figure 4.28).

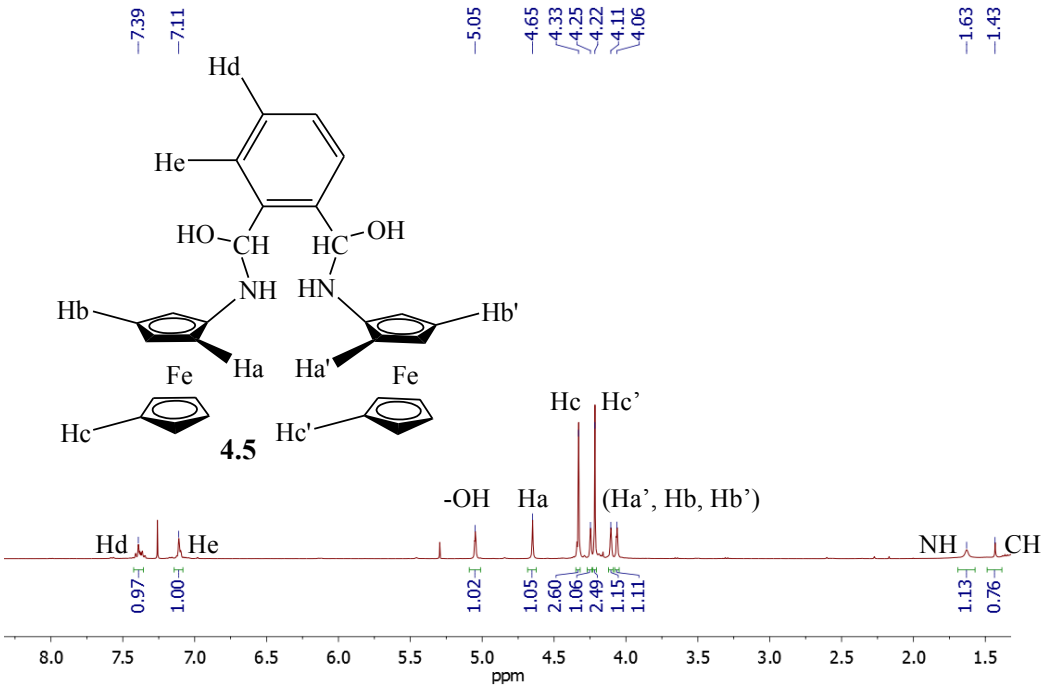

Figure 4.29. ^1H NMR ($CDCl_3$, 298 K, 400 MHz) spectrum of the product obtained from the reaction shown in figure 4.28

However, the ^{1}H NMR spectrum of the crude product obtained (figure 4.29) from the reaction suggested the formation of a hemiaminal compound **4.5**, rather than **4.4**. Although this dark yellow slurry could not be dried properly and thus was not a good sample for elemental analysis, the electrospray spectrum of this crude product also suggested the formation of **4.5**. According to the mechanism of the amine carbonyl condensation reactions,[46] **4.5** undergoes elimination of water to give **4.4**. Therefore, drying agents, including Na_2SO_4 and molecular sieves, and Dean-Stark apparatus were used to drive the reversible reaction shown in figure 4.28 towards the formation of **4.4**. However, **4.5** was again obtained, even when this reaction was carried out in toluene at 110 °C.

Efforts were not continued as this compound cannot be isolated properly, and the synthesis of another type of ferrocene-based diimine ligands, N,N'-substitued ferrocene-1,1'-diyl ligands, was carried out.

4.4. Synthesis of Ferrocen-1,1'-diyl-containing Diimines

4.4.1. Synthesis of 1,1'-bis(amino)ferrocene

The preparation of the starting material for the synthesis of N,N'-substituted ferrocen-1,1'-diyl compounds, $fc(NH_2)_2$, was carried out via the reduction of 1,1'-diazidoferrocene ($fc(N_3)_2$).[13, 47] Extreme care was taken when handling solid $fc(N_3)_2$, since it has been reported to be air- and light-sensitive at ambient temperature, and explosive when heated rapidly above 56 °C. Indeed, it was observed that solid $fc(N_3)_2$ (obtained from reaction shown in figure 4.5) underwent slow degradation at room temperature even when it was stored under a N_2 atmosphere and shielded from the light.[13] However, it was found that the solution of 0.1 M $fc(N_3)_2$ in Et_2O stored under a N_2 atmosphere could be kept in the freezer for a month with little degradation (observed as a dark precipitate). It was also discovered that the more dilute the solution, the more stable is $fc(N_3)_2$ in this solution. Therefore, $fc(N_3)_2$ synthesized in this work was diluted into a 0.05 M Et_2O solution, and then kept in the freezer under an N_2 atmosphere.

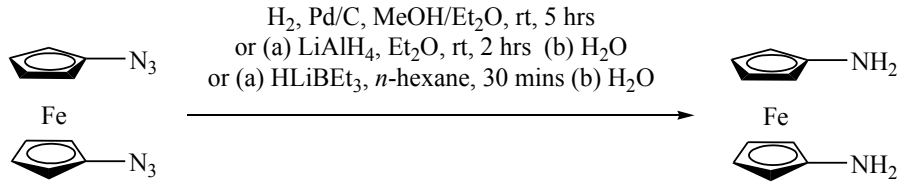

Figure 4.30. Scheme of the synthesis of $fc(NH_2)_2$

The reduction of $fc(N_3)_2$ was then carried out to obtain $fc(NH_2)_2$, and the catalytic reduction of $fc(N_3)_2$ reported by Arnold *et al.*, which involves the hydrogenation of $fc(N_3)_2$ catalyzed by Pd/C (5 % palladium) under atmospheric pressure of H_2 at room temperature, was repeated (figure 4.30, route (i)).[13] However, $fc(N_3)_2$ was observed to be inactive, even when the temperature was raised to 40 °C (a higher temperature was not used as it could lead to the decomposition of $fc(N_3)_2$). Pd/C with a larger percentage of palladium (10 %) and a high pressure of H_2 (4 bar) was also used, but still, none of the $fc(N_3)_2$ was converted.

Therefore, the reduction using $LiAlH_4$, which was proposed by Nesmeyanov *et al.*,[47] was then carried out (figure 4.30, route (ii)). After two hours, the reaction mixture was quenched with H_2O and examined by ^1H NMR spectroscopy. It was found that only 30 % of $fc(N_3)_2$ was converted to $fc(NH_2)_2$. A longer reaction time of 5 hours and a higher reaction temperature of 40 °C did not afforded a better yield of this reaction, and 50 °C led to decomposition products rather than $fc(NH_2)_2$. Consequently, a more reactive reducing agent was required for a more efficient reduction of $fc(N_3)_2$ at room temperature. After a few trials for the reduction of

$fc(N_3)_2$ using various hydride reagents, the super-hydride ($HLiBEt_3$) was found to be an highly efficient reducing agent for $fc(N_3)_2$. Immediate colour change from orange to red was observed when the super-hydride was introduced to the *n*-hexane solution of $fc(N_3)_2$. The resulting reaction mixture was quenched by H_2O after being stirred for 30 mins at room temperature, and the organic phase was dried under an N_2 atmosphere. Pure $fc(NH_2)_2$ was obtained after the removal of *n*-hexane from the solution. For this particular reaction, *n*-hexane was found to be a better solvent than Et_2O, which often led to the formation of by-products rather than $fc(NH_2)_2$. The lower miscibility of *n*-hexane[48] was considered as the reason for the cleaner reaction it afforded. During the reduction of $fc(N_3)_2$ each azide group received the first proton from the hydride, and the other proton from the water added.[49] Side reactions might occur in the aqueous phase and generate by-products, and thus a solvent that is less miscible with H_2O is preferred.

4.4.2. Synthesis of bis-bidentate diimine ligands

The synthesis of the N,N'-substituted ferrocen-1,1'-diyl ligand **4.6** was performed (figure 4.31), as the symmetric analogue of **3.1** (figure 3.4). Using similar reaction conditions for the preparation of **3.1**,[45] **4.6** was obtained as purple solid in a 77 % yield after purification via silica column chromatography using Et_2O as the eluent.

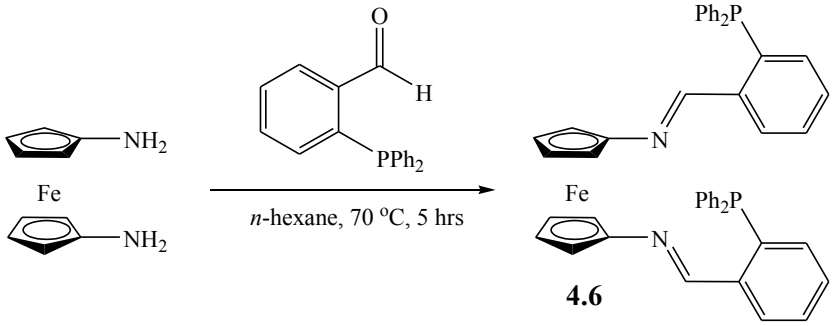

Figure 4.31. Scheme of the synthesis of **4.6**[vi]

The ^1H NMR spectrum of **4.6**, which confirmed the symmetric structure of this ligand, was given in figure 4.32a. The $^{31}P\{^1H\}$ NMR spectrum of **4.6** (figure 4.32b) gives a singlet at -13.7 ppm. Mass and elemental analyses also suggested the formation of **4.6**. For complete characterization, the ^{13}C NMR spectrum (figure 4.33) was also obtained, where the signals for the various carbon environments in this compound are assigned (table 4.5).

[vi] Figure 4.31 adapted from reference 45.

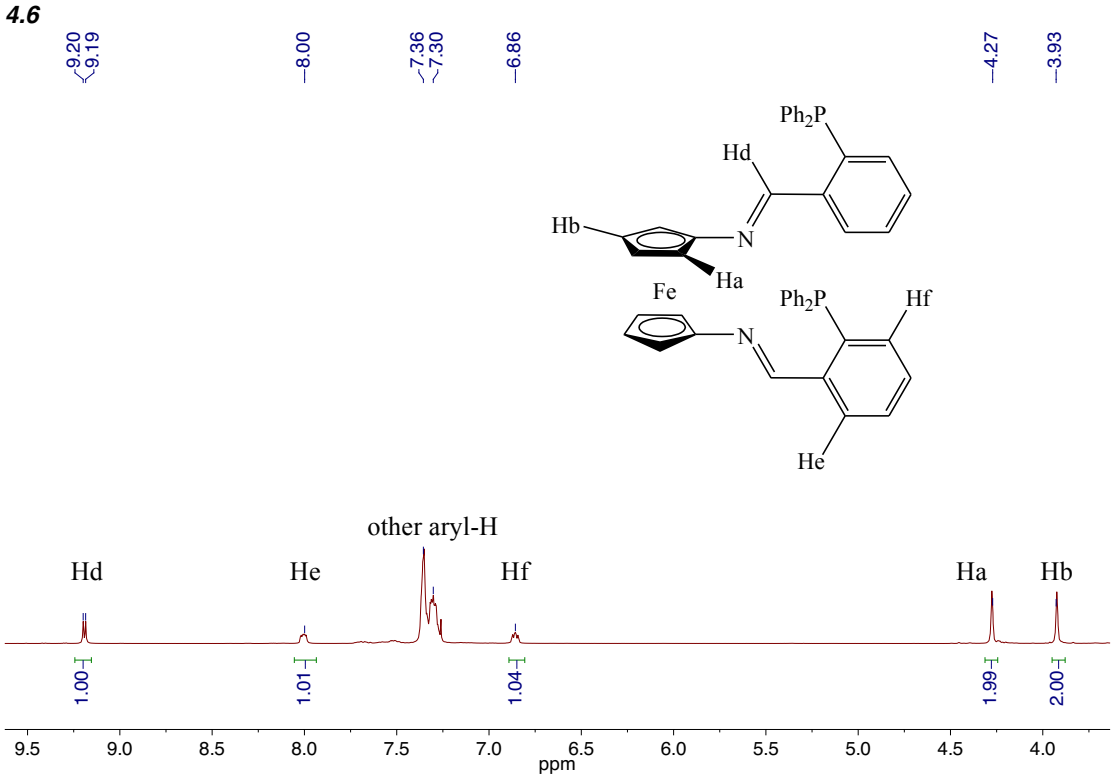

(a)

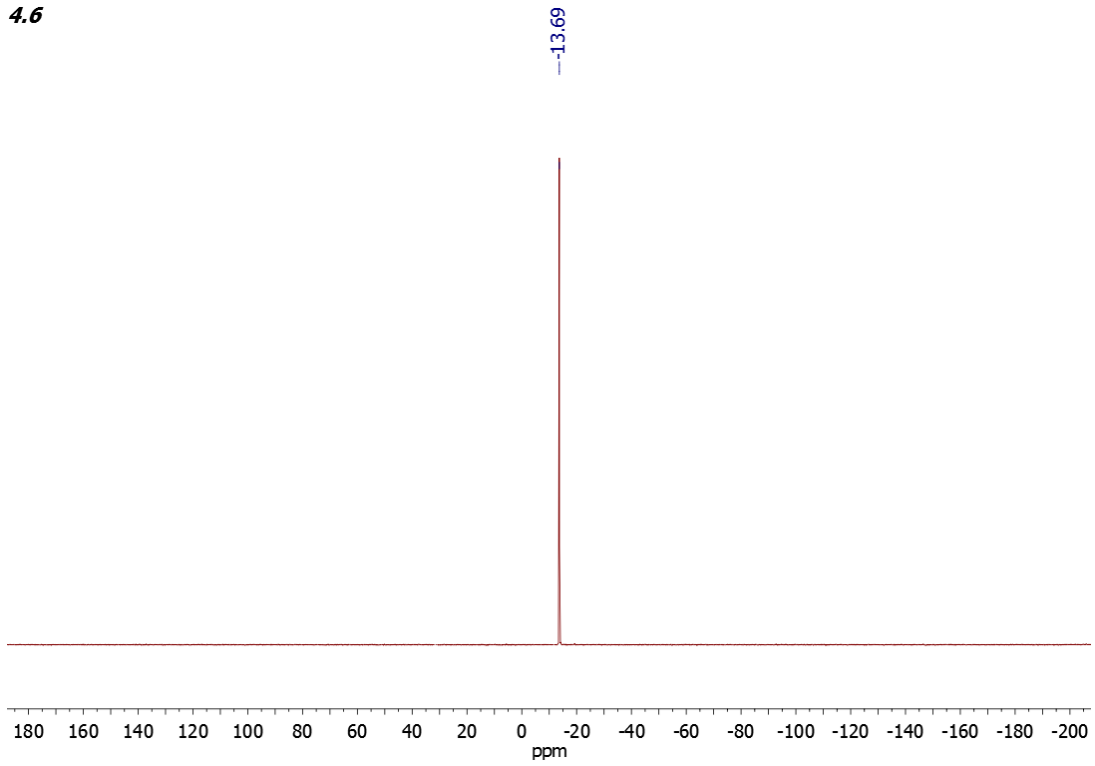

(b)

Figure 4.32. (a) ^{1}H NMR ($CDCl_3$, 298 K, 400 MHz) and (b) $^{31}P\{^{1}H\}$ NMR ($CDCl_3$, 298 K, 162 MHz) spectra of **4.6**

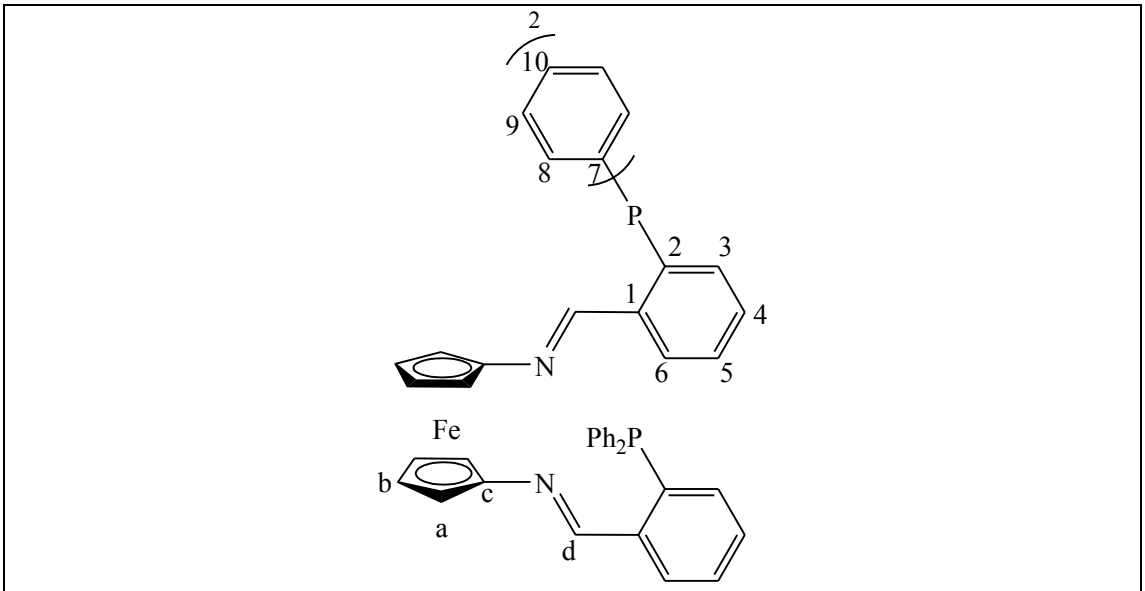

Carbon environment	Chemical shift (ppm)
Ferrocenyl a/b/c/	64.5 / 69.7 / 105.3
Imine d	156.8
Aromatic 1~6	140.0 /137.4 / 133.6 / 129.0 / 130.2 / 127.6
Aromatic 7~10	137.0 / 128.8 / 134.3 / 134.1

Table 4.5. The ^{13}C NMR ($CDCl_3$, 298 K, 100 MHz) spectral data for ligand **4.6**

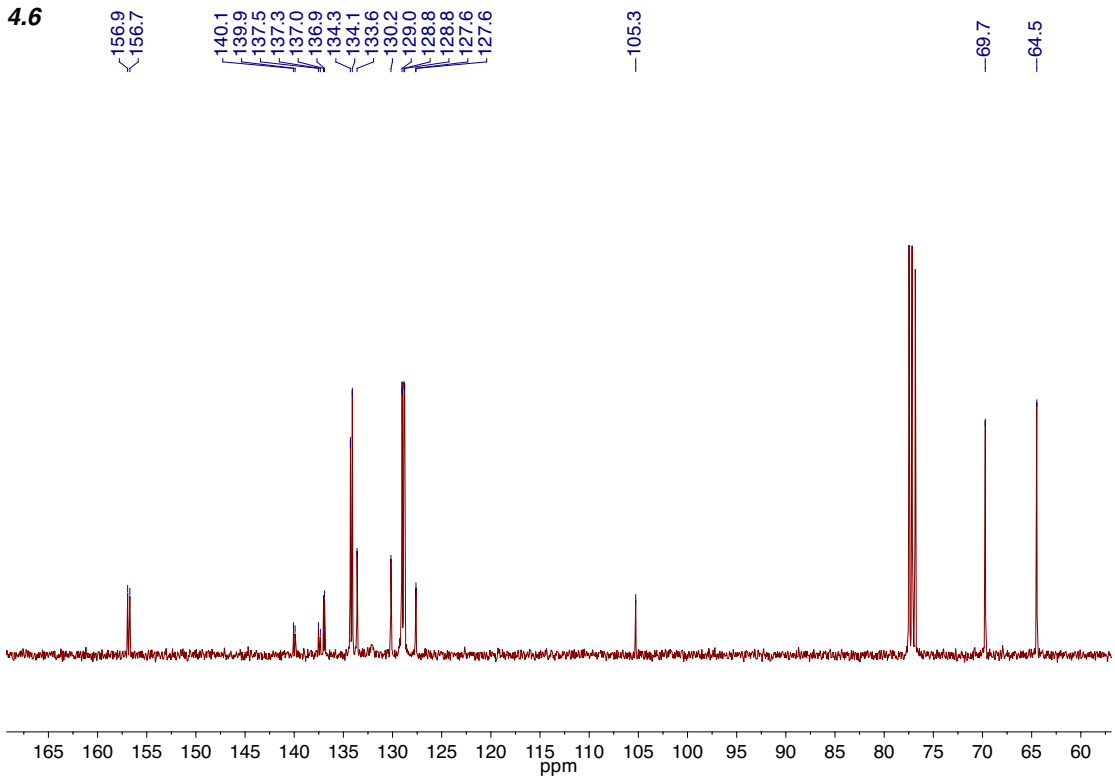

Figure 4.33. ^{13}C NMR ($CDCl_3$, 298 K, 100 MHz) spectrum of **4.6**

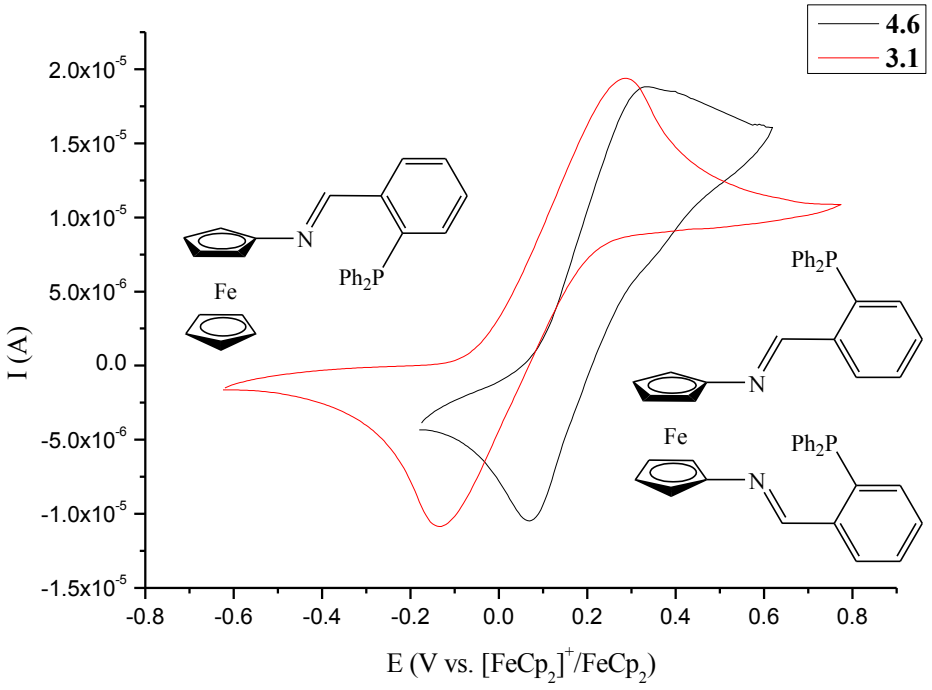

Figure 4.34. Cyclic voltammograms of **3.1** (structure shown on the left side) and **4.6** (10 mM in THF with 0.1 M TBAP, rt, scan rate = 30 mV/s)

Electrochemical characterization of **4.6** was also carried out, and the redox behaviour of this ligand was found to be different from its asymmetric analogue **3.1** (figure 4.34). From the data in table 4.6, it can be seen that the oxidation/reduction potentials of **4.6** are higher than those of **3.1.** This can be easily understood as one more electron-withdrawing imine group is attached to the ferrocene moiety in **4.6** than **3.1**. Also, a larger ΔE_p value was given by **3.1**, suggesting that when the potential on the electrode increased, electrons on the unsubstituted Cp-ring in **3.1** shifted to the iron centre and thus resulted in a slower redox process.

Ligand	ox	red	ΔE_p
3.1	0.289	-0.135	0.426
4.6	0.334	0.070	0.265

Table 4.6. Oxidation and reduction potentials (vs. $[FeCp_2]^+/FeCp_2$) of **3.1** and **4.6** (10 mM in THF with 0.1 M TBAP, rt, scan rate = 30mV/s)

As the bis-bidentate ligand **4.6** had been synthesized and purified, its complexation to palladium was carried out to obtain the complexes shown in figure 4.35 as the desired product. However, similar with the complexation of **3.4** to palladium or **4.1** to iron/cobalt/nickel, the colour of the reaction mixture quickly turned to dark blue upon the addition of palladium to

the DCM solution of the ligand. The ^{1}H NMR spectrum of the dark blue crude product gave only one broad peak at 3.77 ppm, suggesting the paramagnetic nature of the compound(s). While this signal can be assigned to the protons on the Cp-ring of a ferrocen-1,1'-diylium species, no resonance given by the aryl protons was observed. In addition, the product obtained was found to be quite soluble in $CDCl_3$, which is quite different from the solubility of **3.6** (figure 4.36). Furthermore, the $^{31}P\{^{1}H\}$ NMR spectrum of this crude product gave a broad peak at 38.1 ppm, indicating a more deshielded electronic environment for the phosphorus atom than **4.6** (-13.7 ppm). No evidence for the complexation of **4.6** to palladium from mass spectrometry was found.

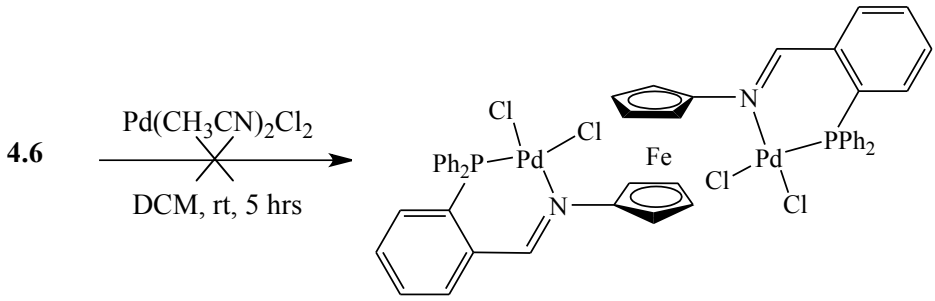

Figure 4.35. Scheme of the unsuccessful complexation of **4.6** to palladium

These facts indicated that (i) the complexation of **4.6** to palladium was unsuccessful, (ii) the ferrocen-1,1'-diyl moieties in **4.6** was oxidized during the reaction, (iii) decomposition of **4.6** might have occurred, which could be caused by its oxidation. Due to time constraints, no further complexation studies of this ligand could be carried out. As the species that was responsible for the oxidation observed in the reactions shown in figure 4.21 and 4.35 has not been identified, investigations on these complexation reactions form an important part of the future work.

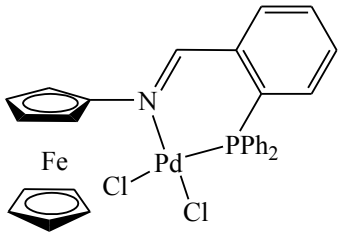

Figure 4.36. Structure of **3.6**, the mono-analogue of the desired product of the reaction shown in figure 4.35

4.5. Conclusion

Some ferrocenyl or ferrocen-1,1'-dyl-incorporated diimines (**4.1**, **4.2**, **4,6**)/diamine (**4.5**) have been synthesized and characterized. The complexation of these diimine compounds to transition metals was found to be complicated. While the instability of the palladium complex of **4.2** in solution was observed, the complexation of **4.1** to nickel/cobalt/iron and that of **4.6** to palladium were unsuccessful. In the latter cases, oxidation of the ferrocenyl or ferrocen-1,1'-diyl species were observed, and the paramagnetic products obtained cannot be identified as their ^{1}H NMR and mass spectra cannot be rationalized.

On the other hand, the synthesis of the whole series of mono- and 1,1'-dihaloferrocenes (X= F, Cl, Br, I) has been successfully carried out. An advanced separation method based on the different oxidation potentials of the species in a mixture, which is named 'oxidative purification', has been successfully applied in the isolation of the halogenated ferrocenes synthesized. It was found to be, so far, the most straightforward approach for obtaining pure mono- and 1,1'-di- haloferrocenes in large quantities.

4.6. References

1. Gibson, V. C.; Long, N. J.; Marshall, E. L.; Oxford, P. J.; White, A. J. P; Williams, D. J. *J. Chem. Soc., Dalton Trans.,* **2001**,1162.

2. Gibson, V. C.; Spitzmesser, S. K.; *Chem. Rev.* **2003**, *103*, 283.

3. Britovsek, G. J. P.; Gibson, V. C.; Wass, D. F. *Angew. Chem. Int. Ed.* **1999**, *38*, 428.

4. Simelling, U.; Auch, T.-C.; Kuhner, O.; Malaun, M.; Kopacka, H.; Bildstein, B. *Z. Anorg. Allg. Chem.* **2003**, *629*, 1334.

5. Johnson, L. K.; Killian, C. M.; Brrokhart, M. *J. Am. Chem. Soc.* **1995**, *117*, 6414.

6. Laine, T. V.; Klinga, M.; Leskela, M. *Eur. J. Inorg. Chem.* **1999**, 959.

7. Laine, T. V.; Lappalainen, K.; Liimatta, J.; Aitolu, E.; Lofgren, B.; Leskela, M. *Macromol. Rapid Commun.* **1999**, *20*, 487.

8. Leine, T. V.; Piiranen, U.; Lappalainen, K.; Klinga, M.; Aitolu, E.; Leskela, M. *J. Organomet. Chem.* **2000**, *606*, 112.

9. Bres, P.-L.; Gibson, V. C.; Mabille, L. D. F.; Reed, W.; Wass, D. F.; Weatherhead, R. H.: World patent, WO 9849208, 1998.

10.Gibson, V. C.; Halliwell, C. M.; Long, N. J.; Oxford, P. J.; Smith, A. M.; White, A. J. P.; Williams, D. J. *Dalton Trans.* **2003**, 918.

11.Gibson, V. C.; Gregson, C. K. A.; Halliwell, C. M.; Long, N. J.; Oxford, P. J.; White, A. J. P.; Williams, D. J. *J. Organomet. Chem.* **2005**, *690*, 6271.

12. Weng, Z.; Koh, L. L.; Hor.; T. S. A. *J. Organomet. Chem.* **2004**, *689*, 18.

13. Shafir, A.; Power, M. P.; Whitener, G. D.; Arnold, J. *Organometallics* **2000**, *19*, 3978.

14.Butler, I. R.; Boyes, A. L.; Kelly, G.; Quayle, S. C.; Herzig, T.; Szewczyk, J. *Inorg. Chem. Commun.* **1999**, *2*, 403.

15. Butler, I. R.; Mussig, S.; Plath, M. *Inorg. Chem. Commun.* **1999**, *2*, 424.

16. Butler, I. R.; Drew, M. G. B.; Greenwell, C. H.; Lewis, E.; Plath, M.; Mussig, Szewczyk, J. *Inorg. Chem. Commun.* **1999**, *2*, 576.

17. Butler, I. R. *Inorg. Chem. Commun.* **2008**, *11*, 15.

18. Butler, I. R.; Broomsgrove, A. E. J.; Fitzpatrick, P.; Vidovic, D.; Thompson, A. L.; Fallis, I. A.; Aldridge, S. *Organometallics* **2010**, *29*, 4762.

19. Atkinson, R. C. J.; Gerry, K.; Gibson, V. C.; Long, N. J.; Marshall, E. L.; West, L. J. *Organometallics* **2007**, *26*, 316.

20. Dong, T. Y.; Lai, L. L. *J. Organomet. Chem.* **1996**, *509*, 131.

21. Dong, T. Y.; Chang, C. K. *J. Chin. Chem. Soc.* **1998**, *45*, 577.

22. Dong, T. Y.; Ho, P. H.; Chang, C. K. *J. Chin. Chem. Soc.* **2000**, *47*, 421.

23. Bebbington, M. W. P.; Bontemps, S.; Bouhadir, G.; Hanton, M. J.; Tooze, R. P.; van Rensburg, H. Bourissou, D. *New J. Chem.* **2010**, *34*, 1556.

24. Park, J.; Quan, Z.; Lee, S.; Ahn, K. H.; Cho, C. W. *J. Organomet. Chem.* **1999**, *584*, 140.

25. Conway, B. G.; Rausch, M. D. *Organometallics*, **1985**, *4*, 688

26. Nesmeyanov, A. N.; Perevalova, E. G.; Nesmeyanova, O. A. *Dokl. Akad. Nauk SSSR*, **1955**, *100*, 1099.

27. Fish, R. W.; Rosenblum, M. *J. Org. Chem.*, **1965**, *30*, 1253

28. Butler, I. R.; Wilkes, S. B.; McDonald, S. J.; Hobson, L. J.; Taralp, A.; Wilde, C. P. *Polyhedron* **1993**, *12*, 129.

29. Kovar, R. F.; Rausch, M. D.; Rosenberg, H. *Organomet. Chem. Synth.* **1971**, *1*, 173.

30. Goeltz, J. C.; Kubiak, C. P. *Organometallics* **2011**, *30*, 3908.

31. Connelly, N. G.; Geiger, W. E. *Chem. Rev.* **1996**, *96*, 877.

32. Cunningham, K. L.; McMillin, D. R. *Polyhydron* **1996**, *15*, 1673.

33. Inkpen, M. S.; Du, S.; Driver, M.; Albrecht, T.; Long, N. J. *Dalton Trans*, **2013**, *42*, 2813.

34. Suenkel, K.; Bernhartzeder, S. *J. Organomet. Chem.* **2011**, *696*, 1536.

35. Bernhartzeder, S.; Suenkel, K. *J. Organomet. Chem.* **2012**, *716*, 146.

36. Hedberg, F.; Rosenberg, H. *J. Organomet. Chem.* **1971**, *28*, C14.

37. Sander, R.; Mueller-Westerhoff, U. T. *J. Organomet. Chem.* **1996**, *512*, 219.

38. Tang, P.; Furuya, T.; Ritter, T. *J. Am. Chem. Soc.* **2010**, *132*, 12150.

39. Yamada, S.; Knochel, P. *Synthesis* **2010**, *14*, 2490.

40. Yamada, S.; Gavryushin, A.; Knochel, P. *Angew. Chem. Int. Ed.* **2010**, *49*, 2215.

41. Shechter, H.; Helling, J. F. *J. Org. Chem.* **1961**, *26*, 1034.

42. Hedberg, F. L.; Rosenberg, H. *Tetrahedron* **1969**, *46*, 4011.

43. Inkpen, M. S. PhD thesis, Imperial College London. 2013

44. Oxford, P. J. PhD thesis, Imperial College London, 2003.

45. Guan, W. MRes report, Imperial College London, 2006.

46. Jerry, M. *Advanced Organic Chemistry reactions, mechanisms and structure* 3rd ed. John Wiley & Sons, New York, 1985.

47. Nesmeyanov, A.; Drozd, V.; Sazonova, V. *Dokl. Akad. Nauk SSSR* **1963**, *150*, 321.

48. Wade, L. G. *Organic Chemistry*: 8th Ed., Pearson Education, 2013.

49. Boyer, J. H. *J. Am. Chem. Soc.* **1951**, *73*, 5865.

Chapter 5

Investigations on Palladium-Catalyzed Suzuki-Miyaura Cross-coupling and Rhodium-catalyzed Hydrogenation Reactions

千磨万击还坚劲，任尔东西南北风。

—— 郑板桥

5.1. Introduction

The previous chapters have focused on redox control of palladium complexes with ferrocene-based ligands for carbonylation processes. Palladium complexes have also found widespread application as efficient catalysts in cross-coupling reactions in general, which play an important role, not only in academic research, but also in billions of pounds of industrial production.[1-7] Heck, Negishi, and Suzuki, who have made significant achievements in the well-defined strategies for the development Pd(II)/Pd(0) catalysts in a variety of cross-coupling processes, were awarded with 2010 Nobel Prize in Chemistry for their contributions in synthetic organic and organometallic chemistry.

In a research study on the synthesis and catalytic applications of palladium ferrocene-based P,C,P Pincer complexes, it has been reported that for the redox partners shown in figure 5.1, the oxidized complex (**A-ox**) was observed to offer higher yields for the Suzuki-Miyaura cross-coupling reactions of aryl halide (X = Br, I) and phenylboronic acid shown in figure 5.1 than its non-oxidized version (**A**).[8] The electronic aspect of the reason behind these findings was not discussed, as this better catalytic performance by **A-ox** can also be seen as a solvent effect. The reactions catalyzed by the oxidized complex were carried out in 1,4-dioxane, which is capable of solvating many inorganic compounds including the base used (K_2CO_3), while those **A-red**-catalyzed reactions were carried out in toluene. Consequently it is possible that the reason why reactions carried in 1,4-dioxane are more active than those in toluene is because solvent molecules of 1,4-dioxane can better stabilize the palladium intermediates involved in the catalytic cycle of these processes, and thus drive the reactions towards the formation of the product.

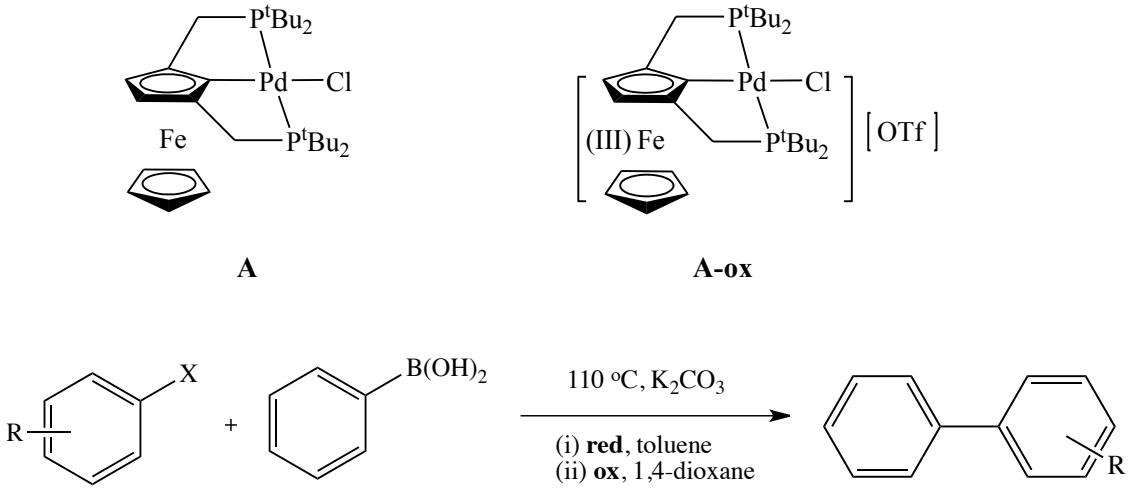

Figure 5.1. Scheme of the cross-coupling reactions catalyzed by **A/A-ox**[i]

[i] Figure 5.1 adapted from reference 8.

However, in spite of this difference in the reaction conditions, it can still be noticed that the electronic change of the ferrocenyl moiety might lead to a different catalytic activity of the palladium centre towards the Suzuki-Miyaura cross-coupling reactions. Therefore, it is of interest to investigate the impact of ligand-based oxidation brought about by palladium redox switches on Suzuki-Miyaura cross-coupling processes for a better insight into the electronic effects in such reactions.

The square-planar rhodium centre has also received great interest in terms of its catalytic activities towards hydrogenation/hydroformylation processes.[9-12] A pioneering demonstration of modifying the reactivity of a rhodium centre via incorporation of a redox active functionality within a ligand framework was described by Wrighton *et al*.[13] It was found that the hydrogenation of cyclohexene catalyzed by **B** is approximately 16-fold faster than **B-ox** (figure 5.2). This drop in catalytic reactivity of the rhodium centre through ligand-based oxidation was indeed rationalized in electronic terms, as the more electron-rich metal centre is believed to promote the oxidative addition of H_2, which is often the rate-determining step in such processes.

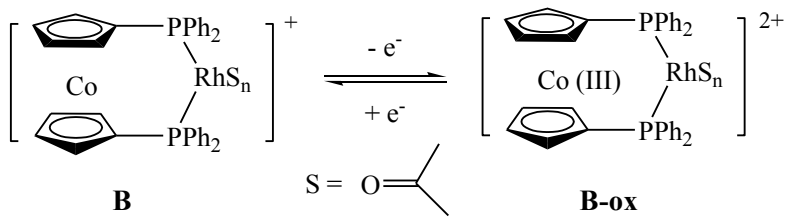

Figure 5.2. Rhodium-based redox switches bearing a cobaltocene-1,1-diyl/-ium ligand

Nonetheless, although the ferrocene-based analogues of complex **B** (figure 5.3) have been synthesized,[14, 15] their electrochemical and catalytic properties have not yet been reported. Therefore, the synthesis of redox-active rhodium complexes bearing ferrocenyl or ferrocen-1,1'-diyl ligands was also carried out in this project, which will be discussed in this chapter, along with the catalytic behaviour of these complexes towards the hydrogenation reactions of styrene.

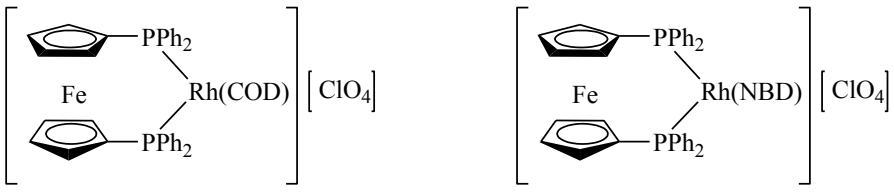

[Rh(dppf)(COD)][ClO_4] [Rh(dppf)(NBD)][ClO_4]

Figure 5.3. Ferrocen-1,1'diyl analogues of complex **B**

5.2. Synthesis of 1,1'-bis(Methylthio)ferrocene-containing Complexes

In previous chapters, redox active ligands obtained from modifications of ferrocenes by phosphines or N-donors, and the utilization of the transition metal complexes bearing these ligands in redox controlled catalytic processes has been discussed. Aside from group 15 atom functionalized ferrocenes, ferrocene derivatives with cyclopentadienyl moieties containing group 16 donor heteroatoms have also been investigated in this project.

5.2.1. Synthesis of methylchloropalladium complexes

The utilization of bidentate symmetric ferrocene-1,1'-diyl ligands was first considered because these typs of compounds possess both a large ligand bite angle, which is favoured by palladium-catalyzed cross-coupling reactions[16], and a redox property. While there is a distinct lack of knowledge in the area of transition metal chelates bearing ferrocene-based [O,O] ligands,[17] one good example of the limited applications of symmetric ferrocen-1,1'-diyl [S,S] ligands in catalysis was the synthesis of the titanium and zirconium complexes, which are catalytically active towards ethylene polymerization, with the dianionic thiolate ligand shown in figure 5.4.[18]

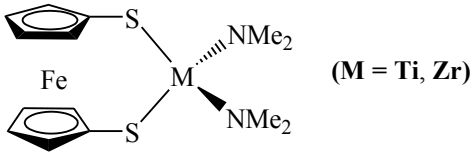

Figure 5.4. Structure of ethylene polymerization catalysts bearing a ferrocene-[S,S] ligand

Furthermore, electrochemical characterization of the dichloropalladium complexes with ligands of the type $Fe(C_5H_4SR)_2$ (S = Me, Ph, ^{i}Bu) suggests that these compounds undergo ligand-based one-electron reversible redox processes (Fe^{II}-Fe^{III}).[19] Therefore, the preparation and chemical oxidation of dichloropalladium 1,1'-bis(methylthio)ferrocene, [Pd(bmsf)Cl_2], was first carried out adopting a literature procedure (figure 5.5). [19]

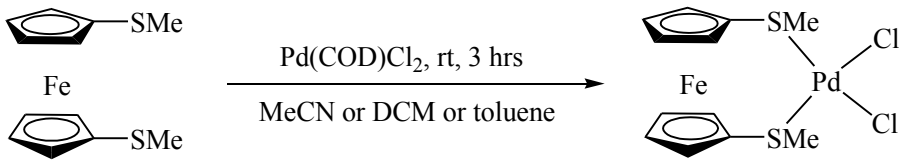

Figure 5.5. Scheme of the preparation of Pd(bmsf)Cl_2

The brown product that readily precipitated from the reaction mixture in MeCN was collected, but found to be quite insoluble. While most organic solvents could not dissolve the

product, a DMSO-d_6 or DCM-d_2 solution of the product could offer ^{1}H NMR spectra with weak signals. As this was not mentioned in related publications, it was thought that there might be a solvent effect as the previous synthesis of [Pd(bmsf)Cl_2] was carried out in benzene.[19] Consequently, other solvents such as toluene and DCM were used for the same reaction. However, products of the same poor solubilities were obtained, and the redox property of the complex could not be characterized electrochemically as the concentration of the solution with electrolyte was too small. Further experiments also show that the complex is also not active towards the oxidation via ferrocenium salts ([$FeCp_2$][PF_6]/[$FeCp_2$][BF_4]) as such a reaction favours a homogeneous environment. As a consequence, it was important to improve the solubility of the complex so that it could be used as a homogeneous catalyst, and the substitution of one of the chlorides on the palladium centre by an alkyl group was considered to be an efficient way to increase the solubility of the compound as the polarity of the complex reduced upon the replacement of an electron-withdrawing substituent by a moderate electron-donating ligand.

Since it is easier to modify the palladium centre before the chelating ligand is involved, the preparation of the alkylchloride palladium complex from [Pd(COD)Cl_2] was carried out via the substitution reaction towards [Pd(COD)MeCl]. After a few trials following the literature procedure[20], [Pd(COD)MeCl] was obtained from the reaction of [Pd(COD)Cl_2] and $SnMe_4$ as a light grey solid.

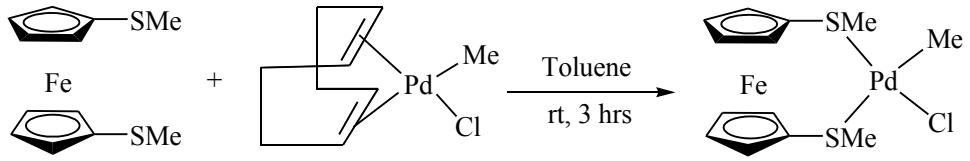

Figure 5.6. Scheme of the synthesis of [Pd(bmsf)MeCl] (**5.1**)

The synthesis of methylchloropalladium 1,1'-bis(methylthio)ferrocene ([Pd(bmsf)MeCl], **5.1**) was successfully carried out via a similar approach towards [Pd(bmsf)Cl_2] (figure 5.6) and a yellow product was obtained in a yield of 81 %. The ^{1}H NMR spectrum of this complex is shown in figure 5.7, with all the signals assigned. The formation of the Me-Pd bond is also confirmed by mass spectrometry, which gave the peak attributable to [Pd(bmsf)Me]$^+$ in the electrospray spectrum. Results from the elemental analysis show good agreement with the calculated valuse. For a better comparison of the S- and P-substituted ferrocene-1,1'-diyl ligand, the phosphine analogue of **5.1**, [Pd(dppf)MeCl] (**5.2**), was also prepared adopting literature methods.[21]

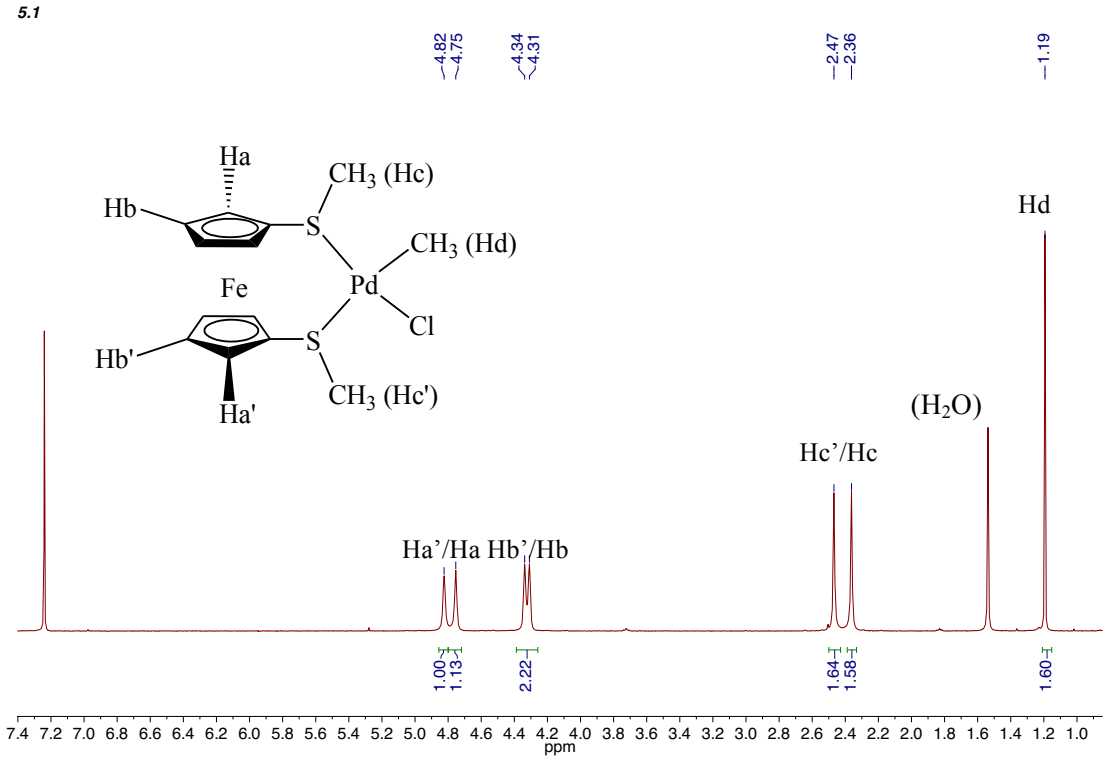

Figure 5.7. ^{1}H NMR ($CDCl_3$, 298 K, 400 MHz) spectrum of [Pd(bmsf)MeCl]

5.2.2. Synthesis of rhodium complexes bearing fc[P, P] and fc[S, S] ligands

Rhodium complexes bearing phosphine ligands have proved to be a useful tool for highly efficient hydroformylation and hydrogenation reactions.[9-12] However, the reactivities of rhodium catalysts containing thio-based chelating ligands have not been well studied. Therefore, the synthesis of the catalyst precursor [Rh(bmsf)(COD)][PF_6] (**5.3**) was carried out using an adopted literature method (figure 5.8).[22]

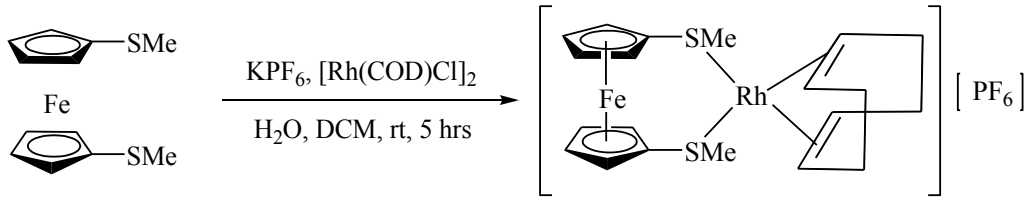

Figure 5.8. Scheme of the synthesis of **5.3**

An aqueous solution of KPF_6 was added to the DCM solution of $[Rh(COD)Cl]_2$ to remove the chloride ligand. This was followed by addition of one equivalent of bmsf ligand in DCM, and the product was obtained after the separation of the organic layer and subsequent removal of the solvent. A brown solid was collected with a yield of 96 %. In its ^{31}P-{^{1}H}NMR spectrum, the multiplets for the counter anion of $[PF_6]^-$ were found at around -135 ppm. The ^{1}H NMR spectrum of **5.3** is shown in figure 5.9.

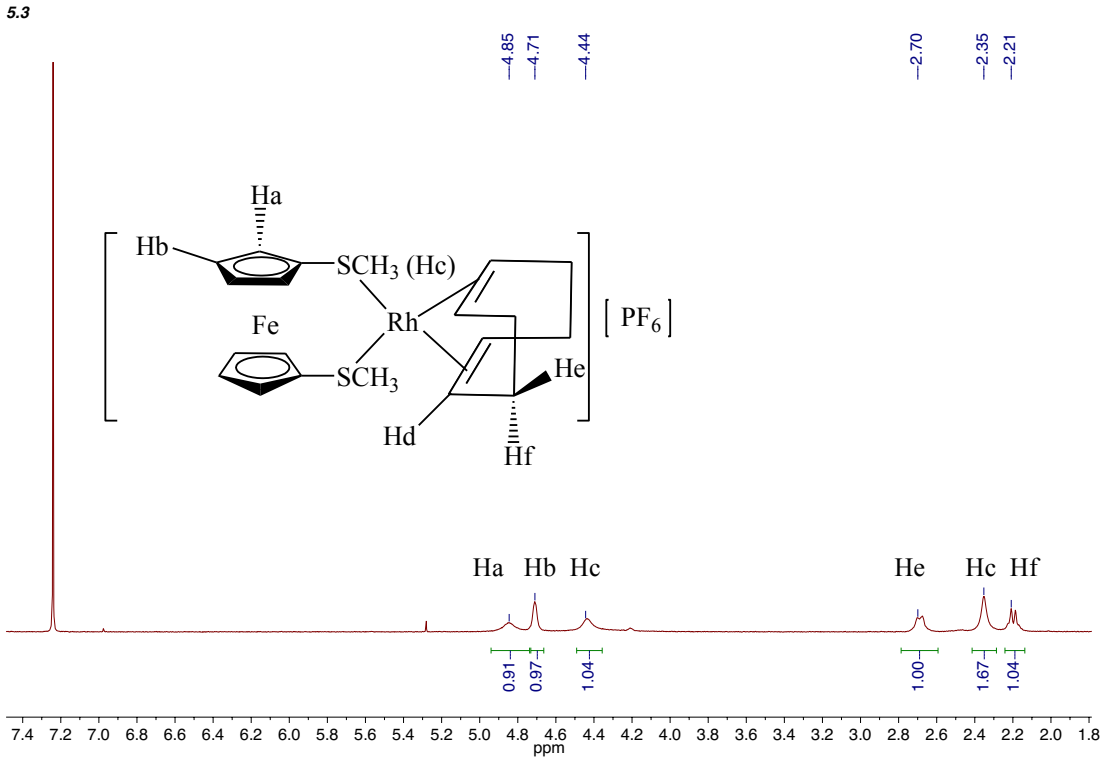

Figure 5.9. ^{1}H NMR ($CDCl_3$, 298 K, 400 MHz) spectrum of **5.3**

It can be seen that although the peaks in the ^{1}H NMR spectrum of **5.3** obtained at room temperature can be identified, these signals are weak due to the low solubility of **5.3** in $CDCl_3$. It was later found that the intensity of the signals given by ^{1}H NMR spectroscopy increases as the temperature, where the spectra were taken, decreases (to 248 K and 223 K). These results suggest that the fluxionality of the Cp-rings and the COD ligand in the molecule is also responsible for the low intensity of the signals in the ^{1}H NMR spectrum of **5.3** at 298 K.

Elemental analysis of **5.3** also gives good results, while only the signals for the ligand $[bmsf]^+$ (278 a. m. u.) and the fragment of $[Rh(bmsf)]^+$ (381 a. m. u.) can be found in the mass spectrum of the complex, which might be a result of the weak binding between the rhodium centre and the COD ligand.

Again, for comparison of the [S,S] and [P,P] functionalized ferrocene ligands, the phosphine analogue of **5.3**, $[Rh(dppf)(COD)][PF_6]$ (**5.4**), was also prepared using a similar procedure.[21] The formation of this compound was confirmed by its ^{1}H NMR spectrum which is similar to that of $[Rh(dppf)(COD)][ClO_4]$.[15] The $^{31}P\{^{1}H\}$ NMR spectrum of **5.4** gives a doublet at 22.4 ppm for the phosphine group, and multiplets at around -145 ppm for the anion of $[PF_6]^-$. Experimental values obtained from elemental analysis show good consistency with the calculated values.

5.3. Studies on the Redox Properties of Complexes

The redox behaviour of **5.2** (figure 5.10) was first investigated via cyclic voltammetry because its dichloro- analogue **2.1** has been mentioned in chapter 2 to undergo ligand-based reversible one-electron oxidation (figure 5.11). Nonetheless, the cyclic voltammogram of **5.2** indicates the irreversible oxidation of this complex, which involves two oxidation processes with a 2 : 1 ratio of the number of electrons involved. The proposed redox behaviour of **5.2** is demonstrated in figure 5.11 after further electrochemical analyses: as the potential on the working electrode increased, the Pd(II) centre in **5.2** was first oxidized to Pd(IV), followed by the oxidation of the ferrocen-1,1'-diyl moiety, which lead to decomposition of the complex.

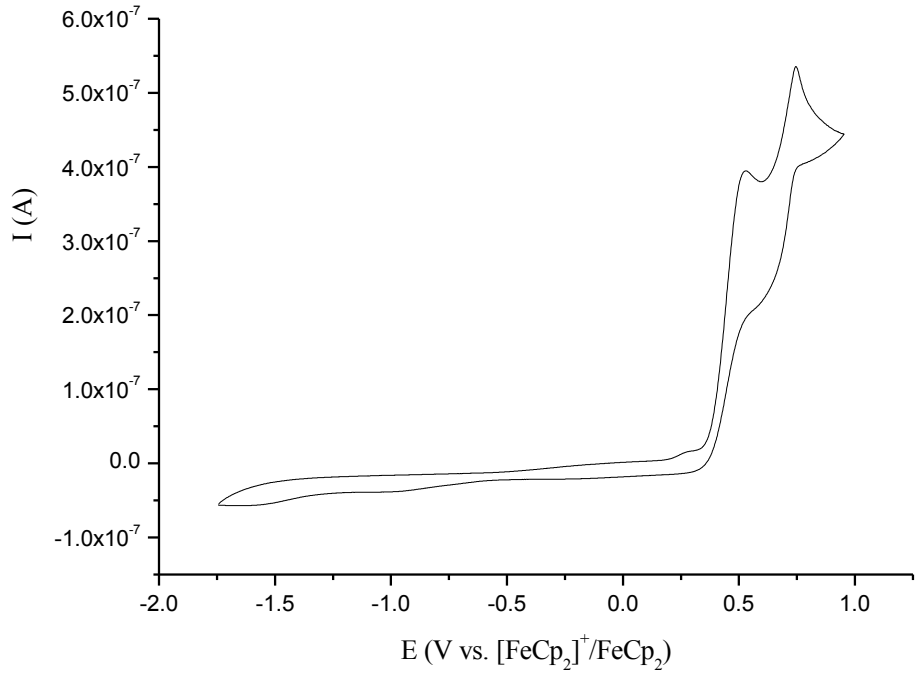

Figure 5.10. Cyclic voltammogram of **5.2** (50 mM in THF with 0.1 M TBAP, rt, 500 mV/s)

Analysis of the crude product obtained from the reaction of **5.2** and $[FeCp_2][PF_6]$ confirmed the instability of **5.2** towards oxidation. The ^1H NMR spectrum of this product suggests its paramagnetic nature by giving broad signals, and the $^{31}P\{^1H\}$ NMR spectrum shows four resonances at 22.5 ppm, 34.9 ppm, 35.4 ppm and 38.4 ppm, none of which can be assigned to **5.1** (38.0 ppm and 11.9 ppm) or the dppf ligand (-17.3 ppm). It was interesting to see that the change of a non-chelating substituent on the palladium centre of **2.1** could cause such a difference on its redox property.

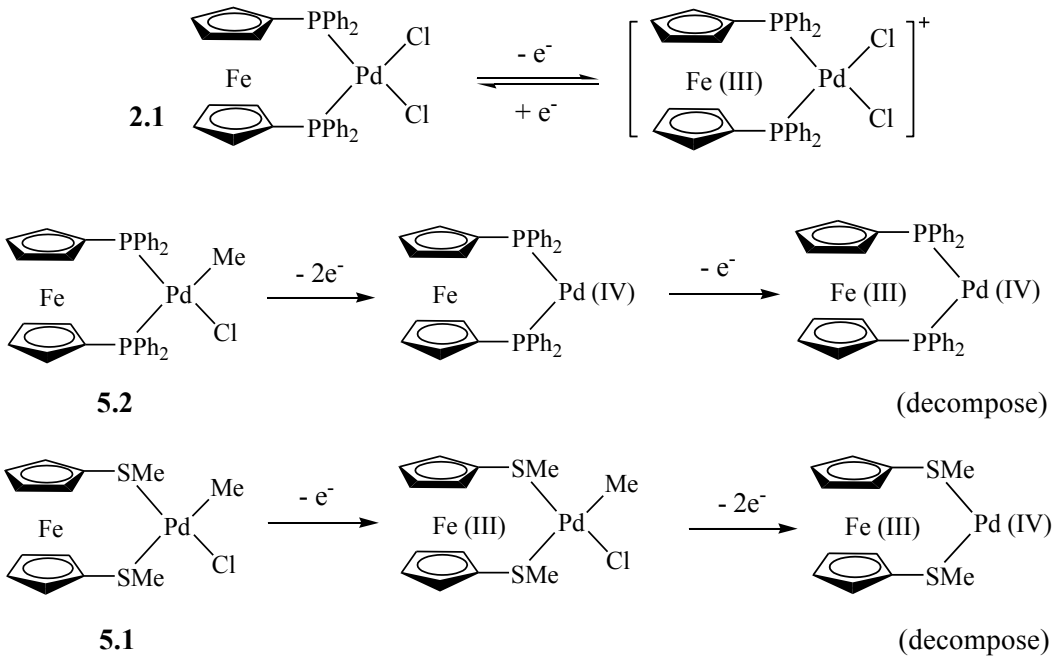

Figure 5.11. Scheme of the redox behaviour of **2.1**, and that proposed for **5.1** and **5.2**

The redox behaviour of **5.1** was found similar to that of **5.2**. The cyclic voltammetry of **5.1** indicated the irreversible oxidation of this complex. However, as suggested by the differential pulse voltammogram of **5.1** (figure 5.12) it was the one-electron oxidation on the iron centre preceding the two-electron oxidation on palladium (figure 5.11).

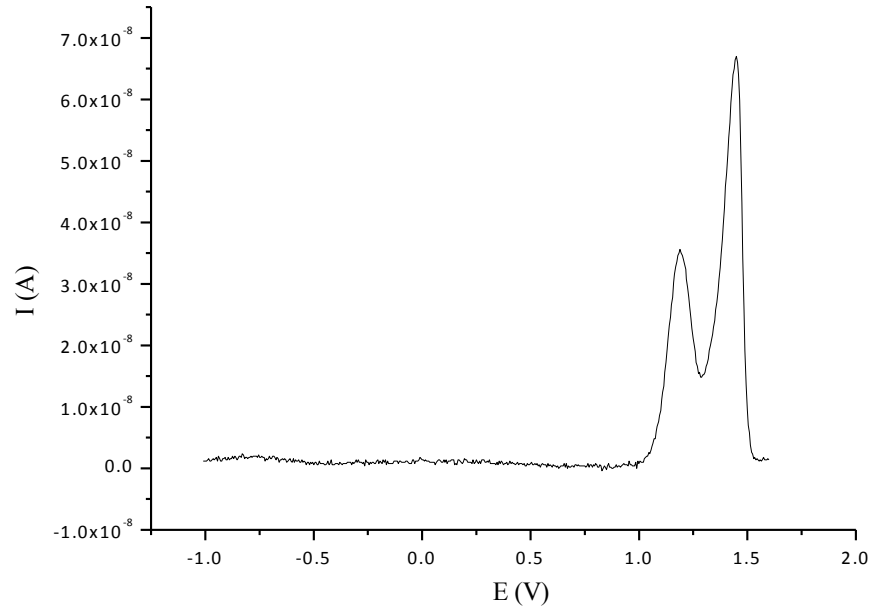

Figure 5.12. Differential pulse voltammogram of **5.1**
(10 mM in THF with 0.1 M TBAP, rt, 500 mV/s)

The electrochemical behaviour of **5.3** was then studied. As suggested by figure 5.13a, this rhodium complex undergoes irreversible oxidation processes. Nevertheless, when the applied potential was set between -1.0 V ~ 0.6 V (vs. $[FeCp_2]^+/FeCp_2$) to focus on the first oxidation peak, a reversible redox process was indicated (figure 5.13b).

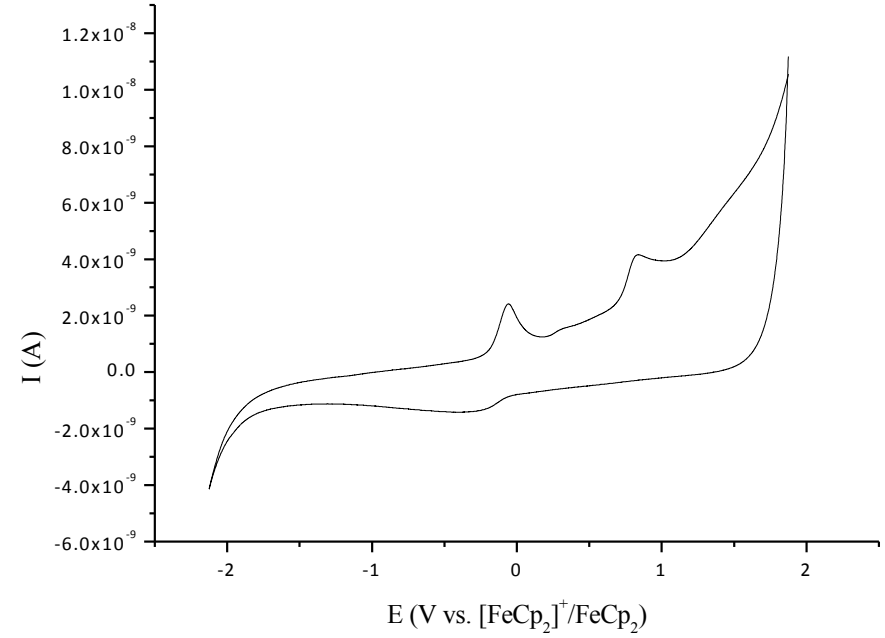

(a)

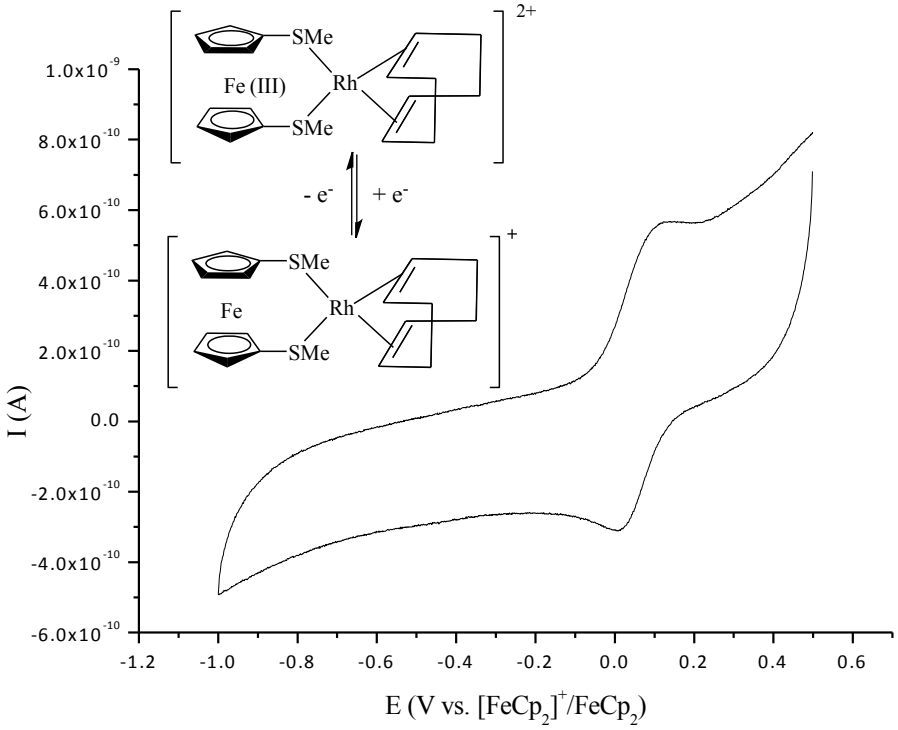

(b)

Figure 5.13. Cyclic voltammograms of **5.3** (50 mM in DCM with 0.1 M TBAP, rt, 200 mV/s)

Therefore, the first oxidation peak in figure 5.12a was assigned to the oxidation of the ferrocen-1,1'-diyl group in **5.3** (figure 5.12b), and the second peak was attributed to the oxidation of the rhodium centre which causes the decomposition of the complex.

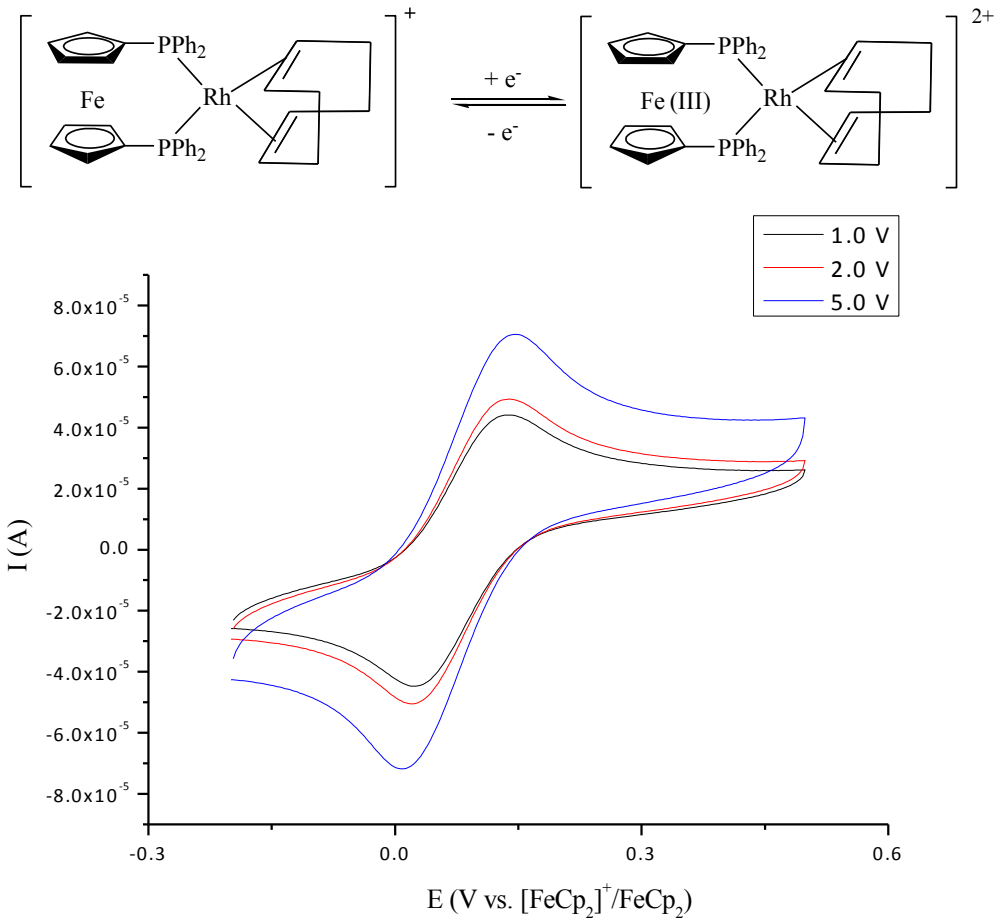

Figure 5.14. Scheme of the ligand-based reversible one-electron redox process of **5.4** and its cyclic voltammogram (50 mM in THF with 0.1 M TBAP, rt) at different scan rates

Finally, the electrochemical behaviour of **5.4** was studied. This complex was found to undergo the ligand-based reversible one-electron redox process shown in figure 5.14. The voltammetric data is summarized in table 5.1.

E_p^A	E_p^C	ΔE_p	$E_p^{1/2}$
0.139	0.025	0.114	0.082

Table 5.1. Selected potentials (V vs. $[FeCp_2]^+/FeCp_2$) from the cyclic voltammogram of **5.4**.

As it was suggested by the cyclic voltammograms of **5.1-5.4** that the only redox-active compound is the rhodium complex bearing the substitutionally-inert redox active dppf ligand, **5.4**, the chemical oxidation of this complex was then carried out in order to study how the catalytic activity of the rhodium centre in **5.4** can be altered by its ligand-based oxidation.

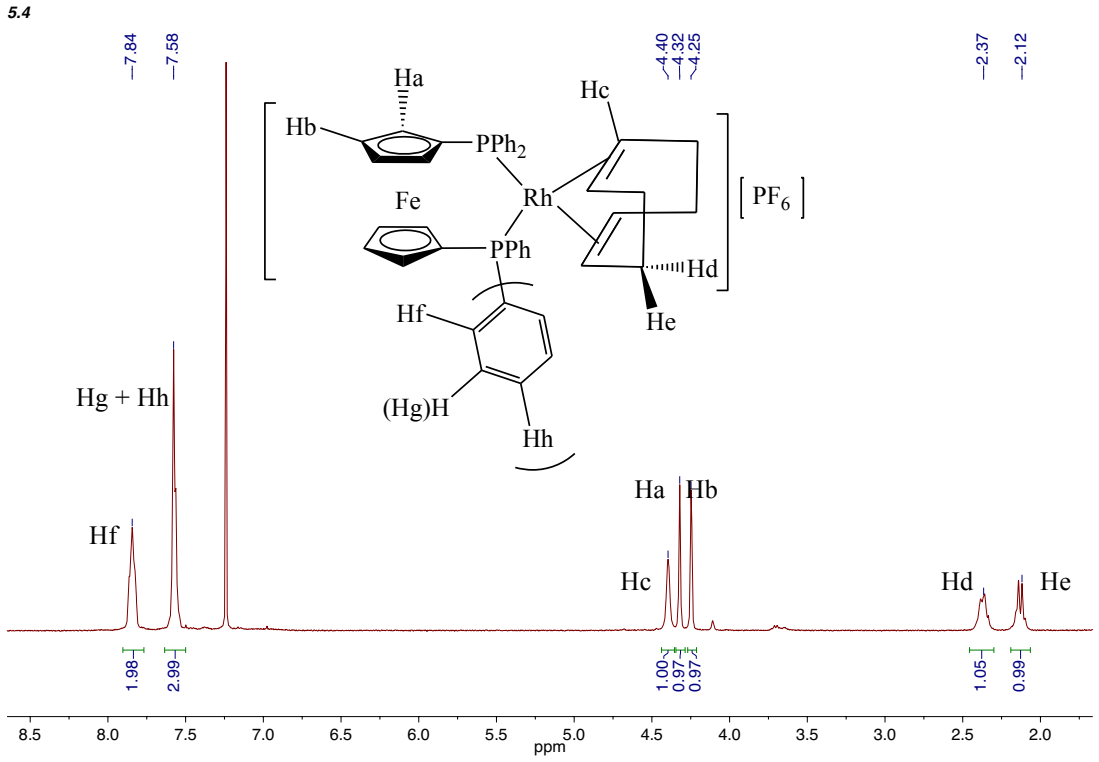

Figure 5.15. ^{1}H NMR ($CDCl_3$, 298 K, 400 MHz) spectrum of **5.4**

The initial study involved the use of a DCM solution of the ferrocenium salt (1 eq. entry 1 in table 5.2), $[FeCp_2][PF_6]$, however, incomplete oxidation of **5.4** was observed in this case. The ^{1}H NMR spectrum of the crude oxidation product shows a mixture of **5.4** and a paramagnetic compound. The downfield shift and broadening of the group of signals at 4.25 ppm, 4.32 ppm and 4.40 ppm for the protons attached to the unsaturated carbons in **5.4** (Hb, Ha and Hd, respectively, in figure 5.15) to 5.13 ppm, 5.30 ppm, 5.60 ppm was observed (table 5.3), which suggested the formation of a ferrocenium compound. Moreover, the $^{31}P\{^{1}H\}$ NMR spectrum of the crude product of the reaction gives two signals at 22.4 ppm and 42.1 ppm, which could be assigned to **5.4** and the oxidation product, and multiplets around -150 ppm for $[PF_6]^-$.

According to the results obtained, it can be seen that more than one equivalent of $[FeCp_2][PF_6]$ was required for the complete oxidation of **5.4**. Nonetheless, due to the anticipated difficulties in the separation of the oxidized complex and the excess ferrocenium

salt,[23, 24] the use of stronger oxidizing agents, instead of increasing the amount of the ferrocenium salt, was considered for the complete oxidation of **5.4**.

Entries	Oxidation agent (in DCM at rt.)	Result
1	$[FeCp_2][PF_6]$ (1 eq.)	Incomplete oxidation
2	$AgPF_6$ (1 eq.)	No oxidation
3	AgOTf (1 eq.)	Decomposition
4	$AgPF_6$ (3 eq.)	Incomplete oxidation
5	$[FeCp_2][PF_6]$ (3 eq.)	Complete oxidation

Table 5.2. Studies on the oxidation of **5.4** carried out using different oxidants

The silver salts have been reported to be powerful oxidants in selective chemical redox processes of organometallic compounds since the oxidizing strength of Ag(I) varies when a different solvent is used to dissolve the mixture substrate and the silver salt.[23, 25] This is because coordinating solvent molecules can form silver complexes with silver salt(s) in solution, which weaken the oxidizing ability of Ag(I). At room temperature, DCM offers Ag(I) the largest oxidation potential of 0.65 V (vs. $[FeCp_2]^+/FeCp_2$) of commonly used solvents.[23] Therefore, the DCM solution of silver hexafluorophosphate ($AgPF_6$, entry 2) was first used to maximize the oxidizing capability of the silver salt, and to avoid the involvement of a different anion. However, no oxidation of **5.4** was found according to the ^1H NMR and $^{31}P\{^1H\}$ NMR spectra of the resulting mixture, while a three-fold excess of the redox agent only offered incomplete oxidation. It was considered that the low reactivity of $AgPF_6$ might be caused by moisturizing of this highly hygroscopic compound during the weighing of it. Therefore a less hygroscopic salt, silver triflate (AgOTf, entry 3), was used. This, however, lead to the decomposition of **5.4**. The two singlets found at -4.0 ppm and -10.0 ppm in the $^{31}P\{^1H\}$ NMR spectrum of the crude product suggest that the phosphines are not coordinating to the rhodium, indicating the dissociation of the dppf ligand from the rhodium centre.

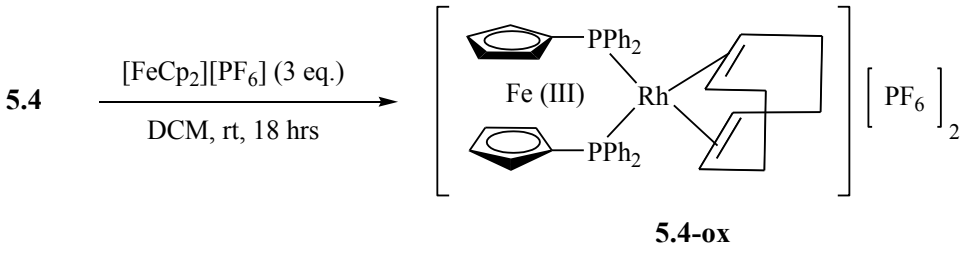

5.4-ox

Figure 5.16. Chemical oxidation of **5.4** using ferrocenium salt

Based on these results, it was found that oxidation of **5.4** with silver salts did not offer advantages than that with ferrocenium salt. As the ferrocenium salt is unlikely to be catalytically reactive in hydrogenation reactions, experiments using excessive $[FeCp_2][PF_6]$ to oxidized **5.4** were carried out, and it was found that 3 equivalents of the oxidant could afford complete oxidation of **5.4** (figure 5.16). However, the excess oxidant $[FeCp_2][PF_6]$ was not separated from the mixture in this case. The selected spectral data for **5.4-ox** were summarized in table 5.3.

Complex	β-hydrogens	α-hydrogens	C=C-H	$^{31}P\{^1H\}$ NMR
5.4	4.25 (dd)	4.32 (p-t)	4.40 (bs)	22.4 (d)
5.4-ox	5.30 (b-dd)	5.60 (b-pt)	5.13 (b-m)	42.1 (d)

Table 5.3. Chemical shifts of selected signals in the ^1H NMR ($CDCl_3$, 298 K, 400 MHz) and $^{31}P\{^1H\}$ NMR ($CDCl_3$, 298 K, 162 MHz) spectra of **5.4** and **5.4-ox**

5.4. Catalytic investigations

5.4.1. Suzuki-Miyaura cross-coupling reactions

The palladium-catalyzed cross-coupling reactions between organoboronic compounds and organic halides in the presence of activating bases (figure 5.17), also known today as Suzuki-Miyaura cross-coupling reactions, have proven to be a powerful technique for a wide range of selective carsebon-carbon bond formation reactions.[26-30] These relatively simple and versatile coupling reactions can be extended to various substrates, and have found wide application for the synthesis of pharmaceuticals and complex natural products.

$$R^1—BX_n + R_2—Y \xrightarrow[\text{Base}]{\text{Pd}} R^1—R^2$$

Figure 5.17. General scheme of Suzuki-Miyaura cross-coupling reactions[ii]
($X_n = (OH)_2$, $(OR)_2$, R_2; Y = Cl, Br, I, OTf)

A general catalytic cycle for Suzuki-Miyaura cross-coupling reactions is described in figure 5.18, which involves the following sequence of steps: (i) oxidative addition of substrate

[ii] Figure 5.17 and 5.18 adapted from reference 36.

to Pd(0) catalytically active species, (ii) transmetallation between Pd(II) intermediate and organoboronic compound, and (iii) reductive elimination releasing the coupling product and reproducing the Pd(0) species.[29] Although each step involves further intermediate processes including ligand exchanges, the generation of R^1-Pd(II)-R^2 and R^2-Pd(II)-Y intermediates has been characterized by isolation or spectroscopic analysis.[31-35]

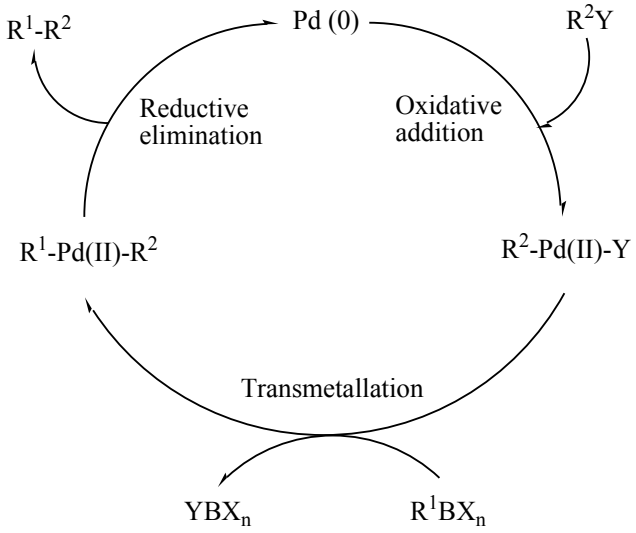

Figure 5.18. General catalytic cycle of Suzuki-Miyaura cross-coupling reactions[ii]

The oxidative addition step is often the rate-determining step in the catalytic cycle, and the reductive elimination readily takes place from *cis*-related R^1-Pd(II)-R^2. The reactivity of the latter step was found to be much higher when both R^1 and R^2 are aryl units than when the R groups are alkyl, suggesting participation of the π-orbital of aryl groups during the R^1-R^2 bond formation.[36] This help to explain why the usefulness of Suzuki-Miyaura cross-coupling reactions have been well documented for the synthesis of biaryl compounds.[37]

Although the mechanism of oxidative addition and reductive elimination sequences are well understood and are presumed to be fundamental processes of general cross-coupling reactions, less is known about the transmetallation step because the mechanism is highly dependent on organometallic intermediates or reaction conditions.[38, 39] It has been reported that organoboronic compounds are quite inert towards organopalladium(II) complexes due to the low nucleophilicity of the boron atom.[36] However, this can be improved by the interaction of the boronic species and a negatively charged base that forms the corresponding boronate species.[40-42] It is therefore crucial for Suzuki-Miyaura cross-coupling reactions to feature the presence of the appropriate bases, which have been reported to have a remarkable effect on activating the organoboronic compounds to the organopalladium(II) halides generated in the catalytic cycle of such reactions. A large range of organic and inorganic bases can be used, either as solutions or as suspensions in the organic solvents.[43, 44]

One of the examples of Suzuki-Miyaura cross-coupling reactions supported by the dppf ligand is shown in figure 5.19.[45] These reactions of phenylboronic acid and aryl bromides show impressive activities and selectivity. The high performance of the catalyst is attributed to the large bite angle of the dppf ligand which increases the interaction between the organic substituents on the diorganopalladium(II) intermediates by forcing the R^1-Pd(II)-R^2 angle to decrease, and thus accelerates the reductive elimination process.[46-48]

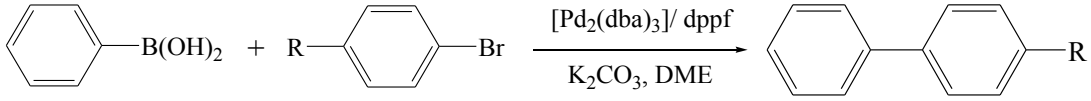

Figure 5.19. Scheme of the Suzuki-Miyaura cross-coupling reaction of phenylboronic acid and aryl bromide (R = MeCO, H)[iii]

In this study, the catalytic behaviour of the palladium complexes bearing symmetric ferrocen-1,1'-diyl ligands, [Pd(bmsf)Cl_2] (**5.1**), [Pd(dppf)Cl_2] (**5.2**), as well as the redox switches of [Pd(dppf)Cl_2] (**2.1**) and [Pd(dppf-Fe^{III})Cl_2][PF_6] (**2.1-ox)**, towards the cross-coupling reaction of 4-bromotoluene (BrPhMe) and phenylboronic acid ($PhB(OH)_2$) was investigated (figure 5.20). These reactions were carried out in THF in the presence of 2 equivalents of K_3PO_4 for 3 hours at the different temperatures of 30 °C, 50 °C and 80 °C, respectively. At least three experiments were carried out for each catalyst at each temperature ($n \geq 3$), and the products obtained from these reactions were analyzed via ^{1}H NMR spectroscopy. The catalytic conversions from BrPhMe to the product, 4-phenyltoluene, are summarized in figure 5.21. In order to rule out the possibilities that the differences in the catalytic conversions offered by the four complexes are due to other factors than their different catalytic activities, all these reactions were repeated with a shorter reaction time of 1 hour. It was found that for each reaction catalyzed by a particular complex at a certain temperature, approximately the same conversions were given from the reactions carried out within 1 hour and those within 3 hours.

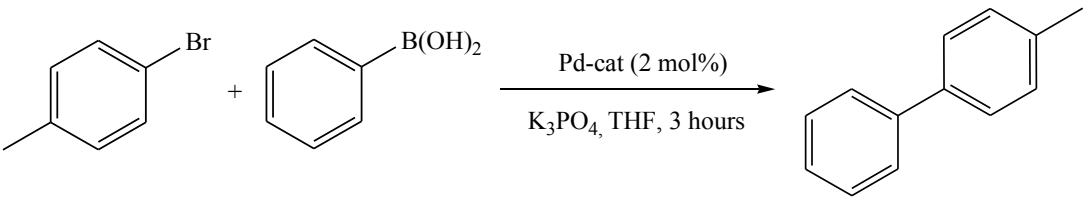

Figure 5.20. Scheme of the cross-coupling reaction of BrPhMe and $PhB(OH)_2$

[iii] Figure 5.19 adapted from reference 45.

It is quite obvious from the column chart that among the four catalysts investigated, **5.1** afforded the lowest yields at each temperature. Moreover, it seems that the catalytic reactivity of this complex decreases with the increase of temperature. This is quite a different case compared with the complexes bearing the dppf ligand, which generally offered better yields of the reaction than **5.1**, and were more catalytically reactive at 50 °C than at 30 °C. It was also observed that for the reactions catalyzed by **5.1** at 80 °C, the reaction mixture turned from yellow, which is the colour of **5.1** in solution, to black immediately after heating. This colour change also occurred at 50 °C and 30 °C, but became slower as the temperature decreased. Since the reactants are white (BrPhMe) or light yellow solid ($PhB(OH)_2$) that readily dissolve in THF to form a clear solution and the inorganic base is a white suspension in the mixture, the catalyst is most likely to be the reason of the colour change. Thus it was considered that the catalytic behaviour of **5.1** might be a result of the relatively low stability of this bmsf-containing complex. As the S atom is more electronegative and thus a weaker σ-donor than the P atom, it is possible that this binding between the bmsf ligand and the palladium centre cleaves when the reaction temperature rises to a certain point, causing the decomposition of **5.1**.

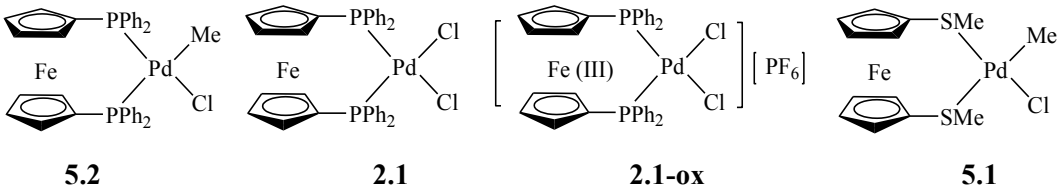

5.2 **2.1** **2.1-ox** **5.1**

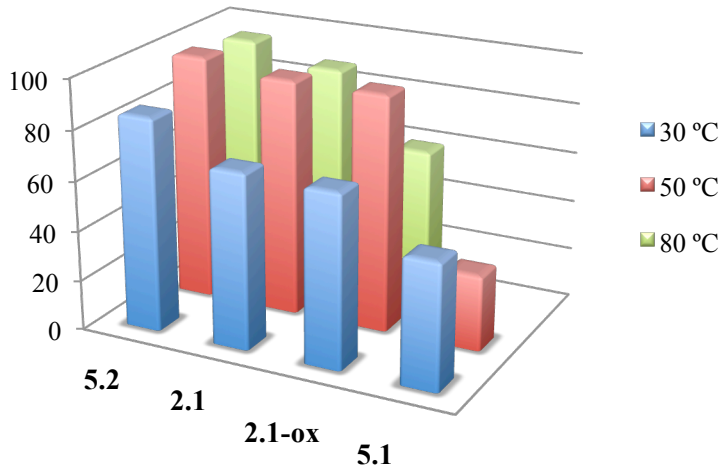

Figure 5.21. Bar chart of the catalytic conversions (%) for the reactions of BrPhMe with $PhB(OH)_2$ catalyzed by **5.1**, **5.2**, **2.1** and **2.1-ox** ($n \geq 3$)[iv]

[iv] Catalytic conversions monitored by ^1H NMR spectroscopy. Data summarized in Chapter 7.

Therefore control experiments studying the stability of **5.1** were carried out to heat the solution of **5.1** and K_3PO_4 in THF under a nitrogen atmosphere from 25 °C, increasing with 5 °C at every 10 minutes. It was observed that the K_3PO_4 suspended yellow solution of **5.1** in THF became a black suspension quickly after the temperature of the mixture reached 65 °C. The mixture was filtered at this point, and the solvent of the filtrate collected was removed. The black solid obtained was analyzed by ^{1}H NMR. The signals can neither be assigned to the complex of **5.1** or the bmsf ligands. The peaks in the region between 4 ppm and 5 ppm, which is often the chemical shift of the signals for the Cp-H of ferrocene-derivatives, indicate compounds other than ferrocene, or mono(methylthio)ferrocene. Thereby the decomposition of **5.1** in THF solution in the presence of K_3PO_4 was confirmed, and the catalytic performance of **5.1** can therefore be explained by its instability towards the increase of temperature.

In the case of the reactions catalyzed by complexes containing the dppf ligand (**5.2**, **2.1**, **2.1-ox**), it was found that (i) complex **5.2**, which is the phosphine analogue of **5.1**, afforded the highest conversions of BrPhMe overall. (ii) All these catalysts offered the best performance at 50 ^{o}C, but became less reactive at 30 ^{o}C. However, compared with the redox switches of **2.1** and **2.1-ox** which both gave a *ca.* 25 % decrease in catalytic conversions when the temperature was changed from 50 °C to 30 °C, **5.2** showed a smaller reduction in its catalytic activity towards this temperature drop. (iii) **2.1**, as well as **5.2**, gave quite similar catalytic results at 50 °C and 80 °C, while there is a decrease in the reactivity of **2.1-ox** at 80 °C. (iv) the redox switches afforded similar conversions at both 30 °C and 50 °C.

The better catalytic performance of **5.2** than **2.1** was explained using the classic catalytic cycle of Suzuki-Miyaura cross-coupling reactions shown in figure 5.18. According to this cycle, both of the catalyst-precursors have to be reduced to [Pd(dppf)] to be catalytically reactive. From this point on, there should be no difference in the catalytic cycle of the reactions catalyzed by **5.2** and **2.1** as they produce the same Pd(0) species before oxidative addition. As a consequence, if both complexes undertook the same mechanism for this particular cross-coupling reaction of BrPhMe and $PhB(OH)_2$, the reason of the higher catalytic conversions afforded by **5.2** than **2.1** can only be attributed to the difference in the rate of the formation of Pd(0) species from these two different catalyst precursors. This is not further discussed as no mechanism study has been carried out in this study.

As to the very similar catalytic performance of the redox switches **2.1**/**2.1-ox**, it was considered that the ferrocen-1,1'-diylium group in **2.1-ox** might somehow be reduced during the catalytic process, and form the same palladium intermediate as **2.1**. Therefore excess oxidant $[FeCp_2][PF_6]$ (3 equivalents from **2.1-ox**), was used for the Suzuki-Miyaura cross-coupling reaction of BrPhMe and $PhB(OH)_2$ catalyzed by **2.1-ox** to ensure that the oxidation state of the ligand is maintained during the reaction (figure 5.22). However, the same catalytic results were given by reactions at each temperature with and without the addition of oxidant.

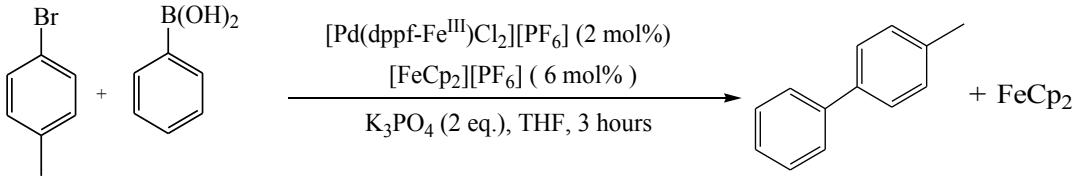

Figure 5.22. Scheme of the Suzuki-Miyaura cross-coupling reaction of BrPhMe and $PhB(OH)_2$ catalyzed by **2.1-ox** in the presence of excess oxidant

Furthermore, signals for ferrocene, as a reduction product of $[FeCp_2][PF_6]$, were found in the ^1H NMR spectra of the crude products of these reactions, as a large singlet at 4.17 ppm. This is consistent with the colour change of the reaction mixture from dark blue to orange observed during the first 15 mins of these reactions. Consequently, it is possible that the oxidized dppf-Fe^{III} ligand in **2.1-ox** was reduced to dppf along with the reduction of the $[FeCp_2][PF_6]$ during the reaction. Therefore, in order to investigate what is responsible for the reduction of $[FeCp_2][PF_6]$, experiments were carried out to heat the mixtures containing $[FeCp_2][PF_6]$ and compound(s) used in the Suzuki-Miyaura cross-coupling reactions of BrPhMe and $PhB(OH)_2$ of the same molar ratio in THF to 50 °C (BrPhMe : $PhB(OH)_2$: $[FeCp_2][PF_6]$: K_3PO_4 : $[Pd(dppf)Cl_2]$ = 1 : 1: 0.06 : 2 : 0.02). These products were examined via ^1H NMR spectroscopy and mass spectrometry. The data obtained is summarized in table 5.4.

No.	Entries (50 °C in THF for 3 hours, Pd = 2.1)	Formation of $FeCp_2$
1	K_3PO_4 + $[FeCp_2][PF_6]$	No
2	$PhB(OH)_2$ + $[FeCp_2][PF_6]$	No
3	BrPhMe + $[FeCp_2][PF_6]$	No
4	K_3PO_4 + $[FeCp_2][PF_6]$ + Pd	No
5	$PhB(OH)_2$ + $[FeCp_2]^+[PF_6]$ + Pd	No
6	BrPhMe + $[FeCp_2][PF_6]$ + Pd	No
7	$PhB(OH)_2$ + K_3PO_4 + $[FeCp_2][PF_6]$	No
8	BrPhMe + K_3PO_4 + $[FeCp_2][PF_6]$	Yes
9	$PhB(OH)_2$ + K_3PO_4 + $[FeCp_2][PF_6]$ + Pd	No
10	BrPhMe + K_3PO_4 + $[FeCp_2][PF_6]$ + Pd	Yes
11	BrPhMe + $PhB(OH)_2$ + K_3PO_4 + $[FeCp_2][PF_6]$	Yes
12	ClPhMe + $PhB(OH)_2$ + K_3PO_4 + $[FeCp_2][PF_6]$ + Pd	Yes

Table 5.4. Studies to probe the cause of the reduction of $[FeCp_2][PF_6]$

It was observed that the reduction of $[FeCp_2][PF_6]$ took place only when BrPhMe and K_3PO_4 were both present. Furthermore, toluene and 4,4'-dimethylbiphenyl were obtained from entries 8 and 10 (table 5.4) with the yield of 18 % and 13%, respectively (figure 5.23). While the biaryl product generated in entry 10 can be easily rationalized as the product of the palladium-catalyzed cross-coupling reaction of BrPhMe, entry 8 is a bit more difficult to explain as no catalyst was added to the mixture.

It has been reported that some transition metal-catalyzed cross-coupling reactions can be carried out with the catalytically active metal species existing as a contaminant in the reaction mixture in trace amounts.[49-51] Therefore, although the possibility that the dehalogenation of BrPhMe in entry 8 was catalyzed by $[FeCp_2][PF_6]$ cannot be completely ruled out, the reaction is more likely to be a transition metal-catalyzed process where BrPhMe was activated by a metal species[52, 53] which exists as an impurity in the reaction mixture. The reason why this reaction did not proceed towards the cross-coupling product of 4,4'-dimethylbiphenyl in this case was probably due to the lack of enough d^8 metal in the reacting system, so the metal adduct of BrMPhMe (M = metal) underwent substitution of Br by H followed by reductive elimination, giving toluene as the product.

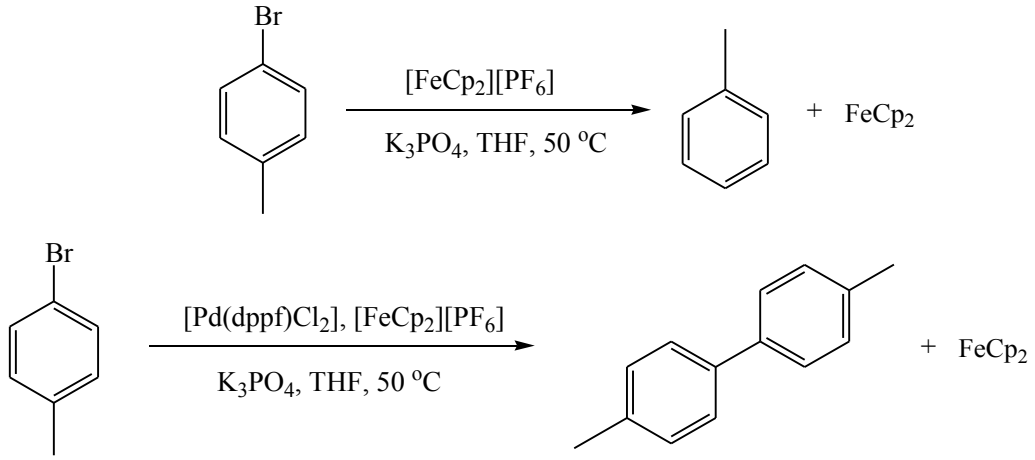

Figure 5.23. Scheme of the reactions taking place in entries 8 and 10 in table 5.4

Although different products were obtained from the reactions in entry 8 and 10, it can be seen that BrPhMe underwent oxidative addition to metal species in both cases, which may cause the reduction of $[FeCp_2][PF_6]$ as the Pd(0) catalytically active species transforms to the $[R^1Pd(II)R^2]$ intermediate (figure 5.18). In the case of entry 11, it was found the formation of ferrocene was not accompanied with cross-coupling or dehalogenation product, suggesting that the reduction of $[FeCp_2][PF_6]$ took place before the completion of a catalytic reaction.

Further evidence comes from the reaction of 4-chlorotoluene (ClPhMe) and $PhB(OH)_2$ in the presence of **2.1** and $[FeCp_2][PF_6]$ under the same conditions (entry 12). Although no

conversion of the substrate was afforded by the catalyst due to the difficulties in the oxidative addition of ClPhMe to [Pd(dppf)] (or [Pd(dppf-Fe^{III})) if not reduced) as a result of the high stability of the Cl-C bond, complete reduction of [$FeCp_2$][PF_6] was again observed (figure 5.24). In this case, the ferrocene is formed in spite of the unsuccessful oxidative addition step, indicating that the Pd(0) species itself can induce the reduction of [$FeCp_2$][PF_6].

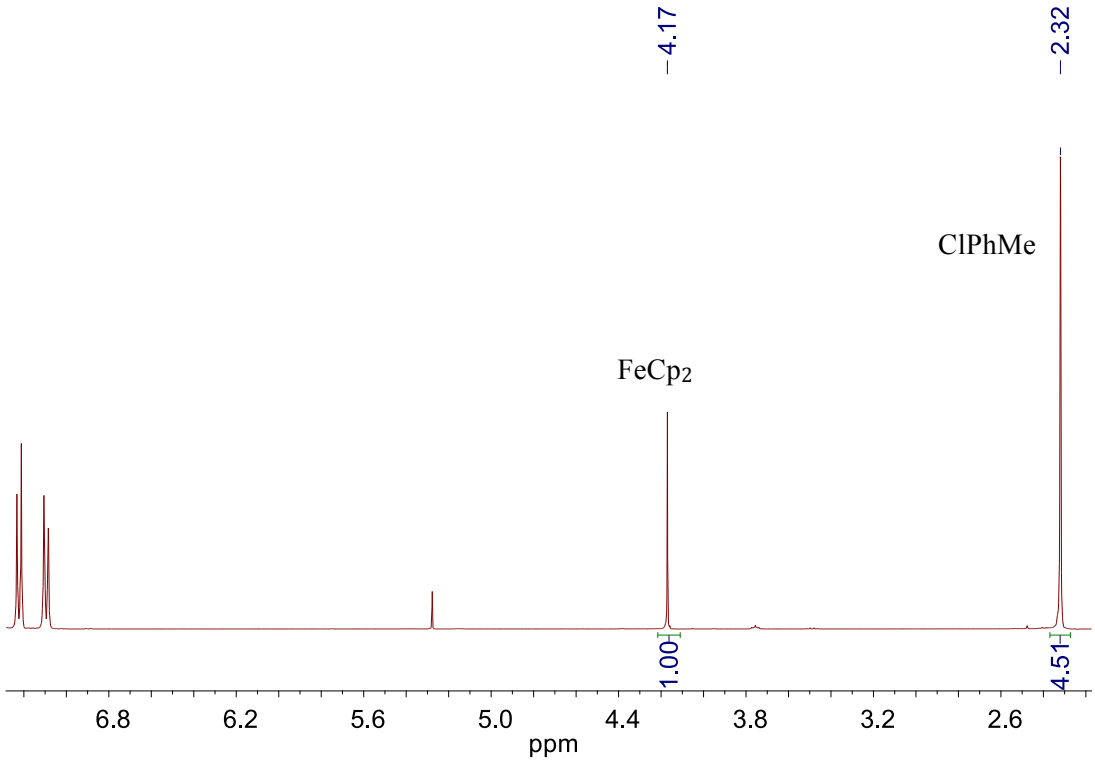

Figure 5.24. ^{1}H NMR spectrum of the reaction mixture from entry 12 in table 5.4

Therefore, the formation of ferrocene observed in the Suzuki-Miyaura cross-coupling reaction of BrPhMe and $PhB(OH)_2$ catalyzed by **2.1-ox** with [$FeCp_2$][PF_6] was caused by the reductive elimination of the catalyst precursor, which gives the Pd(0) species that can reduce the ferrocenium salt. However, this catalyst formation step is not likely to cause the reduction of the ferrocen-1,1'-diylium group in **2.1-ox**. It has been discussed in chapter 2 that the ligand-based oxidation from **2.1** to **2.1-ox** resulted in an increase in the catalytic yield of the alkoxycarbonylation reaction of 2-bromobenzylalcohol, and the oxidative addition and the reductive elimination steps are also included in the catalytic cycle of palladium-catalyzed carbonylation reactions. Consequently, for the Suzuki-Miyaura cross-coupling reactions of BrPhMe and $PhB(OH)_2$ at 30 °C and 50 °C, either the ligand-based reduction of **2.1-ox** took place during the transmetallation step, or **2.1-ox** was not reduced at all but simply afforded the same catalytic conversions as **2.1**.

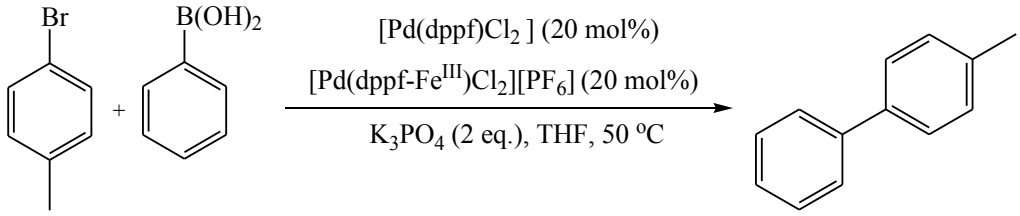

Figure 5.25. Scheme of the Suzuki-Miyaura cross-coupling reaction of BrPhMe and $PhB(OH)_2$ with high catalyst loading

In order to understand whether **2.1-ox** can be reduced during the catalytic process, both the reactions of BrPhMe and $PhB(OH)_2$ catalyzed by **2.1** and **2.1-ox** were repeated at 50 °C using 20 mol% catalyst load (higher concentration of the catalyst for a stronger signal of the catalyst in the ^1H NMR spectrum, figure 5.25). After 3 hours, THF was removed and the crude products were washed with n-hexane, which dissolved both BrPhMe and the product. The solids containing the palladium species obtained upon the completion of the reactions, which are insoluble in n-hexane, were dissolved in $CDCl_3$ and analyzed by ^1H NMR and $^{31}P\{^1H\}$ NMR spectrometry. As to the solution in n-hexane, the solvent was removed and this was analyzed by ^1H NMR spectrometry in $CDCl_3$ to obtain the catalytic conversions of these reactions. The spectral data was summarized in table 5.5.

Catalyst precursor	**β-H (ppm)**	**α-H (ppm)**	**$^{31}P\{^1H\}$ NMR (ppm)**	**Conversion (%)**
2.1	4.24 (dd)	4.69 (dd)	28.63 (s)	92 ± 1
$[Pd(dppf)Cl_2]$	*[4.20 (pt)]*	*[4.40 (pt)]*	*[34.0 (s)]*	
2.1-ox	4.26 (br-s)	4.72 (br-s)	28.18 (s)	92 ± 2
$[Pd(dppf\text{-}Fe^{III})Cl_2][PF_6]$	*[3.92 (br-s)]*	*[4.33 (br-s)]*	*[33.8 (br-s)]*	

Table 5.5. ^1H NMR and $^{31}P\{^1H\}$ NMR ($CDCl_3$, 298 K, 400 MHz) spectral data of the products obtained from the reaction in figure 5.25, and that of **2.1**/**2.1-ox** (in square brackets)

Although the same conversions were afforded by **2.1** and **2.1-ox**, different palladium species were found to be responsible for these catalytic results according to the characteristic signals for the α-hydrogens and β-hydrogens on the substituted Cp ring of the ferrocen-1,1'-diyl/-ium groups in their ^1H NMR spectra. While two doublets of doublets were given by the palladium compound derived from **2.1**, two broad singlets with downfield shifts were found in the spectrum of the product of the **2.1-ox** derivative, suggesting the paramagnetic nature of

this compound and a more electron deficient iron centre. Moreover, the ^{31}P-$\{^{1}H\}$NMR spectra also indicate two different compounds obtained from the two reactions. While these species have not been identified even after mass analyses, it can be confirmed that they are different from **2.1** or **2.1-ox** based on their ^{1}H NMR and $^{31}P\{^{1}H\}$ NMR spectral data (shown in the square brackets in table 5.5). However, it is proposed that these palladium species might be obtained upon the oxidative addition of the Pd(0) catalytically active species, which were formed via the reductive elimination of **2.1** or **2.1-ox**, to the solvent molecule of THF upon the completion of the Suzuki-Miyaura cross-coupling reaction (figure 5.26).

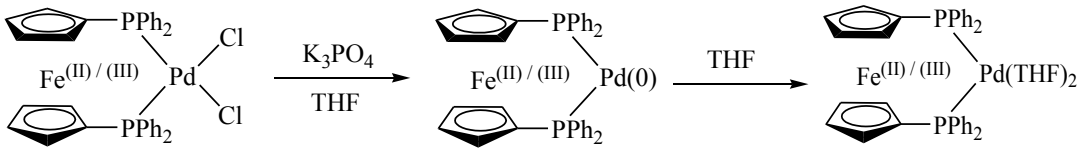

Figure 5.26. Scheme of the formation of Pd(0) species from **2.1/2.1-ox** and the proposed palladium compounds obtained from the completed cross-coupling reaction in THF

Therefore, it is postulated that **2.1-ox** underwent no ligand-based reduction throughout the Suzuki-Miyaura cross-coupling reactions of BrPhMe and $PhB(OH)_2$ in THF with K_3PO_4. Considering that the catalytic reactivities of **2.1** and **2.1-ox** might still be distinguished from the rates of the Suzuki-Miyaura cross-coupling reactions catalyzed by these redox switches, the reactions shown in figure 5.25 were also repeated with the shorter reaction time of 30 mins, and the crude products were analyzed via the same approaches. However, the same spectral data was obtained as shown in table 5.5, suggesting a high rate of these particular reactions.

Although it has not been proved that **2.1** exhibited different catalytic activities than **2.1-ox** towards the same cross-coupling reaction, the similar chemical shifts of the protons and phosphorus atoms in the **2.1** and **2.1-ox** derived species shown in table 5.5 suggest that these catalyst precursors may generate Pd intermediates of similar electronic properties in each steps in the catalytic cycle of this reaction. This could then result in the same catalytic conversions offered by the redox switches.

5.4.2. Rhodium-catalyzed hydrogenation of styrene

The hydrogenation reactions of styrene catalyzed by the redox switches of **5.4/5.4-ox** (figure 5.27) were carried out as a comparative study to the redox-switched rhodium-catalyzed hydrogenation of cyclohexene reported by Wrighton *et al.* (figure 5.2).[13] These hydrogenation reactions were carried out under an atmospheric pressure of H_2 at 120 °C in toluene, with 1 mol% rhodium. **5.3** and the classical Wilkinson catalyst were also used to catalyze this reaction and to compare their catalytic performances with those of **5.4** and **5.4-ox**. Each experiment was repeated 3 times (n = 3), and the products were analyzed by GC

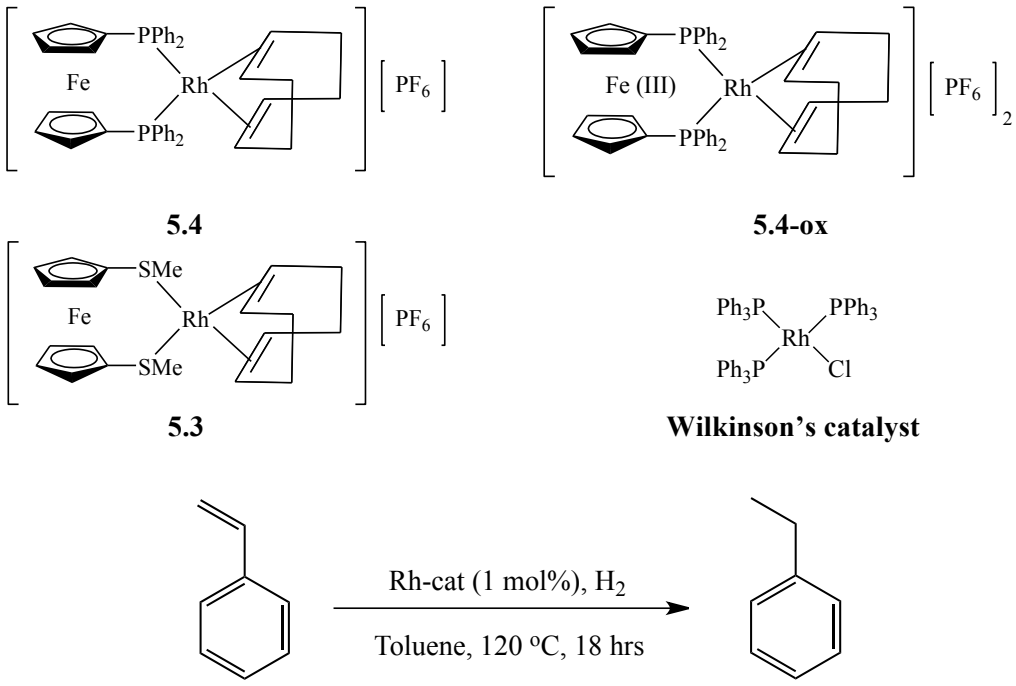

Figure 5.27. Scheme of the hydrogenation of styrene catalyzed by rhodium complexes

The catalytic results are summarized in figure 5.28, and a clear electronic effect can be seen: a more electron-rich rhodium centre afforded a higher conversion of styrene. **5.3**, which has the most electron-deficient rhodium centre due to the weak σ-donation from the S atom to the Rh atom, was found inactive in this hydrogenation reaction. In contrast, **5.4** with a positively charged rhodium centre gave a 63 $\pm$ 1 % conversion, and a lower conversion of 42 $\pm$ 2 % was offered by the more positively charged rhodium centre in **5.4-ox**, while the Wilkinson's catalyst offered the complete conversion of styrene.

In the work by Wrighton *et al.* shown in figure 5.2, the observation that the rhodium complex bearing the ligand of 1,1'-bis(diphenylphosphino)cobaltocene (dppc) offered more rapid hydrogenation of cyclohexane[13] than its cobaltocen-1,1'-diylium version was discussed as being due to the more electron-rich rhodium centre in the dppc-containing complex afforded more rapid oxidative addition of H_2, which is often the rate-limiting step of

hydrogenation reactions. This difference in the rate of the oxidative addition of H_2 to the rhodium centre caused by different electron density on the Rh atom is also considered to be responsible for the catalytic results shown in figure 5.28.

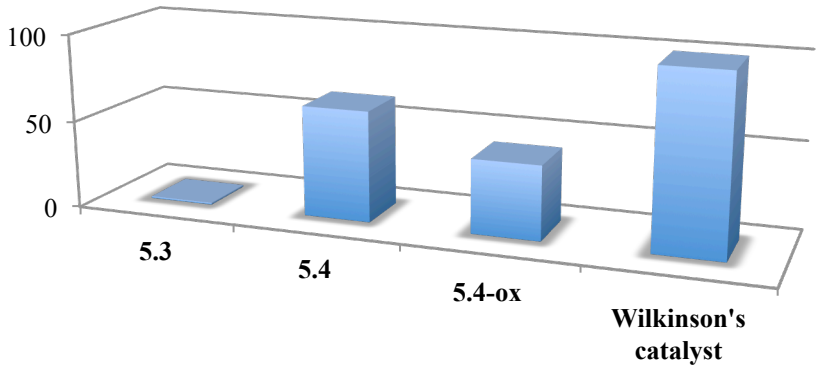

Figure 5.28. Bar chart of the conversions (%) of styrene afforded by rhodium complexes

5.5. Conclusions

The synthesis of the palladium and rhodium complexes bearing the bmsf ligand has been successfully carried out. These complexes were found to exhibit poor catalytic activities in the cross-coupling and hydrogenation reactions investigated compared with their dppf analogues. This is attributed to the weak σ-donation from the S atom to the metal centre, resulting in an electron-deficient palladium/rhodium centre which is not favoured by the oxidative addition of the substrate/H_2.

Investigations into the rhodium-catalyzed hydrogenation reactions of styrene indicate that better catalytic conversions were afforded by the more electron-rich rhodium centre as a result of a more rapid oxidative addition of H_2. The ligand-based oxidation of **5.4** results in about 20% decrease in the catalytic conversion of styrene.

The palladium-catalyzed Suzuki-Miyaura cross-coupling reaction of 4-bromotoluene and phenylboronic acid was more complicated, as the palladium redox switches of **2.1/2.1-ox** offer quite similar conversions of 4-bromotoluene. Excess $[FeCp_2][PF_6]$ was used to keep **2.1-ox** as oxidized, however no difference in the catalytic performance of **2.1-ox** was observed, and the ferrocenium oxidizing agent was found to be reduced to ferrocene. Further investigation show that the Pd(0) catalytically active species is responsible for this reduction. Although it is not clear whether a similar reduction occurred on **2.1-ox**, the signals in the ^1H NMR spectra of the ferrocen-1,1'-diyl/-ium species collected from the completed reactions catalyzed by **2.1/2.1-ox** were found to be of a different type but at similar chemical shifts, which explains the similar catalytic behaviour of this redox switch.

5.6. References

1. Nicolaou, K. C.; Soerensen, E. J. *Classics in Total Synthesis: Targets, Strategies, Methods* VCH: Weinheim, 1996.

2. Nicolaou, K. C.; Snyder, S. A. *Classics in Total Synthesis II: More Targets, Strategies, Methods* VCH: Weinheim, 2003.

3. Magano, J.; Dunetz, J. R. *Chem. Rev.* **2011**, *111*, 2177.

4. Naso, F.; Babudri, F.; Farinola, G. M. *Pure Appl. Chem.* **1999**, *71*, 1485.

5. Hartwig, J. F. *Acc. Chem. Res.* **2008**, *41*. 1461.

6. Martin, R.; Buchwald, S. L. *Acc. Chem. Res.* **2008**, *41*, 1461.

7. Fu, G. C. *Acc. Chem. Res.* **2008**, *41*, 1555.

8. Sheloumov, A. M.; Tundo, P.; Dolgushin, F. M.; Koridz, A. A. *Eur. J. Inorg. Chem.* **2008**, 572.

9. Cullen, W. R.; Kim, T.-J. *Organometallics* **1985**, *4*, 346.

10. Lazzaroni, R.; Setaambolo, R.; Alagona, G.; Ghio, C. *Coord. Chem. Rev.* **2010**, *254*, 696.

11. Gual, A.; Godard, C.; Castillon, S.; Claver, C. *Tetrahedron: Asymmetry* **2010**, *21*, 1135.

12. Cullen, W. R.; Kim, T.-J. *Organometallics* **1983**, *2*, 714.

13. Lorkovic, I. M.; Duff, R. R. Jr.; Wrighton, M. S. *J. Am. Chem. Soc.* **1995**, *117*, 3617.

14. Butler, I. R.; Cullen, W. R.; Kim, T.-J.; Rettig, S. J.; Trotter, J. *Organometallics* **1985**, *4*, 972.

15. Longato, B.; Pilloni, G.; Graziani, R.; Casellato, U. *J. Organomet. Chem.* **1991**, *407*, 369.

16.Hayashi, T.; Konishi, M.; Kobori, Y.; Kumada, M.; Higuchi, T.; Hirotsu, K. *J. Am. Chem. Soc.* **1984**, *106*, 158.

17. Siemeling, U.; Auch, T.-C. *Chem. Soc. Rev.*, **2005**, *34*, 584.

18. Gibson, V. C.; Long, N. L.; Martin, J.; Solan, G. A.; Stichbury, J. C. *J. Organomet. Chem.* **1999**, *590*, 115.

19. McCulloch, B.; Ward, D. L.; Woolins, J. D.; Brubaker, C. H. Jr. *Organometallics* **1985**, *4*, 1425.

20. Riilke, R. E.; Ernsting, J. M.; Spek, A. L.; Elsevier, C. J.; van Leeuwen, P. W. N. M.; Vrieze Kees. *Inorg. Chem.* **1993**, *32*, 5769.

21.Dekker, G. P. C. M.; Elsevier, C. J.; Vrieze, K.; van Leeuwen, P. W. N. M. **1992**, *11*, 1598.

22.Schrock, R. R.; Osborn, J. A. *J. Am Chem. Soc.* **1971**, *19*, 2397.

23. Connelly, N. G.; Geiger, W. E. *Chem. Rev.* **1996**, *96*, 877.

24. Ge, Y. W.; Ye, Y.; Sharp, P. R. *J. Am. Chem. Soc.* **1994**, *116*, 8384.

25. Treichel, P. M.; Essenmacher, G. *J. Inorg. Chem.* **1976**, *15*, 146.

26. Suzuki, A. *Chem. Commun.* **2005**, 4759.

27. Suzuki, A. *J. Synth. Org. Chem., Jpn.* **2005**, *63*, 312.

28. Suzuki, A. *Acc. Chem. Res.* **1982**, *15*, 178.

29. Miyaura, N.; Suzuki, A. *J. Synth. Org. Chem., Jpn.* **1988**, *46*, 848.

30. Miyaura, N.; Suzuki, A. *J. Synth. Org. Chem., Jpn.* **1993**, *51*, 1043.

31.Aliprantis, A. O.; Canary, J. W. *J. Am. Chem. Soc.* **1994**, *116*, 6985.

32. Kochi, J. K. *Organometallic Mechanisms and Catalysis;* Academic: New York, **1978**.

33. Heck, R. F. *Palladium Reagents in Organic Syntheses;* Academic: New York, **1985**.

34. Hartley, F. R.; Patai, S. *The Chemistry of Metal-Carbon Bond;* Wiley: New York, **1985**.

35. McQuillin, F. J.; Parker, D. G.; Stephenson, G. R. *Transition Metal Organometallics for Organic Synthesis*; Cambridge University Press: Cambridge, 1991.

36. Miyaura, N.; Suzuki, A. *Chem. Rev.* **1995**, *95*, 2457.

37. Yanagi, T.; Miyaura, N.; Suzuki, A. *Synth. Commun.* **1981**, *11*, 513.

38. Dieck, H. A.; Heck, R. F. *J. Org. Chem.* **1975**, *40*, 1083.

39. Satoh, Y.; Serizawa, H.; Miyaura, N.; Hara, S.; Suzuki, A. *Tetrahedron Lett.* **1988**, *29*, 1811.

40. Onak, T. *Organoborane Chemistry*; Academic: New York, **1975**.

41. Mikhailov, B. M.; Bubnov, Y. N. *Organoboron Compounds in Organic Synthesis;* Hanvood Academic Publication: Amsterdam, 1983.

42. Pelter, A.; Smith, K.; Brown, H. C. *Borane Reagents*; Academic: New York, **1988**.

43. Miyaura, N.; Yamada, K.; Suzuki, A. *Tetrahedron Lett.* **1979**, *20*, 3437.

44.Miyaura, N.; Yamada, K.; Surrinome, H.; Suzuki, A. *J. Am. Chem. Soc.* **1985**, *107*, 972.

45. Doherty, S.; Robins, E. G.; Nieuwenhuyzen, M.; Knight, J. G.; Champkin, P. A.; Cleggs, W. *Organometallics*, **2002**, *21*, 1383.

46. Casey, C. P.; Whiteker, G. T. *Isr. J. Chem.* **1990**, *30*, 299.

47. Van Leeuwen, P. W. N. M.; Kamer, P. C. J.; Reek, J. N. H.; Dierkes, P. *Chem. Rev.* **2000**, *100*, 2741.

48. Kranenburg, M.; Kamer, P. C. J.; van Leeuwen, P. W. N. M. *Eur. J. Inorg. Chem.* **1998**, *2*, 155.

49.Buchwald, S. L.; Bolm, C. *Angew. Chem. Int. Ed.* **2009**, *48*, 5586.

50. Larsson, P-F.; Correa, A.; Carril, M.; Norrby, P-O.; Bolm, C. *Angew. Chem. Int. Ed.* **2009**, *48*, 5691.

51. Arvela, R. K.; Leadbeater, N. E.; Sangi, M. S.; Williams, V. A.; Granados, P.; Singer, R. D. *J. Org. Chem.* **2005**, *70*, 161.

52. Tsou, T. T.; Kochi, J. K. *J. Am. Chem. Soc.* **1979**, *101*, 7547.

53. Moncomble, A.; Le Floch, P.; Gosmini, C. *Chem. Euro. J.* **2009**, *15*, 4770.

Chapter 6

Conclusions and Future Work

更喜岷山千里雪，三军过后尽开颜。

—— 毛泽东

The work described in this thesis focused on the design and synthesis of ferrocene-based redox-active ligands, the preparation of palladium and rhodium complexes bearing ferrocenyl and ferrocen-1,1'-diyl ligands in both states of charge, and the catalytic applications of these ferrocene/ferrocenium-based complexes in the redox control of the carbonylation reaction of aryl halides, Suzuki-Miyaura cross-coupling reaction of aryl bromide, and the hydrogenation of styrene.

In chapter 2, redox control was first observed in the alkoxycarbonylation reactions of 2-halobenzylalcohol (X= Br, I) catalyzed by the redox partners of $[Pd(dppf\text{-}Fe^{III})Cl_2][PF_6]$ (**2.1-ox**)/$[Pd(dppf)Cl_2]$ (**2.1**), where higher catalytic yields were given by the oxidized complex. Similar improvement on the catalytic performance caused by ligand-based oxidation was later observed for $[Pd(dippf)Cl_2]$ in the same reactions, and for **2.1** in other type of carbonylation reactions. These observations are rationalized as a more electron-deficient palladium centre affords a more difficult oxidative addition step, but more rapid carbonyl insertion, reductive elimination and nucleophilic attack steps in the catalytic cycle. The reactivity of **2.1-ox** was found to depend very much on the temperature and the base used in the reaction.

In these investigations, the performance of the palladium catalysts used was judged only by the yield of the reaction. In order to have a better understanding of the nature of the redox control, kinetic studies can be carried out in the future to see how the rate of the palladium-catalyzed carbonylation reactions studied in this chapter may change with the oxidation state of the ferrocen-1,1'-diyl ligands. Moreover, the cobalt analogues of **2.1/2.1-ox**, $[Pd(dppc)Cl_2]$ /$[Pd(dppc\text{-}Co^{III})Cl_2][PF_6]$, have been synthesized. Therefore the catalytic activities of these cobalt redox partners should be compared with **2.1/2.1-ox** as a future comparative study.

In chapter 3, a different redox control was observed in the alkoxycarbonylation reaction of 2-iodobenzylalcohol catalyzed by the palladium complexes bearing ferrocenyl N-P ligands as the ligand-based oxidation of these complexes resulted in lower catalytic yields. This is seen as a result of the weak σ-donation from the N atom to the palladium centre, where ligand -based oxidation leads to an electron-deficient palladium centre and thus a difficult oxidative addition step. It was quite interesting to see this change in the catalytic behaviour of the palladium complexes bearing ferrocene-based ligands of different chelating atoms caused by ligand-based oxidation. The catalytic results reported in chapter 3 also state the importance of the use of ligands with strong donors as chelating atoms for efficient palladium-catalyzed carbonylation reactions under mild conditions: O- or S-functionalized ferrocenes might not be ideal supporting ligands as the weak donor atoms can cause a difficult oxidative addition step. This conclusion is supported by the catalytic results from the Suzuki-Miyaura cross-coupling and hydrogenation reactions discussed in chapter 5, where palladium/rhodium complexes with bmsf ligand showed poor activities while those with dppf ligand offered good catalytic conversions.

The rhodium-catalyzed hydrogenation of styrene indicated a preference to electron-rich rhodium centres, which is explained via the more rapid oxidative addition of H_2. As the hydro -formylation reactions involve both hydrogenation and carbonylation processes, it would be interesting to see if the catalytic performance of [Rh(dppf)(COD)][PF_6] in hydroformylation reactions can be altered by ligand-based oxidation.

Furthermore, the similar high catalytic conversions afforded by the redox partners of [Pd(dppf)Cl_2] and [Pd(dppf-Fe^{III})Cl_2][PF_6] for the Suzuki-Miyaura cross-coupling reaction of 4-bromotoluene and phenylboronic acid is still unclear, as addressed in chapter 5. It might be worthwhile using a more challenging reaction, for instance, an aryl bromide with strong electron-donating substituents on the aryl group, to see if there is a noticeable difference between the catalytic performances of the palladium redox switches.

On the other hand, oxidative purification reported in chapter 4 offers a promising tool for the separation of compounds with different oxidation potentials. This purification method can be applied to the isolation of general ferrocene-containing species, and extended to the separation of other redox-active organometallic compounds using various oxidants according to the different physical properties of the non-oxidized and oxidized species.

In addition, a more reactive fluorinating agent and a more optimized reaction system for the synthesis of fcF_2 should be studied, as the yield of the reaction of 1,1'-dilithioferrocene-TMEDA and NFSI is very low (5 %). Once the yield can be improved, investigations towards the synthesis of pentafluoroferrocene and eventually decafluoroferrocene can be carried out to obtain the most unusal metallocene ever.

The synthesis of transition metal complexes from the ferrocene-based diimine ligands described in chapter 4 was found to be complicated due to the instability of these complexes, which undergo either decomposition or oxidation. A better understanding of the complexation of these ligands can be achieved by obtaining the crystal structure of these ligands and carrying out structural studies.

Last but not the least, the design of redox-active ligands can be extended to include the use of: (i) a stronger ferrocene-based redox unit, such as biferrocene or bis(ferrocenyl)phosph -ine to exert more significant electronic effect via oxidation; (ii) other metallocenes such as ruthenocene and cobaltocene; and (iii) the use of non-metallocene units, such as tetrathiafulva -lene. Other catalytic processes for redox control should also be explored.

Chapter 7

Experimental

天若有情天亦老，人间正道是沧桑。

—— 毛泽东

7.1. General

All the preparations were carried out using standard Schlenk line and air-sensitive chemistry techniques under an atmosphere of nitrogen. No special precautions were taken to exclude air or moisture during workup, unless stated otherwise. Solvents used for reactions were distilled under nitrogen from appropriate agents. Air-sensitive compounds were kept under nitrogen and stored in sealed vials at room temperature. Chromatographic separations were carried out on silica gel (kieselgel 60, 70-230 mesh). Starting materials were either prepared according to adapted literature procedures (if stated), or purchased from commercial suppliers and used without further purification.

^{1}H NMR, ^{31}P{^{1}H} NMR, ^{13}C{^{1}H} NMR, ^{19}F{^{1}H} NMR and ^{11}B NMR spectra were recorded on a departmental 400MHz Bruker spectrometer. Chemical shifts are reported in δ (ppm) and internally reference to the residual NMR solvent peaks.[1] ^{13}C{^{1}H} NMR spectra were fully assigned where possible using 2D correlation spectroscopy; this could not achieved in some cases due to insufficient sample quantity and solubility limitation. Mass spectrometric analyses were performed by Mr. John Barton and Ms. Lisa Haigh of the Department of Chemistry, Imperial College London. Elemental analyses were conducted by Stephen Boyer of the Science Centre, London Metropolitan University.

Cyclic voltammetry experiments were recorded under an atmosphere of argon in the stated solution with 0.1 M TBAP on a Gamary potentiostat (Gamary Instrument), with a platinum working electrode, a Pt-coil counter electrode and a silver-wire reference electrode (see Chapter 1, Section 1.4.1). Potentials are reported to relative to $[FeCp_2]^+/FeCp_2$, measured against an internal $[FeCp_2]^+/FeCp_2$ or $[FeCp_2]^+/FeCp_2$ reference, where appropriate.

Carbonylation and hydrogenation reactions were carried out on a Radley's multi-reactor carousel connected to a carbon monoxide/hydrogen manifold where up to 12 reactions could be carried out simultaneously under the same conditions. Only 6 reactions were carried out at one time in order to reduce human error. The solid reagent(s) and catalyst placed in the reaction vessels were subject to at least three cycles of freeze-pump-thaw before use to remove any atmospheric air, and the dry degassed liquid reagent(s) and solvent were transferred *via* cannula under an atmospheric pressure of carbon monoxide/hydrogen. Once the mixture had been heated to temperature, the gas cylinder was switched off, and the

remaining carbon monoxide/hydrogen in the reaction vessels was to react. Upon completion of the reaction, the solution of the crude product was cooled to room temperature and filtered through a thin pad of Celite to remove any precipitate. This solution is later prepared for GC analysis. Each reaction entry was repeated for at least three times.

Quantitative analysis *via* gas chromatography was carried out on a Hewlett-Packard 5890 GC fitted with an Agilent 6690 auto-sampler and a flame ionization detection system. The products were separated on a J&W DB-5 column with a cross linked/surface bonded 5% phenyl, 95% methylpolysiloxane stationary phase; length 30 m, I. D. 0.22 mm, film thickness 0.25 mm. 'Barton' was chosen as the analytical method (oven start temperature: 100 ºC for 10 mins, heat rate: 12 ºC /min, end temperature: 240 ºC).

For hydrogenation reactions, catalytic conversions were calculated *via* calculating the response factors from the starting material and the product. For carbonylation reactions, each crude product were made into 10 mL 0.01 M solution of dodecane in ethyl acetate in 10 mL volumetric flasks. Quantification of yield was achieved by calculating the response factors from the products and dodecane, which is the internal standard. Approximately 1 mL of the made-up solution was then transferred into GC vials for analysis.

The GC calibration for the carbonylation products (phthalide, N-benzylbenzamide, benzyl benzoate and 1-isoindolinone) was first carried out. This was achieved by preparing at least 3 samples with different concentrations of phthalide or N-benzylbenzamide in ethyl acetate and a uniform concentration of internal standard solution (dodecane, 0.01 M, 10 mL). The response of the products and internal standard was detected by the GC and analyzed using Clarity software, and the integration (area) of the corresponding peaks was noted from the chromatograms. Then a graph was drawn up of integration of product/ integration of dodecane standard (A_p/A_{std}) versus the concentration of the product/ concentration of the dodecane standard (C_p/C_{std}), which gives a linear relationship. The gradient from this graph which links the integration of the peaks on the chromatogram with the concentration in the vial is known as the response factor (RF) and is different for every product obtained.

An example of the calibration of GC for phthalide is shown in figure 7.1. The linear relationship obtained from the calibration can be rearranged to calculate the concentration of the products ($C_p= [A_pC_{std}]/[A_{std}RF]$) of the carbonylation reactions. The C_p can then be

multiplied by 10 mL (10 mL standard volumetric flask) and divided by the 100% theoretical molar yield of product to give the overall yield.

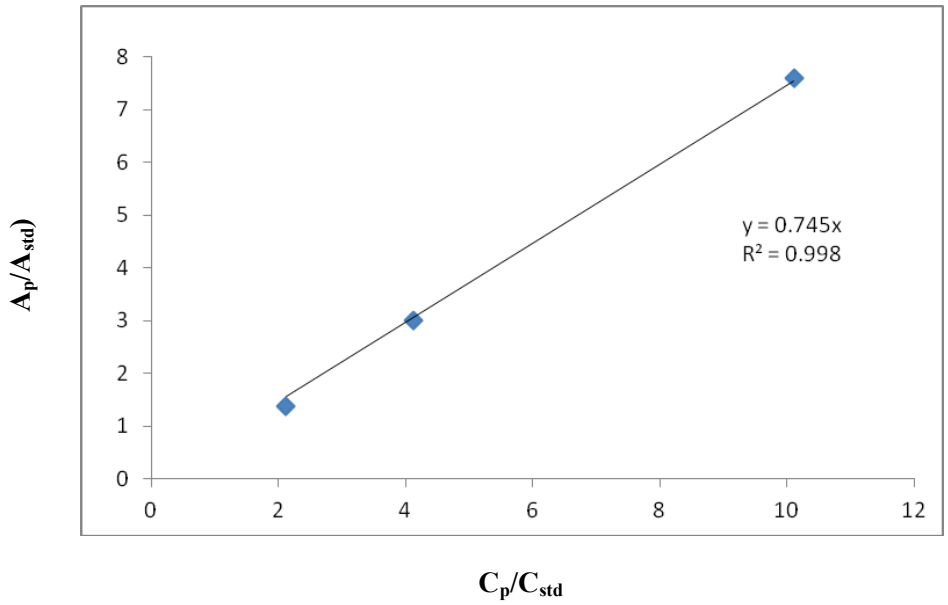

Figure 7.1. The graph for the calibration of GC for phthalide

7.2. Compounds Synthesized in Chapter 2

Dichloropalladium 1,1'-bis(diphenylphosphino)ferrocenium hexafluorophosphate[1]

$[PdCl_2(dppf)][PF_6]$ (2.1-ox)

In a two-necked round-bottomed flasks, the mixture of $[Pd(dppf)Cl_2]$ (0.41 g, 0.55 mmol, 1 eq.) and $[FeCp_2][PF_6]$ (0.18 g, 0.54 mmol, 0.98 eq.) were placed with a stirrer. DCM (15 mL) was added to the mixture, and a dark green solution was formed. After this was left stirring overnight, and the solvent was removed to give a dark green solid, which was washed with toluene (3 × 30mL). A dark green solid was obtained (0.39 g, 86 %). Anal. Calcd. for $C_{34}H_{28}F_6Cl_2FeP_3Pd$: C 46.52, H 3.20. Found: C 46.62, H 3.13. ^{1}H NMR (400 MHz; $CDCl_3$) δ_H: 3.92 (br, Cp-H), 4.33 (br, Cp-H), 7.41 (br, aryl-H). $^{31}P\{^1H\}$ NMR (162 MHz; $CDCl_3$) δ_P: 33.7 (s, PPh_2). MS(ESI) m/z: 735 ($[M\text{-}PF_6]^+$, 55%).

Dichloropalladium 1,1'-bis(di-*tert*-butylphosphino)ferrocenium hexafluorophosphate [$PdCl_2$(dtbpf)][PF_6] (2.2-ox)

In a two-necked round-bottomed flasks, the mixture of [Pd(dtbpf)Cl_2] (130 mg, 0.20 mmol, 1 eq.) and [$FeCp_2$][PF_6] (65 mg, 0.196 mmol, 0.18 g, 0.98 eq.) were placed with a stirrer. DCM (15 mL) was added to the mixture, and a dark green solution was formed. After this was left stirring overnight, and the solvent was removed to give a dark green solid, which was washed with diethyl ether (3 × 30mL). A brown solid was obtained (0.39 g, 88 %). Anal. Calcd. for $C_{26}H_{44}Cl_2F_6P_3FePd$: C 39.17, H 5.57. Found: C 39.12, H 5.49. ^{1}H NMR (400 MHz; $CDCl_3$) δ_H: 4.21 (br, Cp-H), 1.63 (br, -CH_3). $^{31}P\{^1H\}$ NMR (162 MHz; $CDCl_3$) δ_P: 11.0 (s, P^tBu_2), -145.8 (m, PF_6^-, $^1J_{F,P}$ = 683.65 Hz). MS(ESI) m/z:, 290 ([M-Cl_2PF_6]$^{2+}$, 25 %).

Dichloropalladium 1,1'-bis(di-*iso*-propylphosphino)ferrocenium hexafluorophosphate [$PdCl_2$(dippf)][PF_6] (2.3-ox)

In a separate two-necked round-bottomed flasks, the mixture of [Pd(dippf)Cl_2] (120 mg, 0.20 mmol, 1 eq.) and [$FeCp_2$][PF_6] (65 mg, 0.196 mmol, 0.18 g, 0.98 eq.) were placed with a stirrer. DCM (15 mL) was added to the mixture, and a dark green solution was formed. After this was left stirring overnight, and the solvent was removed to give a dark green solid, which was washed with DCM (3 × 30mL). A dark green solid were obtained (0.39 g, 86 %); Anal. Calcd. for $C_{22}H_{35}F_6Cl_2FeP_3Pd$: C 35.71, H 4.77. Found: C 35.62, H 4.72. ^{1}H NMR (400 MHz; CD_2Cl_2) δ_H: 4.47 (br, Cp-H), 4.52 (br, Cp-H), 2.73 (br, -CH-) 1.12 (br, -CH_3), 1.44 (br, -CH_3). $^{31}P\{^1H\}$ NMR (162 MHz; CD_2Cl_2) δ_P: 65.3 (s, P^iPr_2). MS(ESI) m/z: 267 ([M-Cl_2PF_6]$^{2+}$, 30 %)

Synthesis of phthalide

2-Iodobenzylalcohol (0.23 g, 1.0 mmol, 1 eq.)/2-bromobenzylalcohol (0.187 g, 1.0 mmol, 1 eq.) and the selected palladium catalyst (0.05 eq.) were placed under an atmospheric pressure of CO. Dry toluene (5 mL) and triethylamine (0.4 mL, 3.0 mmol, 3 eq.) was added to the mixture under CO. This reaction mixture was heated to 100 ºC/120 ºC for 3 hours/18 hours, filtered through Celite, and the filtrate was collected. The solvent was removed under reduced pressure, and the solid obtained was dissolved in 10 mL stock solution of dodecane

in ethyl acetate (0.01 M) and analyzed by GC.

The data of catalytic yields (%) of phthalide corresponding to the bar charts in section 2.3 is summarized in the following tables.

ArX / **R**	**2.2**	**2.2-ox**	**2.3**	**2.3-ox**	**2.1**	**2.1-ox**
X = Br	100	100	0	50 ± 3	54 ± 3	91 ± 2
X = I	100	100	0	21 ± 2	87 ± 1	94 ± 3

Table 7.1. Data included in figure 2.6 (n ≥ 3)

cat. / **T**	**100 ºC**	**120 ºC**
2.3	0	100
2.3-ox	21 ± 2	100

Table 7.2. Data included in figure 2.11 (n ≥ 3)

Entry / **R**	**2.3**	**2.2**	**2.1**
100 ºC non-ox	0	100	25 ± 1
100 ºC ox	0	74 ± 1	0
120 ºC non-ox	0	100	54 ± 3
120 ºC ox	50 ± 3	100	91 ± 2

Table 7.3. Data included in figure 2.12 (n ≥ 3)

Pd-load	1 mol%	2 mol%	3 mol%	5 mol%
Yield (%)	0	10 ± 3	53 ± 2	91 ± 2

Base (pK_a)	$PhNMe_2$ (5.1)	DABCO (8.7)[i]	NEt_3 (10.8)
Yield (%)	0	68 ± 1	91 ± 2

Table 7.4. Data included in figure 2.14 (n ≥ 3)

[i] pK_1 value of DABCO (1,4-Diazabicyclo[2.2.2]octane).

cat. \ Sol.	Toluene	THF
2.1	54 ± 3	2 ± 1
2.1-ox	91 ± 2	30 ± 5

Table 7.5. Data included in figure 2.16 (n ≥ 3)

Synthesis of N-benzylbenzamide[2]

The mixture of iodobenzene (0.112 mL, 1.0 mmol, 1 eq.)/bromobenzene (0.10 mL, 1.0mmol, 1 eq.), benzylamine (1.0 mL, 10.0 mmol, 10 eq.) (or benzylamine (0.1 mL, 1.0 mmol, 1 eq.) and triethylamine (0.4 mL, 3.0 mmol, 3 eq.)) and the selected palladium catalyst (0.02 eq.) in dry toluene (5 mL) was heated to 100 ºC/120 ºC for 3 hours/18 hours under an atmospheric pressure of CO. After filtration through Celite the mixture was made up to 8 mL with toluene and added with 2 mL stock solution of dodecane in ethyl acetate (0.01 M). The resulting solution was then analyzed by GC.

The data of catalytic yields (%) of N-benzylbenzamide corresponding to the bar charts in chapter 2.4 is summarized in the following tables (n ≥ 3).

Cat. \ PhX	X = I	X = Br
2.1	85 ± 1	82 ± 2
2.1-ox	84 ± 3	30 ± 5

Table 7.6. Data included in figure 2.20 (n ≥ 3)

Cat. \ PhX	X = Br	X = I
2a-neu	83 ± 2	84 ± 2
2a-ox	91 ± 1	100

Table 7.7. Data included in figure 2.21 (n ≥ 3)

2 mol% Pd, THF	1 mol% Pd, Toluene	2 mol% Pd, Toluene
0	80 ± 1	91 ± 1

Table 7.8. Data included in figure 2.23 (n ≥ 3)

Synthesis of benzyl benzoate

The mixture of iodobenzene (0.112 mL, 1.0 mmol, 1 eq.)/bromobenzene (0.10 mL, 1.0mmol, 1 eq.), benzylalcohol (0.1 mL, 1.0 mmol, 1 eq.), triethylamine (0.4 mL, 3.0 mmol, 3 eq.) and the selected palladium catalyst (0.05 eq.) in dry toluene (5 mL) was heated to 120 ºC for 3 hours under an atmospheric pressure of CO. After filtration through Celite, the filtrate was collected. The solvent was removed under reduced pressure, and the solid obtained was dissolved in 10 mL stock solution of dodecane in ethyl acetate (0.01 M) and analyzed by GC.

Synthesis of 1-isoindolinone

The mixture of 2-bromobenzylamine (0.186 g, 1.0 mmol, 1 eq.), triethylamine (0.4 mL, 3.0 mmol, 3 eq.) and the selected palladium catalyst (0.05 eq.) in dry toluene (5 mL) was heated to 120 ºC for 18 hours under an atmospheric pressure of CO. After filtration through Celite, the filtrate was collected. The solvent was removed under reduced pressure, and the solid obtained was dissolved in 10 mL stock solution of dodecane in ethyl acetate (0.01 M) and analyzed by GC.

The data of catalytic yields (%) of benzyl benzoate and 1-isoindolinone corres -ponding to the bar charts in chapter 2.5 is summarized in the table 7.9 (n ≥ 3).

Cat. / **Product**	**1-isoindolinone**	**benzyl benzoate**
2.1	43 ± 5	54 ± 2
2.1-ox	45 ± 4	67 ± 3

Table 7.9. Data included in figure 2.24 (n ≥ 3)

7.3. Compounds Synthesized in Chapter 3

2-(Di-*p*-tolylphosphino)benzylideneiminoferrocene[3] (3.2)

In a 250 mL round-bottomed flask, the mixture of 2-(di-*p*-tolylphosphino)benzaldehyde (0.50 g, 1.57 mmol, 1 eq.) and aminoferrocene (0.32 g, 1.59 mmol, 1.01 eq.) in *n*-hexane was heated to 80 ºC for 18 hours. The resulting solution was dried over K_2CO_3 and the solvent was removed. A red solid was obtained in a 94 % yield (0.74 g). ^{1}H NMR (400 MHz; $CDCl_3$) δ_H: 2.35 (s, 6H, CH_3), 3.96 (s, 5H, Cp-H), 4.19 (pt, 2H, Cp-H), 4.43 (pt, 2H, Cp-H), 6.87 (m, H, Ar-H), 7.31 (pt, H, Ar-H), 7.19 (pt, 4H, PAr'$_2$), 7.22 (pt, 4H, PAr'$_2$), 7.40 (pt, H, Ar-H), 8.11 (dd, H, Ar-H), 9.32 (d, H, N=C-H). ^{31}P{^{1}H} NMR (162 MHz; $CDCl_3$) δ_p: -15.8 (s). ^{13}C{^{1}H} NMR (100 MHz; $CDCl_3$) δ_C: 21.5 (CH_3, *C*-H), 63.4 (Cp-N, *C*-H), 67.3 (Cp-N, *C*-H), 69.7 (Cp, *C*-H), 104.8 (Cp-N, *C*-N), 127.1 (Ar, *C*-H), 128.9 (Ar, *C*-H), 129.6 (PAr'$_2$, *C*-H), 129.7 (PAr'$_2$, *C*-P), 130.2 (Ar, *C*-H), 133.2 (Ar, *C*-H), 133.3 (PAr'$_2$, *C*-H), 134.1 (PAr'$_2$, *C*-H), 134.3 (PAr'$_2$, *C*-H), 138.0 (Ar, *C*-P), 139.1 (PAr'$_2$, *C*-CH_3), 139.8 (Ar, *C*-C=N), 156.7 (C=N). MS (EI) m/z: 502 ([M+H]$^+$, 30 %); MS (ESI) m/z: 519 ([M+H_2O]$^+$, 100 %).

A procedure similar to that for the preparation of **3.2** was used for the synthesis of **3.3** and **3.4**.

2-[bis(3,5-Dimethylphenyl)phosphino)]benzylideneiminoferrocene (3.3)

The mixture of 2-[bis(3,5-dimethylphenyl)phosphino)]benzaldehyde (0.25 g, 0.72 mmol, 1 eq.) and aminoferrocene (0.15 g, 0.75 mmol, 1.04 eq.) in *n*-hexane was heated to 80 ºC for 18 hours. A dark red solid was obtained in a 95 % yield (0.35 g). ^{1}H NMR (400 MHz; $CDCl_3$) δ_H: 2.26 (s, 12H, CH_3), 3.94 (s, 5H, Cp-H), 4.18 (pt, 2H, Cp-H), 4.46 (pt, 2H, Cp-H), 6.88 (m, H, Ar-H), 6.92 (s, 2H, PAr'$_2$), 6.98 (s, 2H, PAr'$_2$), 7.32 (pt, H, Ar-H), 7.40 (pt, H, Ar-H), 8.11 (dd, H, Ar-H), 9.32 (d, H, N=C-H). ^{31}P{^{1}H} NMR (162 MHz; $CDCl_3$) δ_p: -14.7 (s). ^{13}C{^{1}H} NMR (100 MHz; $CDCl_3$) δ_C: 21.5 (CH_3), 63.6 (Cp-N, *C*-H), 67.3 (Cp-N, *C*-H), 69.7 (Cp, *C*-H), 104.7 (Cp-N, *C*-N), 126.9 (Ar, *C*-H), 129.0 (Ar, *C*-H), 130.2 (PAr'$_2$, *C*-P), 131.0 (Ar, *C*-H), 131.8 (PAr'$_2$, *C*-H), 131.8 (PAr'$_2$, *C*-H), 132.0 (PAr'$_2$, *C*-H), 133.6 (PAr'$_2$, *C*-H), 136.2 (Ar, *C*-P), 138.1 (PAr'$_2$, *C*-CH_3), 139.8 (Ar, *C*-C=N), 157.2 (C=N). MS (EI) m/z: 529 ([M]$^+$, 10 %); MS (ESI) m/z: 547 ([M+H_2O]$^+$, 100 %).

2-[bis(3,5-Di-*tert*-butyl-4-methoxyphenyl)phosphino]]benzylideneaminoferrocene (3.4)

The mixture of 2-[bis(3,5-di-*tert*-butyl-4-methoxyphenyl)phosphino]benzaldehyde (0.25 g, 0.44 mmol, 1 eq.) and aminoferrocene (0.09 g, 0.45 mmol, 1.02 eq.) in *n*-hexane was heated to 70 ºC for 5 hours. A dark red solid was obtained in a 90 % yield (0.30 g). Anal. Calcd. for $C_{47}H_{60}FeNO_2P$: C 74.48, H 7.98, N 1.85. Found: C 74.32, H 7.93, N 1.89. ^{1}H NMR (400 MHz; $CDCl_3$) δ_H: 1.32 (s, 36H, CH_3), 3.65 (s, 6H, OCH_3), 3.93 (s, 5H, Cp-H), 4.17 (pt, 2H, Cp-H), 4.43 (pt, 2H, Cp-H), 6.85 (m, H, Ar-H), 7.12 (s, 2H, PAr'$_2$), 7.14 (s, 2H, PAr'$_2$), 7.34 (pt, H, Ar-H), 7.40 (pt, H, Ar-H), 8.16 (dd, H, Ar-H), 9.43 (d, H, N=C-H). ^{31}P{^{1}H} NMR (162 MHz; $CDCl_3$) δ_p: -14.1 (s). ^{13}C{^{1}H} NMR (100 MHz; $CDCl_3$) δ_C: 32.1 (CH_3), 36.1 (*C*-CH_3), 63.7 (Cp-N, *C*-H), 67.2 (Cp-N, *C*-H), 69.7 (Cp, *C*-H), 105.1 (Cp-N, *C*-N), 126.6 (Ar, *C*-H), 128.8 (Ar, *C*-H), 129.9 (PAr'$_2$, *C*-P), 130.1 (Ar, *C*-H), 132.6 (PAr'$_2$, *C*-H), 132.8 (PAr'$_2$, *C*-H), 133.0 (Ar, *C*-H), 139.3 (Ar, *C*-P), 139.6 (Ar, *C*-C=N), 143.9 (PAr'$_2$, *C*-CCH_3), 157.4 (C=N), 160.5 (PAr'$_2$, *C*-OCH_3). MS (EI) m/z: 757 ([M]$^+$, 5 %).

Dichloropalladium 2-(diphenylphosphino)benzylideneiminoferrocene (3.6)

To a 250 mL round-bottomed flask $[Pd(CH_3CN)_2Cl_2]$ (0.12 g, 0.50 mmol, 1 eq.) and **3.1** (0.25 g, 0.53 mmol, 1.05 eq.) was dissolved in 30 mL CH_2Cl_2 and the mixture was left stirring at room temperature for 3 hours. After removal of the solvent the resulting dark product was washed with toluene (3 × 20 mL) and filtered. The solid was gathered and recrystallized from hot MeCN to give dark green product (0.31g, 95 %). Anal. Calcd. for $C_{29}H_{24}Cl_2FeNPPd$: C 53.51, H 3.72, N 2.15. Found: C 53.50, H 3.80, N 2.12. ^{1}H NMR (400 MHz; CD_2Cl_2) δ_H: 3.72 (s, 5H, Cp-H), 4.29 (pt, 2H, Cp-H), 4.85, (pt, 2H, Cp-H), 7.10 (m, H, Ar-H), 7.50 ~ 7.90 (m, 13H, Ar-PPh_2), 8.90 (s, H, N=CH). ^{31}P{^{1}H} NMR (162 MHz; $CDCl_3$): 31.7 (s).

A procedure similar to that for the preparation of **3.6** was used for the synthesis of **3.7** and **3.8**. No meaningful data were obtained from the mass analyses of these complexes.

Dichloropalladium 2-(di-*p*-tolylphosphino)benzylideneiminoferrocene (3.7)

The mixture of $[Pd(CH_3CN)_2Cl_2]$ (0.087 g, 0.35 mmol, 1 eq.) and **3.2** (0.20 g, 0.39 mmol, 1.1 eq.) in DCM (30 mL) was left stirring at room temperature for 3 hours. A dark

purple solid was obtained (0.20 g, 88 %). Anal. Calcd. for $C_{31}H_{28}Cl_2FeNPPd$: C 54.84, H 4.16, N 2.06. Found: C 55.01, H 4.06, N 2.15. ^{1}H NMR (400 MHz; $CDCl_3$) δ_H: 2.42 (s, 6H, CH_3), 4.16 (m, 7H, Cp-H), 4.55 (pt, 2H, Cp-H), 7.10 (m, H, Ar-H), 7.13 (dd, H, Ar-H), 7.32 (d, 4H, PAr'$_2$) 7.52 (pt, H, Ar-H), 7.58 (pt, 4H, PAr'$_2$), 10.01 (s, H, N=CH), 10.74 (m, H, Ar-H). ^{31}P{^{1}H} NMR (162 MHz; $CDCl_3$): 34.3 (s).

Dichloropalladium 2-[bis(3,5-dimethylphenyl)phosphino)]benzylideneiminoferrocene

(3.8)

The mixture of $[Pd(CH_3CN)_2Cl_2]$ (0.096 g, 0.37 mmol, 1 eq.) and **3.3** (0.21 g, 0.41 mmol, 1.1 eq.) in DCM (30 mL) was left stirring at room temperature for 3 hours. A dark purple solid was obtained (0.24 g, 92 %). Anal. Calcd. For $C_{33}H_{32}Cl_2FeNPPd$: C 56.06, H 4.57, N 1.98. Found: C 56.14, H 4.50, N 2.04. ^{1}H NMR (400 MHz; CD_2Cl_2) δ_H: 2.37 (s, 12H, CH_3), 4.20 (s, 5H, Cp-H), 4.28 (pt, 2H, Cp-H), 4.58 (pt, 2H, Cp-H), 7.19 (m, H, Ar-H), 7.25 (d, 2H, PAr'$_2$), 7.30 (s, 2H, PAr'$_2$), 7.33 (s, 2H, PAr'$_2$), 7.59 (pt, H, Ar-H), 7.82 (m, H, Ar-H), 9.89 (s, H, N=CH), 10.71 (m, H, Ar-H). ^{31}P{^{1}H} NMR (162 MHz; $CDCl_3$): 32.5 (s).

Ditriflatepalladium 2-(diphenylphosphino)benzylideneiminoferrocenium triflate[3]

(3.6-ox)

In a 100 mL round-bottomed flask **3.6** (0.13 g, 0.2 mmol, 1 eq.) and silver triflate (0.15 g, 0.6 mmol, 3 eq.) was dissolved in 15 mL DCM. The flask was covered with foil to shield the light, and the mixture was left stirring at room temperature for 3 hours. The resulting suspension was filtered through Celite. The solid was washed by MeCN (3 × 10 mL), and the filtrates were combined. After removal of the solvent, a dark orange oily solid was obtained (wet crude product weight 0.20 g). Anal. Calcd. for $C_{32}H_{24}F_9FeNO_9PPdS_3$: C 37.42, H 2.36, N 1.36. Found: C 35.40, H 1.89, N 2.46. ^{1}H NMR (400 MHz; $CDCl_3$) δ_H: 3.42 (br, Cp-H), 7.53 (br, Ar-PPh_2). ^{31}P{^{1}H} NMR (162 MHz; $CDCl_3$): 78.3 (s). ^{19}F{^{1}H} NMR (377 MHz; $CDCl_3$): -190.7 (br).

A procedure similar to that for the preparation of **3.6-ox** was used for the synthesis of **3.7-ox** and **3.8-ox**. No meaningful data were obtained from the mass analyses of these oxidized complexes.

Ditriflatepalladium 2-(di-*p*-tolylphosphino)benzylideneiminoferrocenium triflate (3.7-ox)

A mixture of **3.7** (0.136 g, 0.2 mmol, 1 eq.) and silver triflate (0.15 g, 0.6 mmol, 3 eq.) in DCM was left stirring for 3 hours at room temperature. The solution was filtered through Celite, the solid was washed by toluene and the filtrates were combined. An orange solid was obtained after the removal of solvent (wet crude product weight 0.22 g). Anal. Calcd. for $C_{34}H_{28}F_9FeNO_9PdPS_3$: C 38.70, H 2.68, N 1.33. Found: C 40.79, H 4.38, N 1.04. ^{1}H NMR (400 MHz; $CDCl_3$) δ_H: 2.02 (br, CH_3), 3.19 (br, Cp-H), 3.49 (br, Cp-H), 9.54 (br, Ar-PAr'$_2$). ^{31}P {^{1}H}NMR (162 MHz; $CDCl_3$): 73.4 (s). ^{19}F{^{1}H} NMR (377 MHz; $CDCl_3$): -170.5 (br).

Ditriflatepalladium 2-[bis(3,5-dimethylphenyl)phosphino)]benzylideneiminoferrocenium triflate (3.8-ox)

A mixture of **3.7** (0.14 g, 0.2 mmol, 1 eq.) and silver triflate (0.15 g, 0.6 mmol, 3 eq.) in DCM was left stirring for 3 hours at room temperature. The solution was filtered through Celite, the solid was washed by chloroform and the filtrates were combined. An orange solid was obtained after the removal of solvent. Anal. Calcd. for $C_{36}H_{32}F_9FeNO_9PdS_{33}$: C 39.91, H 2.98, N 1.29. Found: C 38.83, H 2.95. ^{1}H NMR (400 MHz; $CDCl_3$) δ_H: 1.85 (br, CH_3), 3.75 (br, Cp-H), 3.84 (br, Cp-H), 7.58 (br, Ar-PAr'$_2$). ^{31}P {^{1}H}NMR (162 MHz; $CDCl_3$): 74.6 (s). ^{19}F {^{1}H}NMR (377 MHz; $CDCl_3$): -179.2 (br).

Synthesis of phthalide

The alkoxycarbonylation reaction of 2-iodo-/bromobenzylalcohol was carried out using the same procedure as described in the previous section. The data of catalytic yields (%) of phthalide corresponding to the bar charts in section 3.20 is summarized in table 7.10.

ArX \ **R**	**3.1**	**3.1-ox**	**3.2**	**3.2-ox**	**3.3**	**3.3-ox**
X = Br	13 ± 2	0	0	0	0	0
X = I	88 ± 1	100	83 ± 1	50 ± 2	83 ± 2	50 ± 3

Table 7.10. Data included in figure 3.20 ($n \geq 3$)

7.4. Compounds Synthesized in Chapter 4

2,6-Pyridinedimethylideneiminoferrocene[5] (4.1)

In a 250 mL round-bottomed flask, a mixture of 2,6-pyridinedicarboxaldehyde (0.25 g, 1.85 mmol, 1 eq.) and aminoferrocene (0.74 g, 3.70 mmol, 2 eq.) in *n*-hexane was heated to 50 ºC for 3 hours. The resulting solution was dried over anhydrous Na_2SO_4 and the solvent was removed. A red/purple solid was obtained in a 95 % yield (0. 88 g). Anal. Calcd. for $C_{27}H_{23}Fe_2N_3$: C 64.69, H 4.63 N 8.39. Found: C 65.81 H 5.14 N 7.94. ^{1}H NMR (400 MHz; $CDCl_3$) δ_H: 4.21 (s, 5H, Cp-H), 4.36 (pt, 2H, Cp-H), 4.71 (pt, 2H, Cp-H), 7.84 (pt, H, Py-H), 8.19 (s, H, Py-H), 8.21 (s, H, Py-H), 8.81 (s, 2H, N=C-H). ^{13}C{^{1}H} NMR (100 MHz; $CDCl_3$) δ_C: 63.8 (Cp-N, *C*-H), 68.2 (Cp-N, *C*-H), 70.0 (Cp, *C*-H), 103.5 (Cp-N, *C*-N), 121.8 (Py, *C*-H), 137.3 (Py, *C*-H), 155.3 (Py, *C*-C), 157.6 (C=N). MS (ESI) m/z: 502 ([M+H]$^+$, 100 %).

A procedure similar to that for the preparation of **4.1** was used for the synthesis of **4.2** and **4.6**.

Dichloropalladium 1,3-benzenedimethylideneiminoferrocene (4.4)

A mixture of **4.2** (0.15 g, 0.30 mmol, 1 eq.) and $[Pd(CH_3CN)_2Cl_2]$ (0.077 g, 0.3 mmol, 1 eq.) in DCM was left stirring for 3 hours. A dark purple solid was obtained (0.20 g, 96%). Anal. Calcd. for $C_{28}H_{24}Cl_2Fe_2N_2Pd$: C 49.62 H 3.57 N 4.14. Found: C 47.01, H 3.01, N 2.47.

1,2-Benzenedimethylideneiminoferrocene (4.5)

A mixture of phthaldialdehyde (0.052 g, 0.39 mmol, 2 eq.) and aminoferrocene (0.156 g, 039 mmol, 1 eq.) in toluene was heated to 110 ºC for 5 hours using a Dean-Stark apparatus. A dark yellow oily solid was obtained (wet crude product weight 0.21 g) ^{1}H NMR (400 MHz; $CDCl_3$) δ_H: 1.43 (s, 2H, CH) 1.63 (br, 2H, NH), 4.06 (pt, 2H, Cp-H), 4.11 (pt, 2H, Cp-H), 4.22 (s, 5H, Cp-H), 4.25 (pt, 2H, Cp-H), 4.33 (s, 5H, Cp-H), 4.65 (s, 2H, OH), 5.05 (pt, 2H, Cp-H), 7.11 (s, 2H, Ar-H) 7.39 (pt, 2H, Ar-H). ^{13}C{^{1}H} NMR (100 MHz; $CDCl_3$) δ_C: 52.7 (*C*-O), 66.7 (Cp, *C*-H), 69.3 (Cp, *C*-H), 99.9.0 (Cp-N, *C*-N), 109.8 (Cp-N, *C*-N), 122.7 (Ar, *C*-H), 126.4 (Ar, *C*-H), 127.2 (Ar, *C*-H), 130.0 (Ar, *C*-H), 140.6 (Ar, *C*-CH). MS (ESI) m/z: 534 ([M-2H]$^+$, 40 %).

1,1'-bis[2-(Diphenylphosphino)benzylidene]iminoferrocene (4.6)

A mixture of 2-(diphenylphosphino)benzaldehyde (1.16 g, 4.0 mmol, 2 eq.) and 1,1'-bis -(amino)ferrocene (0.44 g, 2.0 mmol, 1 eq.) in *n*-hexane was heated to 70 ºC for 5 hours. A dark red solid was obtained in a 95 % yield (1.52 g). ^{1}H NMR (400 MHz; $CDCl_3$) δ_H: 3.93 (pt, 4H, Cp-H), 4.27 (pt, 4H, Cp-H), 6.86 (m, 2H, Ar-H) 7.25 ~ 7.40 (m, 24H, Ar-PPh_2), 8.00 (ddd, 2H, Ar-H), 9.32 (d, H, N=C-H). ^{31}P{^{1}H} NMR (162 MHz; $CDCl_3$) δ_p: -13.7 (s). ^{13}C{^{1}H} NMR (100 MHz; $CDCl_3$) δ_C: 64.5 (Cp-N, *C*-H), 69.7 (Cp-N, *C*-H), 105.3 (Cp-N, *C*-N), 127.6 (Ar, *C*-H), 128.8 (PPh_2, *C*-H), 129.0 (Ar, *C*-H), 130.2 (Ar, *C*-H), 133.6 (Ar, *C*-H), 134.1 (PPh_2, *C*-H), 134.3 (PPh_2, *C*-H), 137.0 (PPh_2, *C*-P), 137.4 (Ar, *C*-P), 140.0 (Ar, *C*-C=N), 156.8 (C=N).

Chloroferrocene[6] (FcCl)

1.9 M ^{t}BuLi in pentane (23 mL, 43.2 mmol, 2 eq.) was added dropwise to a stirred solution of ferrocene (4.00 g, 21.5 mmol, 1 eq), potassium *tert*-butoxide (0.03 g, 2.68 mmol, 0.12 eq.) and THF (120 mL) held at -78 °C (acetone/dry ice). The resulting orange suspension was vigorously stirred for 2 hours whereby hexachloroethane (7.65 g, 32.3 mmol, 1.5 eq.) was added against nitrogen. This mixture was stirred for a further 30 minutes at -78°C before allowed to slowly warm to ambient temperature by not adding dry ice, at which point the dark orange solution was carefully quenched with water, extracted two times with CH_2Cl_2 and solvent removed.

The crude product was extracted into *n*-hexane (300 mL), and washed with 0.2 M aqueous $FeCl_3$ (2 x 200 mL). When Fc had been removed (composition monitored by ^{1}H NMR spectroscopy between washings), the organic phase was extracted with water until the washings were colorless, dried over $MgSO_4$ and filtered (50 g silica/*n*-hexane). Evaporation of solvent provided pure FcCl as an orange crystalline solid (3.03 g, 64 %). Anal. Calcd. for $C_{10}H_9FeCl$: C 54.45 H, 4.12. Found: C 54.39 H 4.13. ^{1}H NMR ($CDCl_3$; 400 MHz): δ 4.09 (pt, 2H, Cp-*H*, *J* = 1.83 Hz, 1.85 Hz), 4.24 (s, 5H, Cp-*H*) 4.39 (pt, 2H, Cp-*H*, *J* = 1.89 Hz, 1.90 Hz). ^{13}C{^{1}H} NMR ($CDCl_3$; 100 MHz): δ_C: 66.1 (Cp-Cl, *C*-H), 68.0 (Cp-Cl, *C*-H), 70.4 (Cp, *C*H), 92.5 (Cp–Cl, *C*-Cl). HR-MS EI: m/z 219.9735, ($[M]^+$ calcd: 219.9742).

Fluoroferrocene[7] **(FcF)**

1.6 M ^{t}BuLi in pentane (13 mL, 21.2 mmol, 2 eq.) was added dropwise to a stirred solution of ferrocene (1.90 g, 10.6 mmol, 1 eq), potassium *tert*-butoxide (0.013 g, 1.31 mmol, 0.12 eq.) and THF (30 mL) held at -78 °C (acetone/dry ice). The resulting orange suspension was vigorously stirred for 2 hours whereby NFSI (5.00 g, 15.8 mmol, 1.5 eq.) was added against nitrogen. This mixture was stirred for a further 30 minutes at -78°C before allowed to slowly warm to ambient temperature by not adding dry ice, at which point the dark solution was carefully quenched with water, extracted two times with CH_2Cl_2 and solvent removed.

The crude product was extracted into *n*-hexane (300 mL), and washed with 0.2 M aqueous $FeCl_3$ (2 x 200 mL). When Fc had been removed (composition monitored by ^{1}H NMR spectroscopy between washings), the organic phase was extracted with water until the washings were colorless, dried over $MgSO_4$ and filtered (50 g silica/*n*-hexane). Evaporation of solvent provided pure FcF as a light yellow solid (0.33 g, 15 %). Anal. Calcd. For $C_{10}H_9FeF$: C 58.85 H, 4.45. Found: C 58.72 H 4.35. ^{1}H NMR ($CDCl_3$; 400 MHz): δ_H: 3.79 (pt, 2H, Cp-*H*, *J* = 1.82 Hz, 1.51 Hz, 1.82 Hz), 4.26 (s, 5H, Cp-*H*) 4.30 (pt, 2H, Cp-*H*, *J* = 2.23 Hz, 2.41 Hz, 2.22 Hz). ^{13}C{^{1}H} NMR ($CDCl_3$; 100 MHz): δ_C: 29.7 (Cp-F, *C*-F), 56.1 (Cp-F, *C*-H), 61.0 (Cp-F, *C*-H), 69.3 (Cp, *C*H). ^{19}F-{^{1}H}NMR ($CDCl_3$; 377 MHz): δ_F: -188.8 (s). HR-MS EI: m/z 204.0051, ([M]$^{+}$ calcd: 204.0038).

1,1'-Dichloroferrocene[8] **($fcCl_2$)**

The suspension of 1,1'-dilithioferrocene-TMEDA was produced from ferrocene (9.30 g, 50 mmol, 1 eq.), TMEDA (18 mL, 125 mmol, 2.5 eq.), *n*-hexane (60 mL) and 2.5 M ^{n}BuLi (44 mL, 110.0 mmol, 2.2 eq.) was cooled to -78°C (acetone/dry ice). Hexachloroethane (26.0 g, 110 mmol, 2.2 eq.) was added to the reaction mixture. After slowly raising the reaction to ambient temperature and stirring overnight, the resulting solution was quenched with water (20 mL) and separated, providing yellow solid after solvent removal.

The crude product was extracted into *n*-hexane (300 mL), filtered through Celite and washed successively with 3.0 M aqueous $FeCl_3$ (3 × 200 mL). When contaminants had been removed (composition monitored by ^{1}H NMR spectroscopy between washings), the organic phase was extracted with water until the washings were colorless, dried over $MgSO_4$, and

filtered (50 g silica/*n*-hexane). The solution was dried in vacuo to yield pure $fcCl_2$ as a yellow solid (12.7 g, 75 %). Anal. Calcd. For $C_{10}H_8FeCl_2$: C 47.09 H 3.16. Found: C 47.17 H 3.23. ^{1}H NMR ($CDCl_3$; 400 MHz): δ_H: 4.13 (pt, 4H, Cp-*H*, *J* = 1.96 Hz, 2.28 Hz), 4.41 (pt, 4H, Cp-*H*, *J* = 2.03 Hz, 2.13 Hz). $^{13}C\{^1H\}$ NMR ($CDCl_3$; 100 MHz): δ_C: 68.5 (Cp, *C*-H), 70.1 (Cp, *C*-H), 93.3 (Cp, *C*-Cl). HR-MS EI+: m/z: 253.9367, ($[M]^+$ calcd: 253.9362).

1,1'-Difluoroferrocene (fcF_2)

The suspension of 1,1'-dilithioferrocene-TMEDA was produced from ferrocene (1.86 g, 10 mmol, 1 eq.), TMEDA (3.7 mL, 25 mmol, 2.5 eq.) and 2.5 M ^{n}BuLi (8.8 mL, 22.0 mmol, 2.2 eq.) in Et_2O was cooled to -78°C (acetone/dry ice). NFSI (7.0 g, 22 mmol, 2.2 eq.) was added to the reaction mixture. After slowly raising the reaction to ambient temperature and stirring overnight, the resulting solution was quenched with water (20 mL) and separated, providing yellow solid after solvent removal.

The crude product was extracted into *n*-hexane (300 mL), filtered through Celite and washed successively with 2.0 M aqueous $FeCl_3$ (2 × 200 mL). When contaminants had been removed (composition monitored with ^{1}H NMR between washings), the organic phase was extracted with water until the washings were colorless, dried over $MgSO_4$, and filtered (50 g silica/*n*-hexane). The solution was dried in vacuo to yield pure fcF_2 as a light yellow solid (0.11 g, 5 %). Anal. Calcd. For $C_{10}H_8FeF_2$: C 54.08 H 3.63. Found: C 54.15 H 3.60. ^{1}H NMR ($CDCl_3$; 400 MHz): δ_H: 3.92 (pt, 4H, Cp-*H*, *J* = 1.70 Hz, 1.18 Hz, 1.68 Hz), 4.41 (pt, 4H, Cp-*H*, *J* = 2.16 Hz, 1.09 Hz, 2.14 Hz). $^{19}F\{^1H\}$ NMR ($CDCl_3$; 100 MHz) δ_F: -188.0 (s).

7.5. Compounds Synthesized in Chapter 5

Chloromethylpalladium1,1-'bis(methylthio)ferrocene[9] [Pd(bmsf)(CH_3)Cl] (5.1)

In two separate flasks, bmsf (0.70 g, 2.62 mmol, 1.4 eq.) and [Pd(COD)(CH_3)Cl] (0.50 g, 1.85 mmol, 1 eq.) were added. Both compound were fully dissolved in DCM (15 mL) and filtered before adding them to each other. Upon addition of the solutions to one another, the reaction mixture turned orange. This mixture was left stirring overnight at room temperature

to allow the reaction to go to completion. The solvent was then removed to give a light orange solid. This was washed with toluene (3 × 20mL) to remove the excess bmsf ligand and any other impurities.

A dark yellow solid was obtained (0.65 g, 81%). Anal. Calcd. for $C_{13}H_{17}ClFeS_2Pd$: C 35.86, H 3.91. Found: C 35.72, H 3.72. ^{1}H NMR (400 MHz; $CDCl_3$) δ_H: 4.75 (s, 2H, Cp-H), 4.82 (s, 2H, Cp-H), 4.34 (s, 2H, Cp-H), 4.31 (s, 2H, Cp-H), 2.47 (s, 3H, S-CH_3), 2.36 (s, 3H, S-CH_3), 1.19 (s, 3H, Pd-CH_3). MS(ESI) m/z: 399 ($[M-Cl]^+$, 60%).

(η^4-1,5-Cyclooctadiene)rhodium 1,1'-bis(methylthio)ferrocene hexafluorophosphate[10] [Rh(bmsf)(COD)][PF_6] (5.3)

To an DCM (30 mL) solution of [$(Rh(COD)Cl)_2$] (60 mg, 0.12 mmol, 1.0 eq.), an aqueous solution (10 mL) of KPF_6 (70 mg, 0.36 mmol, 3.0 eq.) was added. The mixture was stirred vigorously for 15 min before bmsf (0.11g, 0.4 mmol, 3.3 eq.) was added. The flask was then covered with an aluminum sheet to shield the light, and the mixture was left stirring overnight during which a dark orange suspension was formed. The solvent was removed using a rotary evaporator, and this crude product was washed with distilled water (3 × 10 mL) and THF (3 × 10 mL). A dark brown solid obtained (62.4 mg, 82 %). Anal. Calcd. for $C_{20}H_{26}S_2RhPF_6Fe$: C 37.86, H 4.13. Found: C 37.69, H 4.09. ^{1}H NMR (400 MHz; $CDCl_3$) δ_H: 2.21 (m, 4H, -CH_2-), 2.70 (m, 4H, -CH_2-), 2.35 (s, 6H, -CH_3), 4.44 (m, 4H, -CH-), 4.71 (s, 4H, α-H), 4.85 (s, 4H, β-H). MS (ESI) m/z: 381 ($[Rh(bmsf)]^+$, 65 %).

(η^4-1,5-Cyclooctadiene)rhodium 1,1'-bis(diphenylphosphino)ferrocene hexafluorophos -phate [Rh(dppf)(COD)][PF_6] (5.4)

To an DCM (30 mL) solution of [$(Rh(COD)Cl)_2$] (0.61 mmol, 300 mg, 1.0 eq.), an aqueous solution (10 mL) of KPF_6 (1.85 mmol, 350 mg, 3.0 eq.) was added. The mixture was stirred vigorously for 15 min before dppf (1.85 mmol, 1.0 g, 3.0 eq.) was added. The flask was then covered with an aluminum sheet to shield the light, and the mixture was left stirring overnight during which a dark orange suspension was formed. The solvent was removed using a rotary evaporator, and this crude product was washed with distilled water (3×10 mL), toluene (3 × 20 mL), and ethanol (3 × 10 mL). An orange solid was obtained (0.40 g, 73%). .

Anal. Calcd. for $C_{42}H_{40}P_3F_6RhFe$: C 55.39, H 4.43. Found: C 55.50, H 4.35. ^{1}H NMR (400 MHz; $CDCl_3$) δ_H: 2.12 (m, 4H, -CH_2-), 2.37 (m, 4H, -CH_2-), 4.25 (s, 4H, α-H), 4.32 (s, 4H, β-H), 4.40 (m, 4H, -CH-). $^{31}P\{^1H\}$ NMR (162 MHz; $CDCl_3$) δ_P: 21.5 (d, PPh_2, $^1J_{Rh,P}$ = 148.96 Hz), -144.2 (m, PF_6^-, $^1J_{F,P}$ = 712.80). No meaningful data obtained from the electrospray mass spectrum.

Suzuki-Miyaura cross-coupling reactions

In a 100 mL two-necked round-bottomed flask with a magnetic stirrer, 4-bromotoluene (1.06 mmol, 0.18 g, 1.0 eq.), phenylboronic (1.64 mmol, 0.20 g, 1.55 eq.), K_3PO_4 (2.12 mmols, 0.45 g, 2.0 eq.), the selected Pd-catalyst (0.02 eq.) and THF (25 mL) were added. The mixture was left stirring for 3 hours/1 hour at 30 ºC/50 ºC/80 ºC. The orange/brown crude product was taken in *n*-hexane and then passed through a thin pad (3 cm) of silica column.

The filtrate was reduced to dryness on a rotary evaporator, and an off-white solid was collected from the flask. This solid was analyzed via ^{1}H NMR, and the catalytic conversions given by the four catalysts are listed in table 7.11.

	80 ºC	**50 ºC**	**30 ºC**
[Pd(dppf)Cl_2] (2.1)	88 ± 1	94 ± 1	69 ± 1
[Pd(dppf-Fe^{III})Cl_2][PF_6] (2.1-ox)	60 ± 2	95 ± 2	68 ± 1
[Pd(dppf)ClCH_3] (5.2)	60 ± 5	97 ± 1	84 ± 1
[Pd(bsmf)ClCH_3] (5.1)	95 ± 1	25 ± 5	50 ± 5

Table 7.11. Catalytic conversions (%) of 4-bromotoluene correspondoing to figure 5.20 in chapter 5 (n ≥ 3)

Hydrogenation reactions

The mixture of styrene (0.57 mL, 5.0 mmol, 1 eq.) and the selected rhodium catalyst (0.01 eq.) in toluene (5 mL) was heated to 120 ºC under an atmospheric pressure of hydrogen. After 18 hours, the solution cooled and filtered through Celite. 1 mL of the clear solution obtained was taken for GC analysis.

7.6. References

1. Koridze, A. A.; Kuklin, S. A.; Sheloumov, A. M.; Dolgushin, F.M.; Lagunova, V. Y.; Petukhova, I. I.; Ezernitskaya, M. G.; Peregudov, A. G.; Petrovskii, P. V.; Vorontsov, E. V.; Baya, M.; Poli, R. *Organometallics*, **2004**, *23*, 4587.

2. Jennings, L. Imperial College London, 2001.

3. Guan, W. MRes Report, Imperial College London, 2006.

4. Gregson, C. K. A. PhD thesis, Imperial College London, 2006.

5. Oxford, P. J. PhD thesis, Imperial College London, 2003.

6. Bernhartzeder, S.; Suenkel, K. *J. Organomet. Chem.* **2012**, *716*, 146.

7. Hedberg, F.; Rosenberg, H. *J. Organomet. Chem.* **1971**, *28*, C14.

8. Inkpen, M. S.; Du, S.; Driver, M.; Albrecht, T.; Long, N. J. *Dalton Trans*, **2013**, *42*, 2813.

9. Dekker, G. P. C. M.; Elsevier, C. J.; Vrieze, K.; van Leeuwen, P. W. N. M. **1992**, *11*, 1598.

10. Schrock, R. R.; Osborn, J. A. *J. Am Chem. Soc.* **1971**, *19*, 2397.

.

APPENDICE

Crystal data and structure refinement for NL0511.

Identification code	NL0511	
Empirical formula	C29 H24 Cl2 Fe N P Pd . 2CH2Cl2	
Formula weight	820.46	
Temperature	173(2) K	
Diffractometer, wavelength	OD Xcalibur 3, 0.71073 Å	
Crystal system, space group	Monoclinic, P2(1)/c	
Unit cell dimensions	a = 14.0498(9) Å	a = 90°
	b = 11.7942(9) Å	b = 104.780(6)°
	c = 20.5110(14) Å	g = 90°
Volume, Z	3286.3(4) $Å^3$, 4	
Density (calculated)	1.658 Mg/m^3	
Absorption coefficient	1.548 mm^{-1}	
F(000)	1640	
Crystal colour / morphology	Black tablets	
Crystal size	0.17 x 0.10 x 0.04 mm^3	
q range for data collection	3.77 to 32.70°	
Index ranges	-21<=h<=14, -17<=k<=17, -30<=l<=29	
Reflns collected / unique	31307 / 11031 [R(int) = 0.1729]	
Reflns observed [F>4s(F)]	5463	
Absorption correction	Numeric analytical	
Max. and min. transmission	0.94383 and 0.81281	
Refinement method	Full-matrix least-squares on F^2	
Data / restraints / parameters	11031 / 20 / 411	
Goodness-of-fit on F^2	1.016	
Final R indices [F>4s(F)]	R1 = 0.0921, wR2 = 0.1707	
R indices (all data)	R1 = 0.1813, wR2 = 0.2058	
Largest diff. peak, hole	3.589, -2.066 $eÅ^{-3}$	
Mean and maximum shift/error	0.000 and 0.000	

Table 2. Bond lengths [Å] and angles [°] for NL0511.

Pd-N(7)	2.065(5)
Pd-P	2.2181(16)
Pd-Cl(2)	2.2866(15)
Pd-Cl(1)	2.3797(15)
Fe-C(11)	2.031(6)
Fe-C(15)	2.036(7)
Fe-C(9)	2.036(6)
Fe-C(13)	2.038(7)
Fe-C(10)	2.042(7)
Fe-C(16)	2.043(6)
Fe-C(17)	2.046(7)
Fe-C(8)	2.046(6)
Fe-C(14)	2.047(7)
Fe-C(12)	2.067(6)
P-C(18)	1.818(7)
P-C(24)	1.825(6)
P-C(1)	1.827(6)
C(1)-C(2)	1.389(9)
C(1)-C(6)	1.423(8)
C(2)-C(3)	1.407(9)
C(3)-C(4)	1.370(9)
C(4)-C(5)	1.378(9)
C(5)-C(6)	1.389(8)
C(6)-C(7)	1.452(8)
C(7)-N(7)	1.274(7)
N(7)-C(8)	1.440(8)
C(8)-C(9)	1.404(9)
C(8)-C(12)	1.425(9)
C(9)-C(10)	1.428(9)
C(10)-C(11)	1.422(10)
C(11)-C(12)	1.431(9)
C(13)-C(17)	1.390(12)
C(13)-C(14)	1.408(11)
C(14)-C(15)	1.408(11)
C(15)-C(16)	1.446(11)
C(16)-C(17)	1.427(10)
C(18)-C(19)	1.371(10)
C(18)-C(23)	1.386(9)
C(19)-C(20)	1.416(11)
C(20)-C(21)	1.343(13)
C(21)-C(22)	1.363(12)
C(22)-C(23)	1.380(10)
C(24)-C(29)	1.390(9)
C(24)-C(25)	1.400(9)
C(25)-C(26)	1.379(10)
C(26)-C(27)	1.384(11)
C(27)-C(28)	1.355(11)
C(28)-C(29)	1.407(9)

N(7)-Pd-P	85.37(14)
N(7)-Pd-Cl(2)	174.43(14)
P-Pd-Cl(2)	94.33(6)
N(7)-Pd-Cl(1)	89.80(14)
P-Pd-Cl(1)	169.15(6)
Cl(2)-Pd-Cl(1)	91.41(6)
C(11)-Fe-C(15)	104.9(3)
C(11)-Fe-C(9)	68.9(3)
C(15)-Fe-C(9)	156.7(3)

C(11)-Fe-C(13)	159.6(3)
C(15)-Fe-C(13)	68.0(3)
C(9)-Fe-C(13)	125.1(3)
C(11)-Fe-C(10)	40.9(3)
C(15)-Fe-C(10)	119.8(3)
C(9)-Fe-C(10)	41.0(3)
C(13)-Fe-C(10)	159.4(3)
C(11)-Fe-C(16)	120.4(3)
C(15)-Fe-C(16)	41.5(3)
C(9)-Fe-C(16)	120.8(3)
C(13)-Fe-C(16)	67.8(3)
C(10)-Fe-C(16)	104.5(3)
C(11)-Fe-C(17)	157.6(3)
C(15)-Fe-C(17)	68.9(3)
C(9)-Fe-C(17)	107.8(3)
C(13)-Fe-C(17)	39.8(3)
C(10)-Fe-C(17)	122.1(3)
C(16)-Fe-C(17)	40.8(3)
C(11)-Fe-C(8)	67.8(2)
C(15)-Fe-C(8)	159.9(3)
C(9)-Fe-C(8)	40.2(2)
C(13)-Fe-C(8)	112.0(3)
C(10)-Fe-C(8)	67.8(3)
C(16)-Fe-C(8)	158.4(3)
C(17)-Fe-C(8)	124.8(3)
C(11)-Fe-C(14)	122.1(3)
C(15)-Fe-C(14)	40.4(3)
C(9)-Fe-C(14)	161.6(3)
C(13)-Fe-C(14)	40.3(3)
C(10)-Fe-C(14)	156.7(3)
C(16)-Fe-C(14)	68.5(3)
C(17)-Fe-C(14)	68.0(3)
C(8)-Fe-C(14)	126.4(3)
C(11)-Fe-C(12)	40.9(2)
C(15)-Fe-C(12)	121.9(3)
C(9)-Fe-C(12)	69.0(3)
C(13)-Fe-C(12)	125.3(3)
C(10)-Fe-C(12)	68.9(3)
C(16)-Fe-C(12)	157.6(3)
C(17)-Fe-C(12)	160.5(3)
C(8)-Fe-C(12)	40.5(2)
C(14)-Fe-C(12)	108.7(3)
C(18)-P-C(24)	105.6(3)
C(18)-P-C(1)	106.6(3)
C(24)-P-C(1)	104.9(3)
C(18)-P-Pd	111.2(2)
C(24)-P-Pd	124.4(2)
C(1)-P-Pd	102.7(2)
C(2)-C(1)-C(6)	119.5(5)
C(2)-C(1)-P	120.2(4)
C(6)-C(1)-P	120.2(5)
C(1)-C(2)-C(3)	120.6(6)
C(4)-C(3)-C(2)	119.2(6)
C(3)-C(4)-C(5)	121.0(6)
C(4)-C(5)-C(6)	121.4(6)
C(5)-C(6)-C(1)	118.2(6)
C(5)-C(6)-C(7)	118.9(5)
C(1)-C(6)-C(7)	122.8(5)
N(7)-C(7)-C(6)	126.9(5)
C(7)-N(7)-C(8)	121.2(5)

C(7)-N(7)-Pd	126.1(4)
C(8)-N(7)-Pd	112.4(4)
C(9)-C(8)-C(12)	110.4(5)
C(9)-C(8)-N(7)	126.3(6)
C(12)-C(8)-N(7)	123.1(5)
C(9)-C(8)-Fe	69.5(3)
C(12)-C(8)-Fe	70.5(3)
N(7)-C(8)-Fe	130.3(4)
C(8)-C(9)-C(10)	107.2(6)
C(8)-C(9)-Fe	70.3(4)
C(10)-C(9)-Fe	69.7(4)
C(11)-C(10)-C(9)	107.7(6)
C(11)-C(10)-Fe	69.2(4)
C(9)-C(10)-Fe	69.3(4)
C(10)-C(11)-C(12)	109.1(6)
C(10)-C(11)-Fe	70.0(4)
C(12)-C(11)-Fe	70.9(4)
C(8)-C(12)-C(11)	105.6(5)
C(8)-C(12)-Fe	69.0(3)
C(11)-C(12)-Fe	68.2(4)
C(17)-C(13)-C(14)	109.7(7)
C(17)-C(13)-Fe	70.4(4)
C(14)-C(13)-Fe	70.2(4)
C(13)-C(14)-C(15)	107.9(7)
C(13)-C(14)-Fe	69.5(4)
C(15)-C(14)-Fe	69.4(4)
C(14)-C(15)-C(16)	107.5(7)
C(14)-C(15)-Fe	70.3(4)
C(16)-C(15)-Fe	69.5(4)
C(17)-C(16)-C(15)	107.0(7)
C(17)-C(16)-Fe	69.7(4)
C(15)-C(16)-Fe	69.0(4)
C(13)-C(17)-C(16)	107.9(7)
C(13)-C(17)-Fe	69.8(4)
C(16)-C(17)-Fe	69.4(4)
C(19)-C(18)-C(23)	120.1(6)
C(19)-C(18)-P	121.3(5)
C(23)-C(18)-P	118.6(5)
C(18)-C(19)-C(20)	119.3(7)
C(21)-C(20)-C(19)	119.9(8)
C(20)-C(21)-C(22)	120.6(7)
C(21)-C(22)-C(23)	121.2(7)
C(22)-C(23)-C(18)	118.9(7)
C(29)-C(24)-C(25)	119.9(6)
C(29)-C(24)-P	120.2(5)
C(25)-C(24)-P	119.5(5)
C(26)-C(25)-C(24)	119.0(7)
C(25)-C(26)-C(27)	120.6(7)
C(28)-C(27)-C(26)	121.3(7)
C(27)-C(28)-C(29)	119.2(7)
C(24)-C(29)-C(28)	119.9(6)